

The local economic impacts of natural disasters

A view from outer space

Manuscript committee: Prof. dr. W.H.J. Hassink  
Prof. dr. J.J. de Laat  
Prof. dr. J.G.M. van Marrewijk  
Prof. dr. I. Noy  
dr. F. Zhou

This research was funded by Utrecht University

ISBN: 978-94-91870-49-1  
U.S.E. Dissertation Series  
USE 064

Printed by Ridderprint, [www.ridderprint.nl](http://www.ridderprint.nl)

© 2022 Vincent Schippers. This dissertation was typeset using  $\text{\LaTeX}$  and is licensed under CC-BY-NC-ND 4.0.  
<https://creativecommons.org/licenses/by-nc-nd/4.0/>

# The local economic impacts of natural disasters

## A view from outer space

De lokale economische impacts van natuurrampen

Een blik vanuit de ruimte

(met een samenvatting in het Nederlands)

## Proefschrift

ter verkrijging van de graad van doctor

aan de Universiteit Utrecht

op gezag van de rector magnificus, prof. dr. H.R.B.M. Kummeling,

ingevolge het besluit van het college voor promoties

in het openbaar te verdedigen op

dinsdag 5 juli 2022 des middags te 12.15 uur

door

Vincent George Schippers

geboren 9 juni 1991

te Leiderdorp

Promotoren: Prof. dr. W.J.W. Botzen  
Prof. dr. M.W.J.L. Sanders  
Prof. dr. B.J.P. van Bavel

Er is altijd licht



---

# Contents

---

Acknowledgements . . . . .	xi
List of Tables . . . . .	xv
List of Figures . . . . .	xvii
<b>1 Introduction</b>	<b>1</b>
1.1 Motivation . . . . .	1
1.2 Objectives and contributions . . . . .	2
1.3 Data and methodology . . . . .	9
1.4 Natural disasters and night lights: a case study of Hurricane Katrina	13
1.5 Going global: the economic impact of weather anomalies . . . . .	14
1.6 New opportunities? Monthly night light data and earthquakes . . . . .	16
1.7 Shaken but not stirred? A case study of the 2016 Kumamoto earthquake	17
<b>2 Night lights in times of catastrophe</b>	<b>19</b>
2.1 Introduction . . . . .	19
2.1.1 Related literature . . . . .	20
2.2 Direct and economic consequences of Hurricane Katrina . . . . .	22
2.2.1 Hurricane Katrina: landfall and economic impacts . . . . .	22
2.2.2 Visible impacts from space . . . . .	25
2.2.3 Regional impacts and recovery in night lights . . . . .	29
2.3 Relating night light changes to economic indicators . . . . .	34
2.3.1 Population changes and night lights . . . . .	35
2.3.2 Other indicators: employment, income, and GDP . . . . .	38
2.3.3 Correlations between night lights and economic indicators . . . . .	39
2.4 Discussion . . . . .	42
2.5 Conclusion . . . . .	44
2.A Figures and Tables . . . . .	46
2.B Cleaning of the night light series . . . . .	49

<b>3</b>	<b>The economic impact of weather anomalies</b>	<b>57</b>
3.1	Introduction . . . . .	57
3.2	Theoretical background . . . . .	60
3.3	Nightlight emissions and weather anomalies at the grid-cell level . .	62
3.3.1	Nightlight emissions . . . . .	62
3.3.2	Weather anomalies . . . . .	63
3.3.3	Population . . . . .	69
3.4	Empirical strategy . . . . .	71
3.5	Main results . . . . .	73
3.5.1	Building the baseline . . . . .	73
3.5.2	Results and interpretation . . . . .	76
3.5.3	Robustness . . . . .	80
3.5.4	Assessing spillovers across longer distances . . . . .	83
3.5.5	Heterogeneity over development levels . . . . .	85
3.6	Conclusion . . . . .	86
3.A	Descriptives and background . . . . .	89
3.A.1	Background information: DMSF night light data . . . . .	89
3.A.2	Interpolation of wind speeds . . . . .	90
3.A.3	Balancing . . . . .	95
3.A.4	Supplementary descriptive statistics . . . . .	97
3.A.5	Rural/urban classification . . . . .	101
3.B	Supplementary tables . . . . .	106
<b>4</b>	<b>Lights out? Earthquakes and local economic activity</b>	<b>117</b>
4.1	Introduction . . . . .	117
4.2	Literature . . . . .	120
4.3	Data . . . . .	123
4.3.1	VIIRS night lights . . . . .	123
4.3.2	Earthquakes . . . . .	126
4.3.3	Night lights and earthquakes: an example . . . . .	132
4.4	Empirical Strategy . . . . .	134
4.5	Results . . . . .	136
4.5.1	Baseline results . . . . .	136
4.5.2	Zooming in: pixel-resolution . . . . .	141
4.5.3	Reflecting on the findings . . . . .	142
4.5.4	Beyond the global average: heterogeneity . . . . .	144
4.6	Conclusion . . . . .	147
4.A	Descriptives, tables and figures . . . . .	150
4.B	Regression Tables and Figures . . . . .	152
4.B.1	Disaster-related power outages . . . . .	157
<b>5</b>	<b>Shaken, but not stirred?</b>	<b>159</b>
5.1	Introduction . . . . .	159
5.2	The April 2016 Kumamoto earthquake . . . . .	164
5.2.1	Direct impacts: fatalities and damages . . . . .	165



5.2.2	Indirect impacts on economic activity, business, and lifelines	166
5.3	Methodology	171
5.3.1	Conceptual framework	171
5.3.2	Night lights	177
5.3.3	Empirical strategy	180
5.4	Results	186
5.4.1	Average effects on night light intensity	186
5.4.2	Zooming in: light intensity for the worst-affected municipalities	189
5.5	Discussion and conclusion	195
5.A	Damages and economic data	198
5.B	Summary statistics and robustness tests	206
5.B.1	Seasonality in the VIIRS time series	209
5.B.2	Difference-in-differences robustness	212
5.C	Case selection	215
<b>6</b>	<b>Conclusion</b>	<b>217</b>
6.1	Main contributions	217
6.1.1	Chapter 2: Night lights and Hurricane Katrina	220
6.1.2	Chapter 3: A global perspective on local weather anomalies	221
6.1.3	Chapter 4: Zooming in on local impacts of earthquakes	223
6.1.4	Chapter 5: Shaken, but not stirred	225
6.2	Discussion on the main findings	226
6.3	Limitations and directions for future research	228
	Bibliography	233
	<b>Nederlandse samenvatting</b>	<b>253</b>
	<b>Curriculum Vitae</b>	<b>261</b>
	<b>U.S.E. Dissertation Series</b>	<b>263</b>



---

## Acknowledgements

---

This journey began in 2014, when I joined Mark in a project on the determinants of losses from natural disasters. This project inspired me to write a research proposal on the importance of institutions for mitigating and adapting to the risk of natural extremes that are associated with ongoing climate change, arguably one of the greatest challenges of this time. What followed over the years after was a challenging and inspiring journey that started with a master's thesis that formed the basis of this dissertation. Soon after I would depart to Munich to work on the first big chapter of my thesis.

During the years I presented my work at conferences and workshops, met dozens of inspiring scholars – some of whom became new friends – and had many opportunities to discuss my work and theirs. In my final year, I joined a research group at the geosciences faculty, the hub on Water, Climate, and Future Deltas, where I met colleagues who again brought entirely new perspectives and who broadened my thinking. As many told me before, writing a PhD thesis is a long and winding process, but I'm glad to conclude at the end that I learned so much while being around smart, kind, and helpful colleagues and friends. For that, some words of gratitude are in place.

First of all, a big thanks to Wouter and Mark for their daily efforts to keep me on track and for giving me the opportunity to explore avenues that were (very!) promising at times, and a meandering dead-end road at others. You challenged me, guided me, and were always available to discuss plans and problems. I truly enjoyed the freedom you gave me at every turn, which allowed me to develop my own questions, analyses, and ultimately my chapters.

Wouter, I cherish our regular meetings, even when they turned into online calls, and your patience and excellent advice when I was stuck in my work. You always read and commented on whatever I sent ahead – something that I do not take for granted. I very much enjoyed our collaboration and look forward to the continuation of working together. Mark, without you this whole project would never have happened. Thank you for your ambition and the way you pushed me to step out of my comfort zone and try new things. You helped me grow as a person and I will always be grateful for having you as a mentor.

Equal thanks go out to you, Bas, for taking me on board in your project and for giving me a second office and another group of inspiring colleagues to exchange thoughts with. Our plans did not quite unfold as intended, but you supported me nonetheless. You always had a sharp eye to challenge what I had become to adopt as standard practice, for which I am grateful.

I thank the members of my reading committee, Prof. dr. Wolter Hassink, Prof dr. Joost de Laat, Prof dr. Charles van Marrewijk, Prof dr. Ilan Noy, and dr. Fujin Zhou, for their time and effort to read and evaluate my thesis. Another word of thanks goes to Prof. dr. Hans Middelkoop and Prof. dr. Walter Immerzeel for joining my defense committee. I also thank my co-authors Thomas Steinwachs, Jasmin Gröschl, and Gabriel Felbermayr for being dedicated co-authors on our ambitious project. I enjoyed my time in Munich and learned a lot from our time together. For my final chapter I had the opportunity to supervise Lia Alscher, at the time a talented bachelor student, who helped with excellent research assistance. Lia, I thank you for your diligent work and I hope our work will find a way to publication in the future. I wish you the best of luck in your career.

Office life as it was in the first years would not have been half as much fun without my ever present roommates of 2.11. Lucia, Timo, Bora, Thomas, and Fujin, you made the days bright when my thoughts weren't. I am grateful for your support and friendship that extends beyond work alone. Lucia, I miss our daily discussions on whatever occupied our minds that day and your warmth of making the office feel like home. Timo, I'm sorry for having Moos lose some excitement over me being gone, but thanks for looking after him anyway. And my compliments for the never-ending supply of nuts and seeds mix! I'm very happy that I can continue calling you my colleague in our new job. Fujin, it was so great to have a colleague working on related matters, I missed you dearly after you left. Bora, you always brought a smile and warmth to the office. It would not have been complete without you. And a special thanks to you Thomas, for always engaging in what at times seemed to turn into endless discussions about, let's be fair, usually my work. It brought great inspiration and much-needed reflection. I will miss you all dearly as my daily office mates.

Dea, Franziska, I miss our weekly Game of Thrones and Stranger Things sessions. Our long talks were a joy and always something to look forward to. Thanks for cooking so much good food and for making the effort of learning and speaking Dutch. I enjoyed that very much and miss these conversations. Thank you Tim for taking me bouldering and meeting a new group of friends, Michiel and Bono for our joint adventure during the master's, and Dieter for our ever-lively discussions. I also thank all other colleagues who kept me company throughout the years at U.S.E., history, and geosciences, with a special mention for the Monotonics – making music together was a welcome and fun distraction. I thank Maarten Zeylmans van Emmichoven and Jelle Treep for their technical support.

At times the PhD could be lonely, especially in the final years. I thank the 'hubbers' for keeping me company, even if it was from a distance as offices were closed pretty

much until the end of my years at Utrecht University. Being part of a group made the days so much less lonely, especially at home. Murray, Frances, Philip, Annisa, Haomiao, Star, Trang, Hans, and Marjolijn, thank you for the opportunity to explore a new field of studies and for the warm welcome you all gave me. Now you can finally truly conclude that ‘I am not a PhD student’. I do wish COVID had not been around, so that we could have shared an office. I am sure we would have moved mountains if our get-togethers would have been a weekly occasion.

Bram, Jordy, thank you for the long and deep conversations about our work and for our friendship. You finished what feels like ages ago, but I remember our nights with perhaps more than a single beer and hours of fierce discussion on identification and badly written sentences. I’m glad to have you back in town Jordy. And Bram, a special and deep thanks goes out to you for keeping me company throughout it all, our endless discussions on our work, and for having a place other than my home office to work regularly. At times you felt like a much-needed mentor to me, especially in times when everything was in lockdown. Thanks for always being around and for always hearing me out and giving advice. Kasper, thank you for our many years of endless conversations on matters concerning the state of the world, society, academia, and what not really. I clearly recall our first days in the office, using a desk phone to celebrate that we had made it to having our own offices. I enjoyed our joint journey and thank you for your continued support throughout the years, it means a lot to me. Thank you Karolien, Fred, Thijs, Kim, and Olivier, for your warmth and for giving me a second home. To all friends and family, you are too many to all name in person, thank you for all cheerful moments, your support, and always hearing me out whenever I had a new story to tell or frustration to share, even if the world of academia was sometimes a world apart to you.

Mom, you deserve the credit that is due: thanks for spotting all those typos and for reading my work. And to Dad, Marten, grandma and grandpa included, thank you for your continued support and endless patience. I couldn’t wish for more.

And finally you, my dearest Arlieke. These years were quite the journey. I think I owe it to your unrelenting care and support that I was able to eventually start this PhD at all. I do not know in what place I would have ended up without your daily push to get me back in the saddle. The years that followed were rough to say the least, but you never let your head down. I cannot be happier that we can close this chapter now and move on. I cherish the moment that we made a new friend, our dog Moos, who’s made every day since a joy. Thank you so much for your support, your smiles, for being my one and only office mate for the last 2 years of this PhD, and for your endless patience in hearing out my troubles, doubts, highs and lows, and especially the words ‘night lights’. I promise I will try to use them less often now that this has come to a close.

And now, on to the next journey.

Vincent Schippers  
Utrecht, May 2022



---

## List of Tables

---

3.2.1	Families of regional economics models . . . . .	61
3.3.1	Representation of natural events in the monthly data vs. the yearly aggregates . . . . .	69
3.5.1	Model Buildup: Impact of Precipitation and Wind on Light Growth .	75
3.5.2	Baseline Results . . . . .	77
3.5.3	Sensitivity Results . . . . .	82
3.5.4	Spillovers Across Longer Distances . . . . .	84
3.5.5	Income Group Heterogeneity, Combined Effects . . . . .	86
3.A.1	Summary Statistics . . . . .	97
3.A.2	Summary Statistics of Satellite-Years for Nighttime Lights . . . . .	98
3.A.3	Lights to GDP Growth Rate Elasticity . . . . .	98
3.A.4	Test for Residual Spatial Autocorrelation . . . . .	99
3.A.5	Comparison of Drought-Effects Across Rural-Urban Neighborhoods .	105
3.B.1	Model Buildup: Impact of Droughts on Light Growth . . . . .	106
3.B.2	Model Buildup: Impact of Cold Waves on Light Growth . . . . .	106
3.B.3	Spatial Error HAC Model following Hsiang (2010) . . . . .	107
3.B.4	Sensitivity: Exclude Population as a Control . . . . .	107
3.B.5	No Time Lags . . . . .	108
3.B.6	Sensitivity to Top-Coding: Excluding Top-Coded Pixels . . . . .	108
3.B.7	Sensitivity to Bottom-Coding: Setting Pixels <DN3 to Zero . . . . .	109
3.B.8	Time Varying Country Characteristics . . . . .	109
3.B.9	Simple Annual Mean of Weather Shocks . . . . .	110
3.B.10	Maximum Weather Shock Intensities, Non-Weighted . . . . .	110
3.B.11	Spatial Radius r=160km . . . . .	111
3.B.12	Global Spillovers . . . . .	112
3.B.13	Non-Linear Damage Functions, Squared . . . . .	113
3.B.14	Non-Linear Damage Functions, Cubic . . . . .	113
3.B.15	All Weather Categories Together . . . . .	114
3.B.16	Income Interaction . . . . .	115
4.3.1	Top 10 most damaging earthquakes between 2012-2016 . . . . .	131
4.5.1	Baseline results: 0.5° grid cells . . . . .	137

4.5.2	Baseline results: 0.5° grid cells . . . . .	139
4.A.1	Summary statistics . . . . .	150
4.B.1	Baseline results: 0.5° grid cells (extended) . . . . .	152
5.2.1	Earthquake impact in selected municipalities . . . . .	165
5.3.1	Impact framework for the short run . . . . .	174
5.3.2	Impact framework for the medium run . . . . .	175
5.3.3	Expected night light impacts for the worst-affected municipalities . . . . .	176
5.3.4	Summary statistics for the treated and control municipalities . . . . .	183
5.A.1	Impact Numbers by Municipality . . . . .	200
5.A.2	Impact Numbers by Prefecture . . . . .	201
5.B.1	Other natural extremes . . . . .	208
5.C.1	Worst earthquakes between 2012-2016 . . . . .	215



---

## List of Figures

---

1.1	Night lights over North America . . . . .	10
2.1	Flood map of New Orleans area . . . . .	23
2.2	Night lights for the City of New Orleans . . . . .	26
2.3	Correlation plot of housing damage and night light reduction in 2005	27
2.4	Housing damage and night lights after Hurricane Katrina . . . . .	28
2.5	Night light intensity in the study region prior to Katrina, 2004 . . . . .	30
2.6	Changes in night light intensity in the study region (2005) . . . . .	31
2.7	Changes in night light intensity in the study region (2006) . . . . .	32
2.8	Night light and economic indicators following Katrina for the 8 most- affected counties . . . . .	37
2.9	Correlations between changes in economic indicators and night lights	41
2.A.10	Distribution of damage to occupied housing units . . . . .	46
2.A.11	Correlations economic indicators and night lights (Zhang calibration)	47
2.A.12	Correlations economic indicators and night lights (fixed effects correction)	48
2.B.1	Corrected night light data (absolute sum of light) . . . . .	52
2.B.2	Corrected night light data (indexed to 2004 = 1) . . . . .	53
3.3.1	Night lights and GDP . . . . .	64
3.3.2	Hurricane Katrina – IBTrACS (l.) vs. Wind Field (r.) . . . . .	67
3.3.3	Kernel Densities of Annual Aggregate Physical Intensities . . . . .	68
3.3.4	Physical Intensities for Wind Speed, Precipitation, Cold and Drought	70
3.A.1	Nightlight emission of Europe and 0.5° grid-cells . . . . .	90
3.A.2	Balancing Wind Speeds – Cells lost when balancing on non-interpolated wind speed data are shown in red. . . . .	92
3.A.3	Semi-Variogram for June 2012. Distance in meters, value labels report the number of bilateral station-distance-pairs per bin. . . . .	92
3.A.4	Kriged maximum wind speed in June 2012 . . . . .	93
3.A.5	Goodness of fit – Standard deviation of Kriged maximum wind speed (in kt) in June 2012, obtained using the ‘leave one out’ technique. . .	93
3.A.6	Spiked pattern obtained with inverse distance weighting as alternative choice of wind speed interpolation. . . . .	94

3.A.7	Balanced Panel - Wind . . . . .	95
3.A.8	Balanced Panel - Temperature . . . . .	95
3.A.9	Balanced Panel - Precipitation . . . . .	96
3.A.10	Balanced Panel - Drought . . . . .	96
3.A.11	Kernel Densities of Monthly Physical Intensities . . . . .	99
3.A.12	Correlations Twoway Demeaned . . . . .	100
3.A.13	Rural/Urban Classification . . . . .	102
3.A.14	Distribution of Cell Properties Across Rural/Urban Clusters . . . . .	103
4.3.1	Night light emission over Europe . . . . .	124
4.3.2	Global maximum shaking of earthquakes included in the Shakemap Atlas 2.0 for 2012-2016 . . . . .	127
4.3.3	Peak ground shaking and potential damage . . . . .	128
4.3.4	Intensity of ground shaking during the April 2015 Gorkha earthquake . . . . .	129
4.3.5	Changes in night light around Kathmandu after April 2015 earthquake in Nepal . . . . .	133
4.5.1	Plotted estimates of lagged coefficients over time . . . . .	140
4.5.2	Lagged coefficients over time: pixel resolution . . . . .	142
4.5.3	Effects by income group: 0.5° grid cells . . . . .	145
4.5.4	Effects by income group: pixel resolution . . . . .	146
4.A.1	Magnitude distribution of included earthquakes . . . . .	150
4.A.2	Distribution of peak ground acceleration of earthquakes included in the Shakemap Atlas 2.0 for 2012-2016 . . . . .	151
4.A.3	Distribution of log radiance for the analysis sample: built-up and persistently-lit pixels in GRUMP urban extents that ever experience non-zero shaking ( $pga > 0$ ) through 2012-2016. . . . .	151
4.B.1	Robustness of the model to alternative fixed effects . . . . .	153
4.B.2	Robustness of the model to alternative shaking variable specifications . . . . .	154
4.B.3	Robustness of the 12-lag model to alternative clustering of standard errors . . . . .	155
4.B.4	The 12-lag model including pre-shock coefficients . . . . .	156
5.2.1	Earthquake location . . . . .	164
5.2.2	Normalized damage distribution across municipalities in Kumamoto prefecture . . . . .	166
5.2.3	Changes in taxable income and net migration . . . . .	169
5.2.4	Changes in business establishments and engaged persons . . . . .	170
5.3.1	Summary of building damage and economic indicators by municipality . . . . .	173
5.3.2	Total sum of light (in natural logarithm) by municipality for the worst-affected cases . . . . .	179
5.3.3	Composition of treatment and control groups on the island of Kyushu . . . . .	181
5.3.4	Average light intensity for the treated and control municipalities . . . . .	182
5.3.5	Indexed taxable income and net migration rate for the treated and control group . . . . .	184
5.4.1	Baseline treatment effect estimates . . . . .	187

5.4.2	Night light intensity for the worst-affected municipalities versus synthetic counterfactuals . . . . .	190
5.4.3	Difference in night light intensity between actual and synthetic counterfactuals for the worst-affected municipalities . . . . .	191
5.A.1	Normalized damages across municipalities in Kumamoto prefecture (total destruction of housing only) . . . . .	198
5.A.2	Building damage in Kumamoto prefecture . . . . .	199
5.A.3	Timing of the resumption of business . . . . .	202
5.A.4	Changes in the number of evacuees and evacuation centers . . . . .	202
5.A.5	Electric power supplying ratios in Kumamoto prefecture . . . . .	203
5.A.6	Change in income and migration . . . . .	204
5.A.7	Change in business activity . . . . .	205
5.B.1	Number of cloud-free nights in April 2016, Kumamoto prefecture . . . . .	206
5.B.2	Number of cloud-free nights by month, 2013-2018 for the 6 prefectures on Kyushu Island . . . . .	207
5.B.3	Number of cloud-free nights in June 2015, Kumamoto prefecture . . . . .	207
5.B.4	Total sum of light (in natural logarithm) by municipality for the worst-affected cases . . . . .	210
5.B.5	Deseasonalized time series by municipality . . . . .	211
5.B.6	Log difference of light intensity for treated vs. control group . . . . .	212
5.B.7	Baseline treatment effect, alternative control group . . . . .	213
5.B.8	Treatment effect, aggregating to months and years . . . . .	214



# CHAPTER 1

---

## Introduction

---

### 1.1 Motivation

In this dissertation I study the local economic impacts of natural disasters. Natural disasters are the result of extreme natural events, natural hazards, that claim lives and cause destruction. Natural hazards can have enormous consequences and are becoming more frequent as a result of climate change (IPCC, 2014). Combined with population growth and increasing urbanization in hazard-prone areas, the likelihood of natural hazards turning into natural disasters, with often devastating consequences to the communities they hit, has been growing. Worldwide, natural disasters claim an average of over 60,000 lives and cost society over 100 billion US dollars in monetary losses per year (CRED, 2021), with economic losses rising substantially over the past decades (Kunkel et al., 1999; Hoeppe, 2016). These adverse impacts affect local production and consumption through effects on human and physical capital, loss of income, and people's savings.

A growing field in economics studies how natural disasters affect our economies and how we can explain differences in impacts and resilience between countries. This research is essential to improve our understanding of how we should deal with the adverse effects of natural disasters and how we can improve mitigation and adaptation strategies.

The economic literature on the impacts and consequences of natural disasters often takes a national perspective and studies aggregate effects of natural disasters on economic growth and development. While effects of natural disasters can be severe for the communities that are directly affected, the effect on national economies in terms of GDP (Gross Domestic Product) and GDP growth is not all that clear. Much conflicting evidence exists in the literature, with studies providing evidence for pronounced negative, insignificant, and in some cases even positive effects on GDP growth rates (Klomp and Valckx, 2014; Botzen et al., 2019). These mixed

results give rise to the question what we are missing: is there no robust evidence for the seemingly intuitive adverse effects that natural disasters are expected to have on our economies, or are these findings the result of a possibly wrong scope of analysis?

In this dissertation I argue that the national perspective is the wrong starting point for studying the effects of natural disasters. While national economies can prove to be resilient, severe adverse shocks can have long-lasting effects on affected regions even in rich countries. This has been shown for example for Hurricane Katrina, which devastated the coastline of Louisiana and Mississippi in August 2005. Adverse effects on the local housing market, labor market, and more generally on consumption and investment, caused a major downturn in the metropolitan area of New Orleans and its surroundings. Hundreds of thousands of individuals were displaced for many months or even permanently, and the thriving city took more than a decade to recover from the devastating floods and the disruptions of everyday life. Yet, even at the state level GDP growth rates were hardly affected in 2005 (Strobl, 2011). Clearly, analyzing the effects of natural disasters at the level of countries hides much of what is going on within them.

I aim to reconcile this discrepancy between the national and the local by zooming in at the local level. I study effects at an order of tens of kilometers, in municipalities (Japan) and counties (United States), and globally at grid cells of half a degree, rather than the order of thousands or millions of square kilometers that make up countries. This allows us to separately investigate what is going on in directly affected areas versus their surroundings. It also makes the comparison between events more adequate: countries come in vastly different sizes, whereas our concept of ‘local’ is roughly equal across the globe. In doing so, I focus on local economic impacts of natural disasters around the world, and study how natural extremes affect local economies.

## 1.2 Objectives and contributions

In the 2000s and early 2010s, most of the economic literature on the economic impacts of natural disasters focused on GDP or GDP growth effects at the national level, i.e. the macro level. Studies typically relate the incidence and recorded losses in terms of fatalities and monetary damages to (changes in) GDP per capita. Strikingly, this strand of literature produced a range of different answers of how natural disasters affect national economies. Effects range from negative (Raddatz, 2009; Hochrainer, 2009; Noy, 2009; Felbermayr and Gröschl, 2014), to insignificant (Cavallo et al., 2013), and even positive (Skidmore and Toya, 2002; Loayza et al., 2012; Fomby et al., 2013). There are several explanations for this ambiguity, and I argue that most of these have to do with geographical scope.

First, natural hazards are localized events that cause destruction in a spatially limited area. The larger a country, the smaller an event of a given size becomes relative to the size of its economy. Comparison of economic impacts of the same natural disaster will therefore give vastly different outcomes in a small versus a

large economy. Moreover, it matters where a natural hazard takes place; extreme winds or flooding hardly matter in Russian Siberia, while the same event striking the coastline of a highly populated delta region can be catastrophic. Human and economic exposure is therefore key when assessing the potential impact of a natural hazard, i.e. a potential natural disaster, but this is lost when analyzing the economic effects at higher levels of administrative aggregation, such as the national level of the United States (see e.g. Strobl, 2011, 2012).

Second, natural disasters can produce winners and losers across affected and unaffected individuals, but also across affected and unaffected locations. Given sufficient size of an affected country, these dynamics arguably take place within national boundaries and cancel out in nationally aggregated GDP statistics. The focus should therefore be on the local level, residing at the meso-level in between the macro-economy and the micro-level of individual households and firms. Of course I am not the first or only researcher to take a meso-level approach and study local impacts of natural disasters. Chang (2010) studies the urban impact of the 1995 Kobe earthquake in Japan, and shows how a large disaster can permanently shift population and production away from the affected urban core. Xiao and Nilawar (2013) study the regional impact of Hurricane Katrina on coastal counties in Louisiana and Mississippi (U.S.) and show markedly lower growth paths for aggregate income and employment for the worst-affected counties in the years after the catastrophe. Related findings are presented by Strobl (2011) on county-level hurricane impacts in the U.S. and Rodriguez-Oreggia et al. (2013) on the effects of natural disasters on human development and poverty at the municipality level in Mexico. As this dissertation progressed, several studies were published that provide insights on impacts of mostly singular events in selected countries (e.g. Brata et al., 2018; Heger and Neumayer, 2019; Nguyen and Noy, 2020). Many other studies exist in the literature, sometimes focusing on historical disasters rather than recent ones (e.g. Xiao, 2011; Hornbeck and Naidu, 2014; Barone and Mocetti, 2014). However, to the best of my knowledge, none of these studies provide a way to systematically compare economic impacts at the local level across the globe.

A third, and arguably the most important concern is our understanding of the determinants of resilience to natural extremes. Understanding these is key to the global discussion on disaster preparedness and mitigation. One finding the macro literature does provide rather unambiguously, is that developing countries bear the largest weight of natural disasters. Especially in terms of death tolls from natural disasters, countries with lower income per capita fare worse (Kahn, 2005; Strömberg, 2007). Governance capacity, institutions, and inequality have been shown to affect how lethal and costly disasters can become (Anbarci et al., 2005; Strömberg, 2007; Toya and Skidmore, 2007; Raschky, 2008; Noy, 2009). But also in terms of national GDP impacts there is evidence that developing countries take the biggest hits (Noy, 2009; Felbermayr and Gröschl, 2014; Berlemann and Wenzel, 2018). Understanding what determines resilience to and successful recovery from natural disasters, especially in developing countries, is therefore evidently an important area of research. However, studying local impacts of natural disasters for low-and medium-income countries is impeded by unavailability of (reliable) data on

income and production at that spatial level.

Fourth, early studies that are important to this literature, such as (Kahn, 2005) and (Skidmore and Toya, 2002; Toya and Skidmore, 2007), study how the impacts of natural disasters differ by levels of development of countries, but do not control for the intensity of the events. This risks comparing apples with oranges since disaster events, typically coming from the EM-DAT database CRED (2021), differ enormously in their consequences. Some of the other early studies do consider this, but use damages or deaths as a proxy for intensity of the events (e.g. Raschky, 2008; Noy, 2009). However, the degree to which natural hazards turn into natural disasters depend on the very level of development of economies in the first place. Felbermayr and Gröschl (2014) show that using loss records introduces endogeneity problems into the regression analyses of these studies: monetary damages tend to be positively correlated to income per capita, while coverage of events is similarly more complete in high income countries. The widely used disaster impact records are therefore problematic. In order to understand the causal effect of natural disasters on economic activity, it is imperative to use an exogenous measure of disaster intensity. The key distinction is that between a natural hazard, i.e. the (probability of a) natural extreme event in a particular place at a particular time, and a natural disaster, which is the materialization of human suffering and material damages as a result of this extreme event. Whereas the former is strictly exogenous to human decision-making, the latter is a result of the interaction of the extreme event with local exposure of people and assets, and their vulnerability to the extreme event. Both exposure and vulnerability depend on human choices of where to live and how to organize society to be resilient (or not) to these shocks (see e.g. van Bavel et al., 2020), making the loss records of natural disasters the wrong metric when the goal is to identify the causal effects of natural extremes on economic outcomes. Felbermayr and Gröschl (2014) therefore propose to use the exogenous physical intensities of natural hazards to study the effects of natural extremes on economic outcomes, and present a dataset at the national level. To go local, however, requires the collection of data on natural extremes around the world at high spatial resolution, combined with data on local economic activity.

We can account fairly well what happened to county-level income and population for the case of Hurricane Katrina (for other examples, see Chang, 2010; Xiao and Nilawar, 2013; Brata et al., 2018; Heger and Neumayer, 2019), but this becomes difficult if not impossible rather quickly as we move to events in countries with lower levels of development. Adequate data to study economic impacts at the desired geographical level of (dis)aggregation is typically not available, while impacts of natural disasters tend to be especially large in developing countries, making them the most relevant cases to study (Noy, 2009; Felbermayr and Gröschl, 2014; Berlemann and Wenzel, 2018). Studies using more traditional measures of regional or local economic activity are thus limited to (typically high-income) countries that provide this data, resulting in selection bias in the literature on local effects of natural events. To avoid such biases and to study the most relevant cases, low-income countries at the very least should not be omitted from these studies.



One of the central challenges in this dissertation is thus that adequate local socioeconomic data to examine local effects of natural disasters is typically not available for many medium- and low-income countries. In fact, even national statistics of GDP tend to come with rather large uncertainty (measurement error) in many developing countries (see e.g. Deaton and Heston, 2010; Jerven, 2010; Johnson et al., 2013). To come to better estimates of economic growth, in pioneering work Henderson et al. (2012) and Chen and Nordhaus (2011) suggest in work to make use of changes in intensity of anthropogenic nighttime light as observed from space by satellites to proxy changes in GDP. Night lights reflect the presence and activity of humans at night. They reflect the presence of buildings, production facilities, roads, and the transportation of people, goods, and services, and as such reflect human economic activity.<sup>1</sup> Night light intensity is observed from space in a globally consistent way for all countries, independent of the capacity of their national statistical offices. This allows for systematic comparison between events and between countries. In their seminal contribution, Henderson et al. (2012) convincingly show that changes in light intensity can be used to proxy changes in GDP. Moreover, the authors show in a global panel of countries that annual up- and downturns of GDP are also reflected in the night lights.

Numerous studies have followed up on this work and started using - the perhaps more obvious - spatial component of the data, which allows researchers to be more flexible in their spatial scope than allowed by official socioeconomic statistics. The papers by Michalopoulos and Papaioannou (2013, 2014) on institutions and subnational development in ethnic homelands in Africa, and Hodler and Raschky (2014b) on regional favoritism of political leaders sparked a literature that uses night lights as a means to study regional economic development (e.g. Alesina et al., 2016; Storeygard, 2016; Henderson et al., 2017a). An enormous literature that uses night light emissions as a proxy for economic activity at various spatial scales then emerged (for excellent overviews, see Donaldson and Storeygard, 2016; Gibson et al., 2020, 2021).

More importantly for the context of this dissertation, researchers have similarly started using this data to study the local economic effects of natural disasters. Early papers from the natural hazards and remote sensing literatures use high-frequency night light data to quickly identify damaged areas after earthquakes (e.g. Hashitera et al., 1999; Kohiyama et al., 2004). The impact of natural disasters on the societies that they impact can clearly be seen from space:

“... damage brought about by an earthquake include not only social stock damage, e.g. bridge damage, building collapse, etc., but also social flow damage, e.g. malfunctions of lifelines such as electricity, water, gas, communication, or transport. As city lights are figuratively used as a symbol of prosperity, a light emitter represents the existence of human activity, e.g. room lights, street lights, advertisement lights, and the

---

<sup>1</sup>This is discussed in a large body of literature. See for example Elvidge et al. (1997); Sutton and Costanza (2002); Ebener et al. (2005); Doll et al. (2006); Sutton et al. (2007); Ghosh et al. (2010).

light intensity can be assumed to be an index of level of human activity. Therefore, a region which becomes darker after an earthquake than at normal times can be considered to have suffered damage.” (Kohiyama et al., 2004)

Both direct damages to buildings and physical assets, as well as impediments to daily social and economic life can thus be reflected by darkening skies.

A young but quickly growing literature studies the local impacts of natural disasters on local economic activity, often using the night light data up to the pixel resolution (Bertinelli and Strobl, 2013; Elliott et al., 2015; Kocornik-Mina et al., 2020).<sup>2</sup> This literature was still in its infancy at the start of this PhD project (end of 2016), and I have contributed to it actively with the chapters in this dissertation, one of which has been published at the time of writing (Felbermayr et al., 2022).

The central objective of this dissertation is to gain a deeper understanding of how natural disasters affect local economic activity through the use of nighttime light. My main research question is: *"How can nighttime light help us understand how natural disasters affect local economic activity around the world?"*

As my dissertation developed, new studies were published, and new insights were acquired that found their way into my work. I also bridge literatures on highly related topics that hardly seem to communicate. Studies that are widely cited in the remote sensing literature are often ignored in economics, and the same can be said vice versa. Papers such as Gillespie et al. (2014) on the impacts of the 2004 Indian Ocean Tsunami on local light emissions in Aceh do not cite the pioneering work by Bertinelli and Strobl (2013), while e.g. Kocornik-Mina et al. (2020), one of the best published works in the field of natural disaster impacts and night lights in economics, does not cite either. While no single piece of research can incorporate all relevant work in these fields, I have combined insights from both literatures to improve our understanding of how we can approach questions of local development and adverse shocks from natural disasters. The result is a mix of methodological case study approaches, remote sensing expertise on the night light data properties and uses, and economic statistical analyses of large panels, all of which benefit from insights gained from the other fields.

The four main chapters of this dissertation contribute to the economic and remote sensing literatures on natural disasters and night lights in a number of ways. First, while this literature has gradually developed, there is a striking lack of studies that investigate how the proxy of night lights for economic activity functions in the context of natural disasters. Most of the papers in this literature rely on the assertions made by Henderson et al. (2012) and the regional development literature that sprouted from this. However, few studies examine how night lights and economic activity relate to each other in times of shock and crisis.

In Chapter 2, I do a detailed comparative case study on Hurricane Katrina that struck the coastline of Louisiana and Mississippi (U.S.) in August 2005. I combine

---

<sup>2</sup>For other relevant related studies, see Gillespie et al. (2014); Mohan and Strobl (2017); Del Valle et al. (2018); Heger and Neumayer (2019); Ishizawa et al. (2019); Miranda et al. (2020); Skoufias et al. (2020, 2021).

existing literature with primary data on population, employment, and income with night light emissions at the county level. I then examine how night light emissions and economic activity relate in the context of this catastrophic natural disaster to assess the usefulness of nighttime light emissions as a proxy for economic activity in the context of natural disasters. In doing so, I bridge a gap between the literature on the economic effects of natural disasters on the one hand, and the study of local disaster impacts through satellite observations in the remote sensing literature on the other. The economic literature generally assumes a stable relation between night light emissions and economic activity to study medium to long-run outcomes, focusing especially on variation in levels in the cross section of space and changes in ‘normal’ times. Instead, the remote sensing literature is often oriented towards identifying damaged areas and to a lesser degree recovery, without focusing on longer-run impacts of adverse events (see e.g. Hashitera et al., 1999; Kohiyama et al., 2004; Zhao et al., 2018). Neither literature combines the insights to assess what the changes in night lights reflect exactly in the context of a natural disaster. In Chapter 2, I test this and show that changes in night light intensity correlate strongly with the degree of damaged housing along the coastline of Mississippi and Louisiana. Moreover, changes in night light intensity provide a meaningful proxy of changes in economic activity over time, especially for decline and recovery of population and employment.

The central question in this literature revolves around identifying local economic impacts of various types of natural disasters, but focusing mostly on the local impacts of hurricanes in different parts of the world. Various studies examine singular disasters (e.g. Gillespie et al., 2014), whereas others focus on particular countries or regions (e.g. Bertinelli and Strobl, 2013; Elliott et al., 2015). These studies show evidence for adverse impacts of natural extremes being reflected in temporarily depressed night light intensity. However, to speak to the macro-economic literature on comparative development, institutions, and resilience to natural disasters, an effort to generalize this approach to the global scale was lacking. For this, we need a dataset that covers both the intensity of natural extremes as well as local economic activity in a global panel.

In Chapter 3, together with co-authors Thomas Steinwachs, Jasmin Gröschl, Gabriel Felbermayr, and Mark Sanders, I build on Felbermayr and Gröschl (2014) and fill this gap by building and analyzing a dataset on local weather anomalies and night light emissions that covers the entire globe. This dataset comes at a resolution of  $0.5^\circ$  (roughly  $55 \times 55$  kilometers at the equator), which roughly match the size of an average county in the United States.<sup>3</sup> We take a first step in estimating the local impacts and associated spillovers to neighboring areas in a global panel of grid cells, and provide evidence for pronounced local adverse effects of weather extremes and positive spillovers to nearby areas. These two contributions form the first part of my thesis.

---

<sup>3</sup>This dataset is available publicly and freely, and can be downloaded at: <https://www.ifo.de/en/ebdc-data/ifo-game>. See (Felbermayr et al., 2022).

An obvious drawback of the DMSP data is its annual frequency, which allows researchers to assess year-on-year changes only. This hides much of the temporal heterogeneity of the impact and recovery phase of natural disasters. Yet, the recovery phase of natural disasters is still the least understood phase of the disaster cycle (Chang, 2010). Ideally, we would be able to separate the impact phase from the recovery phase, as pioneered by Mohan and Strobl (2017). Using a new suite of monthly night light data, produced by the Visible Infrared Imaging Radiometer Suite (VIIRS) on the joint NASA/NOAA Suomi National Polar-orbiting Partnership (Suomi-NPP) satellites, the authors show pronounced adverse effects of typhoon Pam on night light intensity of the South Pacific Islands in the first months after the typhoon. However, roughly half a year after the disaster, night light intensity increases sharply compared to an unaffected control group. Given that most of the literature studying economic impacts of natural disasters – both using night lights and those using national income statistics – work with annual data, the findings by Mohan and Strobl (2017) suggest that using higher frequency data is an important way forward. Moreover, the VIIRS night light data are of much higher quality than the annual DMSP data used in chapters 2 and 3: they have a higher resolution (15 arc seconds, or roughly 500 meters), higher sensitivity (of both very dim and very bright light), and are more precise in attributing light emissions to their source on the surface (Elvidge et al., 2013, 2017). In the remote sensing literature, the use of the newer VIIRS data has therefore overtaken that of the DMSP suite. However, as the VIIRS data has only been available since early 2012, they have hardly been picked up in the economic literature (Gibson et al., 2020, 2021). This is true for natural disaster studies, but also more generally. It is also worth noting that the production of DMSP stable light images was stopped at the end of 2013. Switching to the newer VIIRS data is therefore necessary to study disasters with night light data henceforth. There is therefore a clear gap between the literatures of remote sensing and the economic study of natural disasters. In the second part of my thesis, I make two contributions to fill this gap, and explore the use of the relatively new VIIRS night light data as a proxy for economic activity in the context of natural disasters.

In Chapter 4, I follow up on the work in Chapter 3 by studying the local impacts of natural hazards using the new VIIRS data, but now focusing on earthquakes. As in Chapter 3, I work with a global panel for which I construct a dataset containing the physical intensity of earthquakes and local night light emissions, now based on the VIIRS data. I follow the approach of Chapter 3 and first compile this dataset for grid cells of half degrees. Strikingly, I find very different results from those presented in Chapter 3. No longer being limited by the resolution of climatic data, for which the highest resolution in global data is half degrees, I assess whether zooming in on the pixel level (roughly 500 meters) changes these results.<sup>4</sup> However, the estimates remain entirely statistically insignificant. Testing across a range of different model

---

<sup>4</sup>Many of the studies in this literature do their analysis at the pixel level, but for specific areas (e.g. Bertinelli and Strobl, 2013; Elliott et al., 2015; Mohan and Strobl, 2017) or for other disaster types (for example for floods, see Kocornik-Mina et al., 2020).

specifications, I find no evidence for a statistically significant relation between heavy groundshaking from earthquakes and intensity of local night light emissions. While these results cannot be directly compared to the findings of Chapters 2 and 3, as I switch to both earthquakes and a new suite of night light data, they do raise questions about the use of the newer VIIRS night light data, and night light data in general. Moreover, a recent study by Skoufias et al. (2021) similarly reports a lack of any apparent relation between light emissions as recorded in the VIIRS data and a set of windstorm and earthquake disasters in Southeast Asia. Combined, these findings call for further scrutiny of the VIIRS night light data as a proxy for local economic activity in the context of natural disasters.

In Chapter 5, I therefore take a similar approach as in Chapter 2 and study in detail the effects of a large and devastating earthquake on changes in night light emissions in the monthly data. I do so for the devastating Kumamoto earthquake that hit the southern Kyushu Island of Japan in April 2016. This earthquake was one of the costliest natural disasters in the past decade, and damaged and partly destroyed tens of thousands of houses. I collect and analyze data at the municipal level, which is the lowest level of aggregation for which we have socioeconomic data available. This study is the first to combine recorded building damage and local socioeconomic data on income and population with VIIRS night light data to test the usefulness of VIIRS night light data as a proxy for economic activity in the context of a large natural disaster. Using a comparative case study approach, similar to that in Chapter 2, I then study in detail the economic impacts of the earthquake and assess how short-run adverse impacts on population, business activity, and income are reflected in night light emissions in the VIIRS data.

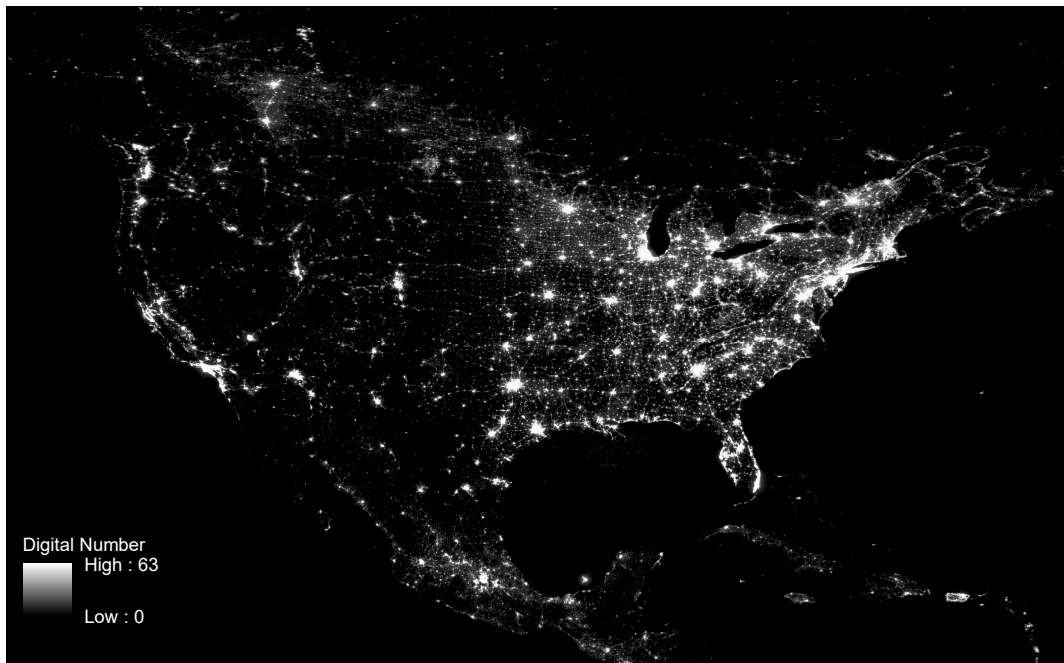
### 1.3 Data and methodology

The challenges in this dissertation are predominantly empirical in nature. Studying the economic impacts of natural disasters requires information on the intensity and spatial extent of the natural extreme events combined with information on affected communities. First, the desired spatial scale requires quantification of natural extremes at a high resolution. Mapping natural hazards over space requires collecting, compiling, and cleaning large amounts of climatic, meteorologic, and seismic data from various sources. For this, I am especially grateful to Thomas Steinwachs, my dedicated and ever-enthusiastic co-author on Chapter 3, who did a large part of the work on climatic and meteorologic data sources. Collection of seismologic data was done by myself, for which I collected and compiled data from the United States Geological Survey (USGS) Shakemaps archive (Allen et al., 2008; Worden and Wald, 2016). These data are processed in geographical information software (GIS) to inspect the data and to clean and prepare tabulated datasets that allow statistical analyses.

While mapping the intensity of natural extremes in space is conceptually easy, the same cannot be said for economic activity. In this dissertation, I use nighttime light emissions as a proxy for local economic activity. What do these night lights look

like? An image of North America by night is displayed in Figure 1.1. The distribution of light strongly resembles that of population, a feature noted decades ago when the first images from the Defense Meteorological Satellite Program Operational Line Sensor (DMSP-OLS in short) were analyzed Croft (1978). Satellites have been observing every location of the planet daily between 8:30-10:00 pm local time. Each satellite orbits the earth 14 times a day and thus ensures global coverage every 24 hours (Doll, 2008). Scientists from the Earth Observation Group of NOAA (the National Oceanic and Atmospheric Association) filter these data for solar glare and moonlight, cloud-cover, lighting features from the aurora, and ephemeral events such as forest fires. The cleaned daily data are then aggregated to produce an annual image of stable average visible light at a resolution of 30 arc seconds (roughly 1 kilometer at the equator), spanning the entire globe between 65° South and 75° North. In a continuously expanding literature, night lights have been shown to be highly correlated with presence of population, economic activity, and more generally with GDP (Elvidge et al., 1997; Doll et al., 2000, 2006; Sutton and Costanza, 2002; Sutton et al., 2007; Ghosh et al., 2010).

Figure 1.1: Night lights over North America



*Note:* own image processing of DMSP-OLS Nighttime light series, version 4, satellite F182010. Night light intensity is measured on a digital number scale, that runs from 0 to 63.

Some advantages of the data are worth mentioning. First, night lights are observed with the same measurement error across the globe, as opposed to the widely varying measurement error on national income statistics (Henderson et al., 2012; Chen and Nordhaus, 2011). Second, global coverage means that we can study all countries in the world, even when they produce no regular income statistics (such as Myanmar, or Somalia). This is relevant in the context of natural disasters, as

these countries do frequently experience extreme natural conditions and can thus be studied using night light emissions. Night lights also objectively reflect all economic activity that emits light, which includes often sizeable informal activity in developing countries that is otherwise omitted from the economic statistics (Schneider and Enste, 2000; Schneider, 2005; Ghosh et al., 2009). A digital archive is available with annual night light data for 1992-2013 (Earth Observation Group, 2016). It is this suite of data that I use in the first two main chapters of the dissertation.

There are also a number of important drawbacks to the annual DMSP data. First, the DMSP satellites have no on-board calibration of recorded light intensity, implying that comparison across time needs post-processing of the data either by using (1) intercalibration techniques (which are common in the remote sensing literature, see Elvidge et al., 2009a; Pandey et al., 2017) or (2) applying statistical techniques in regression frameworks, which is more common in the economic literature (Henderson et al., 2012; Elliott et al., 2015). I will apply both techniques, but rely mostly on the latter in this dissertation. Second, the instrument onboard of the DMSP satellite has a threshold above which no higher light intensity can be detected. This so-called saturation issue plays a role mainly in bright urban centers. In Chapter 2, I discuss this issue in detail. Third, the pixel resolution of is 30 arc seconds, or roughly 1km at the equator, but this dataset is the end product of a cleaning and filtering process of the raw data as recorded by the sensor aboard the satellite. Due to a lack of onboard memory capacity, raw observations of fine pixels are smoothed to blocks of  $5 \times 5$ , causing the footprint of the DMSP night light data to extend to  $2.7 \times 2.7$ km. Further geolocation errors of up to 3 kilometers (Tuttle et al., 2013) imply that the true ground footprint of the DMSP-OLS sensor is roughly  $5 \times 5$ km (Elvidge et al., 2013). Individual 30 arc-second pixels in the final dataproduct are therefore smoothed over 25 square kilometers, introducing (1) substantial spatial autocorrelation between nearby pixels and (2) blurring of light e.g. along urban edges and in zones between urban centers (for the latter, see Gibson, 2021). Changes in a single pixel observation are therefore in fact the smoothed average of changes in a larger area, which introduces serious measurement error into estimations of the effect of shocks on night light intensity as the dependent variable. For this reason, I do not work with pixel-level analyses with the DMSP data in this dissertation. It is important to note that spatial aggregation to larger (administrative) units reduces the magnitude of this problem substantially, as is done in e.g. Michalopoulos and Papaioannou (2013) and Hodler and Raschky (2014b). I apply a similar strategy in Chapters 2 and 3.

To address the need for data on local economic activity that allows separating the impact and recovery phase of natural disasters, I turn to a newer suite of night light data in the second half of the dissertation. Since 2012, the improved VIIRS instrument on the Suomi-NPP satellites produces monthly global stable light images that overcome many of the shortcomings of the annual DMSP data, such as saturation in urban centers and lack of on-board calibration. Moreover, because the VIIRS data have a true ground footprint of  $742 \times 742$  meters, there is no issue of overflow of city lights into their surrounding hinterland (as is the case for the DMSP data, see Elvidge et al., 2013, 2017). I use these newer data in Chapter 4

and 5 to zoom in time to separate the impact from the recovery phase.<sup>5</sup>

It is important to be clear on what night light does and does not inform us about. First, I stress that night light data is no direct substitute for true measurements of local economic activity. Wherever adequate socioeconomic data is available for a specific area of interest, this should be preferred over remotely sensed night lights. However, for many regions we have no alternative.

Second, it is important to clarify that night light does not reflect all types of economic activity equally. Most important is the omission of agricultural production, which tends to emit very little light. Much of its value added is therefore not captured by night light intensity (Keola et al., 2015). From a macro-economic point of view, we may argue that agricultural production is implicitly reflected by consumption and industry (as discussed by e.g. Henderson et al., 2012), even when agricultural production itself emits no light. Wu et al. (2013) use this approach to estimate to what extent agricultural production may be implicitly reflected by nighttime lights, and estimate the agricultural sector to account for approximately 25% of total light radiance for a global study of 169 countries for 1995-2009. However, when taking a subnational or even local approach as I do in this dissertation, this link is arguably broken. I therefore focus mostly on urban effects of natural disasters, and leave out the perspective of agricultural impacts even though they can be sizeable especially in the case of droughts.

Furthermore, the predominant application of night light data is in the context of growth of economic activity, as is the case in studies on urbanization and population (Bennett and Smith, 2017). However, for the direct impact of natural disasters, we are specifically interested in short-term decline. Henderson et al. (2012) test the extent to which night light intensity reflects both positive and negative annual fluctuations and find a symmetric effect that is closely in line with their baseline elasticity of GDP to light growth. In a study on the local economic impacts of hurricanes in Central America, Miranda et al. (2020) repeat this exercise and show similar results. Similar discussions can be found in Elliott et al. (2015) and Kocornik-Mina et al. (2020), and I follow in the footsteps of this literature. In Chapter 2, I further analyze this issue in detail in the context of Hurricane Katrina and show that changes in night light intensity provide a meaningful proxy of changes in economic activity over time in the context of large adverse shocks.

A final consideration is that of micro-level studies.<sup>6</sup> These studies provide essential insights into the well-being of individuals and performance of firms in the aftermath of disasters. The approach of this dissertation does not allow to take this micro-perspective into account. However, an important conceptual notion is that

---

<sup>5</sup>In Chapter 4 I discuss the improvements of the newer VIIRS night light data over the older DMSP data in detail. In Chapters 2 and 3 I also discuss the DMSP data itself in more detail, and particularly address issues with measurement error and saturation of the sensors. Excellent discussions on both suites of night light data can also be found in (Elvidge et al., 2017; Gibson et al., 2020, 2021).

<sup>6</sup>Examples can be found in Leiter et al. (2009); Deryugina et al. (2018); Groen et al. (2020); Noy et al. (2021); Zhou and Botzen (2021).



of mobile residents and firms, versus the immobile nature of fixed physical capital that emits light. As an area is adversely affected by a natural hazard, residents and their economic consumption and production may be displaced elsewhere. In addition, disruptions in one location may incentivize other individuals or locations to substitute for slack demand or supply, giving rise to the presence of spillover effects between affected and unaffected individuals or locations (described by e.g. Xiao, 2011; Xiao and Nilawar, 2013; Carrera et al., 2015). To the extent that night lights are emitted by infrastructure and other fixed physical capital, light represents an immobile area rather than its mobile residents. As will be discussed in Chapter 2, Deryugina et al. (2018) show how mobility of displaced residents is an important mechanism through which affected individuals cope with the shock from a natural disaster, and gives insights into how spatial relocation of individuals may offset losses in the affected area. In Chapter 3, I dive into this matter in detail and show how such spillover effects may be visible across space. I now briefly summarize the outline of the chapters.

## 1.4 Natural disasters and night lights: a case study of Hurricane Katrina

In Chapter 2, I set the stage for the methodology applied throughout this dissertation. The growing literature that studies the local effects of natural disasters by making use of changes in local night light intensity as a proxy for changes in local economic activity (Bertinelli and Strobl, 2013; Elliott et al., 2015; Heger and Neumayer, 2019; Kocornik-Mina et al., 2020) relies heavily on the general relation between night light emissions and economic activity (as established by Henderson et al., 2012; Chen and Nordhaus, 2011). However, natural disasters are events that may (temporarily) shift economies out of their equilibrium (Noy, 2009; Felbermayr and Gröschl, 2014). As a consequence, the relation between night light emissions and economic activity during and in the aftermath of a natural disasters may be different from the relation in ‘normal’ times. Strikingly, there is very little evidence in the literature about this notion, with Gillespie et al. (2014) being one of the few to assess this relationship in detail for households that were affected by the 2004 Indian Ocean tsunami.

In this chapter, I therefore study in more detail to what extent night light emissions reflect changes in economic activity in the context of a catastrophic natural disaster. The central question of this chapter is: *"How do changes in night light intensity relate to economic activity in the aftermath of a large natural disaster?"* Together with my co-author Wouter Botzen, I examine how the severe destruction and subsequent displacement of population and economic activity after Hurricane Katrina is reflected in night light emission of the affected areas in Louisiana and Mississippi. The United States provides an excellent case study as it has reliable records on economic indicators that are relevant in the context of a natural disaster. Specifically, we use data from the U.S. Census Bureau in combination with existing literature to assess the county-level economic effects of the hurricane. We then

assess how and to what extent these effects are reflected in night light emissions of the affected counties. We find that changes in light intensity reflect the pattern of housing damage caused by Katrina, as well as subsequent recovery. The worst-affected counties show the largest declines in night light intensity, while light emissions recover to pre-disaster levels in subsequent years. The relation with our indices for population, employment, and county-level income is not one-on-one, but changes in night light intensity clearly correlate positively and quite strongly with our indicators of economic activity. This chapter showcases how the methodology can be applied, and specifically points towards the value of night light emissions as a means to study impacts at the local level, where we do not have better data at hand.

## 1.5 Going global: the economic impact of weather anomalies

In Chapter 3, I extend the approach discussed in Chapter 2 to the global level, in which I study the local economic impact of the universe of weather anomalies. I do so together with Mark Sanders and my other co-authors Thomas Steinwachs, Jasmin Gröschl, and Gabriel Felbermayr from CESifo in Munich. We take this approach for a number of reasons. First, as discussed above, the economic literature on the economic consequences of natural disasters has produced conflicting results on GDP and GDP growth effects at the national level. Felbermayr and Gröschl (2014) show that at least part of this ambiguity in the literature may be caused by the use of damage records from insurance records and news. Both insurance penetration and monetary damages tend to be positively correlated with GDP per capita, which introduces endogeneity into the regression estimates. Instead, quantifying the size of natural disasters through their physical intensity, rather than through their material damages, Felbermayr and Gröschl (2014) present clear negative effects of severe natural disasters on GDP growth at the country level. However, Strobl (2011) shows that for hurricanes, this national effect does not exist for the United States either at the state or at the federal level. Yet at the county level, GDP growth rates are visibly negatively affected.

This result points towards an interesting phenomenon that we also predict from models of economic geography. Assuming that the spatial pattern of economic activity is in equilibrium prior to an adverse shock of a natural disaster, spillover effects from the shock are to be expected in the network of connected regions. Neighboring locations may (temporarily or permanently) take over activities from the affected area. While poorly studied to date, Xiao and Nilawar (2013) provide an example of such spatial dynamics for the case of Hurricane Katrina, where the counties directly adjacent to the worst-affected area experience significantly higher growth rates in aggregate income and employment than the control group of otherwise unaffected counties in Louisiana and Mississippi. We argue that the results presented by Strobl (2011) may also be explained in a similar fashion. Given

that spillovers arguably take place in geographically nearby areas, spillovers tend to take place within national borders. If such spillovers cancel out adverse effects over space within a country, the aggregated average effect may be an underestimate of the true impact on affected economies.

On top of that, the larger a country, the smaller any given event will be relative to the aggregate economy. We therefore argue that the national perspective is problematic and take the analysis of impacts of extreme weather to the local level, away from varying country sizes or incomparable administrative entities as our unit of observation. This chapter thus answers two related questions. The first focuses on the economic effects of weather extremes at the local level per se: *"How do weather extremes affect local economic activity around the world?"*. The second focuses on the potential indirect effects to neighboring areas: *"Can we observe indirect effects of local weather extremes on local economic activity in neighboring areas?"*

Answering these questions poses a number of challenges. First, quantifying the local intensity of weather anomalies in a global dataset requires a big data collection effort. Building on the efforts of Felbermayr and Gröschl (2014), and in close collaboration with Gabriel Felbermayr, Jasmin Gröschl and Thomas Steinwachs at CESifo Munich, we constructed a database that covers weather conditions in terms of temperature, precipitation, drought, and wind for the entire globe on a monthly basis for the period 1992-2013. The database is constructed at a resolution of  $0.5^\circ$ , being limited by resolution of the climatic data that ensures global coverage. Second, measuring economic activity at this resolution is challenging. No database exists that provides global coverage of local income (per capita), and efforts like the G-Econ project from Yale (Nordhaus et al., 2006) cannot capture local effects of shocks. We therefore propose to use night light emissions as a proxy for local economic activity, following successful applications in various other fields of economic growth (see e.g. Michalopoulos and Papaioannou, 2014; Hodler and Raschky, 2014b). For this chapter, I collect, clean, and prepare the annual DMSP night light data to match this to the data on weather anomalies in the global dataset of  $0.5^\circ$  grid cells. We then build up and estimate a spatial econometric model that allows for identification of local impacts and spatial spillovers to reveal the effect of local extremes on local economic activity. We show that spillovers to neighboring cells exist and typically show the mirror image of the local effect. For wind, precipitation, and cold temperatures, we find negative local effects on night light emissions, while we simultaneously identify positive spatial spillovers to neighboring cells. Splitting the panel by high and low- to middle-income levels, we find that this result is driven by cells in low- and middle-income countries. This echoes a broader result in the literature, pointing out that developing countries already face the heaviest consequences of natural extremes, while in the decades to come climate change is expected to further exacerbate the incidence of extreme weather in these regions.

## 1.6 New opportunities? Monthly night light data and earthquakes

In the second part of this dissertation, I shift the focus to a higher temporal and spatial resolution to focus on the recovery phase after natural disasters, making use of the new suite of VIIRS night light data that comes at monthly intervals. I look specifically at earthquakes, which are relatively underexamined in the literature, and moreover provide an excellent type of natural shock as they tend to be both extremely devastating and are well-studied from a geophysical point of view. While climatic and meteorologic extremes tend to affect larger areas, devastating shaking from earthquakes tends to be quite localized. Being presented with the opportunity to use higher-quality night light data that allows analysis at a high spatial resolution, I explore the effects of earthquakes in a similar fashion as Chapter 3, but now at monthly intervals and at a higher resolution. In doing so, I disentangle the impact phase from the recovery phase, which hitherto was impossible with the use of annual DMSP night light data.<sup>7</sup> From an academic point of view, the lack of economic studies using the newer VIIRS night light data is striking. The literatures on the impacts of natural disasters in economics and remote sensing hardly communicate with each other. To showcase especially the lack of cross-citing remote sensing studies from the field of economics, Gibson et al. (2020) report that as of 2020 none of the major economic publications in this field even mentioned the existence of the newer and potentially better monthly VIIRS data, which over the past years has overtaken publications on the older and discontinued DMSP data. The VIIRS data solves many issues present in the DMSP data, and moreover are available at monthly intervals since April 2012. Unsurprisingly, the newer VIIRS data is suggested to be the way forward by many remote sensing scientists (Elvidge et al., 2013, 2017; Levin et al., 2020).

In line with this notion, I use the monthly VIIRS data to study short-run local economic impacts of earthquakes. I specifically investigate the short-run impacts of earthquakes, and aim to answer the following research question: *"How do earthquakes affect local economic activity around the world?"* Only very few papers exist to which I can directly relate: Mohan and Strobl (2017) are the first to use the monthly VIIRS night light composites to study the impacts of Cyclone Pam on the island economies of the South Pacific Islands, and report sizeable reductions in night light intensity for the first months after the hurricane, followed instead by increases in light intensity later in the year. Nguyen and Noy (2020) use VIIRS night light intensity to study the effect of insurance payments on recovery of economic activity from the 2011 Canterbury earthquake sequence in New Zealand. In this chapter, I provide new evidence of the local impacts of earthquakes using a global panel fixed effects approach.

---

<sup>7</sup>An easy critique to the literature discussed in Chapters 2 and 3 is that power outages may be a (large) part of the explanation for why this literature finds temporary adverse impacts of natural disasters on night light emissions. In this Chapter I address this worry by separating the month with power outages from the months following.

The results, however, are not in line with those from Chapter 3. In a global panel of  $0.5^\circ$  grid cells, I find no statistical effect of groundshaking on local night light emissions. Since the VIIRS data is of much higher quality and has a higher spatial resolution, I zoom in to the pixel resolution of the data (roughly 500 meters) and re-do the analysis to see whether spatial aggregation makes a difference. This does not change the results: using the monthly VIIRS data, I find no relation between earthquakes and local night light emissions.

## 1.7 Shaken but not stirred? A case study of the 2016 Kumamoto earthquake

The findings using the monthly VIIRS data in Chapter 4 are troubling. As Chapter 4 progressed, was revised and further improved, new publications in the field started to cast a different light on the value of the monthly VIIRS night lights. Temporal variability in the data is large (Levin, 2017; Coesfeld et al., 2018), and attempts to control for seasonality or otherwise volatility in time series of individual locations is not always successful. In an attempt to understand to what extent the VIIRS night lights reflect sizeable disasters in Southeast Asia, Skoufias et al. (2021) show the first evidence that the monthly night light composites may not reflect large disasters such as the 2016 Aceh earthquake at all. This finding is evidently worrying and may explain why results of Chapter 4 are inconclusive.

In Chapter 5, I therefore take a similar approach as Chapter 2, and study in detail a case of a major disaster for which I can quantify materialized damages and economic impacts.<sup>8</sup> The central question to this chapter is: *"To what extent can we use monthly VIIRS night lights as a proxy for local economic activity in the aftermath of natural disasters?"* I compare affected areas to unaffected areas to take out the temporal variability in the night light data, and subsequently investigate whether the sizeable economic impacts of the disaster are reflected in changes in night light emissions in the monthly VIIRS data. I do so for one of the costliest earthquake disasters in Japan: the 2016 Kumamoto quake on the Southern island of Kyushu. The earthquake caused over 20 billion US dollars of damages, with tens of thousands of houses being damaged and partly destroyed. The worst-affected municipalities lost up to 30 percent of their annual income. I collect information on building damage, effects on municipal income, population, and business activity, and form a combined expectation on how night light emissions should react. Through a difference-in-differences framework in which I compare affected municipalities to unaffected municipalities from the rest of the island, I then estimate the treatment effect of the disaster on night light emissions.

As will become clear from this chapter, the results are very different from those presented on the case of Hurricane Katrina in Chapter 2. Neither building

---

<sup>8</sup>For this chapter, I supervised Lia Alscher with her excellent BA thesis on this topic, for which she helped with data collection and first investigation. She is co-author on the paper on which Chapter 5 is based.

damage, nor income losses and losses in business activity show any clear reflection in the monthly night light data. With the exception of a single municipality that experienced the destruction of a bridge that formed its primary connection to the region's economic hub, there is no apparent relation between changes in night light intensity and the economic impacts of the earthquake that we identify in this study. While generalizing these findings requires considerably more work, I conclude based on the results of Chapters 4 and 5 that using VIIRS night light data as a proxy for local economic activity in the context of earthquakes is not the way forward. More generally, researchers in this field should be cautious when using the VIIRS data to study the local economic impacts of natural disasters.

I now turn to the four main chapters of my dissertation. These were developed and written as independent papers. Chapter 3 has been published (see Felbermayr et al., 2022), while Chapter 4 has gone through a first iteration of revise-and-submit in a respectable field journal. At the time of writing, Chapter 1 has been submitted to a leading journal on natural hazards and their impacts, with similar plans for Chapter 5. As the papers were written as stand-alone manuscripts, some repetition of arguments that are core to my dissertation is inevitable. Finally, in Chapter 6 I summarize and reflect upon my findings, discuss limitations, and conclude with avenues for future research.

## CHAPTER 2

---

### Night lights in times of catastrophe<sup>\*</sup> A case study of Hurricane Katrina

---

#### 2.1 Introduction

Natural disasters have large social and economic consequences around the world. Impacts of natural disasters are projected to rise as a result of a combination of climate change increasing the frequency and/or severity of extreme weather events and continued urbanization in disaster-prone areas (IPCC, 2014). Studying these impacts, however, is not trivial. For many areas where natural disasters have large impacts, adequate data on local population and economic activity are not available. For this reason, there is a growing literature that studies the local effects of natural disasters by making use of changes in local night light intensity (see e.g. Bertinelli and Strobl, 2013; Gillespie et al., 2014; Elliott et al., 2015; Zhao et al., 2018; Kocornik-Mina et al., 2020). The idea is attractive as night light data is available at high levels of spatial detail, is available consistently over time for the whole globe, and does not suffer from inadequate data collection and measurement error relating to the capacity of (national) statistical offices to measure the state of the economy. Night light intensity is used in a wide range of applications, such as a proxy for economic activity (e.g. Hodler and Raschky, 2014b; Michalopoulos and Papaioannou, 2013), or as a proxy for population and GDP (Elvidge et al., 1997; Sutton and Costanza, 2002; Ebener et al., 2005; Sutton et al., 2007; Ghosh et al., 2010) or GDP growth (Chen and Nordhaus, 2011; Henderson et al., 2012). In other studies night lights are used to study urbanization (Henderson et al., 2003; Zhang and Seto, 2011; Ma et al., 2012), migration in response to flood risk (Mård et al.,

---

<sup>\*</sup>This chapter is based on a paper that is co-authored with Wouter Botzen (Schippers and Botzen, 2022). At the time of writing, the paper is under review at *Natural Hazards and Earth System Sciences* (NHESS), a leading journal on the study of natural hazards and their consequences.

2018), and population displacement due to violent conflict (Li and Li, 2014; Li et al., 2015). However, few studies examine how night lights and economic activity relate to each other in times of severe economic shocks, and there is relatively poor understanding of what changes in night light intensity reflect exactly especially when downturns in lights are considered (Bennett and Smith, 2017).

In this paper, we aim to advance our understanding on this issue by studying in detail the effects of Hurricane Katrina on county-level population, employment, and income for the most heavily affected counties in Mississippi and Louisiana, and then relating these to changes in night light intensity. Hurricane Katrina is one of the biggest hurricanes in recent history in terms of human displacement and economic impacts, located in a country with high-quality sub-national data collection. We exploit this high-quality data by relating local changes in economic activity to changes in night light. Our key goal is to assess to what extent it is possible to capture the regional economic dynamics following damages from a big natural disaster by making use of annual nighttime lights. We show that immediate damages are captured well by a reduction in night light; there is a strong and positive correlation between the degree of housing damage and reduction in light intensity at the county-level. Furthermore, we show that recovery of population, employment and income after Katrina takes years for some of the most heavily affected counties. While not related one-to-one, this dynamic is reflected in a relatively quick recovery of night light intensity in these counties. Our results show that the use of night light data for studying the immediate economic impact of a big natural disaster such as Hurricane Katrina is warranted. Using these data in areas where alternative economic statistics at the desired level of geographical aggregation are absent may therefore allow studying the effects of natural hazards on regional economies.

### 2.1.1 Related literature

Our paper connects to a number of different literatures about natural disasters, climate change, and their economic impact, as well as strands of literature that are concerned with economic development. First, our study connects with the literature on the economic consequences of floods and other natural disasters that uses night lights or economic indicators to proxy these consequences. Specifically for floods, most closely related is the work by Kocornik-Mina et al. (2020), who study the urban impact of large-scale floods in a global sample, using nighttime light intensity as a proxy for local economic activity. The authors find a short-lived negative effect of flooding in the year of the flood, suggesting that economic activity recovers to the pre-flood equilibrium rather quickly. In effect, our case study of Katrina is a part of their broader analysis, which we study in more detail and for which we examine the relationship between decline and recovery of night light and economic activity in detail. Moreover, we show that observable reductions in light intensity are possible for multiple years after the disaster. Similar to Kocornik-Mina et al. (2020), Elliott et al. (2015) find a significant but short-run effect of typhoons on economic activity in cities in coastal China, also proxied by nighttime lights, and Gillespie et al. (2014) who study the impact of the 2004 tsunami in the Indian



Ocean on affected communities in Sumatra, Indonesia.<sup>1</sup>

Second, most economic studies use more traditional indicators of economic activity to study disaster impacts instead of night lights. Strobl (2011) assesses the economic growth impact of hurricanes for US counties and reports a decline in GDP growth in the year of impact of 0.5% on average. Notably, this impact is averaged out at the state level within a year, implying that effects are local in nature. Closely related to this study is work on the economic growth impacts of hurricanes in Central America and the Caribbean (Strobl, 2012), and in a global sample (Hsiang and Jina, 2014; Berlemann and Wenzel, 2018). Heger and Neumayer (2019) study the long-term economic growth impact of the Indian Ocean tsunami of 2004 for Aceh, using both GDP and annual night lights, and find a positive effect that can be explained by the large aid inflow and coordinated reconstruction efforts. Again, no effect on economic growth is observable at the national level. We also relate to a broad literature that studies the impacts of other natural disasters on economic growth (Noy, 2009; Cavallo et al., 2013; Fomby et al., 2013; Felbermayr and Gröschl, 2014).<sup>2</sup> Many of these studies have used aggregate national GDP indicators to study the impacts of disasters which often are local events (see Felbermayr et al. (2022) (Chapter 3) and Botzen et al., 2019). We contribute to this literature by combining insights of impacts on economic activity in the affected region through conventional economic statistics with an analysis of changes in night light activity to assess the value of the latter in studying impacts of natural disasters on local economic activity.

Third, our work relates closely to studies that have examined the social and economic impacts of Hurricane Katrina, which we will discuss in detail in the next section. These studies analyze the effects of Katrina on neighborhoods in New Orleans (Logan, 2006), on the economic welfare of displaced individuals (Paxson and Rouse, 2008; Groen and Polivka, 2008; Deryugina et al., 2018; Groen et al., 2020), business survival and recovery (Jarmin and Miranda, 2009; Basker and Miranda, 2018), and its substantial wider effects on the affected regional economies (Vigdor, 2008; Hallegatte, 2008; Xiao and Nilawar, 2013). We incorporate and synthesize the existing empirical evidence in the next section, before turning to the analysis on the effects of Hurricane Katrina on night light intensity of the affected region.

Fourth, we relate to a growing literature on the use of nighttime light for empirical analysis of economic growth and development, starting with the seminal

---

<sup>1</sup>This work is part of a growing literature that studies the local economic impacts of hurricanes and other natural disasters, often making use of nighttime lights as a proxy for local economic activity. Related papers on hurricanes are Bertinelli and Strobl (2013) on the local economic impact of hurricanes in the Caribbean, Mohan and Strobl (2017) on the short-term impact of cyclone Pam in the South Pacific, Del Valle et al. (2018) on cyclone impacts in Guangdong, China, Ishizawa et al. (2019) on hurricane impacts in the Dominican Republic, and Miranda et al. (2020) on windstorm impacts in Central America more generally. Night lights have also been used to study earthquake impacts (Kohiyama et al., 2004; Fan et al., 2019; Nguyen and Noy, 2020), and a combination of disaster types globally Felbermayr et al. (2022) (Chapter 3) and for Indonesia and Southeast Asia respectively (Skoufias et al., 2020, 2021).

<sup>2</sup>For reviews of this literature, see Cavallo et al. (2011); Klomp and Valckx (2014); Botzen et al. (2019).

contributions by Henderson et al. (2012) and Chen and Nordhaus (2011) and studies with a focus on sub-national development patterns by e.g. Michalopoulos and Papaioannou (2013, 2014), Hodler and Raschky (2014b), and Henderson et al. (2017a). Ghosh et al. (2013) and Donaldson and Storeygard (2016) provide excellent overviews of the various applications of night lights in this literature. Recent tests of the relation between night lights and GDP at the local level using regional, city-level, and prefecture-level data (e.g. Hodler and Raschky, 2014b; Storeygard, 2016; Kocornik-Mina et al., 2020) find light-to-GDP elasticities corresponding to that of Henderson et al. (2012).<sup>3</sup> However, for our purposes we are interested in the relationship between night lights and economic activity in the context of a natural disaster. We contribute to this discussion by presenting new findings about the relationship between night lights and economic activity in shock times for the detailed case study of Hurricane Katrina.

Finally, and more broadly, our study connects with the literature on estimating the costs of climate change, sea level rise, and the increasing risk from hurricanes and flooding that coastal cities face in the near future (Hallegatte et al., 2013; Aerts et al., 2014; de Ruig et al., 2019). We study in this paper one case of a heavily urbanized coastal region that is exposed to the risks of hurricane landfalls. Global warming and sea level rise are expected to aggravate these risks in many parts of the world (IPCC, 2014). Understanding the consequences of hurricanes on coastal economies is therefore important for risk management and planning. Since adequate data to study local economic impacts are not available in large parts of the (developing) world, we contribute to this discussion by assessing the extent to which remotely sensed night light can be of use in this context.

## 2.2 Direct and economic consequences of Hurricane Katrina

We first summarize the immediate impact of Hurricane Katrina, and assess its economic impact on the affected region. We then make the link with visible effects of Katrina on the affected counties from space, by assessing the changes in night light intensity of the affected areas. Subsequently, we assess the recovery in light intensity over the subsequent years, before turning to a comparison between economic impacts and effects on night light intensity.

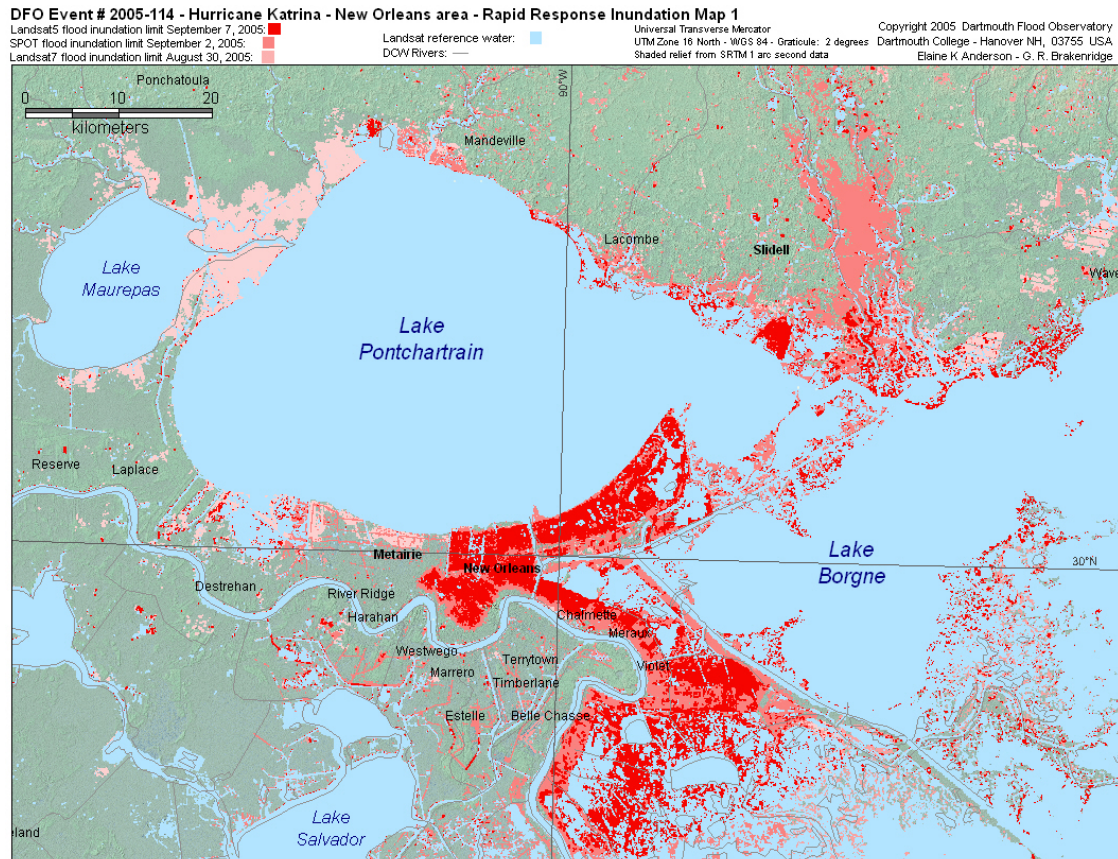
### 2.2.1 Hurricane Katrina: landfall and economic impacts

On 29 August 2005 Hurricane Katrina made landfall close to New Orleans. Although it was downgraded from a Category 5 to a strong Category 3 hurricane, it was an exceptionally large storm when it approached the shoreline with wind speeds up

---

<sup>3</sup>Note that this literature also has critical contributions that show that the lights-to-GDP elasticity is not necessarily equal across the globe and between different regions within countries. See Bickenbach et al. (2016) and Gibson et al. (2020, 2021) for a discussion.

Figure 2.1: Flood map of New Orleans area



*Note:* Image by Dartmouth Flood Observatory (2005), reprinted with permission. Color-coding indicates flooding by August 30, September 2, and September 7 respectively. Note how especially in the eastern part of the city entire neighborhoods were still inundated a week after the hurricane. Knabb et al. (2005) report that the final waters were only cleared five weeks later.

to approximately 200km per hour (Knabb et al., 2005). The storm killed almost 2,000 people and caused substantial damage of \$125 billion in total due to winds, extreme precipitation, and major storm surge flooding (National Hurricane Center, 2018). A large part of these damages occurred in New Orleans that experienced massive flooding of about 80% of its area (Pistrika and Jonkman, 2010). Several levees that were meant to protect the city of New Orleans – which is situated largely below sea level – were overtopped or breached due to the storm surge (see Figure 2.1). Major unanticipated flooding occurred especially in Orleans Parish and St. Bernard Parish. These areas were inundated for a long time as it took 43 days until all flood waters were removed from the city (Knabb et al., 2005). The impact across the City of New Orleans resembles a clear pattern of segregation that was present long before Katrina struck. The parts of the city that proved most vulnerable (see 2.1) were those that were in majority black and low-income neighborhoods, and recovery was also slowest in these areas (Logan, 2006). Other Parishes were mainly affected by wind and less severe flooding of a shorter duration, for which warnings

were issued. As a consequence, more housing units were destroyed in the inner city than in these outside Parishes (Vigdor, 2008). Some areas were never rebuilt. Wider devastating effects were recorded on the south coast of Louisiana and Mississippi, where in some counties well over half of the residential housing stock was damaged severely or completely destroyed.

Hurricane Katrina had large impacts on the population and economic activity in New Orleans that differ between its Parishes and vary over time. Especially the most severely flooded Parishes Orleans and St. Bernard experienced severe population declines in about 2 years after Katrina. The short-term population decline was even more severe. Within a week the population fell from more than 400,000 to almost zero as the city was evacuated. About half of them had returned 2 years later, and population more or less stabilized until mid-2008 (Vigdor, 2008). Deryugina et al. (2018) estimated that a third of the evacuees from New Orleans still had not returned by 2013.

Katrina reinforced a trend of an already shrinking population before Katrina. The city was experiencing continued out-migration due to lacking economic opportunities, which especially applied to the central city (Vigdor, 2008). Economic activity further deteriorated after Katrina, which is reflected in lower employment. The number of private sector jobs declined by approximately 70,000 in the New Orleans metropolitan area (Vigdor, 2008). The most severe decline in employment was observed in services-oriented sectors, which lost part of their customer base due to the population decline. Even though some positive employment growth occurred in the construction sector, this did not offset the declines of well over 10 to 20 percent in most other industries, ranging from business and trade to state and local government services (Vigdor, 2008).

The overall loss in employment indicates that economic activity declined, but this does not necessarily mean that income declined equally. Perhaps surprisingly, the decline of income is only roughly half that of population and employment, mirroring the unequal effect that the hurricane had to different income groups. The low-lying and predominantly poorer and black neighborhoods in the eastern part of New Orleans were hit hardest (Logan, 2006).<sup>4</sup> Some of these neighborhoods were still inundated a week after the hurricane (see Figure 2.1. It were the low-income and primarily African American former residents who in large numbers were unable to return to the city after the disaster (see e.g. Paxson and Rouse, 2008).<sup>5</sup> Groen and Polivka (2008) describe that evacuees suffered substantially in terms of labor market outcomes in the year after Katrina, although on average these effects diminished over time. Moreover, evacuees who did not return to New Orleans had worse labor market outcomes than those who did return in the short run, part of which is explained by individual and family characteristics also discussed by Logan (2006) and Vigdor (2008).

---

<sup>4</sup>The worst-affected neighborhoods had substantially higher numbers of renters, households below the poverty line, and unemployed compared to undamaged communities (Logan, 2006).

<sup>5</sup>This is reminiscent of the out-migration of black population after the Great Mississippi Flood in 1927 reported by Hornbeck and Naidu (2014).

The long-run development of household income of those who lived in New Orleans during Katrina has been analyzed by Deryugina et al. (2018) using tax return data. They find labor income declined shortly after Katrina by \$2,000 and by \$2,300 in 2006 compared with similar households who lived outside of New Orleans when Katrina occurred, mirroring the findings by Groen and Polivka (2008). However, this income decline was gone by 2008, when incomes of Katrina victims were \$1,300 higher (Deryugina et al., 2018). Explanations for this result are that wages in New Orleans increased in the years after Katrina to compensate for local price increases, especially for housing that was in short supply, and that evacuees moved to areas with improved job opportunities and higher wages. In addition, a tightening local labor market with relatively scarce labor supply caused further upward pressure on relative wages (Groen et al., 2020). Focusing on business establishments rather than individuals, Basker and Miranda (2018) find very low survival rates for businesses that incurred physical damage from Katrina, especially for smaller and less productive establishments. Xiao and Nilawar (2013) focus on the regional impacts of the disaster and observe positive spillover effects on income and employment growth from heavily affected counties to their surrounding counties. This pattern suggests the presence of spatial demand shifts away from the core affected area into neighboring, less affected counties. All in all, the social and economic impact of Katrina was enormous.

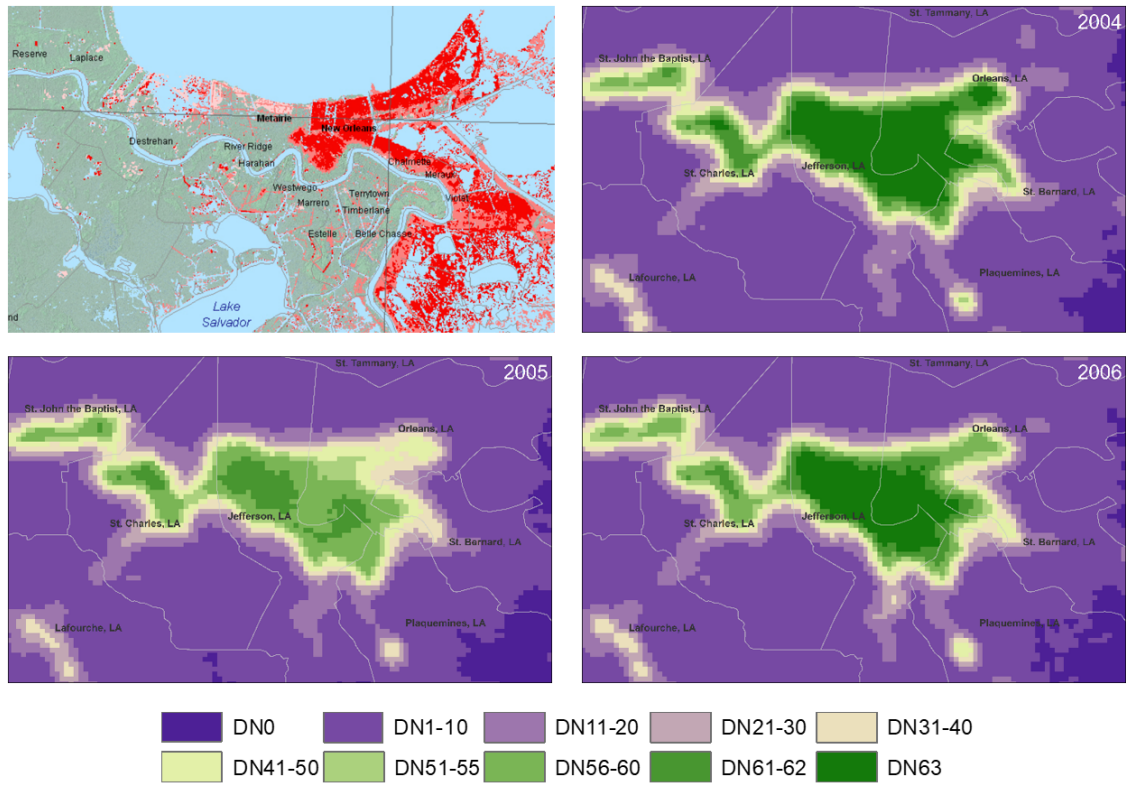
### 2.2.2 Visible impacts from space

A first analysis shows that the devastating impacts of Katrina are visible even from space. We collect the DMSP annual average stable night light composites provided by the National Oceanic and Atmospheric Association, and plot average annual night light intensity for the city of New Orleans below in Figure 2.2. The data comes at a resolution of 30 arc seconds (roughly 1km<sup>2</sup>), and intensity is given in digital numbers ranging from DN0 to DN63 reflecting dark to very bright respectively.<sup>6</sup> Even though New Orleans is a densely urbanized area where brightness of lights is as high as the satellite can record, city lights diminished dramatically in many parts of the city as a result of the flooding and wind damage caused by Katrina. In the eastern part of the city, as well as in its eastern suburbs (Chalmette) night light intensity almost halved, reflecting the severity of flooding in that part of the city. While some recovery is apparent in 2006, notable impacts especially in the eastern part of the city remain visible even in the raw light data. Next, we zoom out and assess direct impacts along the coastline of Louisiana and Mississippi. We collect the damage figures from the U.S. Department of Housing and Urban Development (2006), which reports damage assessments to occupied housing units based on FEMA's data on Individual Assistance Registrants and Small Business Administration Disaster Loan Applications. Damage to housing units is divided

---

<sup>6</sup>Note that while the night light data are provided in a resolution of 30 arc seconds, the sensor resolution is much coarser and represents a ground footprint of roughly 25 square kilometers (Elvidge et al., 2013). For this reason, we do not focus on pixel-level outcomes in this study, but rather use the total sum of light per year at the county level.

Figure 2.2: Night lights for the City of New Orleans



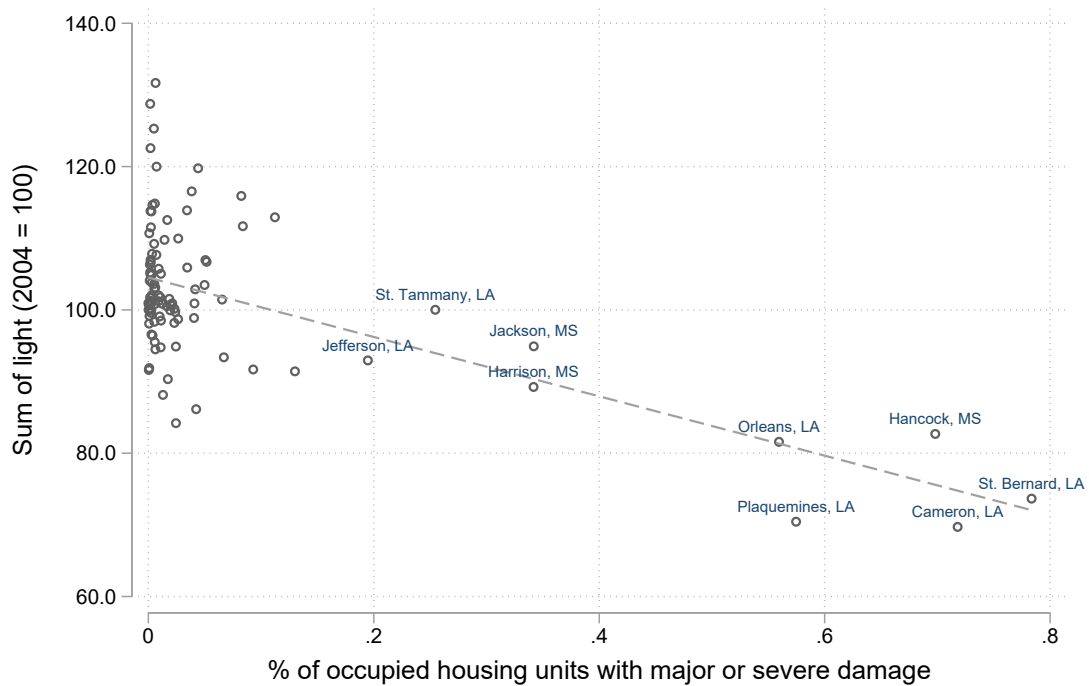
*Note:* excerpt of the Darmouth Flood Observatory flood map reported in 2.1 as reference area (top left). Night lights as observed from space by DMSP-OLS, raw uncorrected data from satellite F15. Brighter areas are indicated by green, whereas purple implies darker areas. Much of the city was at maximum brightness of DN63 in 2004 (top right) but fell below this threshold in the year 2005 (bottom left). Note how especially the eastern part of the city dims and has only partly recovered by 2006 (bottom right). As will be discussed below, it took almost a decade to recover light levels to their old intensities in these neighborhoods.

into three categories: minor damage ( $< \$5,200$ ), major damage ( $\$5,200 - \$30,000$ ), and severe damage ( $> \$30,000$ ). Housing damage of category major and severe as a percentage of total occupied housing units by county is reported below in Figure 2.4a.<sup>7</sup> Damages were extremely high at over 50% in Plaquemines Parish (LA) and Orleans Parish (LA), 70% in Hancock County (MS) and close to 80% in St. Bernard Parish (LA). Four other counties have damages close to or over 20% of their housing stock: Jackson County (MS), Harrison County (MS), and St. Tammany Parish (LA) and Jefferson Parish (LA). In our main analysis, we focus on these eight most severely affected counties. Our main interest is the extent to which we can capture the regional economic dynamics following these damages by making use of the annual nighttime lights. To do so, we start with a simple descriptive analysis of the association between housing damage and light intensity between 2004 and 2005. We first plot changes in the total sum of light by county on the same map (see Figure

<sup>7</sup>The distribution of damages by county is also reported in Figure 2.A.10 of Appendix 2.A.

2.4b below), and find a pattern that is strikingly similar to that of the housing damage map in Figure 2.4a. Indeed, an (unconditional) correlation plot reveals the same pattern, with a correlation of -0.60 that is significant at 1% (see Figure 2.3 below). The immediate impact of Hurricane Katrina is thus evidently captured quite well in the changes in night light intensity.

Figure 2.3: Correlation plot of housing damage and night light reduction in 2005

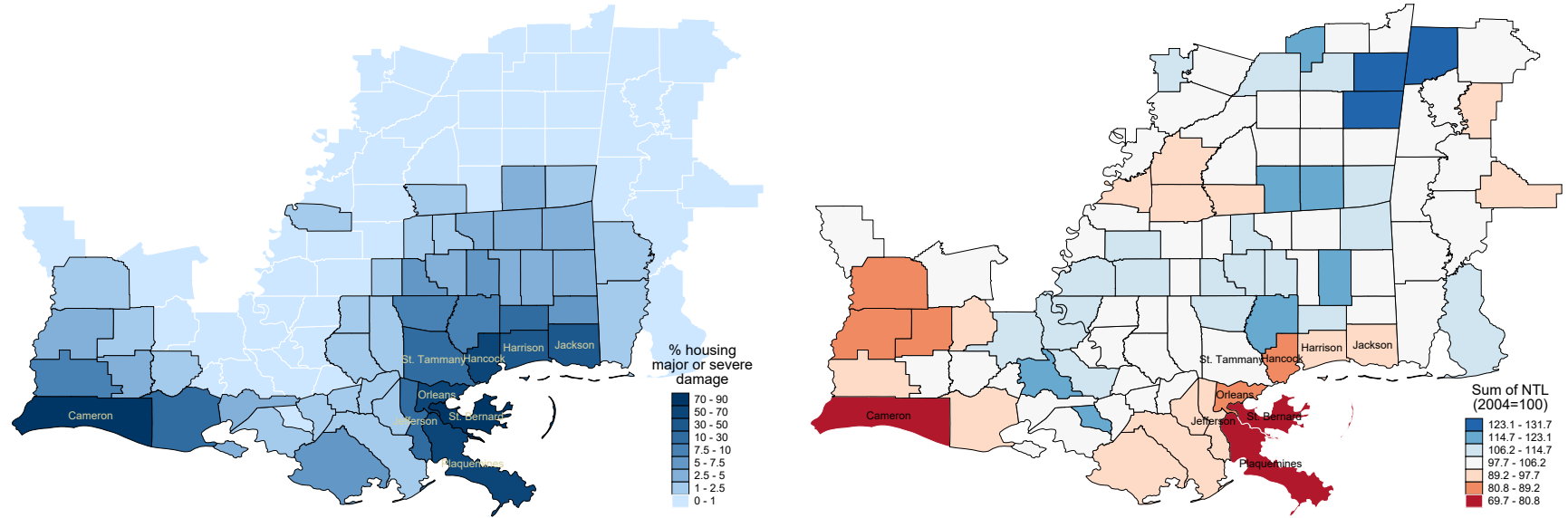


*Note:* Housing damage in 2005 for Louisiana and Mississippi from the U.S. Department of Housing and Urban Development (2006). Night time lights for 2005 are calibrated using the Elvidge et al. (2014) method, discussed in detail in Section 2.2.3 below, indexed to 2004=100. Note that the damage and associated night light reduction for Cameron Parish (Louisiana) is associated with Hurricane Rita that made landfall at the coastline of Texas in 2005. We do not focus on this particular example in the remainder of the paper, as our focus is on Hurricane Katrina.

Figure 2.4: Housing damage and night lights after Hurricane Katrina

(a) Percentage of occupied housing units with major or severe damage from Hurricane Katrina

(b) Night light intensity by county in 2005 relative to 2004 (indexed to 2004=100)



*Note:* (a) Own calculations, based on U.S. Department of Housing and Urban Development (2006) data from FEMA Individual Assistance Registrants and Small Business Administration Disaster Loan Applications. Counties with major/severe damage of 15% or more are labelled in the map. Damages for the counties in Western Louisiana (most notably Cameron, Vermillion and Calcasieu) are related to Hurricane Rita that made landfall at the coastline of Texas later in the year 2005. These are not to be related with the impact of Katrina, but show a similar pattern of damages and night light intensity reductions (see panel b). (b) Based on own calculations. Sum of night light based on calibrated light series using the Elvidge et al. (2014) method, discussed in detail in Section 2.2.3 below. Color-coding based on the standard deviation method.



### 2.2.3 Regional impacts and recovery in night lights

We further illustrate the reductions in light intensity by taking a closer look at the night light images for the affected region at large. However, two features of the night light data make comparison over space and across time challenging. The first issue is the problematic intertemporal and between-satellite measurement differences, due to varying gain settings of the sensor over time and ageing of the satellites (for a detailed discussion see Elvidge et al., 2009b, 2014). This makes it difficult to compare night light intensity within an area over time. In order to facilitate over-time comparison, we calibrate the light composites by making use of the Elvidge et al. (2014) invariant area calibration method.<sup>8</sup>

A second issue is top-coding of light intensity in the DMSP annual night light composites: an upper limit of the DMSP-OLS sensor results in saturation of recorded light intensity at DN63 (Small et al., 2005). This implies that any light intensity above this saturation threshold is not captured in the data. As a result, predominantly bright urban centers are top-coded, as is also the case for the city of New Orleans.<sup>9</sup> This is problematic for several reasons, but specifically results in problems in our case when assessing decreases in night light intensity as a result of Katrina for bright urban centers such as New Orleans: true decreases in night light intensity that take place above the saturation threshold may go undetected in these pixels.<sup>10</sup> We therefore investigate the importance of top-coding for our results.

The distribution of night light intensity values in the study region is presented in Figure 2.5. Clearly the majority of New Orleans city is top-coded, with only its edges falling below the saturation threshold prior to Katrina.<sup>11</sup> Note how similar

---

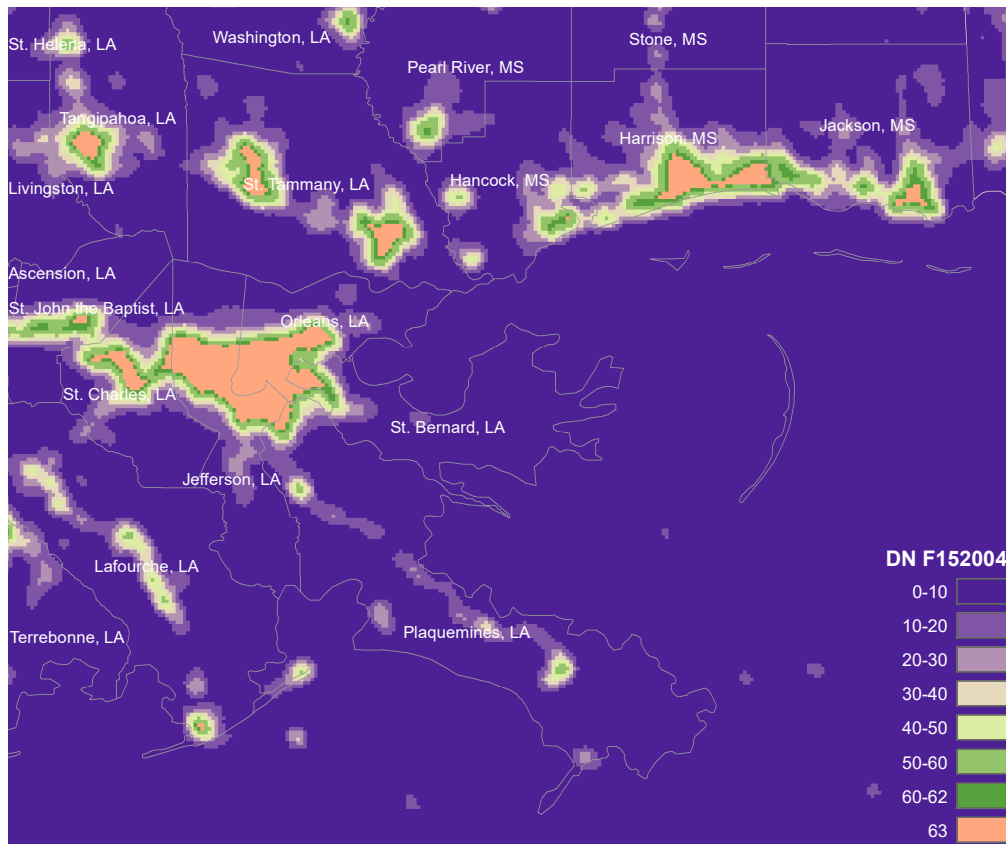
<sup>8</sup>The calibration exercise is based on a reference image for an area where true light intensity remains approximately unchanged throughout the study period, which then allows separating true changes in light intensity from pure satellite measurement error. In Appendix 2.B, we discuss this calibration in detail and also propose alternative methods of adjusting the data: notably an alternative calibration by Zhang et al. (2016) and an econometric fixed effects approach more customary in economics (Henderson et al., 2012). Out of these options, the calibration by Elvidge et al. (2014) performs best for our purposes. In all main results that follow, we therefore use calibrated night light images following the methodology of Elvidge et al. (2014). We test our results for robustness with the alternative calibration proposed by Zhang et al. (2016) and by making use of an econometric panel fixed-effects correction proposed by Henderson et al. (2012) in Appendix 2.A. Our main results are very robust to these alternative correction methods.

<sup>9</sup>Bluhm and Krause (2018) propose a method to impute true light values for top-coded pixels by assuming a Pareto distribution on top lights. Although this approach may be of great value to the general literature that studies economic growth and the spatial distribution of economic activity, we cannot make use of any imputed measures as we study a shock.

<sup>10</sup>The problem is much less severe in low and middle-income countries. There the share of top-coded pixels is close to zero. See Felbermayr et al. (2022) (Chapter 3) and Kocornik-Mina et al. (2020) for a discussion.

<sup>11</sup>There is a third issue with the DMSP data that revolves around overflow, or otherwise referred to as blooming (Bennett and Smith, 2017; Gibson et al., 2020, 2021). Overflow, related to geolocation errors in the DMSP data, results in light intensity being recorded slightly away from its point source, such that urban areas have a larger extent of lit pixels than actual built-up land. This is an issue particularly in studies that use DMSP night light data at high spatial detail, up to the pixel level of the data (e.g. Bertinelli and Strobl, 2013; Kocornik-Mina et al., 2020). Moreover, local economic activity arguably does not reside on square kilometers, but rather in

Figure 2.5: Night light intensity in the study region prior to Katrina, 2004



*Note:* based on own calculations using satellite F15, corrected with the Elvidge et al. (2014) calibration method. Top-coded pixels are indicated in orange. County names in white.

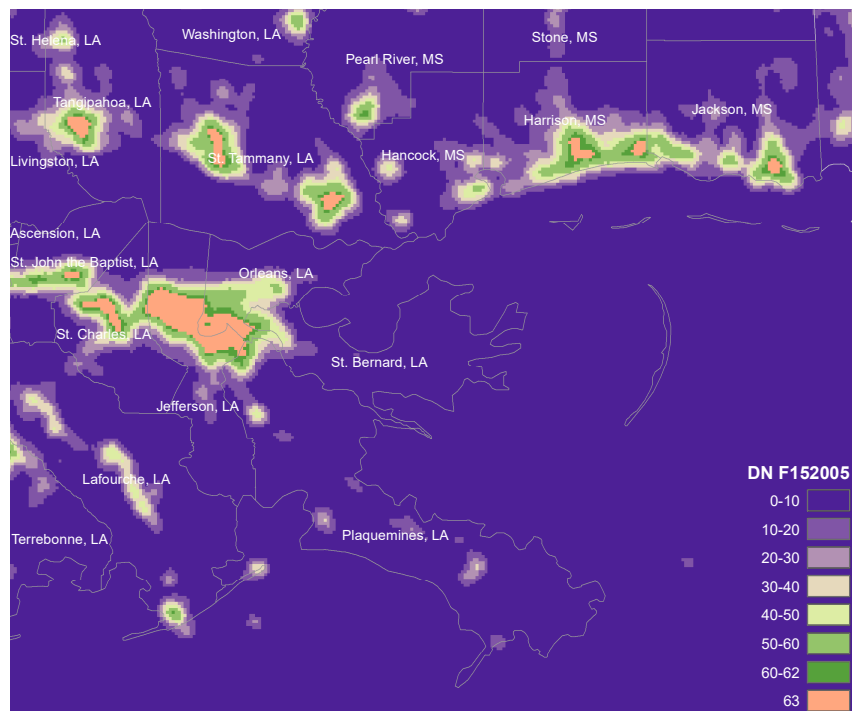
top-coding is present along the urbanized coastlines of Harrison and Jackson County. Of course, this issue is not unique to our particular study area, but is true more generally for high-income countries like the United States. Taking the substantial top-coding in the study area as given, we turn to assessing changes in light intensity after Katrina. Two panels of images now follow to compare the changes over time in 2005 and 2006.

---

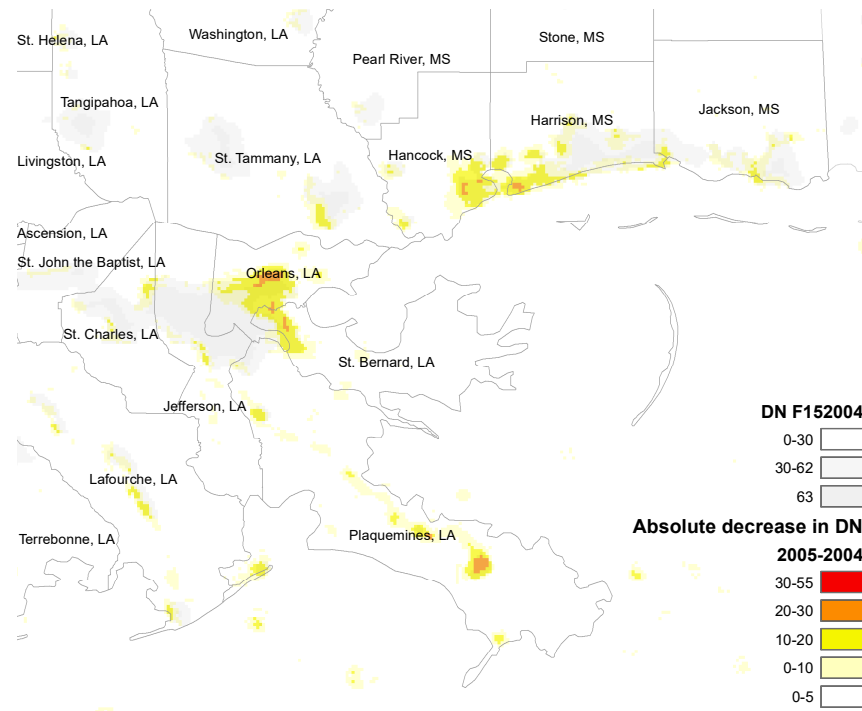
larger economic and administrative (spatial) units. In order to be able to draw a parallel between measured economic activity and night lights, we aggregate night light intensity to the sum of light at the county level. Therefore, the issue of blooming and geolocation errors is of limited concern in our context.

Figure 2.6: Changes in night light intensity in the study region (2005)

(a) Night light intensity in the study region, year of Katrina 2005



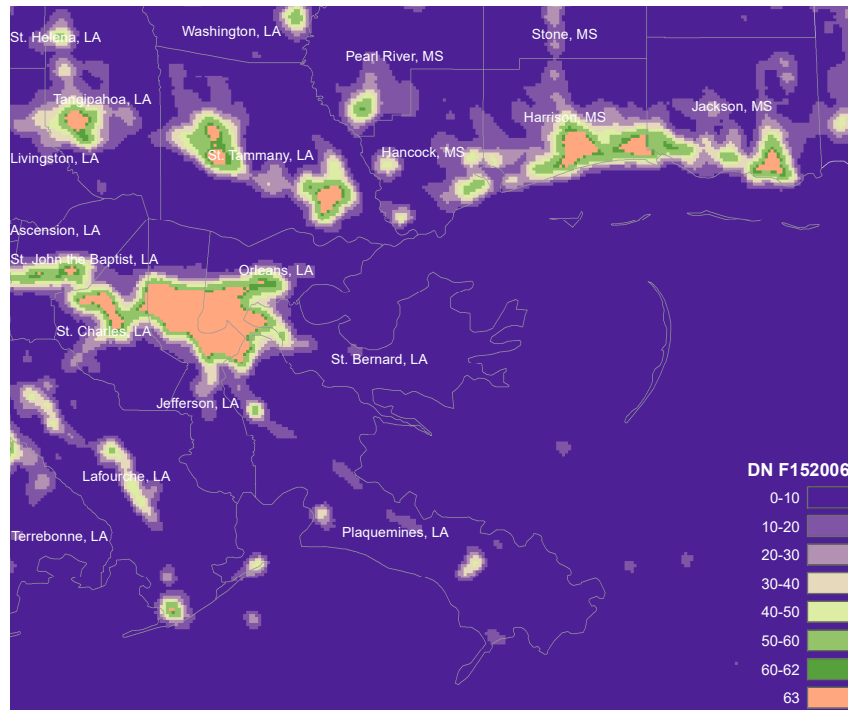
(b) Absolute change in night light intensity from 2004 to 2005



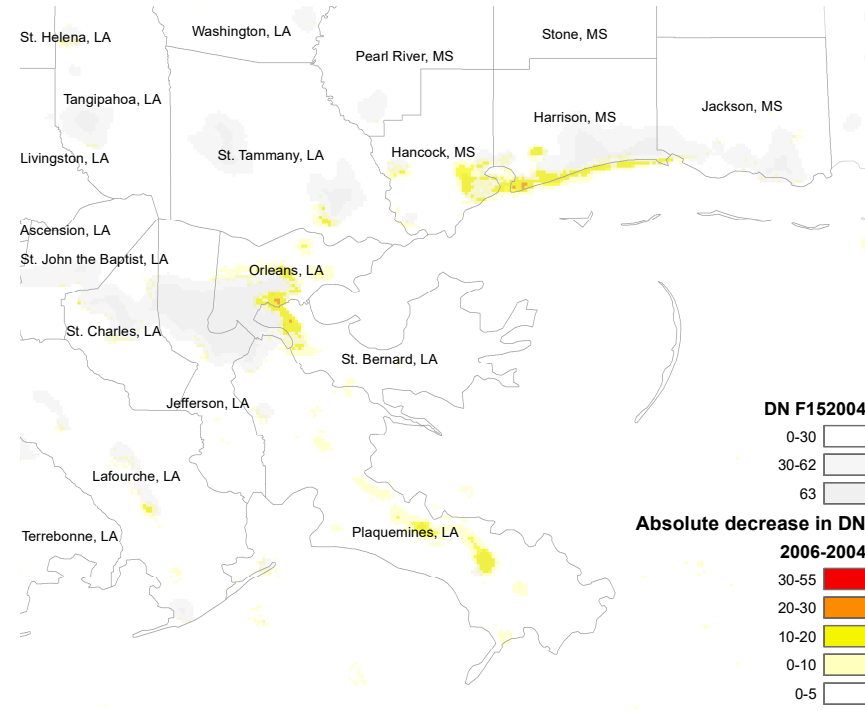
*Note:* (a) based on own calculations using satellite F15, corrected with the Elvidge et al. (2014) calibration method. Top-coded pixels are indicated in orange. (b) based on own calculations using satellite F15, corrected with the Elvidge et al. (2014) calibration method. Absolute difference of pixel DN value between 2004 and 2005.

Figure 2.7: Changes in night light intensity in the study region (2006)

(a) Night light intensity in the study region, year of Katrina 2006



(b) Absolute change in night light intensity from 2004 to 2006



*Note:* (a) based on own calculations using satellite F15, corrected with the Elvidge et al. (2014) calibration method. Top-coded pixels are indicated in orange. (b) based on own calculations using satellite F15, corrected with the Elvidge et al. (2014) calibration method. Absolute difference of pixel DN value between 2004 and 2006.

First, Figure 2.6a gives the distribution of night light intensity across the study region for 2005. Figure 2.6b then plots absolute decrease in night light intensity (the digital number for 2004 subtracted from 2005 for each pixel). Figures 2.7a and 2.7b do the same, but then for 2006 (see below). Focusing first on New Orleans, the immediate effects of Katrina become apparent in the eastern part of the city and in the suburbs of Chalmette, as we saw before even in the raw data in Figure 2.2. Reduction in light intensity is most severe in the northeastern tip of the city, with light reductions of 30 up to 50 points, translating in reductions that amount to well over 50 percent. Moreover, notable reductions occur in previously top-coded parts of the city. Here too reductions run well over 10 percentage points, even though the true decrease in light intensity is likely larger. Note that in the west of the city hardly any change is detected, which is very much in line with the geographical spread of flooding (see Figure 2.1).

Two other main areas that suffer heavy light reduction can be clearly identified from these figures. First, Plaquemines Parish has a long inhabited strip along the Mississippi River ending at the town of Venice, Louisiana, which suffered enormous damages from Hurricane Katrina. Light reductions are evident along the entire river, with the highest reduction located in Venice. Note that no top-coding was present in this area in 2004. The second area is Bay St. Louis, Mississippi, and the coastline along Harrison County. Major light reductions are visible in all urban zones around the bay, notably in Waveland, Diamondhead, and Pass Christian. Reductions in the order of 10-20 points are also visible further along the coastline in Long Beach and Gulfport. Again, no top-coding was present here in 2004.<sup>12</sup>

Next we turn to the year 2006, depicted in Figure 2.7a and 2.7b. A first observation is that the worst reductions in night light have largely disappeared from the map: reductions of over 20 points – compared to 2004 – are rare in 2006. However, the eastern part of New Orleans remains depressed, notably also along the Mississippi river near Chalmette. While a substantial part of the city returns to being top-coded, this is clearly not the case for the north-eastern neighborhoods of the city. This is true even for a large strip that was top-coded in 2004. In a similar vein, the riverbed of Mississippi still shows depressed night light values all the way to the town of Venice. There are signs of recovery around the St. Louis Bay, but light intensity is still 10 to 20 points lower in many parts of the metropolitan area around the bay. Top-coding thus mainly affects the changes that we observe in New Orleans city, thereby affecting the observed changes in light intensity for the Parishes Orleans, St. Bernard, and Plaquemines – which, as will be discussed below, are the counties for which we observe permanent reductions in population and employment. This means that we have to interpret our comparison of changes in night light intensity to changes in economic indicators for these areas with care.

---

<sup>12</sup>These reductions match closely with the damage maps from FEMA for this area, described in detail in Basker and Miranda (2018). Extensive damage along the coastline is reflected by large drops in light intensity, while milder reductions in light intensity are matched by mild damage from the FEMA maps. As with New Orleans city, we find close correspondence between flood zones, property damage, and night light reduction. For a detailed discussion on the FEMA damage maps, see Jarmin and Miranda (2009)

It is likely that the observed reductions in night lights are an underestimate of the true effect on night light intensity. However, even with this caveat in mind, the overall patterns of direct impact and recovery in terms of night light changes are closely in line with our expectations, based on the geographical spread of flooding and on the impact numbers that we know from previous studies.

This is not the end of the story. Our analyses in the subsequent section focus on the following two issues: (1) the extent to which this reduction in night light intensity corresponds with reductions in economic activity, as captured through county level income, employment, population, and GDP, and (2) the extent to which recovery of night light intensity over time corresponds to recovery in these economic indicators. Since the impacts are clearly largest in the defined core group of 8 coastal counties, we collect for these counties annual data on their economic indicators and assess the longer-run impacts of Katrina on their economies. We then compare these developments to changes in night light intensity over time.

## 2.3 Relating night light changes to economic indicators

The economic impact of Hurricane Katrina on the county economies along the coast becomes evident from the graphs in Figure 2.8 (see below), which plot population, aggregate employment and income, real GDP, and night light intensity by county for the years 2000-2018.<sup>13</sup> To allow for a comparison of impacts with recovery over time, we standardize the series of each county to their respective levels in 2004 (2004=1). The graphs are sorted by normalized housing damage, expressed as percentage of total occupied housing units with major or severe damage. Some notes are warranted before discussing the graphs. First, the economic data collected from the Bureau of Economic Analysis are aggregates for calendar years. Hurricane Katrina made landfall in August of 2005, and is hence only captured in the final quarter of 2005. The majority of losses from the hurricane are therefore captured in the records for 2006. We stress that this includes any short-term recovery as well, implying that immediate losses in the first weeks after the hurricane may be partly offset by recovery in subsequent months. Second, a similar notion is important when assessing loss in night light intensity for the counties for 2005 with respect to 2004. As the DMSP night light composites are annual averages, only the months September-December are affected by Katrina's impact – i.e. only one-third of the year. This implies that reduction in night light in the months directly after the impact may be considerably larger than the currently presented figures. Third, population figures come from the Census Bureau midyear population estimates. As these are assessed midyear, the population effect of Katrina is only captured in 2006. All reported figures therefore represent a lower bound of the true short-run

---

<sup>13</sup>The DMSP night light series run up to 2012 only, following the calibration results of Elvidge et al. (2014). Note that the annual stable night light composites from the DMSP-OLS instrument were discontinued after 2013.

effects of Katrina.

We now turn to assessing the impact of Katrina on the worst-affected counties, and start with some general observations. The general patterns are clear and reassuring: reductions in night light intensity are clearly strongest for the most affected counties of St. Bernard, Hancock, Plaquemines, and Orleans, as was also shown in Figures 2.6a-2.7b. All counties experience major or severe damage to housing units of over 50 percent, which is associated with reductions in light intensity of 20 to 30 percent. These reductions are clearly in line with large losses in population. In contrast, the bottom four counties in Figure 2.8 experience smaller housing damage of 20 to 35 percent, and experience much smaller population losses. Harrison, Jackson, St. Tammany, and Jefferson experience smaller economic impacts in comparison to the top four counties in Figure 2.8, and in line with these patterns reduction in night light intensity is smaller at 3 to 13 percent.

### 2.3.1 Population changes and night lights

To facilitate the discussion, we separate the counties into three groups: those with (1) a permanent reduction in population, (2) a temporary reduction in population, and (3) no substantial change. The first group consists of the three most-affected counties in Louisiana – St. Bernard, Plaquemines, and Orleans Parish – plus the less-affected county of Jefferson. The former three experience population losses in 2006 of 24%, 53%, and 76% respectively. This population loss is recovered in part, but population returns to only 80% of pre-Katrina levels by 2018 for Plaquemines and Orleans, and 65% in the case of St. Bernard. In tandem with this development, night light intensity drops between 20 to 30 percent in 2005 and remains depressed below pre-Katrina levels thereafter. However, the decline in night light intensity does not appear to be strictly proportional to population loss; while night light intensity does not decline further than 30 percent, population losses for St. Bernard and Orleans are well over two-fold of their loss in light.

Strikingly, the recovery paths of night light compared to population for these two counties do show remarkable similarity. Growth rates are comparable in the first years following Katrina, which leads St. Bernard to recover its night light intensity to pre-Katrina levels by 2008, and leveling off after that, even though St. Bernard is still 60 and 40 percent below its pre-Katrina population level in 2008 and 2012 respectively. Instead, night light intensity remains permanently depressed at roughly 10 percent below pre-Katrina levels in Orleans. The third county, Plaquemines, experiences an immediate and also permanent reduction of roughly 20% of its population. Night light intensity declines by roughly 30 percent, but shows fast growth in 2006 and 2007. After that, light levels remain permanently depressed slightly below pre-Katrina levels. The fourth county with a permanent reduction in population – albeit less severe at around 7% - is Jefferson, Louisiana. Night light intensity falls by roughly 5% in 2005, and remains permanently depressed until the end of the series in 2012.

The second group consists of counties that experience smaller and only temporary reductions in population: Hancock, Harrison, and Jackson. Population reduction is

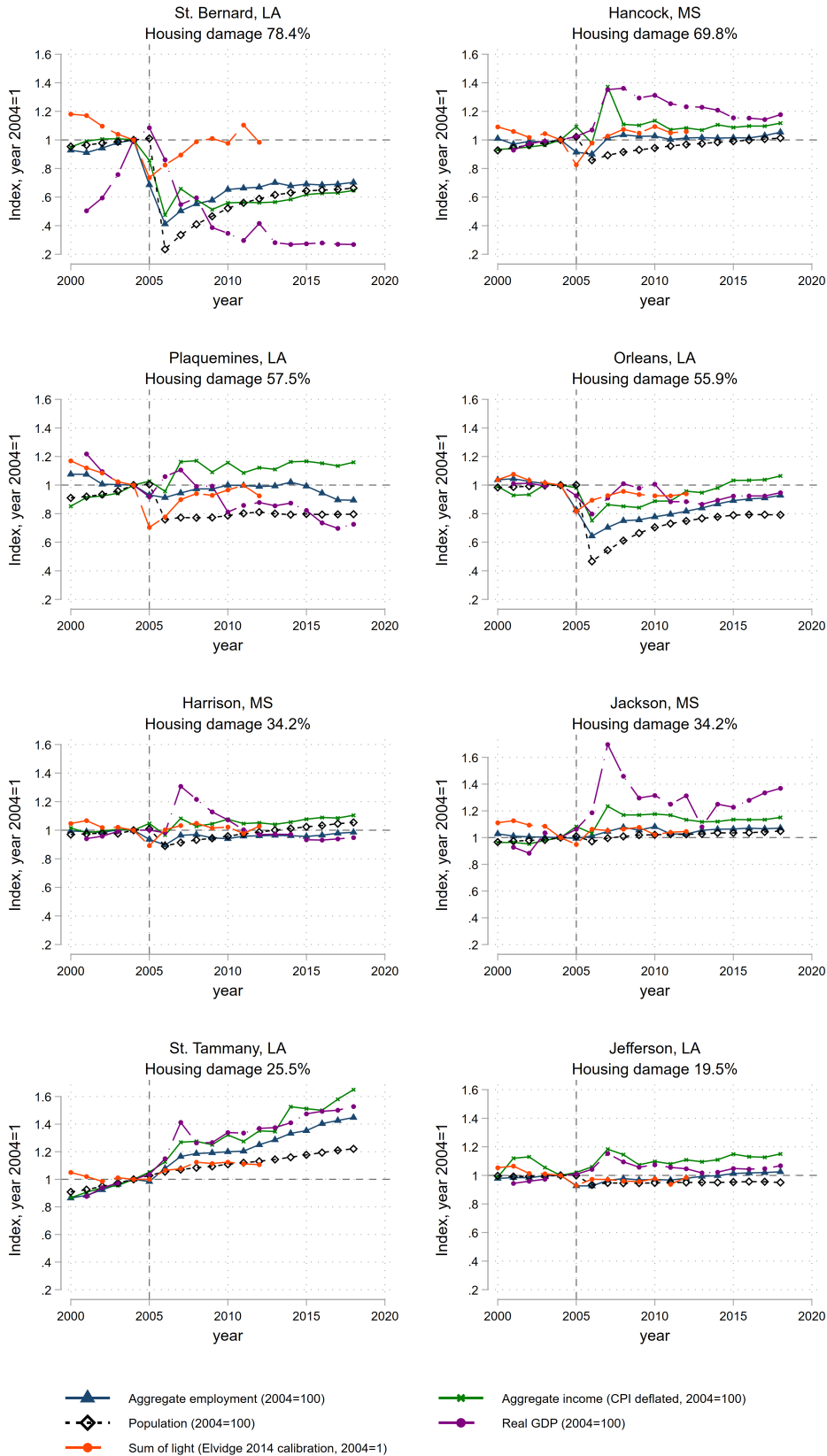
14%, 11%, and 3% matched by a reduction in night light intensity of 20%, 13%, and 8% respectively. For all three counties, night light intensity recovers to or overshoots pre-Katrina levels by the next year, and remains above pre-Katrina levels in subsequent years.

The third classification applies only to St. Tammany, which experiences no population loss at all, even though 25 percent of its occupied housing units had major or severe damage. Population was steadily growing prior to Katrina hit in 2005 at an average rate of 2.5% between 2000-2005, compared to 2.7% in 2006. However, the growth rate does decline substantially in the years after. In line with a lack of any apparent immediate population effect, there is no change in light intensity with respect to 2004. Population growth seems unrelated to light growth before Katrina, while the three years after Katrina are associated with both positive population and light growth. However, while population continues to grow at roughly 1% per year after 2008, night light intensity remains roughly constant at roughly 12 percent above pre-Katrina levels.

As a preliminary conclusion, the effects of Katrina on counties' night light intensity correspond with their respective changes in population, although more so qualitatively than quantitatively. Reductions in light intensity are roughly a third at maximum, whereas population losses were over twofold in some counties. However, recovery patterns in population numbers closely match those of recovery in light intensity.



Figure 2.8: Night light and economic indicators following Katrina for the 8 most-affected counties



*Note:* Based on own calculations. All variables are indexed with 2004=1. Aggregate employment, income, population, and real GDP data come from the U.S. Bureau of Economic Analysis (2020). Night lights are calibrated using the Elvidge et al. (2014) method.

### 2.3.2 Other indicators: employment, income, and GDP

We now extend the discussion to include effects of Katrina on economic activity in the counties, reflected by aggregate employment, income, and GDP. A first observation is that in the first group of counties the loss in employment is considerably smaller than that of total population. Nonetheless, employment losses overall are roughly proportional to losses in total population, and are therefore also closely related to changes in night light intensity.<sup>14</sup> With the exception of all counties experiencing a spike in income in 2007, related to the massive federal recovery assistance funds disbursed in that year (Xiao and Nilawar, 2013), aggregate income changes in relation to Katrina are more heterogeneous. For St. Bernard and Orleans Parish, income changes follow declines in population and employment closely. The six other counties instead experience an increase of aggregate income of up to 10% relative to 2004. In both Hancock and Plaquemines, aggregate income remains 10 to 15 percent above 2004-levels for the entire duration of the study period, even though both counties lost a substantial proportion of their population. In both cases, the increase in income – combined with a substantial growth in GDP in Hancock – may partly explain fast recovery of total night light intensity. The bottom four counties in Figure 2.8 show a consistent pattern: no signs of very substantial impact in either of the economic indicators, and corresponding patterns in aggregate income and GDP, with again a shared spike in 2007. Aggregate income and GDP show a strong correlation for Hancock and Orleans as well, but in St. Bernard and Plaquemines GDP is a lot more variable. Both counties show a notable decline in GDP after 2008, which is not corresponding with similar changes in either employment or aggregate income.

In summary, the impact of Katrina on the counties' economies has clearly not been uniform. While the size of economic effects is related to the extent of damages, there is no stable and unambiguous relation between damages and economic changes in terms of population and income. Some counties experienced lasting population losses, where others – most notably Hancock – recovered fairly quickly and experienced (temporary) booms in income and GDP. In turn, night light intensity does not do a perfect job at capturing these dynamics, but performs as expected in qualitative terms: the heaviest-hit counties show the largest declines in night light intensity, and light intensity recovers to pre-disaster levels in the subsequent years. However, recovery of night light intensity towards pre-Katrina levels is much faster than for population, employment, and income in the heaviest hit counties of St. Bernard and Orleans. Growth in income and employment after Katrina is positively correlated with night light intensity as well. The relation with GDP seems less evident across the 8 counties, compared to the other indicators. However, overall the qualitative patterns are promising: night light intensity can inform us about regional economic downturns in this case study.

---

<sup>14</sup>While employment is proportional to total population, displacement of population may affect the working population differently than the non-working population. As discussed in the effects of Katrina in New Orleans, we know that the low-income segment of New Orleans' population was disproportionately displaced (Logan, 2006).

### 2.3.3 Correlations between night lights and economic indicators

To further structure the discussion, we statistically assess the correlation between the change in total sum of light and the change in economic indicators for the eight affected counties. We distinguish two periods: the period before Katrina (2000-2004), and the period starting in the year of Katrina (2005-2012). Since the population record for 2005 is based on the midyear estimate in July, we limit the population to 2006-2012 for the second period for this indicator only.<sup>15</sup> Results are reported in Figures 2.9a and 2.9b.

The results are rather striking. In the period before Katrina, the correlations are weak and predominantly negative (see Figure 2.9a). The correlation with population is strongest – and negative – driven by light levels that are higher in the period prior to 2004 in all 8 counties. This pattern is visible in all of the counties, while population was either growing or stagnant in these years. This is not the case for employment, which shows close to no correlation with light intensity before Katrina. For both income and GDP, the correlation is again negative but weaker than with population. Note that this likely has to do with top-coding in the night light data, making light intensity unresponsive to economic changes prior to the negative shock caused by Katrina. For GDP specifically the negative correlation is purely driven by St. Bernard Parish – when excluding St. Bernard, the correlation is weak and positive at 0.22.

In stark contrast, there is a clear positive and substantially stronger correlation in the years after Katrina for all 4 indicators (see Figure 2.9b). Unconditional pairwise correlations of 0.65 and 0.54 indicate that the change in night light as a result of Katrina is most closely related to population and employment respectively. The scatterplots clearly reflect that reductions in night light underestimate the reductions in population and employment in some of the counties, as discussed in the previous section. Again, this likely relates to the top-coding issue. It may also be partly explained by the timing of the hurricane in the last part of the calendar year, which implies that the annual light intensity observations are dominated by the 8 months preceding Katrina. Still, the correlation between the change in light intensity and population is strong, while it is moderate for employment.

While similarly positive, the correlation between indexed light intensity and income and GDP is weaker at 0.38. The lower correlation can be explained by developments in the counties Hancock, Harrison, Jackson, St. Tammany, and Jefferson, all of which had income and GDP levels (far) exceeding pre-Katrina levels. Instead, growth in light intensity was much lower for these counties. A notable spike that is visible in all counties is the year 2007, in which relief transfers boost both income and GDP. There appears to be no correlation between these transfers and light intensity for this year, further lowering the correlation with income and GDP. In fact, the correlation between the change in income and GDP between 2006 and

---

<sup>15</sup>Including the 2005 data for population dramatically reduces the correlation from 0.65 to 0.34, purely as a result of the 2005 population figure being unresponsive to the Katrina shock in 2005 by construction – population estimates are midyear and thus precede the landfall of the hurricane.

2007 and the total sum of light is 0.27 and -0.58 respectively – i.e. for GDP there is even a strongly negative correlation with light intensity for this particular year.

The main findings are then twofold: first, the correlation between night light intensity and the four considered economic indicators is much stronger after Hurricane Katrina struck than before.<sup>16</sup> The positive and – in the case of population and employment – strong correlations with economic activity show that changes in night light intensity can be used successfully to capture local effects on economic activity of a large shock such as Hurricane Katrina.

Second, and within the limits of our study, our results suggest that a change in light intensity mostly reflects changes in resident population and the total number of employed people within the affected area, and is less so but positively related to aggregate income and real GDP. We test robustness of these findings to the use of the alternative calibration method by Zhang et al. (2016), as well as to the fixed-effects corrected light data. Results are reported in Appendix 2.A. For the Zhang et al. (2016) calibrated data all correlations for the period 2005-2012 are lower than for the baseline results using the Elvidge et al. (2014) calibration. This can be explained by the anomalous year-corrections in 2010 and 2012, discussed in detail in Appendix 2.B. When excluding 2010-2012, we find similar correlations for the two calibration methods (results available upon request).

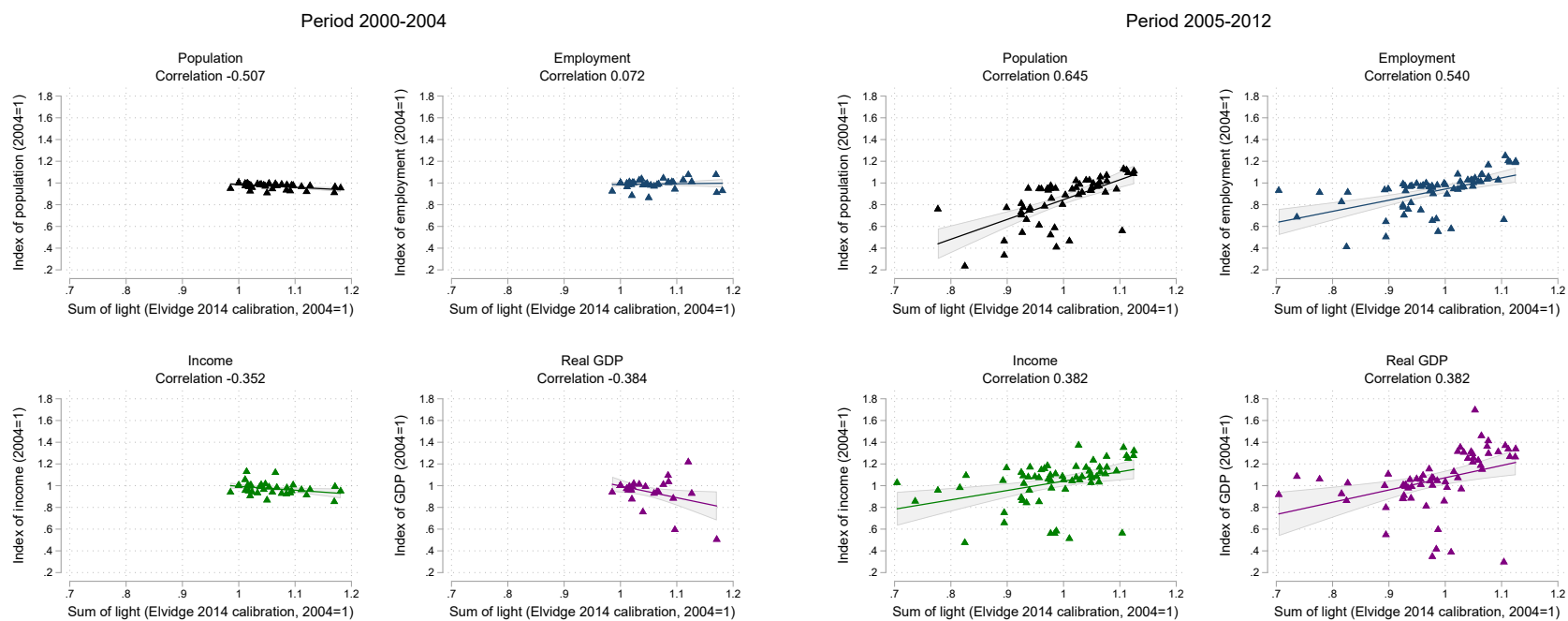
An important remark is that the econometric fixed-effects approach overall yields comparable results (see Appendix 2.B for a discussion on the methodology), but correlations between indexed light and income and real GDP are considerably higher at 0.57 and 0.68 respectively. The correlation with employment increases to 0.75. Moreover, the difference between the correlation coefficients for employment (0.75) and real GDP (0.68) become considerably smaller, signalling that the difference in correlation between light intensity and GDP may not be as large as we conclude on basis of the Elvidge et al. (2014) method. This finding is important with respect to the approaches applied in the other chapters of this dissertation. After taking out common time variation using the fixed effects approach, as I do in these chapters, correlations between light intensity and employment, income, and real GDP become substantially stronger than they are when using the calibrated night light data using the Elvidge et al. (2014) approach.

---

<sup>16</sup>Within the scope of our paper, we cannot answer why the relation between night light and economic activity is rather weak in equilibrium times before the disaster shock, and what can explain the negative correlation with population and income we observe prior to the shock. However, top-coding in the night light data is arguably one important factor. This discussion speaks to a broader literature that uses night light intensity in equilibrium growth regimes to proxy GDP or economic activity more broadly at the subnational level (e.g. Michalopoulos and Papaioannou, 2013; Hodler and Raschky, 2014b; Storeygard, 2016). Part of the explanation may be that top-coding in much of the affected areas prior to the landfall of Katrina obscures otherwise meaningful relations between night lights and income and GDP. Future research can aim to answer these questions by focusing on an event that affected urban areas with a lower degree of top-coding. Alternatively, the results presented in this paper may be indicative of a stronger relation between changes in night light intensity and economic indicators in shock times versus equilibrium times in a high-income country like the United States.

Figure 2.9: Correlations between changes in economic indicators and night lights

(a) Indexed economic indicators and total sum of light by the 8 affected counties before Katrina      (b) Indexed economic indicators and total sum of light by the 8 affected counties after Katrina



Note: (a) based on own calculations. (b) based on own calculations. Population data is for 2006-2012 only.

## 2.4 Discussion

An emerging literature has used night lights to study the local impacts of natural disasters and used changes in night lights as an indicator primarily of local economic activity. Night light analysis of impacts of natural hazards seems especially useful in areas that lack local data of population and economic activity. But often it remains an open question what observed night light changes actually represent, especially in the case of downturns (Bennett and Smith, 2017). In our study we examined changes in night lights following the impacts of Katrina on New Orleans and the coastline of Louisiana and Mississippi. This is a relevant case study for analyzing what changes in night lights represent since for New Orleans both night light data and local population and economic statistics exist. Moreover, a variety of studies examined the direct and indirect socioeconomic impacts of Katrina, which allows for placing our insights into a broader picture of the various effects of the hurricane. The following main lessons emerge from our study.

The immediate effects observed in night lights reflect well the heterogenous severity of direct impacts of the hurricane in the different geographical areas. Flooding and direct damage data indicate that the most severely hit parishes are Orleans and St. Bernard, for which also severe drops in night lights can be observed shortly after Hurricane Katrina. This observation suggests that night lights can be used as an indicator for the short-term severity of a natural disaster and reveal worst hit areas, echoing findings reported by Gillespie et al. (2014) on the impacts of the 2004 Indian Ocean Tsunami in Sumatra.

Moreover, short run changes in night lights reflect observed changes in the population over time. However, there are some limitations to the night light approach. Population losses in some counties, such as Orleans were much more severe than night lights suggest. This may be explained by the fact that Katrina made landfall in August, thus making up only a third of the mean annual night light intensity of the area. Population recovery patterns are overall also seen in the night lights, but the recovery in lights is faster and do not accurately reflect permanent population decline. Economic studies have mainly interpreted changes in night lights as representing changes in economic activity. Our study confirms that there is a correlation between changes in night lights and income and GDP, but the correlation is stronger for population and employment. Also here the recovery of night lights is more optimistic in hard hit counties compared with the actual recovery in income and GDP. Overall, we find that night light changes more strongly reflect population and employment impacts, and less so GDP changes.<sup>17</sup>

---

<sup>17</sup>In Appendix 2.A, we assess correlations between the change in the sum of light intensity and the change in income and GDP with the correction approach using fixed effects in a panel regression framework. In this approach, both the night light and economic variables are demeaned with year fixed effects, and then transformed into index numbers. As discussed in Appendix 2.A, the year fixed effects take out the satellite measurement error, but also all other common temporal variation in the panel of all U.S. counties. Therefore, the correlation results for the fixed effects approach cannot be compared directly to those with the calibration correction. Still, we stress that the correlation between change in total light intensity and aggregate income and aggregate

However, top-coding in urban centers makes part of the change in light invisible to the sensor and is thus not captured in the night light data. In future research, the newer VIIRS data could be used to address the issue of top-coding (see Elvidge et al., 2013).<sup>18</sup> Recent examples are Zhao et al. (2018) and Gao et al. (2020), who study the effects of hurricanes Irma and Maria on light intensity in Puerto Rico and the 2015 Gorkha earthquake in Nepal respectively. However, although the time series for the VIIRS data product is steadily expanding, only disasters after 2012 can be studied with this data. Understanding the effects of more historical examples thus still requires the DMSP data that we use in the current study. We stress that even though top-coding is an issue in the studied area, we can still observe the impacts of the hurricane quite clearly. Studying areas with a lower degree of top-coding, which is a much smaller problem even within urban areas in developing countries (Kocornik-Mina et al., 2020), may therefore reveal stronger relations between light intensity and economic indicators.

Furthermore, most studies in this field report a negative impact of natural disasters on local night lights only in the year of occurrence (e.g. Bertinelli and Strobl, 2013; Gillespie et al., 2014; Elliott et al., 2015; Kocornik-Mina et al., 2020). First, we show here that decreases in night light intensity after severe disasters can extend beyond one year for a disaster of this magnitude. This confirms that changes in night light intensity do not just come from temporary power outages, which remains a worry in some of the studies.

Second, we show that even for this extreme case recovery of night light intensity is rather quick – in the order of a one to a few years – whereas recovery in the economic indicators is much slower. This places conclusions in the literature about fast local recovery based on rebounding of night light in a different perspective. For example, Kocornik-Mina et al. (2020) find that economic activity in cities does not relocate to less risky areas after the occurrence of a major flood in the city, based on the finding that on average no negative effects on light intensity exist beyond the year of the flood. This is the case, even though the authors limit their study to large-scale urban floods that displaced at least 100,000 people. Our results suggest that night light intensity may reflect reductions in population and economic activity only partly, such that relocation of economic activity and population may in reality have occurred. For the case of Katrina, we indeed show that this happens. We therefore stress that night lights serve as a means to proxy local economic impacts in areas where no alternative data is available, but that this only provides part of the picture.

Concluding, even though we observe that night lights seem to be able to capture general patterns in population and economic impacts that can be useful in data scarce regions, they are no substitute for assessments of economic data if the aim is to have a complete understanding of the economic consequences of a natural disaster. In-depth analysis of economic data, such as sectoral impacts and wage development, provides

---

real GDP is 0.57 and 0.68 respectively for the fixed effects method (see Figure 2.A.12b), compared to 0.55 and 0.75 for population and employment respectively.

<sup>18</sup>Although less important in the context of the present study, the newer VIIRS data also address the issue of blooming and the rather coarse native resolution of the DMSP satellite.

more detailed insights than night light data can ever provide. For instance, the economic impacts of Hurricane Katrina were a complex combination of disruptions in certain sectors and positive effects for sectors involved in reconstruction as well as substitution effects between companies within a sector (Vigdor, 2008; Hallegatte, 2008). Such a complexity cannot be disentangled with night light data. Moreover, real wage growth may not follow GDP and employment patterns that night light data partly capture. For example, Deryugina et al. (2018) show based on tax return data that Katrina victims eventually experienced higher wage growth than non-victims. These in-depth analyses of economic data indicate positive long-run economic effects of the hurricane for households that cannot be directly derived from analyses of night light data.

Combining the insights from these studies on the effects of Katrina is important to understand the value of night light data in this context for two reasons. First, night light intensity is spatially explicit and highly detailed, but reflects an immobile area rather than its mobile residents. Focusing on the impacted counties alone therefore makes the analysis blind to general equilibrium effects and potential spillovers of population and economic activity towards neighboring counties. Xiao and Nilawar (2013) provide an example of how such effects occurred in less-affected counties in the case of Katrina, and in Felbermayr et al. (2022) (Chapter 3) I apply this framework more generally in a global analysis of disaster impacts on local economic activity.

Second, displaced population results in lower population numbers in the affected areas, and recovery of an area's economy depends on a combination of return migration, reconstruction, and recovery of and/or new economic activity. Using night light intensity, we can only see the combined result of these processes.

Finally, an important consideration for the interpretation of disaster impacts from night light data is whether or not population and economic trends move in the same direction. In our case these trends did not have opposite effects on night light activity. However, interpretation of night light changes is more ambiguous in case opposite trends occur. For example, several studies find population growth after disasters (Vigdor, 2008), which combined with adverse economic impacts of a disaster would obscure clear trends and hamper a straightforward interpretation of night light data.

## 2.5 Conclusion

The use of night light data is becoming increasingly popular in studies that aim to estimate the impacts of natural disasters on local economic activity. However, it is often unclear what observed changes in night lights exactly represent since they have been used as a proxy for changes in GDP levels or growth, urbanization, and temporary and permanent population movements. Our study contributes to this emerging literature by providing insights into the interpretation of night light changes. In particular, we examined how these changes following a severe hurricane relate with local population, employment, and income statistics. For this purpose



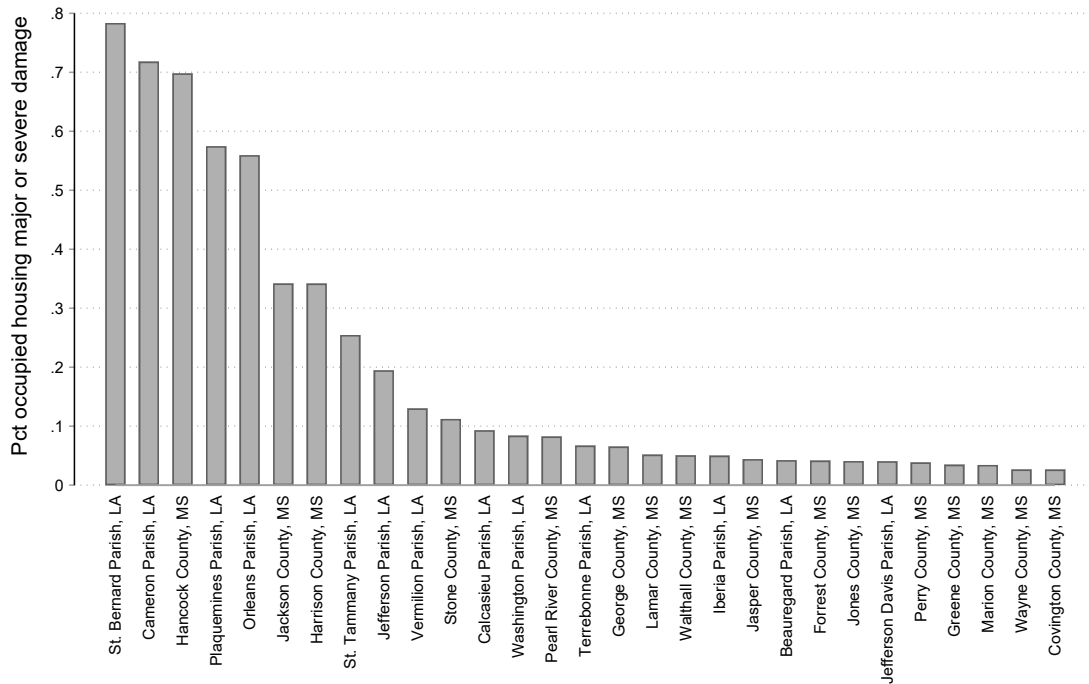
we used Hurricane Katrina as an exemplary case since both detailed night light data and sub-national economic and population statistics are available for the areas impacted by Katrina. Moreover, various previous studies have analysed the social and economic consequences of Katrina, which allows for placing our night light findings in the context of this broader evidence on impacts of this disastrous hurricane.

We find that overall the night light changes reflect the general pattern of direct impacts of Katrina as well as the subsequent recovery. The heaviest-hit counties show the largest declines in night light intensity, and light intensity recovers to pre-disaster levels in the subsequent years. However, recovery of night light intensity towards pre-Katrina levels is much faster than for population and employment and income in the heaviest hit counties. Moreover, our results show that change in light intensity is mostly reflective of changes in resident population and the total number of employed people within the affected area, and less so but positively related to aggregate income and real GDP. The correlation between night light intensity and the considered economic indicators is much stronger after Hurricane Katrina struck than before. The positive and – in the case of population and employment – strong correlations with economic activity show that changes in night light intensity can be used successfully to capture local effects on economic activity of a large natural disaster, such as Hurricane Katrina.

Based on our main results, we conclude that changes in night light intensity prove a valuable proxy for changes in local economic activity following a natural disaster, despite its various shortcomings discussed in this paper. Analysis of disaster impacts using night light data are ideally complemented with detailed analysis of economic data which provide additional more in-depth insights into disaster impacts, like we discussed for our case. Nevertheless, in areas where such economic data is unavailable, our results suggest that night light data can be used to approximate the impacts of natural disasters on regional economies. Future research can conduct similar analyses as conducted in this paper for other natural disasters to improve our understanding of the interpretation of night light data for direct impact and recovery, especially for disaster events of a less extreme nature than Hurricane Katrina.

## 2.A Figures and Tables

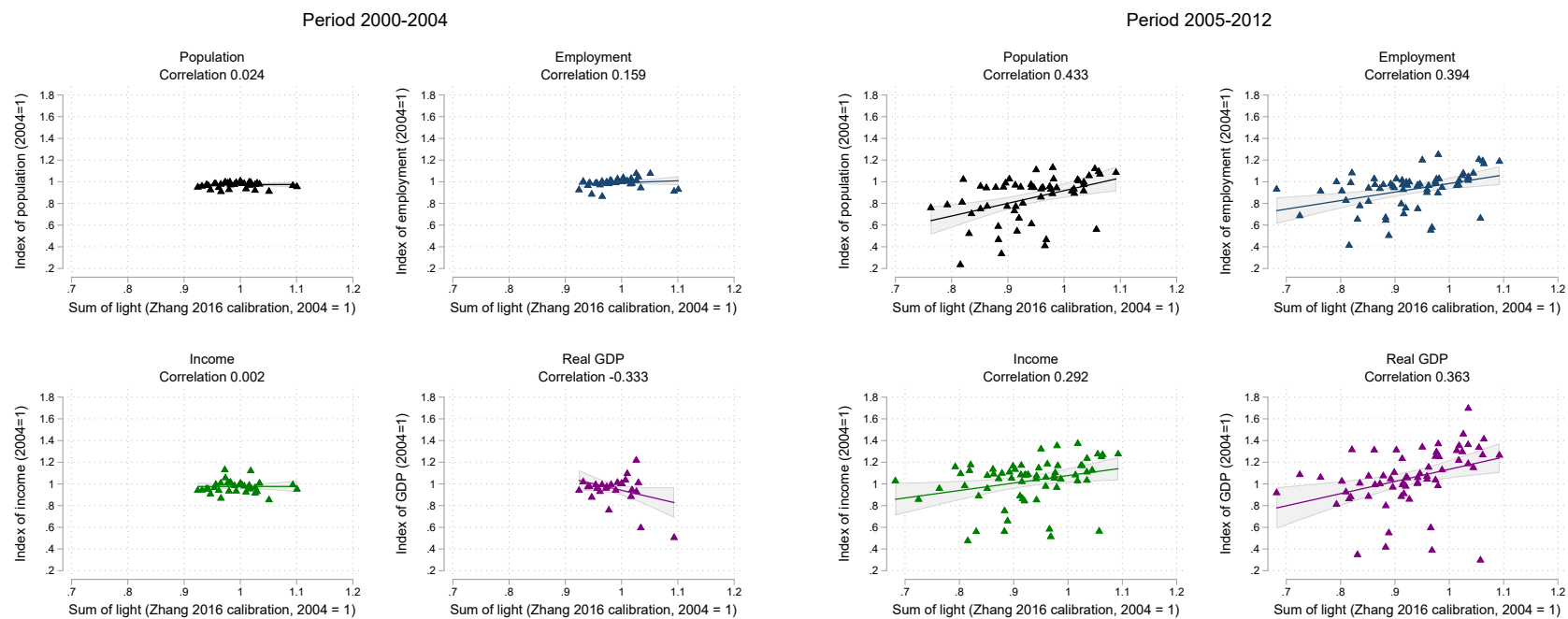
Figure 2.A.10: Distribution of damage to occupied housing units



*Note:* Based on own calculations. Damage figures from the U.S. Department of Housing and Urban Development (2006). Note that the extremely high housing damage figure for Cameron Parish relates to Hurricane Rita rather than Katrina, as is the case for the counties Vermilion and Calcasieu.

Figure 2.A.11: Correlations economic indicators and night lights (Zhang calibration)

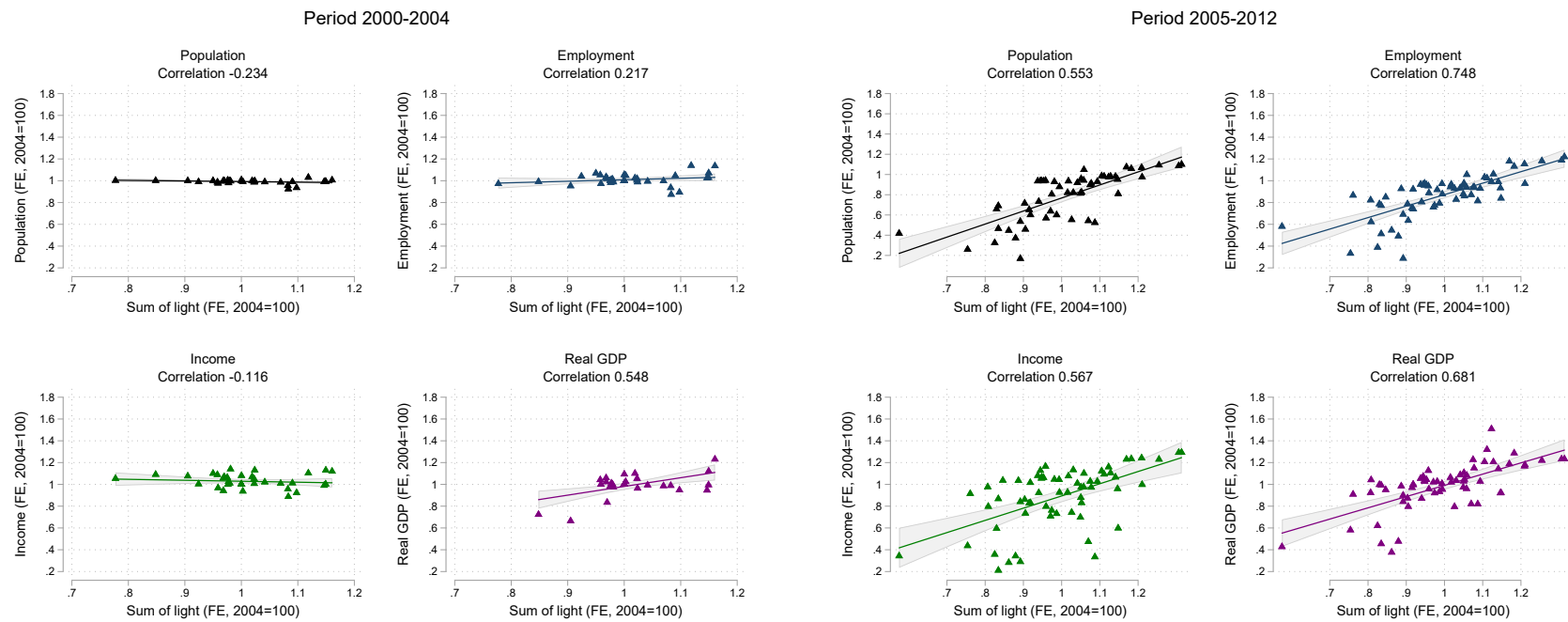
(a) Indexed economic indicators and total sum of light by the 8 affected counties before Katrina. (b) Indexed economic indicators and total sum of light by the 8 affected counties after Katrina



Note: Night lights based on Zhang et al. (2016) calibration, indexed to 2004 = 1. Population data is for 2006-2012 only.

Figure 2.A.12: Correlations economic indicators and night lights (fixed effects correction)

(a) Indexed economic indicators and total sum of light by the 8 affected counties before Katrina.      (b) Indexed economic indicators and total sum of light by the 8 affected counties after Katrina



*Note:* Night lights based on fixed-effects correction, indexed to 2004 = 1. See Appendix 2.B for methodology. Population data is for 2006-2012 only.

## 2.B Cleaning of the night light series

The DMSP annual composite data is known for its problematic intertemporal and between-satellite measurement differences, making it difficult to compare night light intensity over an area across time. The problem stems from the lack of systematic recording of changes in gain settings of the DMSP-OLS sensor that vary across time and between satellites. The reason for this is the main function of the satellite being to detect moonlight clouds, rather than that of artificial night light per se (Elvidge et al., 2009a). As a result, while the annual composites retain a range of DN0 to DN63 (with DN meaning digital number), the true respective radiance associated with these digital numbers varies between the different satellite-year composites. This makes direct comparison of raw digital numbers across years problematic.

A number of approaches have been suggested in the literature, which can be generally grouped into two main classes. First, the approach from remote sensing is to calibrate the annual composite images to a reference image, being either an area that is assumed to have invariant night light intensity over time (e.g. Elvidge et al., 2009a, 2014; Wu et al., 2013), or by making use of a globally or regionally consistent bias across images (e.g. Zhang et al., 2016; Li et al., 2013a). The basic idea of the invariant area method is that any differences in night light intensity between yearly images is the result of measurement error, and thus contains the difference in gain settings between the various satellite-year images. By globally calibrating the year-images to this reference area, a ‘corrected’ time series is produced. A meta-analysis of this approach is discussed in detail by Pandey et al. (2017), who find that among the existing calibration studies Zhang et al. (2016) and Elvidge et al. (2014) produce the most consistent calibration results, with only marginal differences between the two when assessing the global images.<sup>19</sup>

The second approach finds its origin in the economic literature that makes use of night lights, and applies a panel fixed effect setting to address measurement error in night light intensity over time (e.g. Chen and Nordhaus, 2011; Henderson et al., 2012). The basic idea here is that the gain setting changes affect the images in a globally consistent manner, such that estimating a dummy coefficient for changes across years to a reference base year effectively takes out any difference in sensitivity to light intensity across satellite-years.<sup>20</sup> It is important to note that this

---

<sup>19</sup>For example, Elvidge et al. (2009a, 2014) propose Sicily as a candidate invariant area. This area is found to have the best spread of night light intensity across the spectrum of DN0 to DN63. Moreover, and most importantly, true light intensity is found to be largely stable for 1992-2013 for this area. Relying on the resulting invariant area assumption, all images are then calibrated to the image for this area in 1999 (satellite F12) using a second-order polynomial fit. Calibrated digital values that exceed the maximum range of DN63 are truncated at DN63. When assessing the global performance of this calibration method, Pandey et al. (2017) also truncate the lower-bound of the digital values at DN0. I follow their example here.

<sup>20</sup>Chen and Nordhaus (2011) separately control for satellite fixed effects, besides the common year fixed effects. We do not do so here since we make use of single satellite-years rather than taking the average of satellite-years when multiple satellite images are available in a year (I discuss this in more detail in Felbermayr et al. (2022) (Chapter 3)). We use the following satellite-years: F101992-94, F12 1995-98, F141999, F152000-06, F162007-09, F182010-13.

correction is applied at the aggregated county level, rather than at the pixel-level, as is the case for the intercalibration methods. We thus first compute the sum of light intensity by county-year based on the uncorrected images. We know from Strobl (2011) that hurricanes do not affect national GDP growth rates in the United States, and moreover that impacts at the county level net out at the state level within a year. It is therefore safe to assume that we can use the universe of U.S. counties to control for common changes in night light intensity, that are unrelated to the landfall of Hurricane Katrina. Note that this also takes out all other changes that are common to the entire United States in night light intensity, resulting from country-wide economic conditions, technological advance, and energy costs (Henderson et al., 2012).<sup>21</sup> While commonly accepted in the economic literature, the fixed effect approach relies on the assumption that taking out the mean of changes across years is sufficient to correct for measurement changes across time, whereas the calibration method allows for a non-linear effect of the gain settings on the range of digital values in the light composites. This makes the two methods slightly different in their approach for correcting for the measurement differences across time. While not explicitly accounting for non-linearities, however, the fixed effect approach does not rely on assumptions of an invariant area.

In this appendix we compare the results of the calibration and fixed effects corrections to the raw data for the 8 counties that were most heavily affected by Hurricane Katrina. The calibration series were produced with the coefficients for the second-order polynomial fits reported in Zhang et al. (2016) and Elvidge et al. (2014) respectively. The raw image digital values for each satellite-year composite are then recalculated using the coefficients from the respective studies. In both cases, values were truncated to DN0 at the lower end and to DN63 at the upper end, before aggregating the images to sum of light (SOL) for the U.S. counties (following Elvidge et al., 2014; Pandey et al., 2017).

The series corrected with the year fixed effect approach were constructed by first computing the SOL for all U.S. counties (3079 in total) based on the raw images, and then adjusted as follows: (1) We estimate a general OLS model, with SOL from the raw images as the dependent variable, and a set of year dummies as the explanatory variable (2) From this linear model we compute corrected night light intensity by subtracting the estimated coefficients for the year dummies from each county-year observation

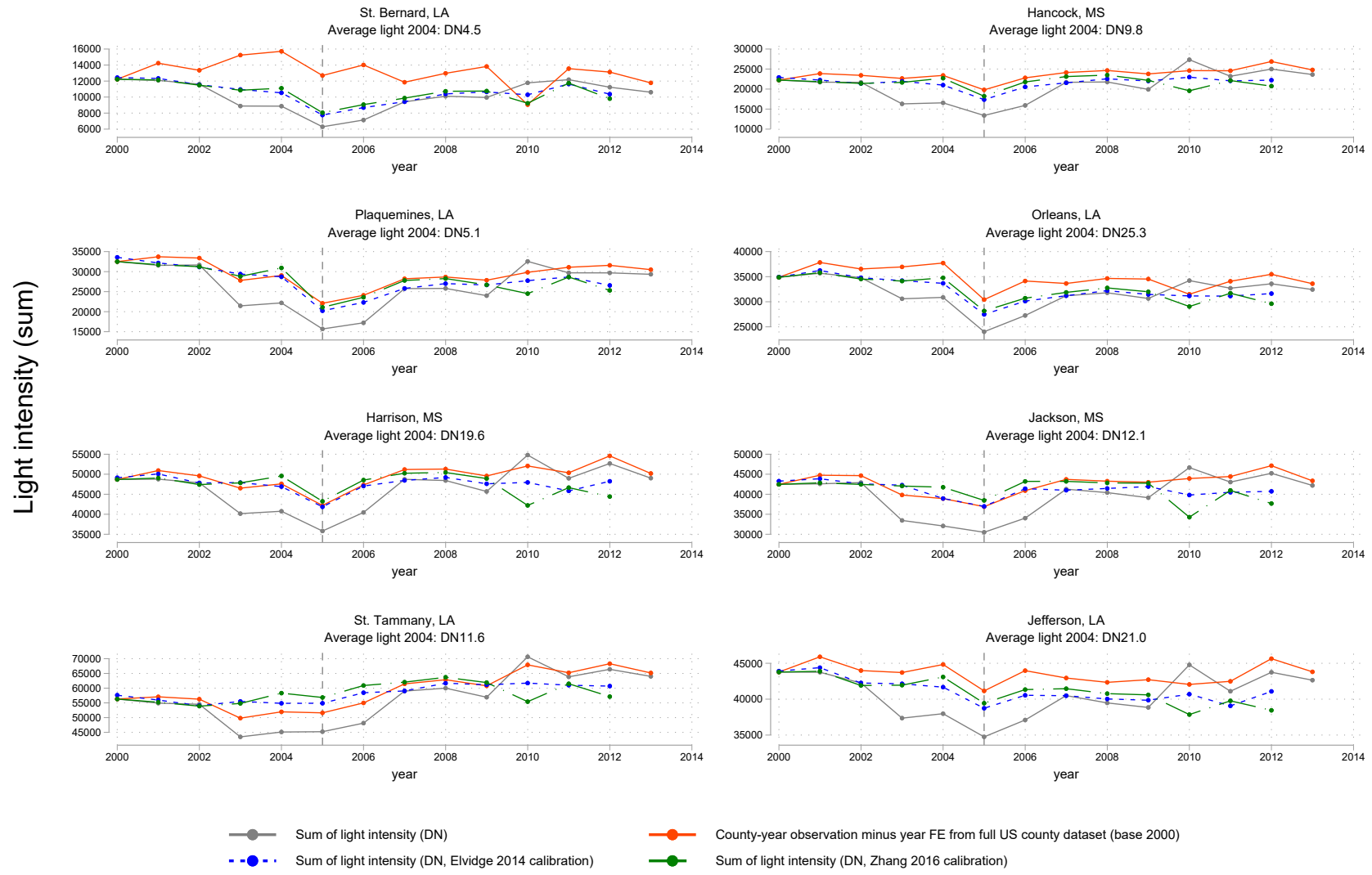
We now discuss the results of the various correction methods. In figures 2.B.1 and 2.B.2 below, we plot the raw series combined with the two calibrated series, and the series corrected with the year fixed effects. Figure 2.B.1 reports the total sum of light by county. The first and most important observation is that the three alternative corrections to the raw night light data show a high degree of similarity. Note how they are more stable over time than the raw series, notably in the period 2002-2007, and how – with the exception of St. Bernard – the two classes

---

<sup>21</sup>This also implies that when we relate changes in fixed-effects corrected night light intensity to the respective economic indicators in Section 2.2.3, we also demean the economic indicators on year dummies.

of correction methods follow each other closely. Especially the dip from 2003-2007 in the raw data is evident when compared to the corrected series. This dip is not specific to the affected counties, but instead is a feature shared by the entire panel of U.S. counties and is thus taken out in the corrected series.

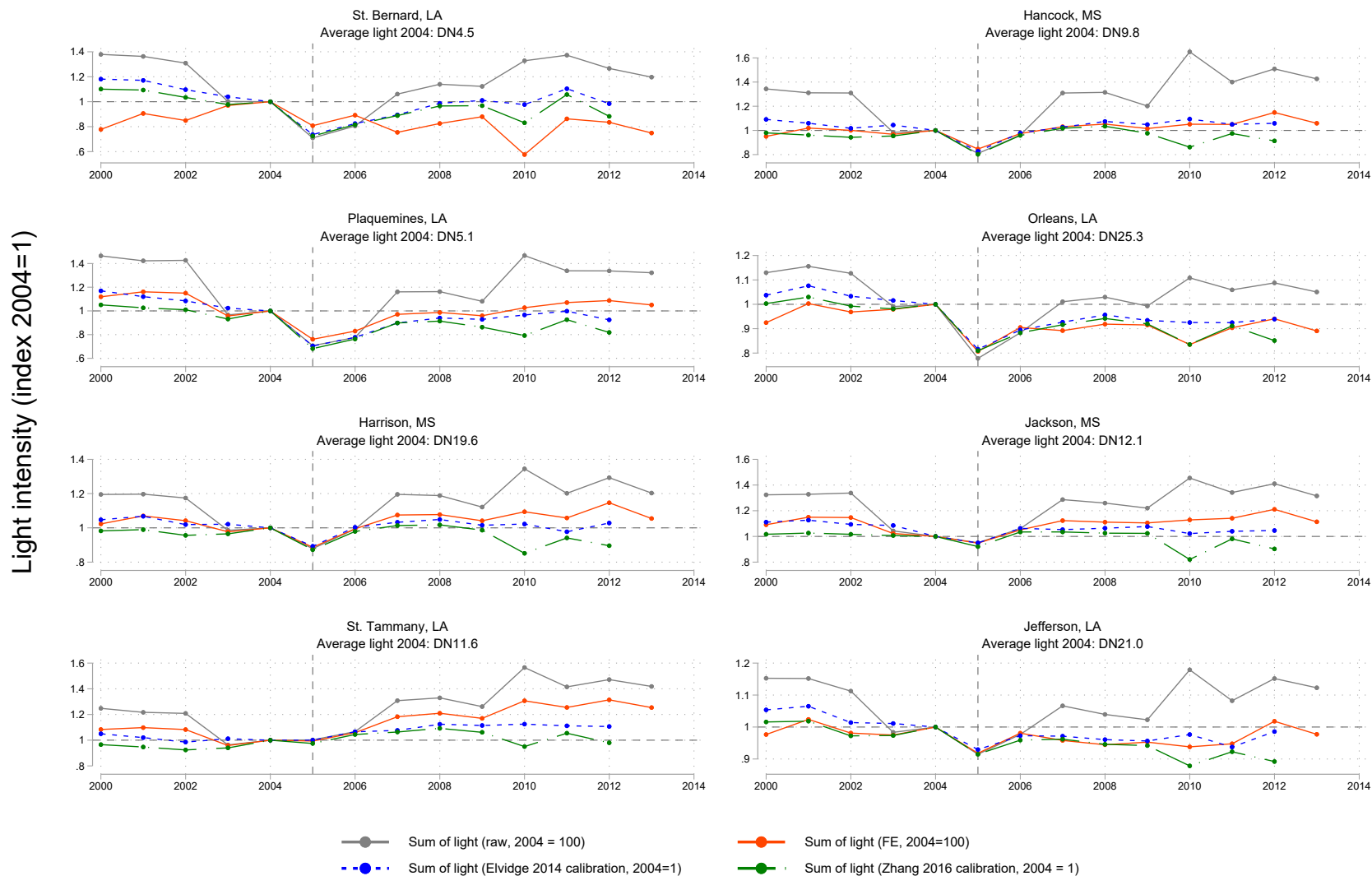
Figure 2.B.1: Corrected night light data (absolute sum of light)



Note: 4 series: raw data (gray), fixed-effect adjustment, invariant area calibration (Elvidge et al., 2014), and global consistent bias calibration (Zhang et al., 2016). Total sum of light by county (SOL).



Figure 2.B.2: Corrected night light data (indexed to 2004 = 1)



Note: 4 series: raw data (gray), fixed-effect adjustment, invariant area calibration (Elvidge et al., 2014), and global consistent bias calibration (Zhang et al., 2016). Total sum of light by county, indexed to 2004=1.

The case of St. Bernard stands out, since its year fixed effect correction deviates strongly from the other three series in both absolute terms and in terms of qualitative behavior. This can be explained by its low level of average light intensity with respect to the other counties. In 2004, St. Bernard has an average DN value of DN4.5, compared to the U.S. mean of DN7.3, while the mean of the other 7 main affected counties is DN14.9. Hence, the fixed effects correction likely under-corrects the digital values for the latter 7 counties, while it over-corrects the values for St. Bernard. This also explains why we find no such deviations between the fixed effects correction and the calibration corrections for the other counties. While the fixed effect method relies on fewer assumptions and may be preferred in impact regression frameworks where the focus is on causal impact identification (such as in Bertinelli and Strobl, 2013; Elliott et al., 2015; Kocornik-Mina et al., 2020), the calibration corrections prove more reliable in producing stable county-specific series for the current application. Since our focus is on absolute light levels, the excessive measurement error for individual cases – such as the clear overcorrection of light changes in low-light counties such St. Bernard – hinders the analysis.

Even though corrected absolute levels help us when assessing recovery after Katrina, we can show that regardless of the correction method the changes over time are fairly stable across the correction methods. Figure B2 reports changes over time in indexed series, with 2004 = 1. A number of observations are to be made: (1) the immediate impact of Katrina on the total sum of light in the 8 affected counties is close to identical between the 4 series. That is, while absolute levels may differ, the relative change from 2004 to 2005 is identical across the various series; (2) again, the two calibration methods show striking similarity; (3) as with the absolute levels in Figure 2.B.1, St. Bernard stands out with its fixed effect correction, which clearly does not perform as intended. Another important feature of the raw data becomes evident when setting it off against the corrected series: while the raw data suggests a relatively quick recovery from Katrina in the subsequent years, both the calibration and fixed effect correction methods indicate that growth in night light intensity is not specific to these counties (suggesting a recovery from the negative shock), but is shared by the entire United States. Especially the year 2010 is associated with a massive increase in light intensity, which seems to stem mostly from the switch to a new satellite (F18), and thus a new instrument with different gain settings. Once we correct for this common feature in the data, recovery appears in fact slower and for a number of counties the sum of light does not return to pre-Katrina levels at all within the available data period.

Although the two calibration methods produce comparable results, the years 2010 and 2012 are important exceptions. Pandey et al. (2017) report that in a global sample, the calibration methods by Zhang et al. (2016) and Elvidge et al. (2014) produce only marginally different results. However, for a subset of countries, among which importantly is the U.S., the Zhang et al. (2016) method performs worse than Elvidge et al. (2014) in smoothing the time series specifically for the years 2010 and 2012. This is reported in detail in Zhang et al. (2016, pp. 5826-5827). This pattern is clearly visible for the subset of counties considered in this study (see Figure 2.B.1 and 2.B.2). While the Elvidge calibration produces rather smooth

series for the period 2009-2012, the Zhang calibration series clearly show drops in 2010 and 2012, which for e.g. the Mississippi counties are comparable in size to the declines in night light intensity in 2005 as a result of Katrina. Comparison to county figures for population, income, and GDP indicate no apparent reason for this dip, and no other natural disaster or adverse event is able to explain this substantial reduction in night light intensity suggested by the Zhang calibration series. This is further supported by a similar stability in the fixed-effects corrected series for the respective Mississippi counties. As a result of this, we use only the calibration method of Elvidge et al. (2014) in the main results, and test robustness of our findings to the fixed effects correction and to the alternative Zhang et al. (2016) calibration in Appendix 2.A. Results prove to be rather stable.



---

## The Economic Impact of Weather Anomalies\*

---

### 3.1 Introduction

In this paper, we present and analyze a unique database to study the economic impact of weather anomalies.<sup>1</sup> Our data allow us to investigate how such anomalies affect economic activity at the local level. Weather anomalies and especially extreme weather events, such as storms, floods, cold spells, and droughts, have a significant impact on our economies and societies (e.g., Frame et al., 2020). Moreover, global warming is likely to increase both the frequency and intensity of weather anomalies in decades to come; (e.g., IPCC, 2014). Finally, the world population grows and ever more people and economic activities occur in vulnerable areas, such as low-lying river-deltas and coastal regions (e.g., Kunkel et al., 1999). Understanding what drives the economic impact of weather anomalies should therefore be high on the research agenda.

The direct material damage and impact on human lives caused by storms, droughts, temperature or precipitation anomalies is quite evident (Kahn, 2005; Kunkel et al., 1999). At the same time, our understanding of the economic consequences of such events is still rather limited. Early papers in this field have investigated the relationship between direct damage, death toll, and economic

---

\*This chapter is published in World Development (Felbermayr et al., 2022). I thank my co-authors Gabriel Felbermayr, Jasmin Gröschl, Mark Sanders, and Thomas Steinwachs for our close collaboration. My contribution to this paper was the collection, cleaning, and compiling of night light data for the dataset that we present in this paper, as well as background and literature research, conceptualization, investigation, econometric analysis (in close collaboration with Thomas Steinwachs), and writing of the paper.

<sup>1</sup>We will consistently refer to "weather anomalies" that we define as extreme weather events *relative* to the normal weather in a given location. Not all such weather anomalies are therefore extreme events by absolute standards and/or result in natural disasters. They are defined as deviations from the normalized, seasonally adjusted, local means.

development (see Kahn, 2005). Building on their findings, a growing literature (e.g., Cavallo et al., 2013; Felbermayr and Gröschl, 2014; Noy, 2009; Strömberg, 2007) has used cross-country data to investigate the effect of natural disasters on economic development and growth.<sup>2</sup> In this literature, findings are mixed and depend on the types of data and country sample used, as well as on the types of events studied (Cavallo et al., 2013; Felbermayr and Gröschl, 2014; Raddatz, 2007).

Several data and specification issues can explain this ambiguity. First, many studies use data on the incidence of natural disasters from insurance records or news. For example, many papers use the EM-DAT database provided by the Centre of Research on the Epidemiology of Disasters (Guha-Sapir et al., 2021). This introduces reporting, selection, and endogeneity biases, as both insurance penetration and damages are highly correlated with development. To tackle this issue, Felbermayr and Gröschl (2014) proposed and collected a database covering the entire globe and containing information on the physical intensities of geological and meteorological events at the country level. Using this more comprehensive data, Felbermayr and Gröschl (2014) show that there is a bias in the EM-DAT data and find a clear negative impact of weather events on country-level economic activity (i.e. GDP). Aggregating the impacts of local weather events to the country or even lower-level administrative units, however, remains theoretically problematic (Botzen et al., 2019). Models of economic geography predict that the spatial pattern of economic activity is in equilibrium and a shock to that spatial equilibrium implies that spillover effects will occur. That is, economic geography models predict that neighboring locations (temporarily or permanently) take over activities from the affected area and so direct impacts can *spill over* to adjacent locations. Such offsetting dynamics are averaged out in aggregation and thereby the estimated effects of weather anomalies on the affected economy are biased downward.<sup>3</sup> In addition, aggregation causes measurement errors and attenuation bias (Noy, 2009).

In this paper, we therefore take the analysis of impacts of weather anomalies to the local level, away from varying country sizes or incomparable administrative entities as our unit of observation. Building on Felbermayr and Gröschl (2014)'s data-collection efforts, we now present their global data on weather anomalies with their exact location and intensity. The challenge in estimating the local economic impact of such anomalies is to find a reasonable proxy for economic activity at a matching spatial resolution. We follow Henderson et al. (2012) and use average annual night-time light emission as an approximation of economic activity.<sup>4</sup> To

---

<sup>2</sup>For comprehensive literature reviews, see Cavallo et al. (2011), Klomp and Valckx (2014) and Botzen et al. (2019).

<sup>3</sup>For example, Strobl (2011) illustrates for the United States that hurricane effects are pronounced at the county level, whereas effects average out at the state level within a year. The author finds no effect of hurricanes on national economic growth rates.

<sup>4</sup>Night-time light emissions have been used to study poverty (Ebener et al., 2005; Elvidge et al., 2009a), the informal economy (Ghosh et al., 2009), ethnic inequality (Alesina et al., 2016; Jean et al., 2016) ethnic favoritism (De Luca et al., 2018), civil conflict (Hodler and Raschky, 2014a), institutions and development (Michalopoulos and Papaioannou, 2013, 2014), and urbanisation and city growth (Storeygard, 2016; Henderson et al., 2017b). In addition, and specifically related to our study, Bertinelli and Strobl (2013), Gillespie et al. (2014), Elliott et al. (2015), Heger and

the best of our knowledge, we are the first to match the night-light emission data collected by the US Air Force Defense Meteorological Satellite Program (DMSP) to the gridded Geological And Meteorological Events (GAME) database and thus obtain a balanced panel of 24,184 grid-cells covering all land mass around the globe (excluding Antarctica) with a resolution of  $0.5^\circ \times 0.5^\circ$  (approximately  $55 \times 55$  km at the equator). The resulting GAME-LIGHTS database covers 197 countries for the period 1992 to 2013 and is available online<sup>5</sup>. Using spatial econometric panel techniques, we then provide evidence on the local impact and spillover effects of various types of weather anomalies on (the change in) night-time light emissions. Our baseline results show a reduction in night-time lights after wind, low temperatures and high precipitation anomalies. On average, the negative impacts on the growth in night-time lights are moderate in size and range between 0.1-0.3 percentage points. For these types of events, we find evidence of *positive* spillover effects on neighboring cells. We also find that weather anomalies are generally very localized phenomena. Neighboring cells benefit from a weather shock and take over some of the economic activity that is lost in the affected area.<sup>6</sup> This implies that effects measured at larger geographical units typically hide the true impact at the local level and, to the best of our knowledge, we are the first to show this in a data set that covers the globe. Finally, our data show that these patterns are heterogeneous across income groups and mainly driven by cells in low- and middle-income economies. This confirms the finding in Felbermayr and Gröschl (2014) that oversampling in high-income regions will bias estimates and global coverage of events is useful in avoiding such biases.

Dry spells also seem to be associated with lower night-light emissions, but we find negative effects only in the spatial spillovers. Note, however, that droughts are slow-onset events mostly affecting agricultural output that in turn is not highly correlated with night lights (Keola et al., 2015; Beyer et al., 2018). The negative spillover effect of dry spells is largely driven by rural cells, suggesting that a lack of precipitation causes indirect negative growth impacts in more rural economies. Furthermore, our estimated coefficients suggest that spatial spillovers from weather anomalies are very local and dissipate quickly beyond the directly neighboring cells.

We make three clear contributions to the literature. First, our data set is publicly

---

Neumayer (2019), Kocornik-Mina et al. (2020), and Nguyen and Noy (2020) have used night-light emission data to proxy for the local impacts of hurricanes, typhoons, and floods, respectively.

<sup>5</sup>The dataset is available under DOI-number: 10.7805/Game-Lights-2021 and can be downloaded at: <https://www.ifo.de/en/ebdc-data/ifo-game>

<sup>6</sup>Recent studies suggest that indeed indirect impacts can be significant and economic activity moves to unaffected regions. Xiao and Nilawar (2013) show for Hurricane Katrina that demand shifts from the core to the edge of the disaster area. Lenzen et al. (2019) analyse effects of a large cyclone in an input-output model, showing that indirect damages spill over in upstream supply chains and may be quite large relative to direct damages. Moreover, Boustan et al. (2020) find that disasters significantly increase out-migration rates in the US, caused by falling productivity and labor demand. Studying a flash flood in Brazil, Lima and Barbosa (2019) show that directly affected municipalities suffered a substantial decrease in production and that significant spillovers to neighboring regions exist. Noy et al. (2021) show for the 2011 flood in Thailand that directly affected households experience negative business income and indirectly affected households suffer an income loss that is nearly as large as that of directly affected households.

available at DOI: 10.7805/Game-Lights-2021 and <https://www.ifo.de/ebdc-data/ifo-game> and allows research to take the next step toward quantifying the impact of weather anomalies on the economy at the local level. Second, our results clearly show that extreme weather events should indeed be studied at a high spatial resolution, as effects are local and average out at higher aggregation levels.

Third, our results show that indeed weather anomalies have a significant negative impact on the local economy, even if these negative effects are often temporary and partially compensated by increasing economic activity in surrounding areas. Our results are consistent with theories of economic geography, in which the spatial pattern of economic activity tends toward an equilibrium that adjusts over time after local negative shocks hit (Capello, 2015; Botzen et al., 2019). Finally, these results have immediate policy relevance, as they imply that more extreme weather as a consequence of global climate change can have significant effects on the economic geography of regions, countries and continents.

In the remainder of the paper, we first provide some theoretical background in Section 3.2. Section 3.3 describes the data compiled and used in this paper, while we discuss the features of the spatial panel estimation techniques we use in Section 3.4. Results from our estimations and their economic interpretation, are discussed in Section 3.5. Section 3.6 concludes and sets the agenda for future research.

## 3.2 Theoretical background

The fields of economic geography and regional economics provide us with several models that one can use to predict the spatial economic impact of negative shocks to supply and/or demand (see Capello, 2015, for a detailed overview). We have summarized this literature in Table 3.2.1, which shows seven broad families of regional economics models that can be identified.

First we list the models' key assumptions in column 2. Under "Key Output Variables", we then list the variables on which these models make predictions, where regional gross product (RGP) in the directly affected and neighbouring regions are the most important for our purposes. Weather anomalies can enter the models through a slightly varying list of key-input variables listed in column 4. Here, all models have capital stock and labour, as well as reconstruction demand and transport costs in common. We assume the direct impact of weather anomalies is negative on the first and positive on the second pair. Columns 5 and 6 then list the predicted signs of the impacts on the listed outcome variables for the short- and long-run for economically integrated regions. Columns 9 and 10 give a short explanation and some key references for each model family. From this table, we can conclude that theory is indeed ambiguous on the predicted effects and that the time frame can matter a great deal for the predictions. We therefore chose not to formulate strict hypotheses on effects for affected and neighboring cells and rather let the data tell us what effects we observe. We also take from the literature that we should control for population density and initial economic activity levels.



Table 3.2.1: Families of regional economics models

Model Family	Key Assumptions	Key Output Variables	Key Input Variables	Predicted Outcomes		Remarks	Key References
				Short Run	Long Run		
Location Models	Uniform Demand		Capital (-)	-,+,-	-,+,-	Location models predict that economic activity is agglomerated or spread in space in location equilibrium. This location equilibrium can be upset temporarily or permanently by weather anomalies.	Weber (1909), Hotelling (1929), Hoover (1948), Salop (1979)
	Optimal Production Location	RGP <sub>i</sub> ,	Labor (-)	-,+,-	-,+,-		
	Constant Transportation Costs	RGP <sub>-i</sub> ,	Recon Demand (+)	+,+,0	0,0,0		
	Abstract Uniform Space	RGPDensity <sub>i</sub>	Transport Costs (+)	-,-,+	0,0,0		
	Agglomeration Economies		Spillovers (-)	-,-,+	-,+,-		
Land Rent Models	Point Demand		Capital (-)	-,+,-	-,+,-	Land-Rent models assume that demand is concentrated (in an urban center) and that land rent adjusts to establish spatial equilibrium. Again, this equilibrium can be upset by weather anomalies affecting land rent.	Von Thünen (1826), Alonso (1960), Muth (1961)
	Optimal Production Location	RGP <sub>i</sub> ,	Labor (-)	-,+,-	-,+,-		
	Constant Transportation Costs	RGP <sub>-i</sub> ,	Recon Demand (+)	+,+,0	0,0,0		
	Abstract Uniform Space	LandRent <sub>i</sub>	Transport Costs (+)	-,-,+	0,0,0		
	Agglomeration Economies		Spillovers (-)	-,-,-	-,-,-		
Central Place Models	Heterogeneous Demand		Capital (-)	-,+,-	-,+,-	In Central-Place models, the focus is on the structure of urban systems of n-order. They assume a hierarchy of products and services. Weather anomalies can upset the urban system depending on their intensity and where they hit.	Christaller (1933), Lösch (1944)
	Optimal Production Location	RGP <sub>n</sub> ,	Labor (-)	-,+,-	-,+,-		
	Product Specific Transport Costs	RGP <sub>n-i</sub> ,	Recon Demand (+)	+,+,0	0,0,0		
	Abstract Uniform Space	PopDensity <sub>n</sub>	Transport Costs (+)	-,+,-	-,+,-		
	Agglomeration Economies		Spillovers (-)	-,-,-	-,-,-		
Growth Pole Models	Uniform Demand		Capital (-)	-,-,-	-,-,-	In Growth Pole models, dominant firms constitute a growth pole (gp). The gp is the engine of growth for the region around it. If it is negatively affected, the entire region around it suffers.	Perroux (1955)
	Optimal Production Location	RGP <sub>gp</sub> ,	Labor (-)	-,-,-	-,-,-		
	Constant Transport Costs	RGP <sub>-i</sub> ,	Recon Demand (+)	+,+,0	0,0,0		
	Abstract Diversified Space	Growth <sub>gp</sub>	Transport Costs (+)	-,-,-	-,-,-		
	Agglomeration Economies		Spillovers (-)	-,-,-	-,-,-		
Innovation Diffusion Models	Uniform Demand		Capital (-)	-,+0	+,+,+	In these models, innovations diffuse as an infectious disease using logistic diffusion curves. The infection rate and vulnerable population can be determined by regional characteristics. Non-geographic concepts of distance and proximity have been shown to matter.	Hägerstrand (1952), Griliches (1957), Mansfield (1961)
	Optimal Production Location	RGP <sub>i</sub> ,	Labor (-)	-,+0	-,-,0		
	Logistic Diffusion	RGP <sub>-i</sub> ,	Recon Demand (+)	+,+,0	0,0,0		
	Diversified Relational Space	Growth <sub>i</sub>	Transport Costs (+)	-,+,-	-,+,-		
	Heterogenous Absorptive Capacity		Absorption Cost (+)	0,0,-	0,0,-		
Spillover and Network Models	Uniform Demand		Capital (-)	±,±,±	±,±,±	In these models, innovations diffuse through a variety of networks and relationships, making a region part of a network. The richness of the models implies that predictions are not unequivocal, but negative shocks ripple through the network.	Acs et al. (1994), Audretsch and Feldman (1996), Frenken et al. (2007)
	Optimal Production Location	RGP <sub>i</sub> ,	Labor (-)	±,±,±	±,±,±		
	Relationships as Channels	RGP <sub>-i</sub> ,	Recon Demand (+)	±,±,±	±,±,±		
	Diversified Relational Space	Growth <sub>i</sub>	Transport Costs (+)	±,±,±	±,±,±		
	Heterogenous Absorptive Capacity		Absorption Cost (+)	±,±,±	±,±,±		
New Economic Geography	Symmetric Demand		Capital (-)	0,0,0	0,0,0	By introducing imperfect competition and increasing returns in stylized space, new economic geography models can explain the dynamic specialization pattern over space and time. They predict asymmetric effects of weather anomalies; when more advanced regions are hit, effects will trickle down, but not up.	Vernon (1966), Krugman (1979), Venables (1996), Grossman and Helpman (1991)
	Optimal Production Location	RGP <sub>n</sub> ,	Labor (-)	-,-,0	-,-,0		
	Increasing Returns to Scale	RGP <sub>n-i</sub> ,	Recon Demand (+)	+,+,0	0,0,0		
	Diversified Stylized Space	Growth <sub>n</sub>	Transport Costs (+)	-,-,0	0,0,0		
	Imperfect Competition		Absorption Cost (+)	0,0,0	0,0,0		

Based on Capello (2015) and additional desk research. RGP=Regional Gross Product; Density=refers to a variable expressed per square kilometer; Growth=the percentage change in a variable and subscripts *i*, *n* and *gp* refer to the region *i* that may be of (city)rank *n* or a growth pole *gp* (if applicable). Subscripts *-i*, *n - 1*, and *-gp* refers to regions that are not *i*, of one rank less *n - 1* or not the *gp*, respectively.

## 3.3 Nightlight emissions and weather anomalies at the grid-cell level

### 3.3.1 Nightlight emissions

Following the seminal contribution by Henderson et al. (2012) scholars proposed using night-light emissions as a proxy for economic activity and started to explore these data to study local economic activity in a variety of applications; for a survey, see Donaldson and Storeygard (2016).<sup>7</sup>

For our purposes, using night lights as a proxy for economic activity has three important benefits: First, measurement error in official GDP statistics is correlated with the level of income per capita, whereas in night lights it is not. Second, night light information is consistently available for all countries of the world at a standard spatial resolution and temporal interval. Thus, countries can be included even if they rarely provide reliable administrative statistics but frequently experience anomalous weather events (e.g., Myanmar or Somalia). Third, official statistics typically fail to account for activity in the sizeable informal economy.<sup>8</sup> This is highly relevant as weather anomalies tend to affect the poorest members of society most, who are most likely to be active in the informal economy. In light of these advantages, others have also used night lights to assess the impact of weather anomalies at the local level. For example, Bertinelli and Strobl (2013), Elliott et al. (2015), and Kocornik-Mina et al. (2020) have studied hurricane, typhoon, and flood impacts on night-light emissions, respectively. Although all papers in this relatively new literature either had a limited regional focus or evaluated the impact of a specific disaster type, their findings strengthen the case for assessing impacts of weather anomalies using night-light emissions at the local level. To the best of our knowledge, we are the first to have combined these data with different types of weather anomalies for the entire globe.

The raw data stem from the US Air Force Defense Meteorological Satellite Program (DMSP) and contains the annual mean night light intensity of each pixel on a satellite image as a digital number (DN). To turn the raw data into a useful proxy for human activity in a given location, some data cleaning is necessary. First, we exclude all pixels that do not cover any land surface. Second, we follow the literature in dropping all pixels in gas flaring zones identified by Elvidge et al. (2009b).<sup>9</sup> Third, as on-board sensors degrade over time, the DMSP launches a new

---

<sup>7</sup>Night-time light emissions have been shown to strongly correlate with economic activity at the country level (cp. Henderson et al., 2012; Nordhaus and Chen, 2015; Pinkovskiy and Sala-i Martin, 2016). An emerging literature analyzes smaller sub-national units: Michalopoulos and Papaioannou (2013, 2014) focus on ethnic homelands, Hodler and Raschky (2014b) on sub-national administrative units, Storeygard (2016) on cities, Henderson et al. (2017a) on uniform grid-cells, and Bleakley and Lin (2012) on locations along rivers as natural features.

<sup>8</sup>See, e.g., Schneider and Enste (2000) and Schneider (2005) for estimates on the informal economy and Ghosh et al. (2009) for a study using night-light data to estimate the size of the informal sector in Mexico.

<sup>9</sup>This affects approximately 2,300 grid-cells or 0.89% of the global land area. Appendix 3.A.1

satellite every three to six years. In 12 of the 22 available years, two satellites were in orbit simultaneously. We deal with years in which more than one composite night-light image is available by choosing the satellite with the best mean coverage of valid nights per pixel in a given year to maximize our geographic coverage (summary statistics on the satellite-years reported in Table 3.A.2 in the Appendix). Finally, if the number of valid nights for a pixel is zero (i.e. no observations in that year), it is dropped from the data. We then aggregate the cleaned night-light data to the  $0.5^\circ \times 0.5^\circ$  grid-cells and compute the log change in annual mean light intensity as our proxy for changes in local economic activity.<sup>10</sup>

Figure 3.3.1 illustrates the link between grid-cell level lights growth and country level GDP growth over time for nine countries in our sample. The graphs show that within countries, there is quite some variation in night-light growth. Also, there are clear co-movements of GDP growth and night-light growth, especially for Turkey, Chile and Columbia. However, it is also clear that we need to be careful in interpreting night-light emission data as a proxy for economic activity. Average light to GDP elasticities may, for example, not remain stable, especially if weather anomalies occur.<sup>11</sup>

### 3.3.2 Weather anomalies

The independent variables of interest measure the physical intensity of meteorological events. We first compile a new data set of monthly observations from various sources

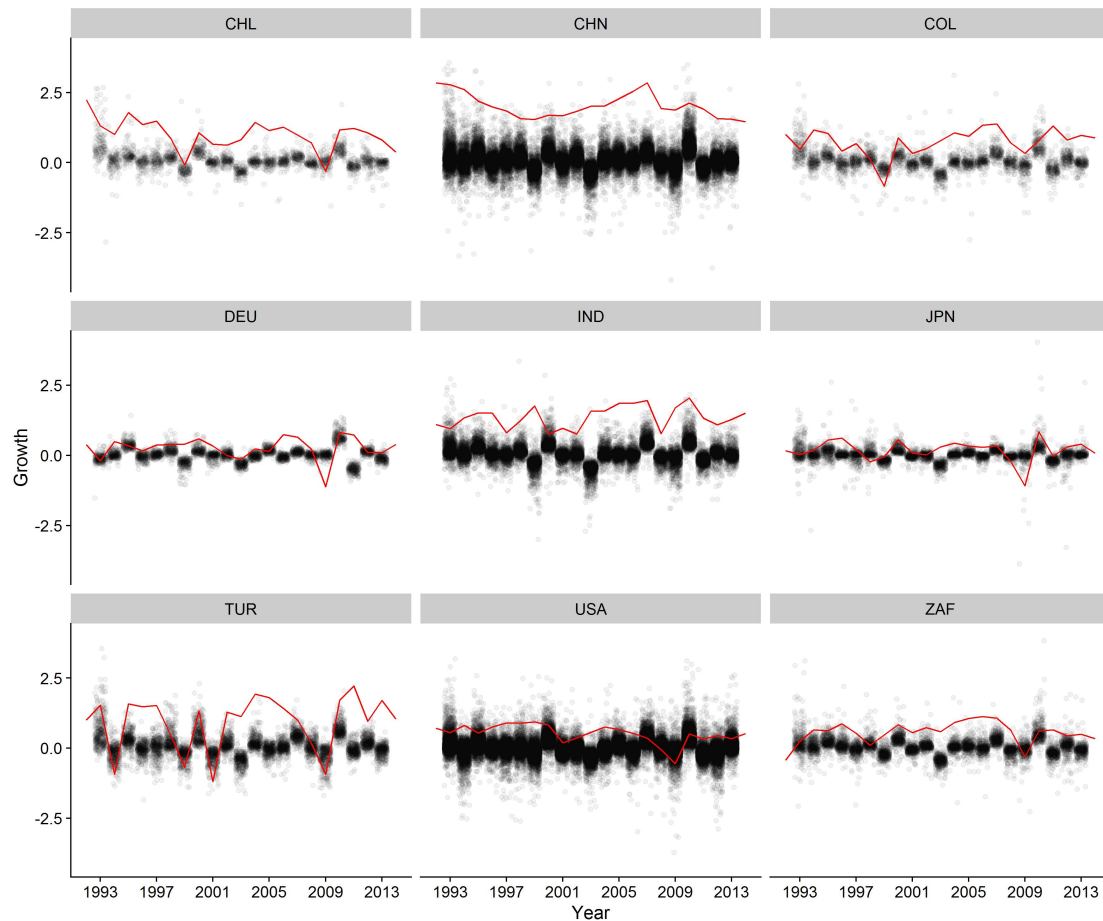
---

provides supplementary information on the data generation.

<sup>10</sup>This variable captures more intense light from previously lit pixels as well as pixels lighting up in the grid-cell area. To convert changes in annual night-light emission into more familiar GDP-growth effects, Henderson et al. (2012) and Storeygard (2016) estimated lights-to-GDP growth elasticities of approximately 0.3. Aggregating our data to the country level we find an aggregate lights-to-GDP elasticity of 0.37, that is not significantly different from 0.3. Detailed results are shown in Table 3.A.3 in the Appendix. We use area-weights and our full panel of 197 countries from 1992 to 2013. Restricting the regression to the same time frame as Henderson et al. (2012), we obtain an elasticity of 0.35, also insignificantly different from 0.3. The time variation in light emission explains more than a quarter of the variation in GDP in countries over time (within  $R^2$  of 0.273). Moreover, the country level elasticity of night-lights to population density (0.10) is statistically not different from the elasticity of GDP to population density (0.13).

<sup>11</sup>The relationship between emitted light and economic activity may change, for example, due to power blackouts or the destruction of power infrastructure. Taking the average annual night-light emissions at the grid-cell level ameliorates the problem of short-term power outages, as most weather events that damage power infrastructures (e.g., storms or heavy rain) typically come with dense cloud cover, and drops in light intensity in the nights immediately after the event, are less likely to be recorded. Power outages that last long enough to be part of our annual average evidently also hamper economic activity and are thus part of the impact of interest. Another issue may be that the average elasticity at the country level hides potentially large differences in the light emission to GDP relationship across cells. This becomes more problematic when activity in grid-cells is highly concentrated in a few economic sectors, when sectoral light-to-value-added elasticities and/or when the sensitivity of output to weather events differ greatly across sectors. As the sectoral specialization of a grid-cell changes only slowly over time (e.g., Content and Frenken, 2016; Malmberg and Maskell, 1997) we tackle this issue by taking out cell fixed-effects in our estimation method.

Figure 3.3.1: Night lights and GDP



*Note: Jitter-plots represent the increase in the log of annual average light emission at the grid-cell level by country. Line-plots represent annual country level GDP growth (scaled by factor 0.2 to compress the vertical scale).*

at the  $0.5^\circ \times 0.5^\circ$  grid-cell resolution for the entire globe – the gridded GAME database. While the paper ultimately uses data at the annual level to match the light emission data, it is essential to collect intensity data at the monthly level to account for seasonality. The gridded GAME database now covers the period 1979 to 2014 and contains earthquakes, volcanic eruptions, storms, droughts, precipitation, and temperature anomalies. In this paper, we focus on weather-related events only. We describe how we have constructed our weather anomalies in detail below.

## Precipitation

Monthly **precipitation** data in millimeters were collected from the University of East Anglia Climatic Research Unit Time-Series (CRU TS 3.23, Harris et al., 2014). The CRU provides homogenized gauge data from weather stations around the world in a consistent format. As precipitation can be discontinuous in time and space, climate scientists apply sophisticated reanalysis methods to produce high-quality

estimates for monthly precipitation covering all land area (excluding Antarctica) at a  $0.5^\circ$  resolution (see Harris et al., 2014). We identify extreme precipitation events by cell within a month, which considers location-specific seasonality. Following the climatological literature (cp. Kraus, 1977; Nicholson, 1986), we calculate precipitation anomalies by subtracting the long-run (1979–2014) mean precipitation observed in a cell for a given month (i.e., each January, February, March) and standardize cell precipitation by dividing it by the corresponding long-run standard deviation for the cell for that particular month:

$$\gamma_{i,m,t}^{prec} = \frac{x_{i,m,t}^{prec} - \bar{x}_{i,m}^{prec}}{\sigma_{i,m}^{prec}}, \text{ where } i = \text{cell}, m = \text{month}, t = \text{year}.$$

This indicator measures both positive and negative precipitation anomalies expressed in standard deviations from the cell mean for a specific month. Positive precipitation anomalies may cause extensive damage, particularly if flooding occurs.<sup>12</sup> As night lights – our dependent variable – are given as annual averages, we aggregate the monthly physical intensities to an annual mean intensity indicator for the purpose of this study. First, as we do not want to average precipitation over dry and wet months, we drop observations below zero, so only months with positive precipitation deviations are considered. Second, to match anomalies to the annual average light emissions, we calculate a rolling-window weighted annual mean  $D_{i,t}^p$ , using for each month the number of months remaining in the year as its weight in year  $t$ , while taking the remainder as the weight for year  $t + 1$ :

$$D_{i,t}^p = \sum_{m=1}^{12} \left[ \gamma_{i,m,t}^p \cdot \frac{12-m}{12} + \gamma_{i,m,t-1}^p \cdot \frac{m}{12} \right]$$

where  $i$  is cell,  $m$  is month,  $t$  is year, and  $p$  is the type of weather shock. This ensures an annual measure in which an anomaly can affect light growth for 12 consecutive months, regardless of the month in which it takes place.<sup>13</sup> Potentially longer lasting impacts are assessed by including a temporal lag of the precipitation variable into the regressions, as will be discussed in section 3.4. The resulting measure for **precipitation** intensity in a given year is thus the time-weighted average of positive deviations from the long-run monthly mean (both in mm) in a cell, expressed in standard deviations from its sample cell mean.

---

<sup>12</sup>To analyze flood events, the extent and depth of floods at the grid-cell level would be preferable, as provided selectively by the Dartmouth Flood Observatory. However, these are not available globally and consistently. Kocornik-Mina et al. (2020) use maps of 53 selected large floods in the period 2003–2008 to study their impact on economic activity in urban areas at a very fine  $1 \times 1$  km resolution, also using annual DMSP night lights. Their estimates suggest economic effects in a similar order of magnitude as the ones found in our study and they exhibit a similar dynamic. Moreover, the authors find very similar results when using excessive precipitation rather than a direct flood-indicator in their analysis. See also, for example, Damania et al. (2017). Still, one should not interpret excessive precipitation as a flood event.

<sup>13</sup>When an extreme event takes place in September of 1995, its intensity weighs for only 4/12 on the intensity measure for 1995 and for 8/12 in that of 1996. As a robustness test we also obtained results using the simple annual mean and the maximum. All results remain comparable and are available on request.

## Droughts

In addition to global precipitation, CRU also provides the information to compute the Standardized Precipitation-Evapotranspiration Index (SPEI). This index considers the amount of water coming in (precipitation, PRE) and going out (evapotranspiration, PET), resulting in a water balance for each cell in any given month. We follow Vicente-Serrano et al. (2010) in constructing a cell-specific monthly SPEI that has zero mean and a standard deviation of one. Negative values in the SPEI indicate drought events. Hence, to aggregate to an annual average **drought** indicator, we include only the negative values and take the absolute value to obtain a drought indicator that is standardized across cells in a similar fashion as for precipitation.<sup>14</sup> The same rolling-window weighting by months, as above, is then applied to obtain a drought-intensity measure for each cell and year.

## Cold Spells

Anomalous **cold** spells can also disrupt social and economic activity. To capture such events, we collect gridded  $0.5^\circ$  resolution land-surface temperatures from the Climate Prediction Center (CPC) of the National Oceanic and Atmospheric Administration (NOAA). Analogous to our measure for precipitation anomalies, temperatures are normalized by subtracting the long-run (1979–2014) cell mean temperature for a given month and dividing this by the cell’s long-run standard deviation for that month:

$$\gamma_{i,m,t}^{temp} = \frac{x_{i,m,t}^{temp} - \bar{x}_{i,m}^{temp}}{\sigma_{i,m}^{temp}}, \text{ where } i = \text{cell}, m = \text{month}, t = \text{year}.$$

Again, this indicator gives both positive and negative temperature anomalies. To isolate the information for cold spells, we drop values above zero and express the remaining negative values in absolute terms. The annual cold-spell intensity indicator gives us the rolling-window weighted-average negative deviations of surface temperature from the long-run monthly mean at the cell level, measured in standard deviations from its own mean.

## Storms

Finally, for **storms**, we create a measure using information on monthly maximum sustained wind speeds from two distinct sources. The International Best Track Archive for Climate Stewardship (IBTrACS) Version v03r09 provides the geolocation on tropical cyclone centers with respective pressure and wind speeds (Knapp et al., 2010a,b). The Global Summary of the Day (GSOD) statistics<sup>15</sup> contain wind speeds,

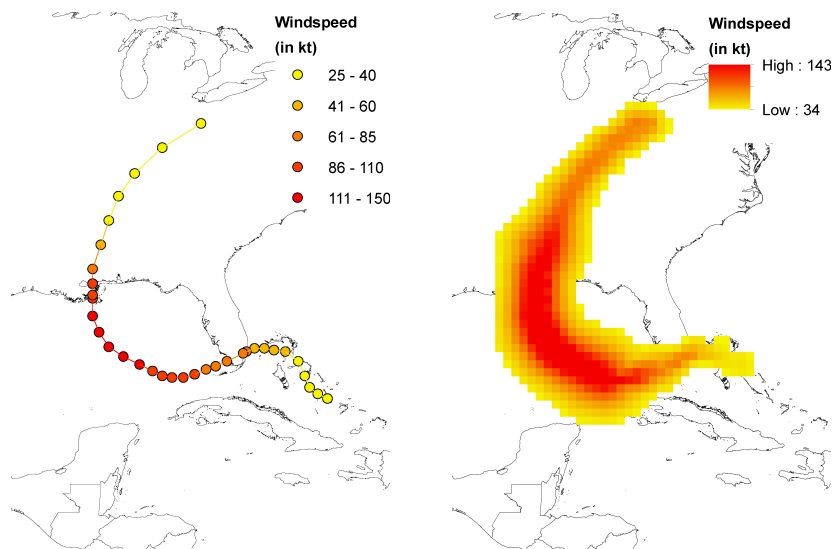
---

<sup>14</sup>Note that droughts are often accompanied by heat waves that enter the SPEI on the evapotranspiration side. As the two are closely correlated, we do not report results for a separate indicator for heat waves.

<sup>15</sup><ftp://ftp.ncdc.noaa.gov/pub/data/g sod>.

also of non-hurricane winds, measured at weather stations. Obtaining wind speeds at the grid-cell level poses a challenge as data are available only if weather stations and/or cyclone information is present in a cell (cp. Figure 3.A.2 in the Appendix). To fill the gaps, we apply two types of interpolation techniques. We use a wind-field model provided by Geiger et al. (2018) to generate continuous gridded wind fields around cyclone data from IBTrACS. Figure 3.3.2 shows Hurricane Katrina as an example of how raw data are transformed into a wind field.

Figure 3.3.2: Hurricane Katrina – IBTrACS (l.) vs. Wind Field (r.)

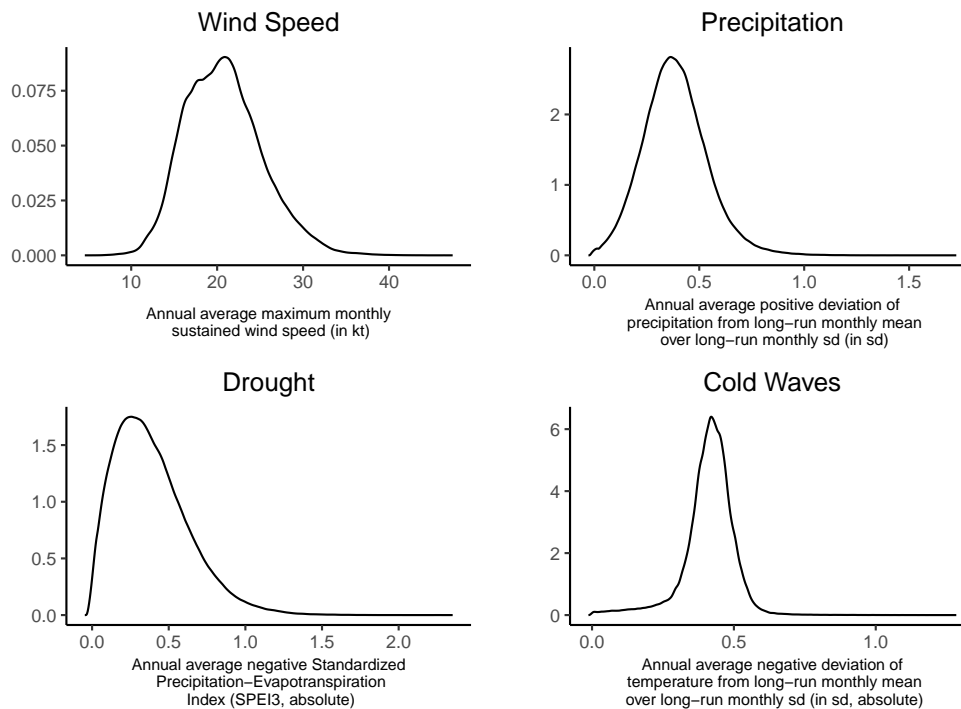


This provides wind speed estimates for cells in cyclone paths. However, many cells do not experience a cyclone in any given month. To complete our panel, we therefore combine GSOD data with a global kriging spatial interpolation algorithm (cp. Krige, 1951).<sup>16</sup> Applying this kriging algorithm, we obtain the predicted maximum sustained wind speed for any given cell and month. Obviously, precision of resulting wind-speed measures drops with distance to actual weather-station measurements. We therefore replace the cell's kriged station wind speed with the wind-field information on hurricanes, cyclones or typhoons, if any such event has affected the cell. Our resulting wind-speed indicator is the (imputed) maximum sustained wind speed for a cell-month combination measured in knots. Again, our annual measure of wind intensity is constructed by taking the rolling-window weighted average maximum sustained wind speed in knots. We do not normalize on the cell-month average wind speed here, as wind causes damages above speeds that are roughly similar across the globe.

Figure 3.3.3 presents the distributions of our annual aggregated physical intensities. Note that by construction, the range of the distribution of weighted annual

<sup>16</sup>Haslett and Raftery (1989) were the first to adopt kriging to model the spatial distribution of Irish wind power resources using historical wind-speed data. Using daily European climate data, Hofstra et al. (2008) show that kriging performs best out of six interpolation methods. Our exact procedure is described in detail in Appendix 3.A.2.

Figure 3.3.3: Kernel Densities of Annual Aggregate Physical Intensities



*Note:* Density distributions of aggregate annual physical intensities. All measures are reported over the full sample.

averages is smaller than at the monthly level. Table 3.3.1 provides some well-known examples of events and shows how these are reflected in our yearly aggregates in comparison to the monthly data. The examples show that well-known weather anomalies typically lie far above their cell means and in the tail of the cell-specific distributions.

In Figure 3.3.4 we show our measures for wind speed, precipitation, cold and drought for some of the years for which Table 3.3.1 indicates we should be seeing anomalies. The drought in Zimbabwe, the high wind speeds for Katrina at the coastline of Louisiana and Mississippi and the excessive rain in Tennessee clearly show up in our data. The record cold spell in the UK of 2010 stands out less clearly, as cold spells tend to stretch larger geographical areas, but clearly shows as a sizeable temperature anomaly. Note that the spread of cold temperature deviations in terms of standard deviations from local means is smaller than for e.g. precipitation anomalies, as shown in Figure 3.3.3. Table 3.A.1 in the Appendix provides full-summary statistics on yearly aggregates for our estimation sample.



Table 3.3.1: Representation of natural events in the monthly data vs. the yearly aggregates

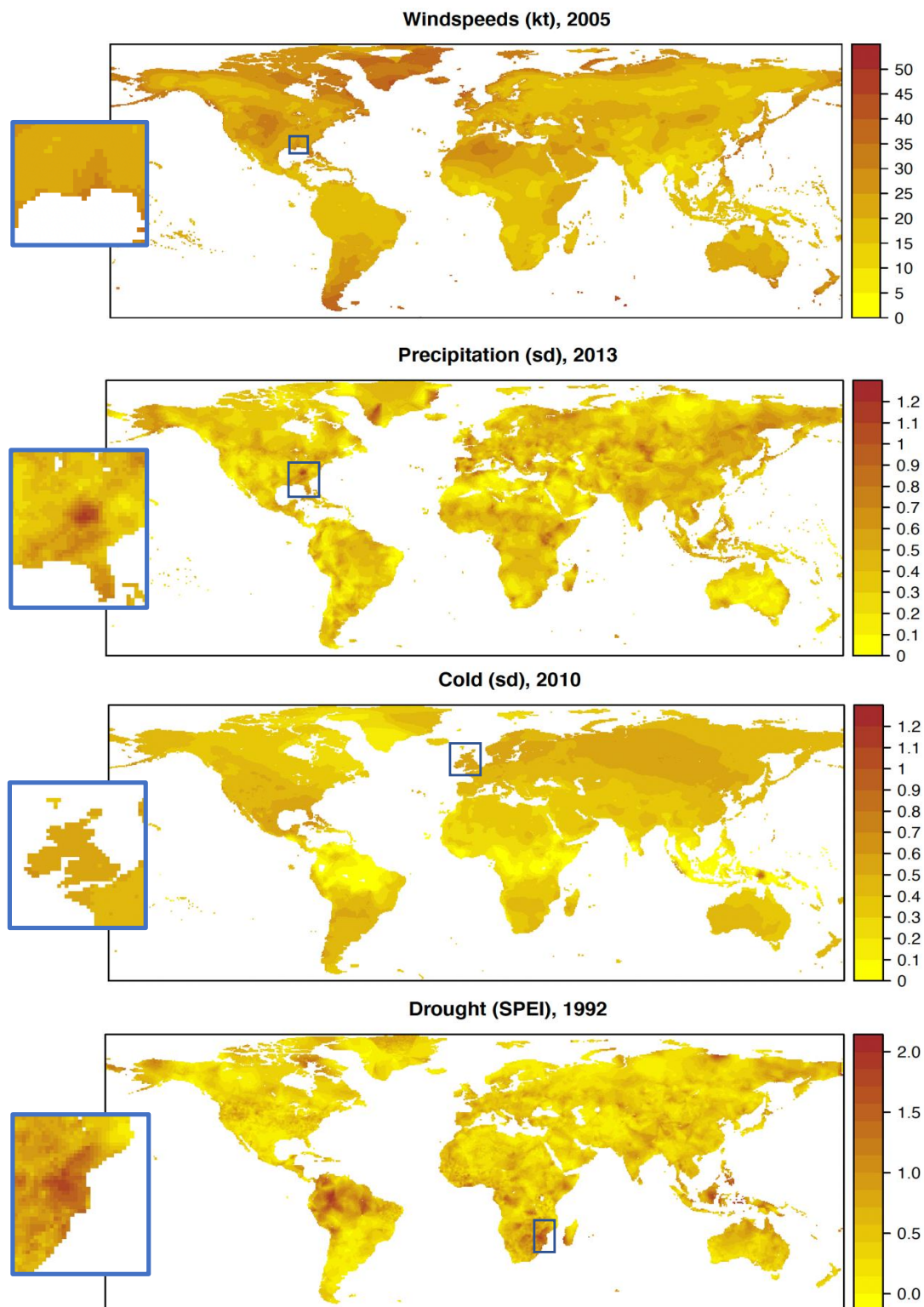
Event	Date	Place	Lat	Lon	Month	Year	C-Mean	C-SD
Hurricane Katrina	08/2005	New Orleans, USA	28.75	-89.25	138 kt	38.3 kt	28.9 kt	3.4 kt
Odisha Cyclone	10/1999	Odisha, India	19.75	86.25	128 kt	24.8 kt	17.8 kt	3.2 kt
Extreme Rain & Flash-Flood + Heavy Prec. (Ohio Winterstorm)	06/2013 12/2013	Maryville, Missouri, USA	35.75	-83.75	2.66 4.16	1.52	0.43	0.35
Torrential Rains	11/1994	Kairo/Nile Valley, Egypt	30.25	32.25	4.56	0.56	0.23	0.15
UK Record Winter	12/2010	Country-Wide, UK	55.25	-2.25	2.30	0.67	0.43	0.09
Heavy Coldwave	07/2003	Cuzco Region, Peru	-12.75	-71.25	2.04	0.59	0.49	0.11
Drought (prolonged)	01/2012	Country-Wide, Mexico	20.25	-104.25	1.63	0.80	0.52	0.17
Drought (prolonged)	02/1992	Country-Wide, Zimbabwe	-21.25	31.75	2.89	1.38	0.44	0.40

*Note:* Columns *Lat* and *Lon* represent geographic coordinates of grid cell centroids for reported values. *Month* represents maximum index realizations of respective events in the monthly raw data, observed in the month of occurrence. *Year* represents the corresponding (simple mean) aggregate over 12 months of the year. *C-Mean* and *C-SD* refer to cell-specific distributions of yearly aggregates.

### 3.3.3 Population

As our aim is to use changes in light emission as a proxy for changes in economic activity, we want to control for population. Population data at the pixel level is available from the Gridded Population of the World (GPWv4) data set (Center for International Earth Science Information Network (CIESIN) at Columbia University, 2016). The data contain five-year target estimates based on census inputs gathered at the lowest available administrative unit. CIESIN distributes the census population uniformly across space within the census area, excluding water bodies. Importantly, note that the GPW data is *not* constructed using lights as an input factor. We aggregate this pixel data to our grid-cells. To interpolate the years between the given five-year periods, we assume stable exponential population growth. This implies that we can control for the trend in population growth but, by construction, cannot capture the possible relocation of population after weather events.

Figure 3.3.4: Physical Intensities for Wind Speed, Precipitation, Cold and Drought



*Note:* the maps show the corresponding intensity measure for wind speed in 2005 (Hurricane Katrina in Louisiana), precipitation in 2013 (extreme rain in Tennessee), cold in 2010 (record winter UK) and drought in 1992 (Zimbabwe). Event regions are cropped on the left.

### 3.4 Empirical strategy

To identify the effects of local weather anomalies on night-light emissions at the grid-cell level, we first propose a simple panel fixed-effects growth estimation. In this simple model, within-cell variation of year-to-year growth in average night-light emission is regressed on the intensity of weather anomalies in that year. Hence, identification relies on the divergence from the predicted growth path in the case of a weather anomaly, the realization of which is unpredictable and exogenous in time and location. As changes in night-light emissions cannot conceivably cause the weather to change, we argue that we can interpret the results as the impact of weather anomalies on economic activity. Our baseline model is the following:

$$\Delta \ell_t = \ell_{t-1} \varphi + \mathbf{D}_t \boldsymbol{\beta}^0 + \mathbf{X}_t \boldsymbol{\delta}^0 + \boldsymbol{\nu} + \boldsymbol{\pi} + \mathbf{u}_t \quad (3.4.1)$$

where the  $K \times 1$  vector  $\Delta \ell_t \equiv \ell_t - \ell_{t-1}$ , captures the growth rate in night-time light emissions expressed in yearly changes of the logarithm of mean night-light intensity  $\ell_t \equiv \ln(\overline{\text{light}}_t)$  for each of the  $K$  grid-cells in year  $t$ .  $\mathbf{D}_t$  is a  $K \times P$  matrix of intensities (and temporal lags) for  $P$  types of weather anomalies (storms, precipitation, droughts, and cold spells) and  $\mathbf{X}_t$  is a  $K \times N$  matrix of  $N$  control variables (population) at the grid-cell level.  $\boldsymbol{\pi}$  denotes year fixed-effects to control for global economic trends, such as technological progress, energy costs, and the global business cycle. More importantly, year fixed-effects also control for changed sensitivity of sensors across satellites and the degradation of sensors with satellite age (see Henderson et al., 2012).  $\boldsymbol{\nu}$  denotes cell fixed-effects. These control for time-invariant local unobservable determinants and absorb the location-specific baseline risk. Cell fixed-effects also control for general climatic conditions (to the extent that these are stable over time), as suggested by Auffhammer et al. (2013).

Consequently, identification relies on atypical variations in our weather variables *for that cell*. In addition, when treating light emission as a proxy for economic activity, cell fixed-effects control for cell-specific but time-invariant components in the elasticity of GDP to night-light emissions.<sup>17</sup> Cell fixed-effects also control for inherent systematic measurement error in night lights across latitude (e.g., due to stray light, aurora, and the solar cycle) and for overall topography and other unobserved geographic determinants. We first explore this basic model to take the analysis from the national to the grid-cell level and to show very basic correlations.

Zooming in on the grid-cell level, however, we violate the assumption that errors are uncorrelated across units of observation. Our proposed  $0.5^\circ \times 0.5^\circ$  grid-cell resolution coincides with the resolution of the data records on meteorological and climatological events and has the advantage that observational units are

---

<sup>17</sup>Such patterns are likely to be heterogeneous in space due to large variation in local, regional, and national factors, such as institutional quality, infrastructure, and sectoral specialization. Areas dominated by agriculture, for example, emit little to no additional light as economic activity grows (Keola et al., 2015), whereas rail infrastructure can transport more goods and people at lower light intensities than road networks. To the extent that these differences and land-use patterns are time-invariant, they are controlled for by cell fixed-effects.

entirely exogenous. As these cells also cut up actual economic units (e.g., cities or metropolitan areas), however, this introduces spatial correlation by construction. As discussed before, economic geography and regional economic models predict that economic activity tends toward a spatial equilibrium and economic activity is therefore spatially correlated (Capello, 2015). When cells are positively or negatively affected by weather anomalies, these models imply that the shock will propagate through space and spill over to neighboring cells. These spillovers will be positive if neighboring cells take over and substitute for activity in the directly affected cell. They will be negative if neighboring cells also suffer from economic disruption and a drop in demand through a complementary relationship. We want to show and account for the implied spatial (inter)dependence of night-light growth and weather events and should therefore employ appropriate spatial methods (cp. Halleck Vega and Elhorst, 2015; LeSage and Pace, 2009) to simultaneously model local treatment effects and spillover effects to neighboring cells. Specifically, we propose using the Spatial Durbin Error Model (SDEM) (cp. Anselin, 2013; Halleck Vega and Elhorst, 2015) with cell and year fixed-effects.<sup>18</sup> In this model, weather anomalies not only affect light growth in cells in which they are recorded, but can also affect light growth in neighbouring cells. We estimate a fully specified spatial panel model of the form

$$\begin{aligned}\Delta \ell_t &= \ell_{t-1}\varphi + \mathbf{D}_t\beta^0 + \mathbf{X}_t\delta^0 + \mathbf{W}^r\mathbf{D}_t\beta^1 + \mathbf{W}^r\mathbf{X}_t\delta^1 + \nu + \pi + \mathbf{u}_t \\ \mathbf{u}_t &= \rho\mathbf{W}^r\mathbf{u}_t + \varepsilon_t\end{aligned}\quad (3.4.2)$$

where  $\mathbf{W}^r$  is a time-invariant  $K \times K$  dimensional spatial weights matrix that accounts for the spatial spillovers.<sup>19</sup> In the baseline specification, we choose a radius  $r$  of 80 km. This implies that effectively all eight adjacent cells in the grid are considered neighbors at the equator, where grid-cells are about  $55 \times 55$  kilometers.<sup>20</sup> The cutoff at 80 km is arbitrary, but robustness tests suggest that it is appropriate.<sup>21</sup>

<sup>18</sup>We find spatial spillovers from weather anomalies to be highly localized. We thus prefer an SDEM over the often-used Spatial Durbin Model (SDM) specification. For a discussion, see Halleck Vega and Elhorst (2015). In the robustness section, we also discuss the results with the SDM model with global spillovers. We find similar qualitative results and moreover confirm that spillovers are indeed a confined local phenomenon.

<sup>19</sup>Following Conley (2008), the spatial-weights matrix is specified as binary and isotropic. This implies that its elements are equal to one for all neighboring cells within the spatial radius  $r$  around a given cell's center and zero for all cells beyond that radius. This imposes a strict balancing restriction on the panel such that the same set of neighbours is used for a specific cell across all years in the sample. This implies that we drop cells that have zero light intensity between 1992–2013 from the panel. Additionally, our approach requires cells to have at least one neighbor, such that cells without neighbors must be dropped from the analysis. This affects mainly dark regions and some small island states. The balanced panels for each weather variable are plotted in Figures 3.A.7 through 3.A.10.

<sup>20</sup>Using a constant metric distance ensures that the geographic area of neighbors remains constant over latitude, but it leads to the inclusion of a larger number of cells along the longitudinal axis the further one moves from the equator.

<sup>21</sup>To test whether the results are sensitive to the spatial radius, we later increase the distance cutoff to 160 km. Results are qualitatively robust while magnitudes of spillovers decrease with distance. For further discussion, see robustness section 3.5.3.

By interacting determinants with  $\mathbf{W}^r$ , we allow local outcomes in night-light growth to depend not only on the local treatment but also on the treatment of neighbors.  $\beta^1$  and  $\delta^1$  are thus average local spillover effects of a marginal change in the respective explanatory variable in *one* neighboring cell.<sup>22</sup>

We account for the possibility of regional clustering in unobserved characteristics by allowing for spatial auto-correlation in the error term  $\mathbf{u}_t$ . This strategy allows for consistent estimation of the local economic impact of weather events together with spillover effects to neighboring locations.

## 3.5 Main results

This section presents the results of our analysis. We start with building up the model, by first estimating a simple fixed effects regression, and then adding the spatial components of our model. First, we show that night-light emissions change in cells that experience weather anomalies. Next, we show that (compensating) spatial spillovers exist. This emphasizes the importance of analyzing the economic impacts of weather events at a high spatial resolution. For most types of anomalies, we find that directly affected cells suffer while surrounding areas benefit, even if these effects are typically temporary.

### 3.5.1 Building the baseline

Table 3.5.1 presents results for precipitation in columns (1) to (4) and wind in columns (5) to (8). The simple ordinary least square (OLS) model in column (1) follows Bertinelli and Strobl (2013) and Elliott et al. (2015), including cell and year fixed-effects. It suggests a positive effect of excessive precipitation on night-light growth. This finding has also been reported in earlier work; see Felbermayr and Gröschl (2014) for a discussion. Control variables, such as initial light levels and population, have the expected negative and positive signs, respectively. Note that excluding population from our regressions does not change the results; see Table 3.B.4 in the Appendix. However, the OLS specification does not account for spatial dependence and spatial autocorrelation. We first account for spatial dependence, by introducing the spillover component for our weather anomaly variables in a "spatial lag of X" (SLX) model in column (2), following Halleck Vega and Elhorst (2015). The local effect of excessive precipitation now turns negative, while the spatially weighted term is positive and both coefficients are statistically significant at the 1% level. Hence, while the local impact of precipitation anomalies is negative, a cell's night-light growth is positively affected by excessive precipitation in neighboring

---

<sup>22</sup>As neighboring cells are likely to be affected by related weather shocks, we calculate spatial autocorrelation of each demeaned independent variable in our baseline regression (see Figure 3.A.12 in the Appendix). Depending on the type of shock, time lags of weather events show correlations between 0.28 and 0.62 from one period to the next, while spatial correlations between the local effect of an event and shocks in neighboring cells are 0.9. The latter correlation is high, as expected, but not sufficient for perfect multicollinearity. Hence, we are confident that we can identify local and spatial effects separately in our data.

cells. Point estimates on lagged night-light intensity and population remain stable and highly significant. In column (3), we add a temporal lag to the SLX model to allow for dynamic effects. While contemporaneous effects remain stable, a reversal of signs in lagged local treatment and spatial spillovers suggest that the impacts tend to be reversed after a year.

However, the SLX model does not account for linkages between cells that are not directly related to weather anomalies. When we test for the absence of such residual spatial autocorrelation (RSA) in the SLX model using a Moran's  $I$  test (Moran, 1950), we indeed find that it is rejected.<sup>23</sup> Therefore, we present the results of our preferred specification, the SDEM model that augments the SLX model with Baltagi-type spatial errors in column (4). This reduces the magnitude of point estimates on both local and spillover effects, but the signs remain the same.<sup>24</sup>

Turning to winds in columns (5) to (8), we find negative local effects of storms on changes in night-time light across all model specifications. These effects continue to be significant in the first lag. The magnitude of point estimates varies across specifications and is more than halved between the OLS (column [5]) and the preferred SDEM model (column [8]).

Similar model comparisons for droughts and cold spells can be found in Tables 3.B.1 and 3.B.2 in the Appendix, but are not discussed in detail here. All types of weather events show the presence of spatial spillovers and RSA, such that our choice for the SDEM model over other approaches is justified for all types of weather events.

---

<sup>23</sup>The test shows a positive and statistically significant value for all weather variables in a spatial lag of X (SLX) regression with two-way cell and time fixed-effects (see Table 3.A.4 in the Appendix). This suggests the presence of spatial clustering. All tests suggest the SDEM model is preferred in our data. To account for RSA, we apply Baltagi et al. (2007) type spatial auto-correlation in the residuals. We rely on a Maximum-Likelihood approach for spatial panel models provided by Millo and Piras (2012) and Millo (2014) to also address possible non-linearity in  $\rho$ . In line with the results of Moran's  $I$  test, the spatially auto-regressive parameter  $\rho$  is positive and significant at the 1% level. Results of the SLX model excluding the spatial error component are shown in Tables 3.5.1 and 3.B.1 to 3.B.2 in the Appendix.

<sup>24</sup>We also test an ordinary least squares (OLS) model with standard errors adjusted for spatial clustering following the procedure implemented by Hsiang (2010). Estimates are highly comparable to the reported SLX results across all weather variable types. Results are reported in Appendix Table 3.B.3.

Table 3.5.1: Model Buildup: Impact of Precipitation and Wind on Light Growth

Dependent Variable: $\Delta \ln(\text{lights}_t)$								
	precip.				wind			
	(1)	(2)	(3)	(4)	(5)	(6)	(7)	(8)
$\text{weather}_t$	0.0115*** (0.0029)	-0.0613*** (0.0078)	-0.0752*** (0.0081)	-0.0310*** (0.0070)	-0.0051*** (0.0003)	-0.0102*** (0.0009)	-0.0010 (0.0010)	-0.0020** (0.0009)
$\text{weather}_{t-1}$			0.0481*** (0.0077)	0.0219*** (0.0069)			-0.0143*** (0.0010)	-0.0090*** (0.0009)
$W \cdot \text{weather}_t$		0.0114*** (0.0011)	0.0138*** (0.0011)	0.0049*** (0.0013)		0.0008*** (0.0001)	-0.0002 (0.0001)	0.0000 (0.0002)
$W \cdot \text{weather}_{t-1}$			-0.0079*** (0.0011)	-0.0021 (0.0013)			0.0015*** (0.0001)	0.0008*** (0.0002)
$\ln(\text{pop}_t)$	0.0412*** (0.0028)	0.0250*** (0.0027)	0.0250*** (0.0027)	0.0257*** (0.0013)	0.0404*** (0.0028)	0.0238*** (0.0027)	0.0236*** (0.0027)	0.0247*** (0.0013)
$W \cdot \ln(\text{pop}_t)$		0.0149*** (0.0009)	0.0149*** (0.0009)	0.0112*** (0.0006)		0.0145*** (0.0008)	0.0143*** (0.0008)	0.0108*** (0.0006)
$\ln(\text{lights}_{t-1})$	-0.4090*** (0.0032)	-0.4123*** (0.0032)	-0.4122*** (0.0032)	-0.4367*** (0.0011)	-0.4109*** (0.0032)	-0.4146*** (0.0032)	-0.4152*** (0.0032)	-0.4387*** (0.0011)
$\rho$				0.0672*** (0.0000)				0.0672*** (0.0000)
Method	OLS	SLX	SLX	SDEM	OLS	SLX	SLX	SDEM
Observations	502,026	502,026	502,026	502,026	507,864	507,864	507,864	507,864

*Note:* \*\*\*, \*\*, \* denote significance at the 1%, 5% and 10% level. Specifications (1) to (3) and (5) to (7) are estimated by panel OLS, (4) and (8) is estimated by Maximum Likelihood. Standard errors (in parentheses) allow for heteroskedasticity and clustering at the cell level in specifications (1) to (3) and (5) to (7). Cell and year fixed effects included but not reported. Spatial radius is  $r=80$  km. Yearly weather intensities reflect time-weighted rolling averages over 12 subsequent monthly observations.

### 3.5.2 Results and interpretation

Table 3.5.2 summarizes the main results for each type of weather anomaly using our preferred SDEM model. Note that, as we proxy for economic activity with night-light emission, we must be careful not to over-interpret the meaning of our coefficients. It is entirely possible that this proxy is less reliable for some types of weather anomalies than others and for some geographic regions than others. Further, we show results for sudden-onset and short-duration events such as wind and rain as well as slow-process and longer lasting events, such as droughts and cold spells. We should therefore not be surprised to see different effects on these different types of events. Patterns look similar for most types: storms, precipitation anomalies, and cold spells; but magnitudes differ quite a bit. Droughts stand out as different and will be discussed separately below.

First, consider the results on wind. Months with high winds that increase the annual average wind-speed measure by one knot are on average associated with a decline in lights growth of 0.2 percentage points.<sup>25</sup> With all the caveats we have discussed in Section 3.3.1, we can use our estimated light-to-GDP growth elasticity of 0.37 to develop an idea of the economic significance of such shocks. A one standard deviation increase in the yearly wind speed measure then leads to a reduction of income growth below the local growth path by 0.33 percentage points on average.<sup>26</sup> Interestingly, a large proportion of the impact only kicks in with a time lag, as opposed to earlier results reported for storms in Bertinelli and Strobl (2013) and Elliott et al. (2015), who find no persistent decline of night light for grids of 1km<sup>2</sup> in the Caribbean and coastal Chinese cities beyond the years of occurrence, respectively. After one period, an increase in the yearly wind-speed measure by one knot reduces lights growth by 0.9 percentage points, corresponding to a reduction in GDP-growth of 1.49 percentage points for a one standard deviation increase.<sup>27</sup> On average, the contemporaneous spatial spillover effects of strong winds are statistically insignificant. After one period, a positive spillover effect suggests an increase in local lights growth by 0.08 percentage points if in *one* of the neighboring cells the yearly mean wind speed is higher by one knot. This implies an increase in income growth by 0.13 percentage points for a one standard-deviation increase in

---

<sup>25</sup>Averaging wind speeds implies that we inflate our coefficient. A 12-knots-stronger wind in January shows up as a 1 knot stronger average sustained wind speed in the annual measure, whereas a 12-knots stronger wind caused the damage. As damages are also measured as an average reduction in night lights, this effect is averaged out and biases our coefficients toward zero further. Coefficients can therefore not be interpreted as point estimates of the impact of a single storm on local night-light emissions. This would require higher frequency data on both dependent and independent variables.

<sup>26</sup>This is calculated as the GDP growth effect of a one standard deviation increase in the annual wind measure (4.49, see Table 3.A.1) multiplied by a wind-speed coefficient of -0.0020, by 100 and by the lights-to-GDP growth rate elasticity of 0.37:  $[-0.002 \cdot 100] \cdot 0.37 \cdot 4.49 = -0.33$ .

<sup>27</sup>Note that the first temporal lag of the direct and spillover effects is foremost a control variable to rule out lasting impacts of potential previous events. It is entirely possible that extreme winds or cold spells have longer-lasting negative effects than excessive precipitation. Using up to 10 time lags and computing cumulative effects, we can show that there is some oscillation of weather effects around a path; results can be obtained from the authors on request.



wind.<sup>28</sup> Note that Bertinelli and Strobl (2013) and Elliott et al. (2015) also look for signs of potential spatial spillover effects. However, rather than explicitly modeling direct spillovers as we do, they average wind intensity over the set of a cell and a range of its neighbors. Both studies find little evidence for spatial spillovers, while we find strong evidence for their existence albeit with a time lag. Note that the size of our grid-cells ( $0.5^\circ$  compared to  $1 \text{ km}^2$ ) is considerably larger. Spatial spillovers in their approach are thus estimated over a much smaller distance and would be part of the local effect in our approach. In our data, we test the robustness for larger, not smaller, distances, and find that spillovers are mostly concentrated in neighboring cells within an 80 kilometer range.<sup>29</sup>

Table 3.5.2: Baseline Results

<b>Dependent Variable: <math>\Delta \ln(\text{lights}_t)</math></b>				
	<b>wind</b>	<b>precip.</b>	<b>drought</b>	<b>cold</b>
$\text{weather}_t$	-0.0020** (0.0009)	-0.0310*** (0.0070)	0.0083* (0.0048)	-0.0762*** (0.0153)
$\text{weather}_{t-1}$	-0.0090*** (0.0009)	0.0219*** (0.0069)	0.0005 (0.0047)	-0.0326** (0.0149)
$W \cdot \text{weather}_t$	0.0000 (0.0002)	0.0049*** (0.0013)	-0.0044*** (0.0009)	0.0218*** (0.0027)
$W \cdot \text{weather}_{t-1}$	0.0008*** (0.0002)	-0.0021 (0.0013)	0.0010 (0.0009)	-0.0195*** (0.0026)
$\ln(\text{pop}_t)$	0.0247*** (0.0013)	0.0257*** (0.0013)	0.0276*** (0.0014)	0.0244*** (0.0013)
$W \cdot \ln(\text{pop}_t)$	0.0108*** (0.0006)	0.0112*** (0.0006)	0.0115*** (0.0006)	0.0106*** (0.0006)
$\ln(\text{lights}_{t-1})$	-0.4387*** (0.0011)	-0.4367*** (0.0011)	-0.4329*** (0.0011)	-0.4379*** (0.0011)
$\rho$	0.0672*** (0.0000)	0.0672*** (0.0000)	0.0676*** (0.0000)	0.0672*** (0.0000)
Observations	507,864	502,026	468,174	506,037

*Note:* \*\*\*, \*\*, \* denote significance at the 1%, 5% and 10% level. All specifications are SDEM and are estimated by Maximum Likelihood. Standard errors in parentheses. Cell and year fixed effects included but not reported. Spatial radius is  $r=80$  km. Yearly weather intensities reflect time-weighted rolling averages over 12 subsequent monthly observations.

<sup>28</sup>If a storm hits multiple cells simultaneously, aggregate spillovers from the neighborhood accumulate.

<sup>29</sup>There might be some interconnection between weather events, such as wind or rainfall. As we are confined to those cells that contain information on all event types, we lose information when combining all types of weather anomalies in one single regression; see Table 3.B.15 in the Appendix. For this reason, we chose not to have the combined regression as our preferred specification, still acknowledging that events might occur simultaneously. The results are similar with some loss of significance. Hence, we are convinced that our wind measure captures storms rather than flooding events, for example.

Next, we look at precipitation anomalies. We find that light growth falls on average by 3.1 percentage points if the yearly precipitation measure increases by one unit. Note that a one-unit increase in precipitation corresponds to a one cell-specific standard deviation more rain *on average* in a given year. This would be rather massive (imagine a month with 12 standard deviations higher than normal rainfall, or three with rainfall at four standard deviations above normal). For this reason, the standard deviation in our rainfall measure is small. Using our estimated lights-to-GDP elasticity, a one standard-deviation increase in the rainfall measure on average leads to a decline in local income growth of 0.17 percentage points. With a one-period lag, the recovery from a one-unit increase in the yearly rainfall measure leads on average to a 2.2 percentage-points increase in lights growth, corresponding to a 0.12 percentage-point increase in local income growth. The one-unit increase in precipitation anomalies in a neighboring cell within 80 km leads on average to spillovers increasing local lights growth by 0.5 percentage points implying a 0.03 percentage-point increase in income growth for a one standard deviation increase in one neighbor's yearly precipitation measure. Finally, we find no significant effect of spatial spillovers in the year after a precipitation event. The qualitative findings resemble those reported by Kocornik-Mina et al. (2020) on city-level flooding effects, who find no local treatment effect on the level of night-light intensity beyond the year of occurrence. Our results show a sign reversal that suggests a similar dynamic pattern at the grid-cell level.<sup>30</sup>

The interpretation of our results for cold spells follows a similar logic. Our unit of measurement is once again expressed in standard deviations from the long-run cell-mean surface temperature. A one-unit increase in our measurement then corresponds to a temperature that is on average one standard deviation below its monthly long-run cell mean. Such a unit increase can thus reflect a very cool summer or a very cold winter, a year with a few extremely cold months or one with consistently cooler monthly average temperatures. In Table 3.5.2, one unit increase in our cold anomaly measure reduces lights growth on average by 7.6 percentage points in the base period and by 3.3 percentage points after one period. The associated declines in local income for a one standard-deviation increase in cold spells, however, are only 0.25 and 0.10 percentage points, respectively. Spatial spillovers suggest that some economic activity is shifted to neighboring locations in the current year, increasing their lights growth on average by 2.2 percentage points (or a 0.07 percentage point increase in local income growth) for a one standard deviation increase in cold spells in one neighboring cell. For the following period, we observe a sign reversal in a similar order of magnitude. For wind, precipitation, and cold-weather anomalies we can thus conclude that the impact on the local economy is negative and statistically and economically significant and that important spatial spillovers typically arise.

---

<sup>30</sup>Note, however, that we do not find a significant sign reversal for the time lag of the spillover, suggesting that spillovers from floods may be more persistent over larger distances than those discussed in Kocornik-Mina et al. (2020), who find no evidence for persistence of relocation of economic activity at the city level.

Results on droughts stand out as different. A one-unit increase in our drought measure, corresponds to a 0.8 percentage point *increase* in local night-light emission, while a neighboring cell experiences a *decrease* in lights by 0.44 percentage points. Both effects turn statistically insignificant in the following year. Note that our unit of droughts is the absolute value of the SPEI index, which combines cell-specific precipitation and evapotranspiration. A one-unit increase in the measure therefore corresponds to a one standard-deviation increase in excessive evapotranspiration relative to a balanced water situation.<sup>31</sup> We are not surprised that the effects of droughts on night light turn out different. First, droughts primarily affect agricultural outcomes but because agricultural production is not necessarily associated with light emission in most parts of the world, an effect on our proxy for economic activity may be small.<sup>32</sup> Second, droughts are often slow-onset events that usually last months or even years. Hence, their effects can be expected to be less concentrated than for events like storms, excessive precipitation, or cold spells. Because of the slow onset, the effects of droughts on economic activity might reveal themselves not immediately within the year of the onset of a drought but rather after some time. However, from an input-output perspective, agricultural production does provide intermediary inputs to light-emitting industrial production and consumption. Hence, agricultural activity may be reflected in night-light emissions associated with consumption and intermediary industry output at the country level. Our high spatial resolution then makes it likely that the shock and its impacts are spatially separated.<sup>33</sup> When droughts depress agricultural output in a grid-cell, it is likely that this reduces consumption and intermediary industry output primarily in nearby urban areas. To test this hypothesis, we classify the data into predominantly urban or non-urban  $0.5^\circ \times 0.5^\circ$  cells (see Appendix 3.A.5 for more details). Table 3.A.5 in the Appendix shows a decomposition of the direct and spillover effects of droughts along this classification. In line with our hypothesis, we find evidence for negative spatial spillovers from rural to nearby urban cells, whereas we find no evidence for spillovers from urban to non-urban cells. There are only weak spillovers between urban neighbours, where the positive direct effect of a drought is nearly three times as large in urban compared to non-urban cells.

Overall, we find clear impacts of weather anomalies on local night light emissions, both in affected cells and in its neighboring cells. We do find that effects across weather shocks differ in magnitude, regarding spillover effects from neighboring cells, and with respect to their effects over time and distance.

---

<sup>31</sup>The SPEI accounts for excess evapotranspiration in the last three months. See Section 3.3.2.

<sup>32</sup>While night-lights typically correlate with activity in the industrial and services sectors (Doll et al., 2006; Ghosh et al., 2010), agriculture (and forestry) emit less or no visible light as they expand (Keola et al., 2015). See Gibson et al. (2021) for a discussion.

<sup>33</sup>Wu et al. (2013) use aggregate night-lights at the country level to estimate the extent to which night-lights implicitly reflect agricultural production. In a sample of 169 countries observed from 1995 to 2009, their results suggest that the agricultural sector accounts for 25% of total light radiance at the country level.

### 3.5.3 Robustness

We have tested the sensitivity of the results and found that the presented patterns are highly robust to a range of alternative approaches and modeling decisions. We start with testing for a variety of sources of sensitivity in the data and our weather intensity variables.

First, the results are largely robust to the well-known problem that the sensors on the satellite do not reliably register light above and below certain threshold values (for a detailed discussion, see Bluhm and Krause, 2018). Excluding pixels for which the sensor was saturated (the maximum value of DN63) in the construction of the dependent variable results in virtually identical results, see panel A of Table 3.5.3.<sup>34</sup> Systematic measurement error also exists at the lower end of recorded light intensity (see Elvidge et al., 2009a). To investigate if bottom coding biases our results, we set all pixels below DN3 to zero in Panel B. Results show that baseline results are robust – except the contemporaneous treatment effect of storms becomes insignificant.

Second, we test the sensitivity of the weather-intensity variables. We start with taking the simple annual mean of monthly weather intensity variables, rather than the rolling average discussed in the data section. Results are reported in panel C of Table 3.5.3, showing similar qualitative findings.<sup>35</sup> Moreover, we consider taking the maximum monthly intensity within a year rather than the average of all 12. This implies focusing only on the most extreme month, such that the focus shifts further to extreme weather events only. Results are comparable in terms of sign and significance; see panel D of Table 3.5.3.<sup>36</sup>

Third, we turn to modeling decisions. Our sensitivity analysis shows that results remain qualitatively robust when including country-specific year fixed-effects; see panel E of Table 3.5.3. While this allows us to control for time-varying country characteristics (e.g., institutions, policies or overall infrastructure), it reduces our degrees of freedom and, importantly, restricts identification to countries beyond a minimum critical geographic size.<sup>37</sup> We therefore refrained from including these in

---

<sup>34</sup>Full results for all robustness checks are reported in Appendix 3.B.

<sup>35</sup>While local effects of storms on light growth decrease slightly in magnitude, results are consistent for precipitation and increase by factor 2.9 for droughts and by 1.2 for cold spells. Spillover effects are consistent for storms, decrease slightly for precipitation and droughts and increase by one-half for cold spells. Generally, results remain unchanged in sign and significance levels, but it also becomes clear that not accounting for the timing of events within the year introduces significant bias in the magnitude of estimated coefficients.

<sup>36</sup>While we gain or lose some statistical significance on some of the weather shocks, one result stands out. For precipitation, the sign reversal on the time lag vanishes, implying that considering more extreme rainfall we find more persistent consequences. Further, the positive spillover coefficient on the time lag is in line with this pattern while we lose statistical significance on the spillover in the contemporaneous period.

<sup>37</sup>After dropping cells from the data set that ever have zero light intensity, and cells that have no neighboring cells (see data section for discussion), some countries contain only a single non-zero cell. This affects some countries that are predominantly dark, and some very small island states. Country-by-year fixed-effects then imply that we lose these observations for identification of our effect of interest.

our baseline model. General patterns on weather shocks also remain qualitatively and quantitatively stable when we test whether weather shocks are interrelated by estimating a model with all four shocks in one regression.<sup>38</sup> Results are reported in Table 3.B.15 in the Appendix. We lose significance only on the negative contemporaneous treatment for wind (potentially due to missing a lot of crucial coastal cells) and the positive spillover for precipitation. Not controlling for first period lags leads the wind effects to be statistically significant in the first period (column [2]) already, while other types of anomalies remain similar to the lag structure in column (1). From this, we conclude that assessing the effects on weather shocks separately does not bias our results. Population may be considered a problematic control variable since it is not well-measured on the timescale of interest. Reassuringly, excluding population as a control variable has virtually no effect on the effects of interest (results reported in Appendix Table 3.B.4). Also, if we exclude temporal lags, results remain robust; see Table 3.B.5 in the Appendix.

Finally, both Strobl (2011) and Hsiang and Jina (2014) emphasize the importance of the potentially non-linear relation between hurricane exposure, wind damage, and the effect on economic growth. Similarly, the relation between temperature shocks and economic activity may also be non-linear, with a threshold above which an impact will occur. We therefore test for non-linearity by estimating squared and cubed weather variables, reported in Tables 3.B.13 and 3.B.14. Overall, the results are robust and very similar to our baseline coefficients. Not surprisingly, and due to the construction of our weather shock measures, magnitudes for the impact of precipitation and cold on night-light growth are very similar to our baseline. Only the positive coefficient on droughts in the contemporaneous period loses statistical significance under the assumption of a quadratic or a cubic intensity variable. Winds drop strongly in magnitudes and the effects of the SPEI index on droughts approximately halve the spillover effects. From this we conclude that the local impact of weather shocks on growth in night-lights is approximately linear. This is in line with Hsiang and Jina (2014), who conclude that local loss in wind damage is linear and that growth effects of cyclone exposure appears to be approximately linear in cyclone intensity.

---

<sup>38</sup>The direct effect of droughts and the spillover effect of precipitation become insignificant, suggesting multicollinearity might be present between the different weather anomaly types.

Table 3.5.3: Sensitivity Results

<b>Dependent Variable: <math>\Delta \ln(\text{lights}_t)</math></b>				
	<b>wind</b>	<b>precip.</b>	<b>drought</b>	<b>cold</b>
<b>PANEL A: Top-Coding: Excluding Top-Coded Pixels</b>				
weather <sub>t</sub>	-0.0019** (0.0009)	-0.0329*** (0.0070)	0.0091* (0.0048)	-0.0752*** (0.0152)
weather <sub>t-1</sub>	-0.0090*** (0.0009)	0.0222*** (0.0069)	0.0012 (0.0048)	-0.0318** (0.0149)
W · weather <sub>t</sub>	-0.0000 (0.0002)	0.0052*** (0.0013)	-0.0046*** (0.0009)	0.0219*** (0.0027)
W · weather <sub>t-1</sub>	0.0008*** (0.0002)	-0.0023* (0.0013)	0.0011 (0.0009)	-0.0200*** (0.0027)
<b>PANEL B: Bottom-coding: Setting Pixels &lt;DN3 to Zero</b>				
weather <sub>t</sub>	-0.0007 (0.0009)	-0.0265*** (0.0070)	0.0082* (0.0048)	-0.0852*** (0.0154)
weather <sub>t-1</sub>	-0.0106*** (0.0009)	0.0290*** (0.0069)	0.0015 (0.0048)	-0.0291* (0.0150)
W · weather <sub>t</sub>	-0.0001 (0.0002)	0.0042*** (0.0013)	-0.0041*** (0.0009)	0.0242*** (0.0027)
W · weather <sub>t-1</sub>	0.0010*** (0.0002)	-0.0022* (0.0013)	0.0007 (0.0009)	-0.0217*** (0.0027)
<b>PANEL C: Simple Annual Mean of Weather Shocks</b>				
weather <sub>t</sub>	-0.0032*** (0.0007)	-0.0289*** (0.0055)	0.0243*** (0.0039)	-0.0613*** (0.0137)
weather <sub>t-1</sub>	-0.0064*** (0.0007)	0.0011 (0.0055)	-0.0060 (0.0038)	-0.0540*** (0.0133)
W · weather <sub>t</sub>	-0.0002 (0.0001)	0.0018* (0.0010)	-0.0037*** (0.0007)	0.0337*** (0.0025)
W · weather <sub>t-1</sub>	0.0008*** (0.0001)	0.0030*** (0.0010)	-0.0000 (0.0007)	-0.0504*** (0.0019)
<b>PANEL D: Maximum Annual Intensity, Non-Weighted</b>				
weather <sub>t</sub>	-0.0004*** (0.0001)	-0.0023** (0.0009)	0.0072*** (0.0017)	-0.0105*** (0.0040)
weather <sub>t-1</sub>	-0.0004*** (0.0001)	-0.0016* (0.0009)	0.0005 (0.0017)	0.0043 (0.0040)
W · weather <sub>t</sub>	-0.0001** (0.0000)	-0.0003 (0.0002)	-0.0017*** (0.0003)	0.0089*** (0.0007)
W · weather <sub>t-1</sub>	0.0001** (0.0000)	0.0006*** (0.0002)	-0.0002 (0.0003)	-0.0115*** (0.0007)
<b>PANEL E: Time Varying Country Characteristics</b>				
weather <sub>t</sub>	0.0004 (0.0010)	-0.0312*** (0.0070)	0.0062 (0.0049)	-0.0360** (0.0179)
weather <sub>t-1</sub>	-0.0049*** (0.0010)	0.0117* (0.0069)	0.0009 (0.0049)	-0.0390** (0.0175)
W · weather <sub>t</sub>	0.0003** (0.0002)	0.0043*** (0.0013)	-0.0041*** (0.0009)	0.0165*** (0.0029)
W · weather <sub>t-1</sub>	0.0009*** (0.0002)	-0.0022* (0.0013)	0.0017* (0.0009)	-0.0144*** (0.0028)

*Note:* \*\*\*, \*\*, \* denote significance at the 1%, 5% and 10% level. All specifications are SDEM and are estimated by Maximum Likelihood. Standard errors in parentheses. Cell and year fixed effects included but not reported in all specifications. Cell and country-year fixed effects included for the time-varying country characteristics analysis but not reported. Spatial radius is r=80 km. Yearly weather intensities reflect time-weighted rolling averages over 12 subsequent monthly observations. Simple annual mean uses non-weighted mean over all monthly observations within a year. Maximum yearly intensities reflect non-weighted maxima within a year.

### 3.5.4 Assessing spillovers across longer distances

To investigate whether spillovers propagate over larger distances, we estimated our baseline model with a doubled radius of 160 kilometers. A radius of 160 km effectively captures the 8 first and 16 second order neighbors of a cell at the equator; the affected area is enlarged from roughly 150km x 150km to 250km x 250km. The results in panel A of Table 3.5.4 show that the magnitude of spillovers declines the further one moves away from the affected grid-cell (full results reported in Appendix Table 3.B.11). This implies that spatial spillovers of weather shocks from neighboring cells are indeed rather local phenomena and their impact declines with distance. Moreover, results on local effects are robust to doubling the neighborhood radius, except for cold spells, where we lose statistical significance of the lagged local effect. For droughts, we find weak evidence of a reversal of the positive effect in the time lag, but also stronger evidence for the aforementioned positive contemporaneous local-treatment effect.

We also present results for the more general Spatial Durbin Model (SDM), which allows spillovers to propagate beyond a cell's local neighborhood.<sup>39</sup> As discussed by Anselin (2013) and Halleck Vega and Elhorst (2015), the SDM model implies a *global* notion of spillover effects as opposed to *local* spillover effects in the SDEM model. A useful feature of the SDM model is that it parameterizes the global spillover effect and thus allows us to assess the average decline of spillovers over distance.

Equation 3.5.1 presents the global spillover model:

$$\Delta \ell_t = \ell_{t-1}\gamma + \lambda \mathbf{W}^r \Delta \ell_t + \mathbf{D}_t \beta^0 + \mathbf{X}_t \delta^0 + \mathbf{W}^r \mathbf{D}_t \beta^1 + \mathbf{W}^r \mathbf{X}_t \delta^1 + \nu + \pi + \varepsilon_t \quad (3.5.1)$$

Using  $(\mathbf{I} - \lambda \mathbf{W})^{-1} = \mathbf{I} + \lambda \mathbf{W} + \lambda^2 \mathbf{W}^2 + \lambda^3 \mathbf{W}^3 + \dots$ , direct effects are reflected in the diagonal and spillovers in the off-diagonal elements of  $(\mathbf{I} - \lambda \mathbf{W})^{-1}[\beta^0 + \mathbf{W} \beta^1]$  and  $\lambda$  is the spatial autoregressive coefficient from equation (3.5.1), which quantifies the degree to which spillovers propagate from one cell to the next.

Table 3.5.4 panel B reports the mean-direct effect, obtained by averaging over all diagonal elements, in square brackets. These effects are comparable to our local effects of respective weather shocks in the SDEM baseline specification.<sup>40</sup> Spillover

---

<sup>39</sup>A potential advantage of this approach is that it explicitly enforces global compliance with the stable unit treatment value assumption (SUTVA) by allowing observational units not only to interfere within an exogenously defined neighborhood, but across all contiguous locations. Explicit SUTVA enforcement in local spillover models is confined to observational units defined as local neighbors, implying compliance beyond the local neighborhoods by assumption. The similarity of point estimates presented for SDM and SDEM specifications provides support that SUTVA violation is not a concern in the baseline model. The disadvantage of the SDM model, however, is that local and global spillover components cannot be disentangled, while it is exactly the local spillover component that we are most interested in. Moreover, potential ripple effects by construction stop wherever there are 'holes' in the grid, as is the case when a cell has no economic activity in it. How this affects our results is untractable. We therefore prefer the SDEM over the SDM model for our application.

<sup>40</sup>The row-wise mean across all connected (non-sparse) off-diagonal elements corresponds to, but has a very different interpretation than the spillover coefficient in our baseline results. The row-wise mean captures how a cell is affected if any other cell, which is part of its contiguously connected spatial neighborhood, is affected by a weather shock.

Table 3.5.4: Spillovers Across Longer Distances

Dependent Variable: $\Delta \ln(\text{lights}_t)$				
	wind	precip.	drought	cold
<b>PANEL A: Radius r=160km</b>				
weather <sub>t</sub>	-0.0016** (0.0007)	-0.0249*** (0.0057)	0.0125*** (0.0041)	-0.0849*** (0.0136)
weather <sub>t-1</sub>	-0.0052*** (0.0007)	0.0158*** (0.0057)	-0.0075* (0.0040)	-0.0129 (0.0133)
W · weather <sub>t</sub>	-0.0000 (0.0000)	0.0008** (0.0004)	-0.0015*** (0.0003)	0.0061*** (0.0009)
W · weather <sub>t-1</sub>	0.0001* (0.0000)	-0.0000 (0.0004)	0.0005* (0.0003)	-0.0060*** (0.0008)
<b>PANEL B: Global Spillovers</b>				
weather <sub>t</sub>	-0.0046*** [-0.0044] (0.0007)	-0.0279*** [-0.0259] (0.0060)	-0.0016 [-0.0029] (0.0041)	-0.0974*** [-0.0794] (0.0122)
weather <sub>t-1</sub>	-0.0095*** [-0.0093] (0.0007)	0.0198*** [0.0189] (0.0059)	0.0017 [0.0017] (0.0041)	-0.0858*** [-0.0908] (0.0119)
W · weather <sub>t</sub>	0.0005*** [0.0000] (0.0001)	0.0037*** [0.0001] (0.0009)	-0.0010* [-0.0001] (0.0006)	0.0217*** [0.0010] (0.0017)
W · weather <sub>t-1</sub>	0.0008*** [0.0000] (0.0001)	-0.0021** [-0.0001] (0.0009)	-0.0001 [0.0000] (0.0006)	0.0015 [-0.0003] (0.0017)
λ	0.0671*** (0.0000)	0.0671*** (0.0000)	0.0675*** (0.0000)	0.0671*** (0.0000)

*Note:* \*\*\*, \*\*, \* denote significance at the 1%, 5% and 10% level. All Panel A is SDEM, Panel B is SDM. All regressions are estimated by Maximum Likelihood. Standard errors in parentheses. Cell and year fixed effects included but not reported in all specifications. Spatial radius is r=160 km in Panel A and r=80km in Panel B. Yearly weather intensities reflect time-weighted rolling averages over 12 subsequent monthly observations. Global Spillovers show average effects translated with spatial multiplier in square brackets. Full results are shown in Tables 3.B.11 and 3.B.12 in the Appendix.

coefficients have the same signs and statistical significance, while the small estimate for  $\lambda$  indicates that spillover effects dissipate fast in space (full results on global spillovers are reported in Table 3.B.12). In conclusion, the results on both the increased radius for the SDEM model and the global spillovers in the SDM model show that spillover effects of weather events are mostly local and vanish quickly beyond an 80-km radius.



### 3.5.5 Heterogeneity over development levels

Our focus has been on the global average impact of local weather shocks. As some countries or regions are better able and prepared to handle weather anomalies than others, such an approach could hide important heterogeneity (see e.g. Raddatz, 2007; Noy and Nualsri, 2011; Dell et al., 2012). We have estimated our models including country- and year-fixed effects for a global panel of cells to prevent this heterogeneity from biasing our estimates. However, to gain a more intuitive understanding of our results, this section explores heterogeneity across income groups. Richer countries tend to be better equipped to handle shocks because income directly affects their willingness and ability to pay to prevent negative impacts. In higher income regions one would also expect higher opportunity costs of allowing weather anomalies to disrupt economic activity. Moreover, income may proxy for a host of other relevant characteristics of affected cells, such as institutional quality, risk attitudes, and government effectiveness. We first classify all cells depending on whether they belong to high- or low- (and middle-) income countries.<sup>41</sup>

To estimate the effects, we include interaction terms of the local weather shock and its spatial spillovers for cells classified as low and middle income. Resulting coefficients show by how much the treatment effects in low- and middle-income countries differ from those in high-income countries. Table 3.5.5 shows the combined effects obtained from these interaction regressions.

Our estimates suggest that negative wind effects are driven by cells located in low- and middle-income countries in the year of occurrence and thereafter. Moreover, the lagged negative effect in low- and middle-income cells is nearly three times larger than in high-income cells. This finding strongly resembles that of Berlemann and Wenzel (2018), who similarly find negative GDP growth effects of hurricanes to be driven entirely by developing countries. Positive lagged spatial spillover effects appear for all income levels, but are also 50% stronger in poorer cells. For excessive precipitation and cold spells, the negative treatment and positive spillover effects are entirely driven by low- and middle-income cells. In fact, for cold spells in high-income cells we now find an increase in lights growth in the period of occurrence and negative growth thereafter, with negative spillovers in the following year. The positive local treatment effect on droughts also appears exclusively in cells of low- and medium-income countries, as does the direct negative spillover effect. Overall, this provides strong evidence that our baseline local average treatment and spillover effects are generally driven by cells in low- and middle-income countries. In line with expectations, most of our baseline results disappear and, for cold spells, they even reverse for cells in high-income countries. This may be due to better preparedness in the case of weather anomalies and corresponds well to earlier findings in the literature that developing and poor countries are vulnerable to the impact of weather anomalies (cp. Raddatz, 2007; Noy and Nualsri, 2011; Dell et al., 2012). These results also indicate that the income dimension warrants further research.

---

<sup>41</sup>The binary categorisation of income groups follows World Bank lending groups from the year 2000. Cells in high income countries account for 31% of the sample, while those in low and middle income countries account for the remaining 69%.

Table 3.5.5: Income Group Heterogeneity, Combined Effects

Dependent Variable: $\Delta \ln(\text{lights}_t)$				
	wind	precip.	drought	cold
<b>high income</b>				
weather <sub>t</sub>	-0.0015 (0.0016)	0.0171 (0.0118)	-0.0120 (0.0093)	0.2442*** (0.0389)
weather <sub>t-1</sub>	-0.0042*** (0.0015)	0.0249** (0.0117)	0.0081 (0.0092)	-0.0680* (0.0384)
W · weather <sub>t</sub>	-0.0001 (0.0003)	0.0015 (0.0021)	-0.0020 (0.0016)	0.0077 (0.0059)
W · weather <sub>t-1</sub>	0.0006** (0.0003)	-0.0040* (0.0021)	0.0029* (0.0016)	-0.0224*** (0.0059)
<b>low and middle income</b>				
weather <sub>t</sub>	-0.0021* (0.0011)	-0.0534*** (0.0087)	0.0147*** (0.0056)	-0.1133*** (0.0169)
weather <sub>t-1</sub>	-0.0119*** (0.0011)	0.0192** (0.0085)	-0.0010 (0.0055)	-0.0193 (0.0165)
W · weather <sub>t</sub>	0.0001 (0.0002)	0.0064*** (0.0016)	-0.0052*** (0.0011)	0.0191*** (0.0031)
W · weather <sub>t-1</sub>	0.0009*** (0.0002)	-0.0007 (0.0016)	0.0000 (0.0010)	-0.0170*** (0.0030)
Observations	506,142	500,787	467,691	504,525

*Note:* \*\*\*, \*\*, \* denote significance at the 1%, 5% and 10% level. All specifications are SDEM and are estimated by Maximum Likelihood. Cell and year fixed effects and controls as in baseline included but not reported. Spatial radius is  $r=80$  km. Yearly weather intensities reflect time-weighted rolling averages over 12 subsequent monthly observations. Estimates present combined effects, adding up coefficients from interaction terms. Significance levels are obtained using a two-sided t-test. Full regressions in Table 3.B.16.

### 3.6 Conclusion

We presented a new data set, the gridded GAME-LIGHTS database, which allows us to analyze the economic impacts of weather anomalies at the grid-cell level. We compiled this data set by matching data on weather-related events to data on night-time light emissions as a proxy for local economic activity. The resulting data set contains a balanced panel of over 24,000 grid-cells with a resolution of  $0.5^\circ \times 0.5^\circ$  (approximately  $55 \times 55$  km at the equator) covering the land area of 197 countries from 1992 to 2013. Using spatial econometric panel techniques, we analyze this data and provide new evidence on the local impact and spillover effects of various types of weather events on the growth of night-time light emissions.

Controlling for a set of year- and cell-fixed effects and accounting for spatial autocorrelation in the error term, results show that storms, cold spells, and precipitation anomalies all tend to reduce local light growth and have positive contemporaneous or lagged spatial spillover effects within an 80-km radius. These effects are

economically significant. Using a lights-to-GDP elasticity of 0.37, we show that a one-standard deviation increase in wind speeds reduces income growth by 0.33 percentage points, whereas a one-standard deviation increase in precipitation or decrease in temperature will decrease local income growth by 0.17 or 0.25 percentage points, respectively. Local income growth rebounds in the case of precipitation anomalies, whereas it decreases further after a cold spell, and spatial spillover effects are positive for both types of events. In contrast, the link between local light emission and droughts is weakly positive, with negative spillovers on neighbor cells. That result is mostly driven by urban cells, where droughts cause light emissions to rise, while spillovers from rural to urban cells are negative. Finally, our results show that cells in low- and medium-income countries tend to respond more to weather anomalies than high-income countries.

Concluding, we can draw some important practical implications from our results. First, it seems only fair that high-income countries lead climate-mitigation efforts. Arguably, they are the primary source of greenhouse gas emissions causing climate change while especially low- and middle-income countries will suffer the consequences. Our results also imply that the latter should contribute to the global fight against climate change in their own self-interest. Moreover, as weather anomalies cause mostly positive spillovers and are generally localised phenomena it would be efficient to finance climate adaptation policies regionally. That is, by pooling the risks in a region spanning multiple cells, the positive spillovers can help cushion the negative impacts in an affected cell. Moreover, extensive insurance coverage of weather-related damages should be economically feasible even if the portfolio is spread over a relatively small area.

Our biggest contribution, however, is to break ground for future research by providing a global data set for analysing the impact of exogenous shocks to local economies and the spatial distribution of economic activity. As we have indicated, model predictions are still ambiguous and imprecise. Our results can guide future theory development in this area while our data allow for more rigorous empirical testing. Next steps could include investigating what mechanism dominates in causing spatial spillovers at the local level or how various economic factors, households, or firms react to the weather anomalies studied here. As indicated, the dimension of income and development levels warrants special attention in this respect. This allows future research to generate more precise theories and more detailed policy implications on local private insurance, regional public adaptation, or international climate-change mitigation mechanisms.

#### **Addendum to the published paper:**

As this chapter went through the revision and publication process, together with Thomas Steinwachs and Jasmin Gröschl I have taken some first steps of our proposed research agenda concerning the mechanisms that may explain the observed spatial spillovers. We are interested in answering to what extent connectivity between cells in our study drives the spillover effects that we identify in Chapter 3. Preliminary results are presented in a working paper that is not part of this dissertation (this working paper is available as a CESifo Working Paper; see Gröschl et al., 2020). We

combine the presented GAME-LIGHTS database with global geographic information on international borders and road networks. Using the same identification strategy as in this chapter, we first split neighborhoods (i.e. the  $\mathbf{W}^r$  spatial weights matrix) in their respective national parts and study border effects. In a second and more flexible approach, we use weights of the amount of (major) road connections between cells as a measure of connectedness, and estimate how connectedness affects the previously estimated global average spillover effects by type of weather anomaly. Results are promising and suggest that the global average spillovers that we identify in this chapter indeed follow sensible economic channels. First, international borders limit economic relocation due to extreme weather to domestic neighboring cells. Second, the existence of major road connections between cells are key drivers of spatial spillover effects. Without a transport network between cells, we identify essentially no spatial spillovers. At the time of writing, research efforts in this area are therefore promising and I put it on the agenda for future research.

## 3.A Descriptives and background

### 3.A.1 Background information: DMSP night light data

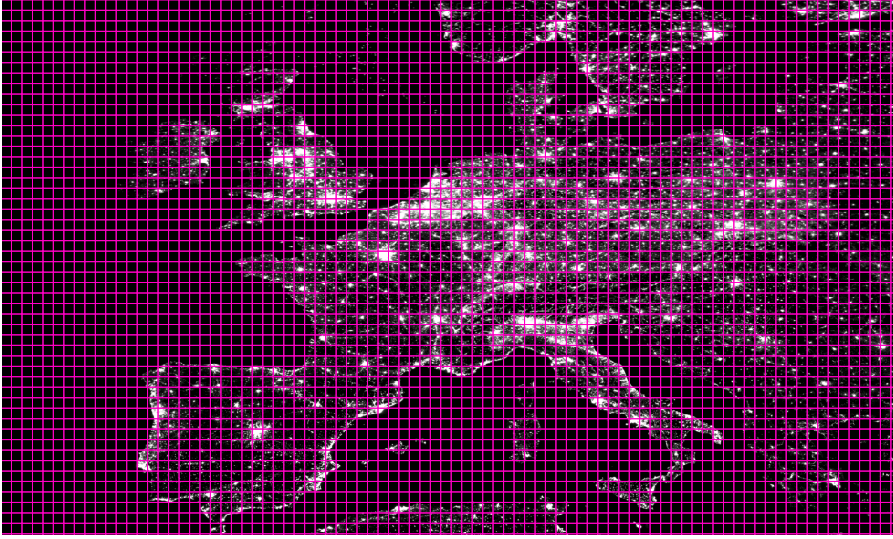
The United States Air Force DMSP satellites were originally used to detect moonlit clouds, with lights from human settlements being a byproduct that is recorded by the DMSP Operational Linescan System sensor on-board. Figure 3.A.1 shows the grid and raw data for Western Europe. The sensor records light intensity with a DN between 0 and 63. Satellites have been observing every location of the planet daily between 8.30 pm and 10 pm local time between 1992 and 2013. Each satellite orbits the earth 14 times a day and thus ensures global coverage every 24 hours (Doll, 2008). The satellites have a 3000 km swath, from which data of the center half is used to produce images at a nominal resolution of 0.56 km. The data are smoothed on-board to produce an average of  $5 \times 5$  pixel blocks resulting in a data resolution of approximately 2.7 kilometers at the equator. After smoothing, the data are delivered at a resolution of 30 arc seconds, representing half a minute, or 1/120th of a degree. This gives data for approximately 0.86 square kilometers at the equator, with surface area decreasing in absolute terms when moving away from the equator.

The Earth Observation Group of NOAA then processes the raw data using an advanced algorithm, which cleans the raw data. Lights from the center half of the 3000 km swath are selected because these have better geo-location, are smaller and have more consistent radiometry (Earth Observation Group, 2016). Sunlit data and glare are then excluded based on the solar elevation angle and similarly moonlit data is excluded on basis of the moonlit half of the lunar cycle. Subsequently, only cloud-free observations are included and lighting features from the aurora are excluded from the data (Baugh et al., 2010). The exclusion of aurora lighting concerns high-latitude zones and affects approximately 10,000 people or 0.0002% of the world population (Henderson et al., 2012). Finally, ephemeral events such as forest fires and other background noise are removed to produce stable average visible light products that reflect annual average human produced light emission into space at a 30 arc second resolution between 65°South and 75°North (Earth Observation Group, 2016).

The average number of valid nights for a given cell in the satellite-years is 41.4 and typically ranges between 20 to 100. The share of unlit pixels ranges from only 1% in the Netherlands to 99.47% and 99.89% for the sparsely populated countries Mozambique and Canada (Henderson et al., 2012, pp. 1000). A contrasting example to Mozambique and Canada can be found when comparing Bangladesh and the Netherlands. Both have high population density, Bangladesh having twice the density of the Netherlands with an average of 1,080 people per square km between 1992–2008. Yet, average light intensity is only 2 for Bangladesh, whereas it is 23.5 in the Netherlands. With GDP per capita (purchasing power parity, constant 2005 US Dollars) being 35 times higher in the Netherlands, this indicates that light intensity informs not only about whether there is human life present in a certain area, but also about the relative income per capita (see, e.g., Elvidge et al., 2009b; Ghosh

et al., 2010).

Figure 3.A.1: Nightlight emission of Europe and 0.5° grid-cells



*Note:* night-light data cleaned and prepared as described. Raw data comes from satellite F182010.

A direct comparison of average light intensity can be misleading if population size in a given area is not taken into account: The average light intensity of Canada is lower than that of Bangladesh while income per capita is much higher in Canada. Moreover, light usage per person may vary across countries due to cultural differences in night-light use and customs of timing of economic activity across day and night. This is why Henderson et al. (2012) stress that night-light intensity is better used as a proxy for income growth rather than income levels.

### 3.A.2 Interpolation of wind speeds

Using the algorithm by Hiemstra et al. (2008), we classify the data into bins by breaking up distances  $\mathbf{d}$  between all point locations of weather stations. For each distance bin  $\bar{\mathbf{d}}$ , the cross-sectional empirical (or experimental) semi-variance of observed maximum wind speeds across  $n$  observations at any given point in time is defined by equation (3.A.1).  $z(x_i)$  is a set of random variables, representing the respective wind speeds in any given location  $x_i$ . By assumption, the correlation between two random variables  $z(x_i)$ ,  $z(x_j)$  depends only on their bilateral spatial distance, irrespective of their location (i.e., stationarity of the second moment of  $z(x_i)$ ). Thus,  $z(x_i + \bar{\mathbf{d}})$  captures the wind speed realizations observed  $\bar{\mathbf{d}}$  distance units away from location  $x_i$ .

$$\hat{\gamma}(\bar{\mathbf{d}}) = \frac{1}{2} \cdot \frac{1}{n(\bar{\mathbf{d}})} \sum_{i=1}^{n(\bar{\mathbf{d}})} (z(x_i + \bar{\mathbf{d}}) - z(x_i))^2 \quad (3.A.1)$$

Since the empirical semi-variogram cannot be computed at all possible distances  $\mathbf{d}$ , we fit a model function for each period for which parameters are fully determined

by the data. The best fit in line with the experimental semi-variogram is achieved by the Stein (1999) parametrization of the Matérn model<sup>42</sup> (3.A.2) with gamma function  $\Gamma$  and a modified Bessel function  $K_\nu$ . The nugget (the intercept of the fit) is fixed at zero.<sup>43</sup>  $\sigma^2$  is the so-called *sill* of the model, which under stationarity of the second moment is simply an estimate of the variance  $Var[z(x_i)]$ .  $\nu$  and  $\kappa$  are non-negative smoothing and range parameters, respectively. All parameters are determined by available global wind speed data for any given month.

$$\gamma(\mathbf{d}) = \begin{cases} 0 & \text{if } |\mathbf{d}| = 0 \\ \sigma^2 \left[ 1 - \frac{1}{2^{\nu-1}\Gamma(\nu)} \left( 2 \frac{|\mathbf{d}|\sqrt{\nu}}{\kappa} \right)^\nu K_\nu \left( 2 \frac{|\mathbf{d}|\sqrt{\nu}}{\kappa} \right) \right] & \text{if } 0 < |\mathbf{d}|, \nu > 0 \end{cases} \quad (3.A.2)$$

The resulting functional fit increases monotonically as a function of distance and is deployed to spatially interpolate the maximum wind speed for any location on the global grid. Note that this interpolation technique allows mapping recorded wind speeds to surrounding locations. For areas that are very sparsely covered with weather stations, this inevitably results in a smoothing effect over larger distances. This introduces a downward bias in the recorded wind speeds: obtained estimates may be considered a lower bound. We achieve full global coverage by using all stations within a search radius of 2,000 km as predictors. Figure 3.A.3 shows the semi-variogram obtained for June 2012. Figure 3.A.4 visualizes the corresponding spatially interpolated maximum wind speeds and Figure 3.A.5 assesses the fit of these predicted values, using a leave-one-out technique. Figure 3.A.5 shows the intrapolated windspeeds with the alternative method using inverse distance weighting, resulting in a very spiked pattern.

---

<sup>42</sup>We test five different variogram models (spherical, exponential, Gaussian, Matérn, and M. Stein's parametrization of the Matérn model). Note that the Matérn model includes the exponential model as a special case and the Gaussian model as a limit case ( $\nu \lim \inf$ ).

<sup>43</sup>A zero nugget constrains deviation of predicted from preserved values at very short distances.

Figure 3.A.2: Balancing Wind Speeds – Cells lost when balancing on non-interpolated wind speed data are shown in red.

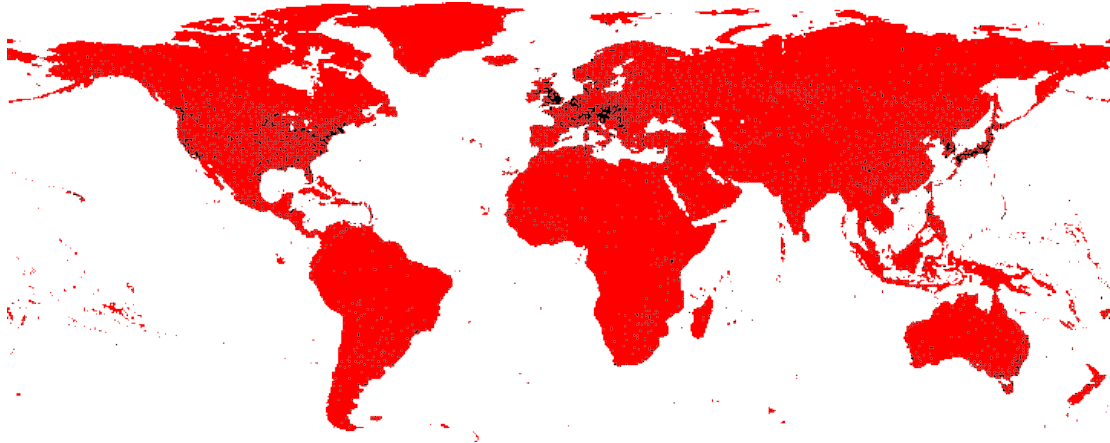


Figure 3.A.3: Semi-Variogram for June 2012. Distance in meters, value labels report the number of bilateral station-distance-pairs per bin.

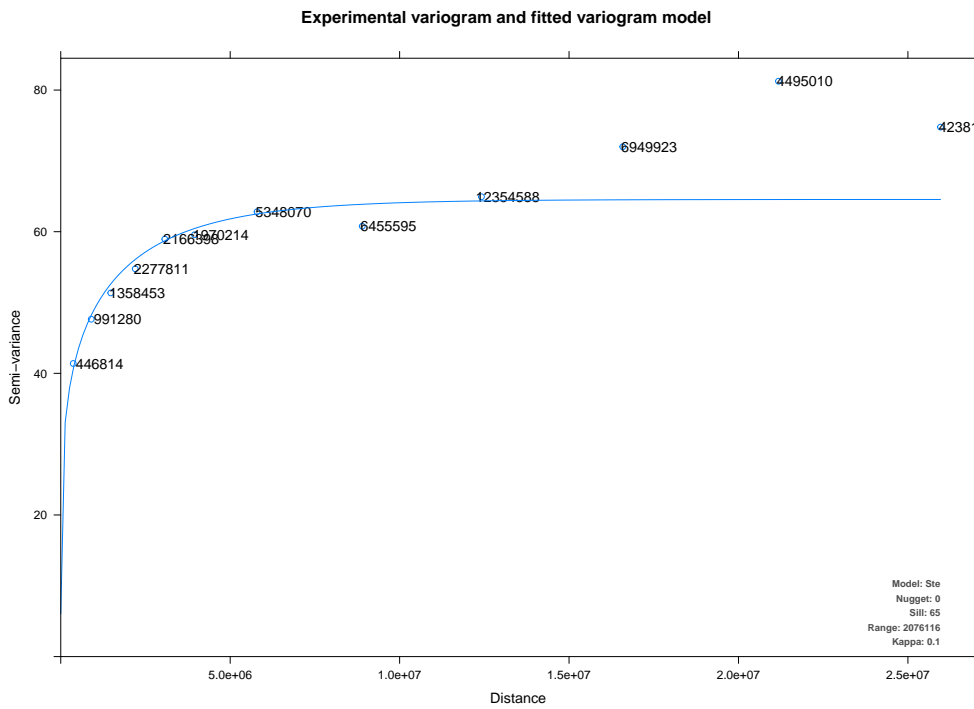




Figure 3.A.4: Kriged maximum wind speed in June 2012

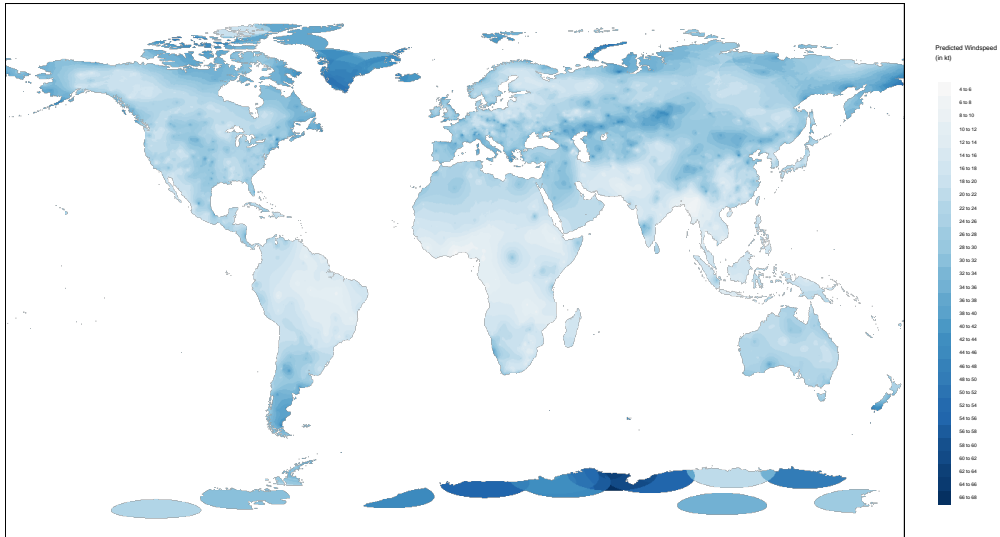


Figure 3.A.5: Goodness of fit – Standard deviation of Kriged maximum wind speed (in kt) in June 2012, obtained using the ‘leave one out’ technique.

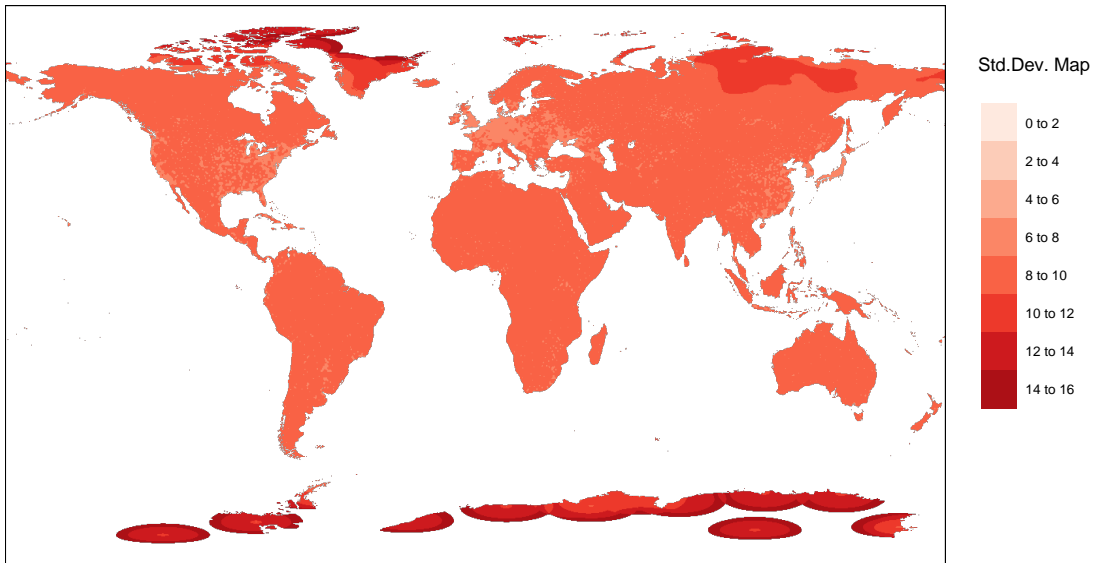
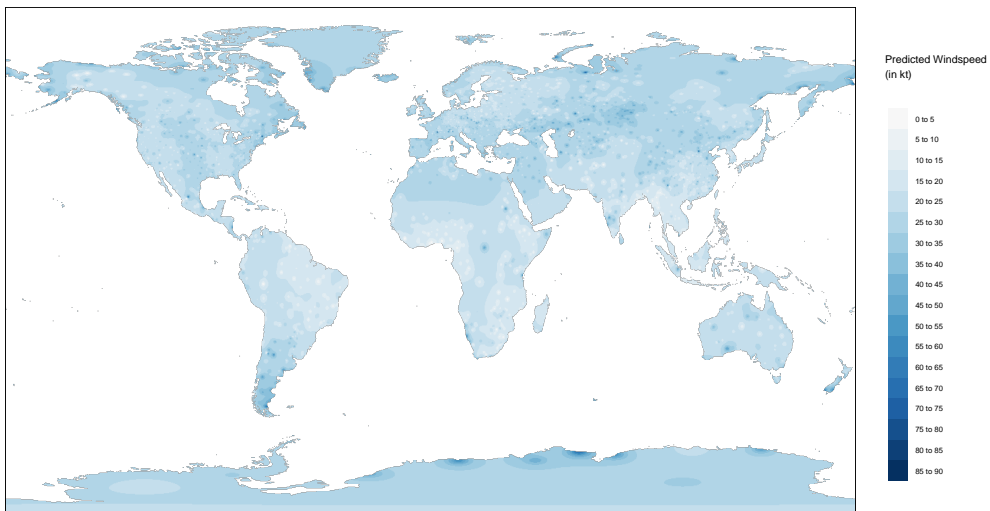
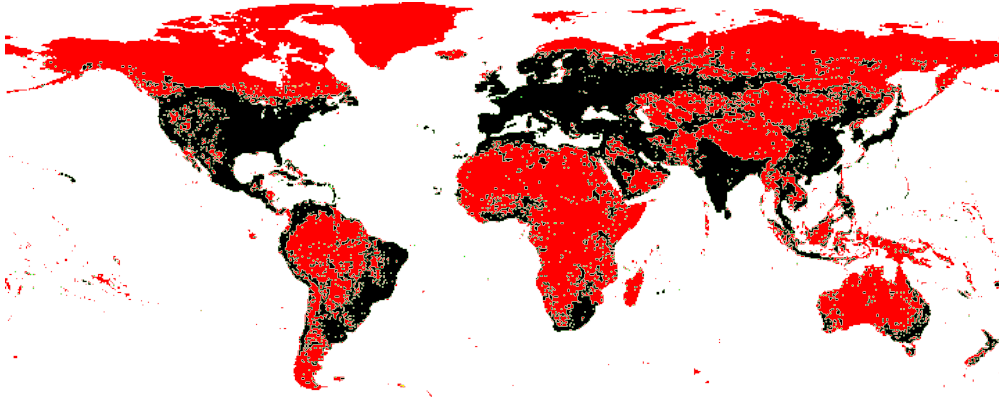


Figure 3.A.6: Spiked pattern obtained with inverse distance weighting as alternative choice of wind speed interpolation.



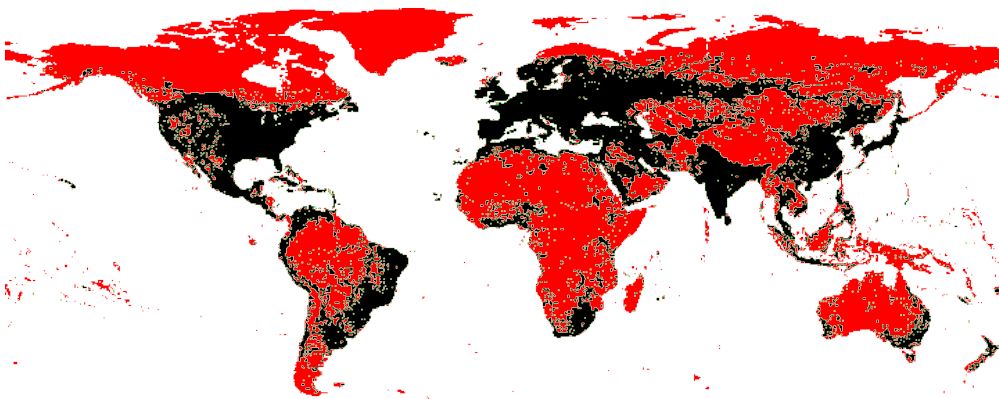
### 3.A.3 Balancing

Figure 3.A.7: Balanced Panel - Wind



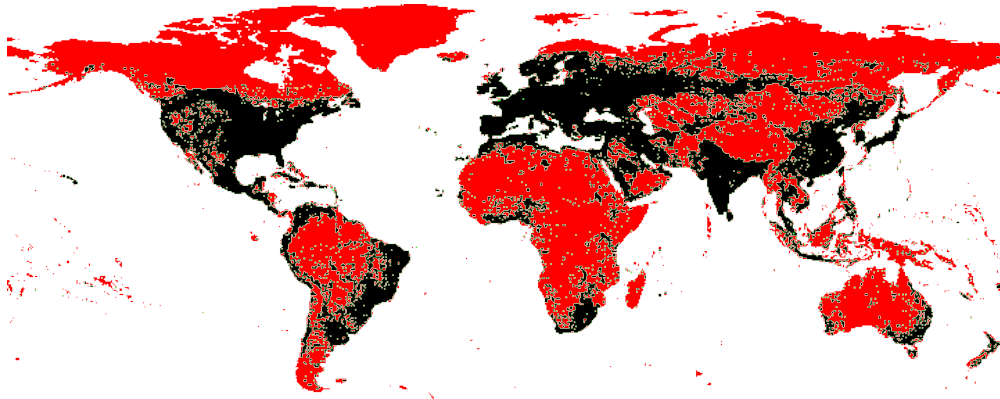
*Note:* Global distribution of grid-cells preserved in balanced panel. Physical indicators used for balancing: Winds. Red: Dropped because of zero absolute light emission in at least one period. Yellow: Dropped because of zero population in at least one period. Green: Dropped because no neighbors found within 80 km radius, or because of singleton country. Black: Preserved, i.e., balanced and consecutive with at least one neighbor each and at least two cells per country. Number of years: 21. Number of preserved cells: 24,184.

Figure 3.A.8: Balanced Panel - Temperature



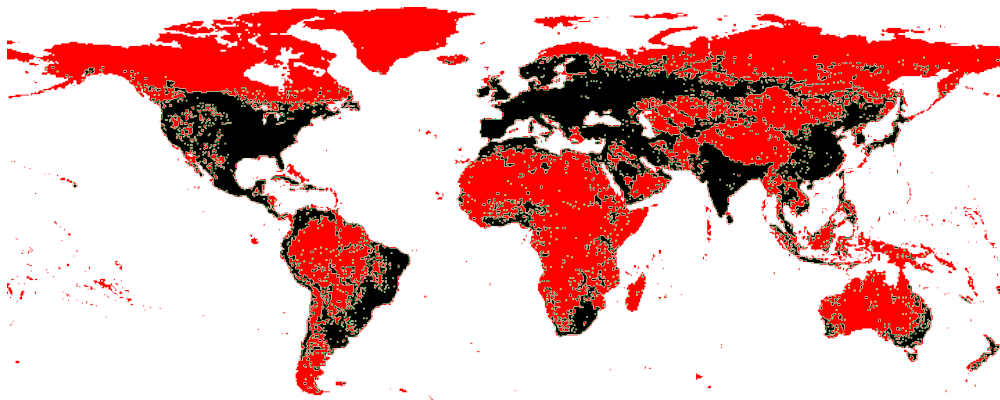
*Note:* Global distribution of grid-cells preserved in balanced panel. Physical indicators used for balancing: Temperature. Red: Dropped because of zero absolute light emission in at least one period and because of missing values in the physical intensity measure. Yellow: Dropped because of zero population in at least one period. Green: Dropped because no neighbors found within 80 km radius, or because of singleton country. Black: Preserved, i.e., balanced and consecutive with at least one neighbor each and at least two cells per country. Number of years: 21. Number of preserved cells: 24,097.

Figure 3.A.9: Balanced Panel - Precipitation



*Note:* Global distribution of grid-cells preserved in balanced panel. Physical indicators used for balancing: Precipitation. Red: Dropped because of zero absolute light emission in at least one period and because of missing values in the physical intensity measure. Yellow: Dropped because of zero population in at least one period. Green: Dropped because no neighbors found within 80 km radius, or because of singleton country. Black: Preserved, i.e., balanced and consecutive with at least one neighbor each and at least two cells per country. Number of years: 21. Number of preserved cells: 23,906.

Figure 3.A.10: Balanced Panel - Drought



*Note:* Global distribution of grid-cells preserved in balanced panel. Physical indicators used for balancing: Drought. Red: Dropped because of zero absolute light emission in at least one period and because of missing values in the physical intensity measure. Yellow: Dropped because of zero population in at least one period. Green: Dropped because no neighbors found within 80 km radius, or because of singleton country. Black: Preserved, i.e., balanced and consecutive with at least one neighbor each and at least two cells per country. Number of years: 21. Number of preserved cells: 22,294.

### 3.A.4 Supplementary descriptive statistics

Table 3.A.1: Summary Statistics

<b>statistic</b>	<b>n</b>	<b>mean</b>	<b>st. dev.</b>	<b>min</b>	<b>max</b>
$\Delta \ln(\text{lights})$	507,864	0.045	0.392	-8.246	8.217
$\Delta \ln(\text{lights NTC})$	468,111	0.046	0.394	-8.139	8.109
$\Delta \ln(\text{lights} \leq \text{DN55})$	507,528	0.048	0.402	-0.030	8.002
$\Delta \ln(\text{lights} \geq \text{DN3})$	507,024	0.045	0.397	-8.246	8.217
$\Delta \ln(\text{lights} \geq \text{DN8})$	390,957	0.045	0.483	-8.311	8.424
$\ln(\text{lights})$	507,864	0.264	1.724	-7.090	4.142
$\ln(\text{lights NTC})$	468,111	0.135	1.672	-7.090	4.093
$\ln(\text{pop}_t)$	507,864	10.639	2.165	-14.390	16.822
<b>time-weighted physical intensities</b>					
wind	507,864	20.766	4.486	5.478	46.528
cold	506,037	0.412	0.089	0.000	1.271
precip.	502,026	0.385	0.151	0.000	1.697
drought	468,174	0.387	0.242	0.000	2.305
<b>simple mean of yearly physical intensities</b>					
wind	507,864	20.735	4.552	4.957	48.036
cold	506,037	0.410	0.093	0.000	1.372
precip.	502,026	0.386	0.182	0.000	1.841
drought	468,174	0.386	0.277	0.000	2.322

Table 3.A.2: Summary Statistics of Satellite-Years for Nighttime Lights

Satellite-Year	DN							Cloud-Free Nights
	0	1–2	3–8	9–15	16–25	26–62	63	(Mean)
F101992	84.97%	0.00%	4.00%	1.89%	0.73%	0.85%	0.09%	15.2
F101993	86.34%	0.00%	6.19%	1.65%	0.70%	0.86%	0.00%	31.2
F101994	86.39%	0.00%	6.21%	1.58%	0.69%	0.89%	0.10%	14.7
F121995	84.97%	0.00%	6.26%	1.92%	0.84%	1.08%	0.10%	40.9
F121996	84.79%	0.00%	6.58%	1.82%	0.82%	1.04%	0.09%	40.2
F121997	84.81%	0.00%	5.90%	1.99%	0.85%	1.10%	0.11%	36.3
F121998	82.93%	0.00%	6.01%	2.25%	0.93%	1.18%	0.12%	40.2
F141999	78.35%	0.03%	7.65%	1.45%	0.66%	0.89%	0.08%	37.1
F152000	84.64%	0.00%	7.19%	2.31%	0.92%	1.15%	0.11%	48.7
F152001	81.82%	0.00%	7.49%	2.11%	0.89%	1.15%	0.09%	47.1
F152002	84.02%	0.00%	7.52%	2.19%	0.91%	1.19%	0.09%	53.4
F152003	82.19%	0.19%	8.24%	1.30%	0.63%	0.86%	0.06%	45.8
F152004	84.56%	0.52%	8.57%	1.27%	0.62%	0.89%	0.05%	53.9
F152005	83.91%	0.61%	8.90%	1.37%	0.69%	0.95%	0.06%	59.4
F152006	84.23%	0.56%	8.63%	1.36%	0.67%	0.96%	0.06%	51.6
F162007	84.16%	0.00%	8.16%	1.99%	0.87%	1.20%	0.09%	53.7
F162008	84.32%	0.00%	8.08%	1.92%	0.86%	1.19%	0.10%	47.4
F162009	85.55%	0.00%	6.74%	1.90%	0.87%	1.17%	0.12%	32.0
F182010	83.11%	0.00%	6.43%	3.39%	1.47%	1.87%	0.18%	54.6
F182011	83.56%	0.00%	7.85%	2.44%	1.06%	1.44%	0.14%	54.6
F182012	84.25%	0.00%	6.06%	2.89%	1.20%	1.59%	0.17%	49.4
F182013	84.61%	0.00%	6.16%	2.83%	1.16%	1.57%	0.16%	58.8

*Note:* Summary statistics are provided for post-cleaning night light satellite-years. Light pixels are considered only on-land, not in gas-flaring zones and not in vicinity of volcanoes (see data section). Exception: The mean number of cloud-free nights is constructed using the raw data product, as downloaded from NOAA.

Table 3.A.3: Lights to GDP Growth Rate Elasticity

Dependent Variable:	ln(GDP in const. LCU)	ln(pop density)
ln(light)	0.348*** (0.092)	0.369*** (0.069)
ln(GDP in const. LCU)		0.132*** (0.031)
adj. $R^2$	0.999	0.998
within $R^2$	0.240	0.273
$N$	3229	4167

*Note:* \*\*\*, \*\*, \* denote significance at the 1%, 5% and 10% level. All models use panel OLS. Standard errors (in parentheses) are robust to heteroskedasticity. Country and year fixed effects included but not reported. Years 1992–2008 in first column, 1992–2013 in remaining columns. 197 countries in sample.

Figure 3.A.11: Kernel Densities of Monthly Physical Intensities

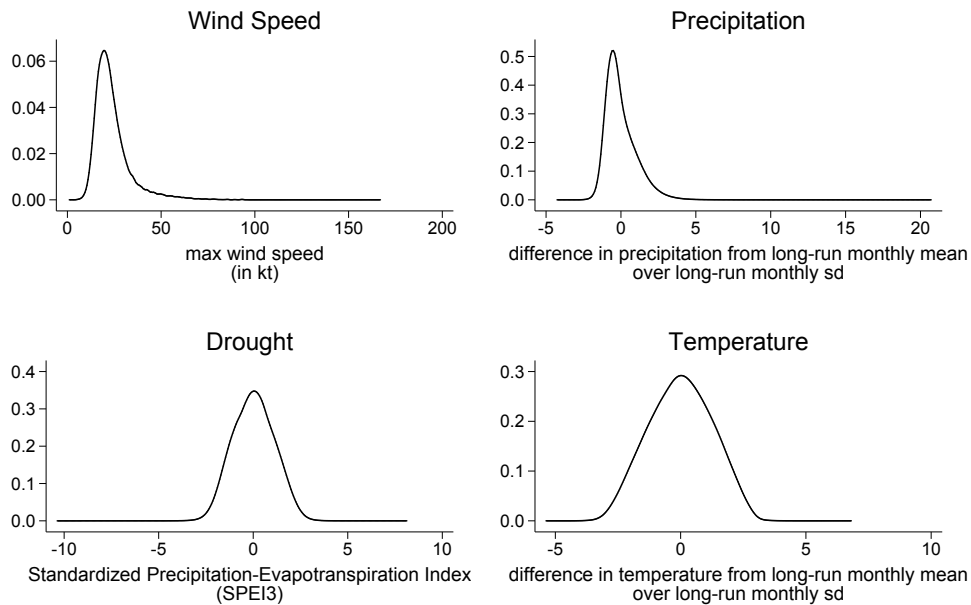


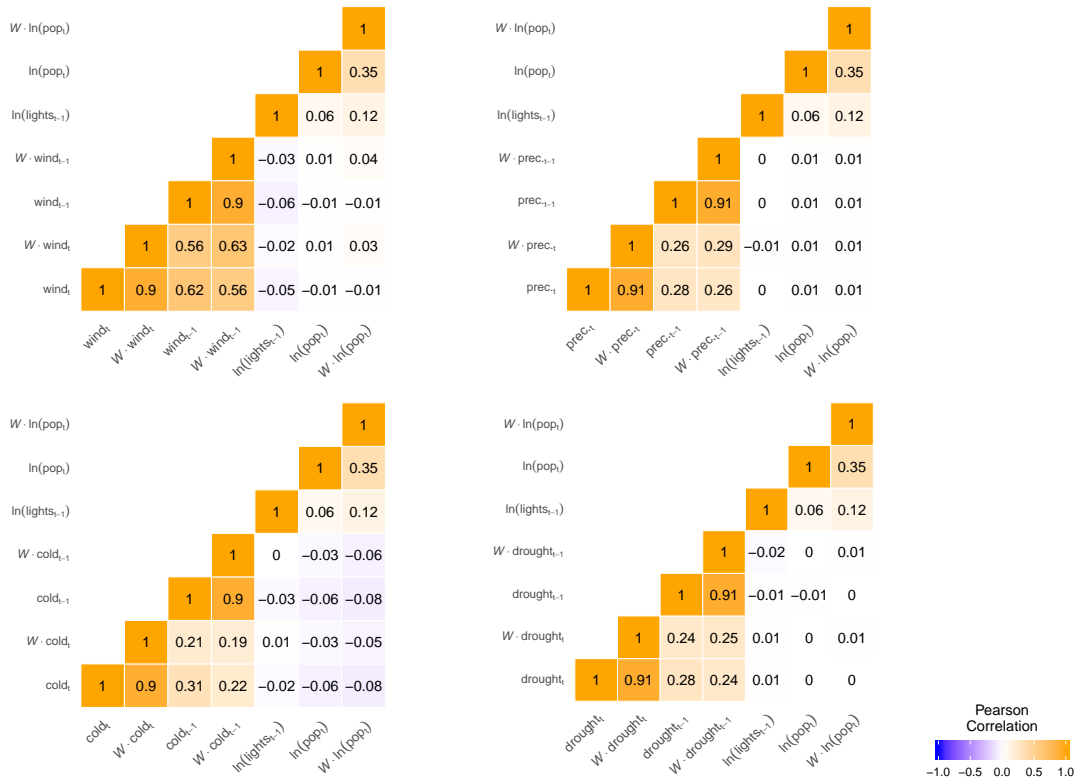
Table 3.A.4: Test for Residual Spatial Autocorrelation

**Global Moran's  $I$  Test for regression residuals of SLX model**

	wind	precip.	drought	cold
<b>Sample Estimates</b>				
Observed Moran's $I$	0.4466	0.4496	0.4530	0.4459
Expected Moran's $I$	-0.0001	-0.0001	-0.0001	-0.0001
<b>Test Statistics</b>				
Moran's $I$ stat. s.d.	596.16	596.66	579.01	594.28
Two-sided p-value	2.2e-16	2.2e-16	2.2e-16	2.2e-16

*Note:* Global Moran's  $I$  Test for spatial autocorrelation in the residuals of estimated linear SLX models, compare column (3) of tables 3.B.1–3.B.2. The Null Hypothesis of no residual spatial autocorrelation (RSA) is overwhelmingly rejected. Observed Moran's  $I$  are positive throughout, suggesting positive RSA (i.e., spatial clustering).

Figure 3.A.12: Correlations Twoway Demeaned





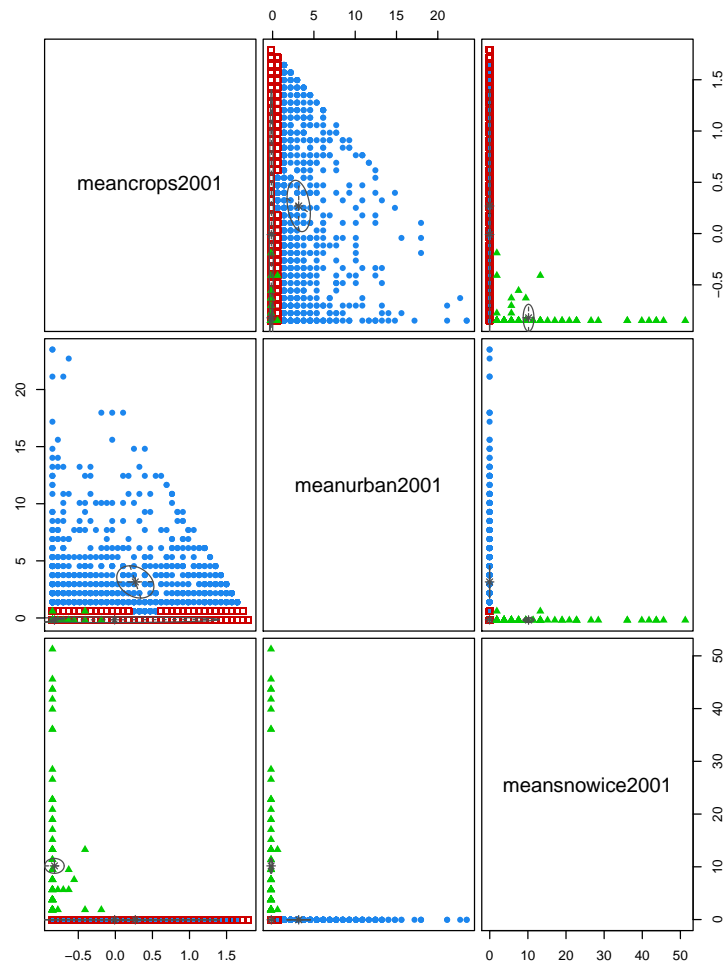
### 3.A.5 Rural/urban classification

To test the hypothesis that the observed negative spillover effects of droughts are mainly driven by treated non-urban (potentially rural/agricultural) cells that negatively affect nearby urban (or residential) locations, cells need to be classified into predominantly urban vs. non-urban areas. For this purpose, we use the MODIS Land-use Data provided by the FAO for year 2001. These land-use data include information on the extent of urban or crop areas at a spatial resolution of 15 arc-seconds (i.e., roughly 500 meters), obtained from MODIS satellite imagery using a supervised decision tree classification algorithm with region-specific parameters (Schneider et al., 2009). Urban land-use comprises all human-constructed elements (e.g., buildings and roads), while crop land-use comprises all kinds of cultivated fields. Pixel locations are defined according to the type of land-use they are *dominated* by (i.e., coverage of at least 50% of a given pixel unit). Urban areas follow a defined minimum mapping unit approach, considering only contiguous patches of built-up land that are greater than one square kilometer. We aggregate the data to  $0.5^\circ \times 0.5^\circ$  grid-cell units by computing the cell level shares of each land-use pixel type. Testing the hypothesis requires classifying each cell as either “urban” or “non-urban” in a mutually-exclusive fashion. Due to the presence of snow/ice and other vegetation, crops and urban shares do not sum up to one at the cell level. Moreover, cells with a relatively high share of urban pixels compared to the global distribution may simultaneously also have a relatively high share of rural pixels, and vice versa. Consequently, it is unclear ex-ante, what threshold should be imposed on land-use shares to make a binary distinction.

To solve this classification problem, we apply an off-the-shelf unsupervised machine learning algorithm provided by Scrucca et al. (2016) that uses three input components: The shares of urban, crop, and snow-ice pixels (vs. other vegetation) per cell in the year 2001. Using the Bayesian Information Criteria (BIC), the algorithm picks the best fit across a range of classification models. It chooses an ellipsoidal, equal volume and shape (EEV) Gaussian finite mixture model fitted by expectation-maximization, to classify cells into three categories representing cells that are mostly urban (1,038), mostly non-urban/rural (21,163), and none (93). Thus, about 5% of ever-lit cells in the sample represent mostly urban areas. Figure 3.A.13 depicts the classification outcome along the three input-dimensions.

Figure 3.A.14 depicts the distributions of key variables for the obtained classes. The top two graphs are dedicated to the distribution of input components used by the classification algorithm. Most cells classified as rural have no or only small urban pixel shares. However, the reverse conclusion is not true: The graph on the top right suggests that cells classified as urban may simultaneously have very high crop shares. This observation seems reasonable, given the arbitrary layout of the grid-cells combined with the fact that cultivated croplands are often located in the outskirts of urban areas. The lower two graphs turn to the distributions of the mean night-light intensity (left) and of population (right). Neither of these variables has been used as inputs for classification but are relevant for empirical identification and thus serve to assess the class validity. The plots suggest that both mean night-light

Figure 3.A.13: Rural/Urban Classification

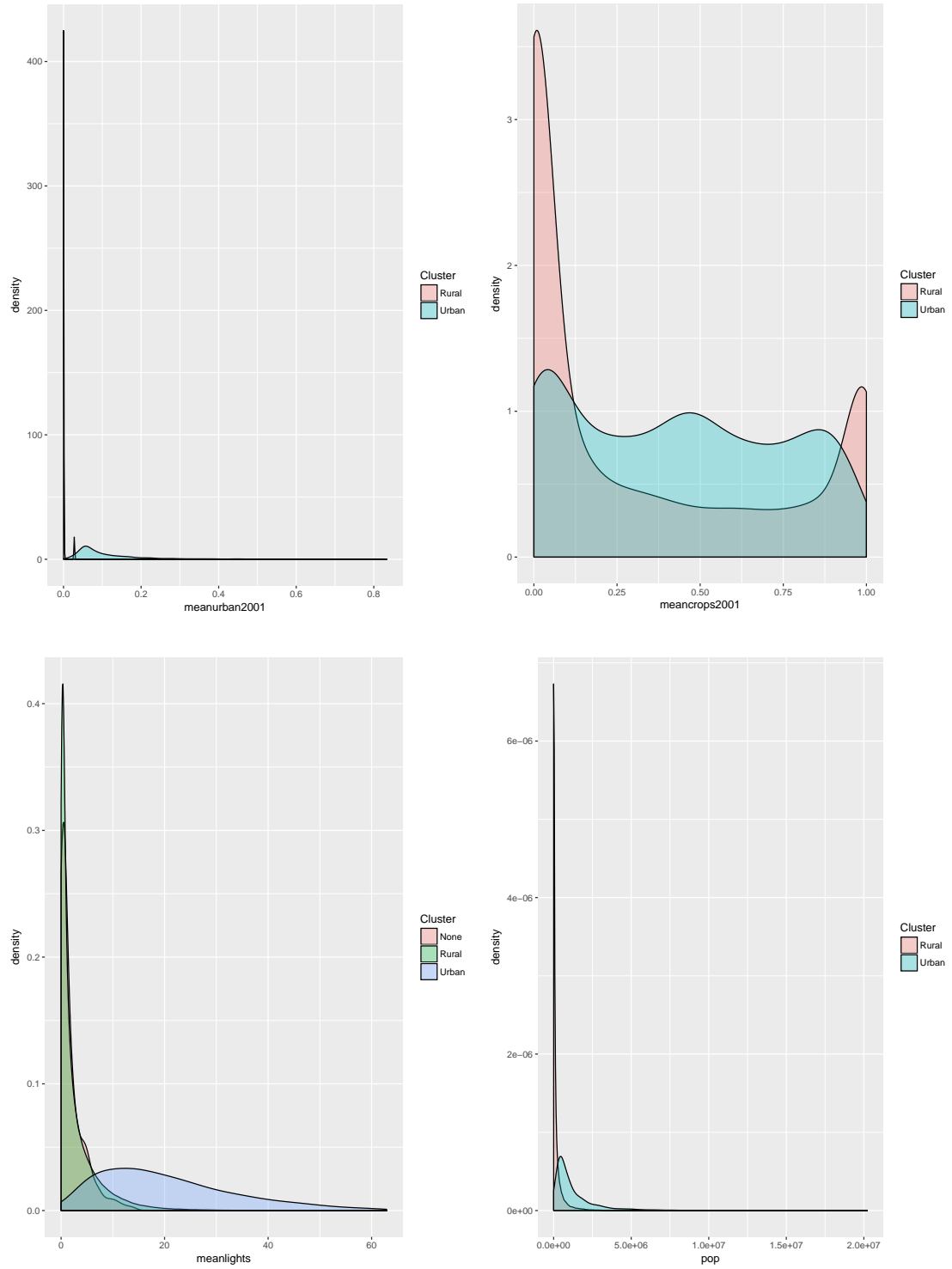


*Note:* Classification of Rural and Urban Cells in a Gaussian finite mixture model fitted by Expectation-Maximization (EM) algorithm. Ellipsoidal, equal volume and shape (EEV) model with 3 input components: Shares of urban, crop, and snow-ice pixels per cell in year 2001. All input components centered and scaled by their standard deviation for efficiency reasons. Log-Likelihood: 39,242.11, number of observations: 22,294 cells, number of estimated parameters: 23, Bayesian Information Criteria (BIC): 78,253.94, Integrated Complete-data Likelihood (ICL): 77,970.27. Best fit across range of classification models provided by 'mclust 5' R package (Scrucca et al., 2016), using BIC as selection criterion. 21,163 cells classified as rural (red), 1,038 as urban/residential (blue), 93 as none (green).

intensity and population are overall higher for urban than for rural cells, which is very reasonable.

Finally, to offer a more tractable alternative to the classification with non-supervised learning, we test a “simple” selection rule. This baldly classifies all cells as urban that have a share of urban pixels which is larger than zero. This approach leads to about twice as many cells being classified as urban, potentially including also those that have only very small urban areas. While it is reasonable

Figure 3.A.14: Distribution of Cell Properties Across Rural/Urban Clusters



to assume that about 10% urbanization at a global scale may be too high, results are qualitatively similar. To decompose the local and spillover effects of droughts according to cell classification, we estimate the following model:

$$\begin{aligned}
\Delta \ell_t &= \ell_{t-1} \gamma + \mathbf{D}_t \beta^0 + [\mathbf{D}_t \times \text{urban}] \beta^1 & (3.A.3) \\
&+ \mathbf{W}_{\text{non-urban}}^r \mathbf{D}_t \beta^2 + [\mathbf{W}_{\text{non-urban}}^r \mathbf{D}_t \times \text{urban}] \beta^3 \\
&+ \mathbf{W}_{\text{urban}}^r \mathbf{D}_t \beta^4 + [\mathbf{W}_{\text{urban}}^r \mathbf{D}_t \times \text{urban}] \beta^5 \\
&+ \mathbf{X}_t \delta^0 + \mathbf{W}^r \mathbf{X}_t \delta^1 + \nu + \pi + \mathbf{u}_t \\
\mathbf{u}_t &= \rho \mathbf{W}^r \mathbf{u}_t + \varepsilon_t.
\end{aligned}$$

$\mathbf{W}_{\text{urban}}$  and  $\mathbf{W}_{\text{non-urban}}$  represent mutually exclusive subsets of neighborhoods. Since these subsets potentially have systematic differences in the number of neighbors, spillover-components are standard-normalized to allow direct comparison of coefficient magnitudes. Results for both classifiers (clustering and simple) are summarized in Table 3.A.5.

Results suggest that negative spillovers from non-urban to urban cells drive the aggregate spillover, with magnitudes about twice as strong as from non-urban to non-urban cells. This supports the hypothesis that negative drought spillovers are driven by the rural-to-urban channel. We still find spillovers within pairs of non-urban cells, potentially due to residual urban structures in cells classified as non-urban. There is no evidence for spillovers from urban to non-urban cells and only weak evidence within urban neighborhoods. Overall, the positive direct effect is nearly three times as large in urban cells compared to non-urban ones. The relevant spillover effects from non-urban to urban cells are about a third higher with the machine-learning clustering approach than if the simple classification rule is applied. This suggests that the distinction between urban and non-urban cells provided by machine-learning may be more precise but does not exclusively drive qualitative findings.

Table 3.A.5: Comparison of Drought-Effects Across Rural-Urban Neighborhoods

Dependent Variable: $\Delta \ln(\text{lights}_t)$		clustering	simple
direct effects	<b>non-urban cells</b>		
	drought <sub>t</sub>	0.0243*** (0.0039)	0.0227*** (0.0040)
	drought <sub>t-1</sub>	-0.0046 (0.0039)	-0.0038 (0.0039)
	<b>urban cells</b>		
	drought <sub>t</sub> × urban	0.0593*** (0.0172)	0.0463*** (0.0123)
	drought <sub>t-1</sub> × urban	-0.0289* (0.0172)	-0.0204* (0.0123)
spillover effects	<b>to non-urban cells</b>		
	from non-urban cells		
	$W_{\text{non-urban}} \cdot \text{drought}_t$	-0.0080*** (0.0015)	-0.0079*** (0.0015)
	$W_{\text{non-urban}} \cdot \text{drought}_{t-1}$	-0.0004 (0.0015)	-0.0006 (0.0015)
	<b>to urban cells</b>		
	$W_{\text{non-urban}} \cdot \text{drought}_t \times \text{urban}$	-0.0094* (0.0051)	-0.0062* (0.0036)
	$W_{\text{non-urban}} \cdot \text{drought}_{t-1} \times \text{urban}$	0.0046 (0.0051)	0.0037 (0.0036)
	<b>to non-urban cells</b>		
	from urban cells		
	$W_{\text{urban}} \cdot \text{drought}_t$	-0.0012 (0.0011)	-0.0004 (0.0011)
	$W_{\text{urban}} \cdot \text{drought}_{t-1}$	-0.0005 (0.0011)	-0.0005 (0.0011)
	<b>to urban cells</b>		
$W_{\text{urban}} \cdot \text{drought}_t \times \text{urban}$	-0.0042** (0.0019)	-0.0050*** (0.0019)	
$W_{\text{urban}} \cdot \text{drought}_{t-1} \times \text{urban}$	0.0034* (0.0019)	0.0025 (0.0019)	
<b>controls</b>			
$\ln(\text{pop}_t)$	0.0276*** (0.0014)	0.0276*** (0.0014)	
$W \cdot \ln(\text{pop}_t)$	0.0115*** (0.0006)	0.0115*** (0.0006)	
$\ln(\text{lights}_{t-1})$	-0.4329*** (0.0011)	-0.4329*** (0.0011)	
$\rho$	0.0676*** (0.0001)	0.0676*** (0.0000)	
Observations	468,174	468,174	

*Note:* \*\*\*, \*\*, \* denote significance at the 1%, 5% and 10% level. All specifications are SDEM and are estimated by Maximum Likelihood. Standard errors in parentheses. Cell and year fixed effects included but not reported. Spatial radius is  $r=80$  km. Yearly weather intensities reflect time-weighted rolling averages over 12 subsequent monthly observations.  $W_{\text{urban}}$  and  $W_{\text{non-urban}}$  represent mutually exclusive subsets of neighborhoods. Spillover-Components standard-normalized to allow comparison across subsets within regressions.

### 3.B Supplementary tables

Table 3.B.1: Model Buildup: Impact of Droughts on Light Growth

Dependent Variable: $\Delta \ln(\text{lights}_t)$				
	(1)	(2)	(3)	(4)
drought <sub>t</sub>	-0.0229*** (0.0021)	0.0262*** (0.0055)	0.0345*** (0.0057)	0.0083* (0.0048)
drought <sub>t-1</sub>			-0.0296*** (0.0058)	0.0005 (0.0047)
W · drought <sub>t</sub>		-0.0080*** (0.0008)	-0.0099*** (0.0008)	-0.0044*** (0.0009)
W · drought <sub>t-1</sub>			0.0073*** (0.0008)	0.0010 (0.0009)
ln(pop <sub>t</sub> )	0.0432*** (0.0030)	0.0267*** (0.0029)	0.0266*** (0.0029)	0.0276*** (0.0014)
W · ln(pop <sub>t</sub> )		0.0149*** (0.0009)	0.0149*** (0.0009)	0.0115 (0.0006)
ln(lights <sub>t-1</sub> )	-0.4054*** (0.0033)	-0.4086*** (0.0033)	-0.4084*** (0.0033)	-0.4329*** (0.0011)
$\rho$				0.676*** (0.0000)
Method	OLS	SLX	SLX	SDEM
Observations	468,174	468,174	468,174	468,174

Note: \*\*\*, \*\*, \* denote significance at the 1%, 5% and 10% level. Specifications (1), (2), and (3) are estimated by panel OLS, (4) is estimated by Maximum Likelihood. Standard errors (in parentheses) allow for heteroskedasticity and clustering at the cell level in specifications (1), (2), and (3). Cell and year fixed effects included but not reported. Spatial radius is r=80 km. Yearly weather intensities reflect time-weighted rolling averages over 12 subsequent monthly observations.

Table 3.B.2: Model Buildup: Impact of Cold Waves on Light Growth

Dependent Variable: $\Delta \ln(\text{lights}_t)$				
	(1)	(2)	(3)	(4)
cold <sub>t</sub>	0.0134** (0.0068)	-0.1765*** (0.0184)	-0.1227*** (0.0194)	-0.0762*** (0.0153)
cold <sub>t-1</sub>			-0.0293* (0.0176)	-0.0326** (0.0149)
W · cold <sub>t</sub>		0.0323*** (0.0025)	0.0307*** (0.0026)	0.0218*** (0.0027)
W · cold <sub>t-1</sub>			-0.0229*** (0.0024)	-0.0195*** (0.0026)
ln(pop <sub>t</sub> )	0.0409*** (0.0028)	0.0236*** (0.0027)	0.0233*** (0.0027)	0.0244*** (0.0013)
W · ln(pop <sub>t</sub> )		0.0148*** (0.0008)	0.0142*** (0.0008)	0.0106*** (0.0006)
ln(lights <sub>t-1</sub> )	-0.4097*** (0.0032)	-0.4141*** (0.0032)	-0.4138*** (0.0032)	-0.4379*** (0.0011)
$\rho$				0.0672*** (0.0000)
Method	OLS	SLX	SLX	SDEM
Observations	506,394	506,394	506,037	506,037

Note: \*\*\*, \*\*, \* denote significance at the 1%, 5% and 10% level. Specifications (1), (2), and (3) are estimated by panel OLS, (4) is estimated by Maximum Likelihood. Standard errors (in parentheses) allow for heteroskedasticity and clustering at the cell level in specifications (1), (2), and (3). Cell and year fixed effects included but not reported. Spatial radius is r=80 km. Yearly weather intensities reflect time-weighted rolling averages over 12 subsequent monthly observations.

Table 3.B.3: Spatial Error HAC Model following Hsiang (2010)

Dependent Variable: $\Delta \ln(\text{lights}_t)$				
	wind	precip.	drought	cold
weather <sub>t</sub>	-0.0010 (0.0014)	-0.0744*** (0.0112)	0.0342*** (0.0080)	-0.1219*** (0.0275)
weather <sub>t-1</sub>	-0.0143*** (0.0014)	0.0477*** (0.0108)	-0.0292*** (0.0079)	-0.0301 (0.0253)
W · weather <sub>t</sub>	-0.0002 (0.0002)	0.0137*** (0.0019)	-0.0098*** (0.0013)	0.0306*** (0.0043)
W · weather <sub>t-1</sub>	0.0015*** (0.0002)	-0.0079*** (0.0018)	0.0072*** (0.0013)	-0.0228*** (0.0041)
ln(pop <sub>t</sub> )	0.0237*** (0.0020)	0.0250*** (0.0020)	0.0267*** (0.0021)	0.0234*** (0.0020)
W · ln(pop <sub>t</sub> )	0.0142*** (0.0011)	0.0149*** (0.0011)	0.0149*** (0.0012)	0.0141*** (0.0011)
ln(lights <sub>t-1</sub> )	-0.4153*** (0.0035)	-0.4123*** (0.0035)	-0.4085*** (0.0037)	-0.4139*** (0.0035)
	-0.0018 (0.0050)	-0.0052 (0.0051)	-0.0058 (0.0053)	-0.0033 (0.0051)
Observations	507,864	502,320	468,384	506,394

Note: \*\*\*, \*\*, \* denote significance at the 1%, 5% and 10% level. All specifications adapt the Spatial Error HAC Model methods by Conley (1999) as implemented by Hsiang (2010). Standard errors (in parentheses) allow for heteroskedasticity, spatial autocorrelation and temporal autocorrelation over 3 periods. Cell and year fixed effects included but not reported. Spatial radius is r=80 km. Yearly weather intensities reflect time-weighted rolling averages over 12 subsequent monthly observations.

Table 3.B.4: Sensitivity: Exclude Population as a Control

Dependent Variable: $\Delta \ln(\text{lights}_t)$				
	wind	precip	drought	cold
weather <sub>t</sub>	-0.0024*** (0.0009)	-0.0302*** (0.0070)	0.0080* (0.0048)	-0.0893*** (0.0153)
weather <sub>t-1</sub>	-0.0094*** (0.0009)	0.0232*** (0.0069)	-0.0007 (0.0047)	-0.0476*** (0.0149)
W · weather <sub>t</sub>	0.0001 (0.0002)	0.0050*** (0.0013)	-0.0044*** (0.0009)	0.0225*** (0.0027)
W · weather <sub>t-1</sub>	0.0008*** (0.0002)	-0.0020 (0.0013)	0.0011 (0.0009)	-0.0187*** (0.0026)
ln(lights <sub>t-1</sub> )	-0.4368*** (0.0011)	-0.4347*** (0.0011)	-0.4307*** (0.0011)	-0.4361*** (0.0011)
$\rho$	0.0672*** (0.0000)	0.0672*** (0.0000)	0.0676*** (0.0000)	0.0672*** (0.0000)
Observations	507,864	502,026	468,174	506,037

Note: \*\*\*, \*\*, \* denote significance at the 1%, 5% and 10% level. All specifications are SDEM and are estimated by Maximum Likelihood. Standard errors in parentheses. Cell and year fixed effects included but not reported. Spatial radius is r=80 km. Yearly weather intensities reflect time-weighted rolling averages over 12 subsequent monthly observations.

Table 3.B.5: No Time Lags

Dependent Variable: $\Delta \ln(\text{lights}_t)$				
	wind	precip	drought	cold
weather <sub>t</sub>	-0.0077*** (0.0007)	-0.0248*** (0.0067)	0.0086* (0.0045)	-0.1052*** (0.0136)
W · weather <sub>t</sub>	0.0005*** (0.0001)	0.0043*** (0.0012)	-0.0042*** (0.0009)	0.0193*** (0.0025)
ln(pop <sub>t</sub> )	0.0248*** (0.0013)	0.0257*** (0.0013)	0.0276*** (0.0014)	0.0248*** (0.0013)
W · ln(pop <sub>t</sub> )	0.0109*** (0.0006)	0.0113*** (0.0006)	0.0115*** (0.0006)	0.0110*** (0.0006)
ln(lights <sub>t-1</sub> )	-0.4384*** (0.0011)	-0.4367*** (0.0011)	-0.4329*** (0.0011)	-0.4378*** (0.0011)
$\rho$	0.0672*** (0.0000)	0.0672*** (0.0000)	0.0676*** (0.0000)	0.0672*** (0.0000)
Observations	507,864	502,026	468,174	506,037

Note: \*\*\*, \*\*, \* denote significance at the 1%, 5% and 10% level. All specifications are SDEM and are estimated by Maximum Likelihood. Standard errors in parentheses. Cell and year fixed effects included but not reported. Spatial radius is r=80 km. Yearly weather intensities reflect time-weighted rolling averages over 12 subsequent monthly observations.

Table 3.B.6: Sensitivity to Top-Coding: Excluding Top-Coded Pixels

Dependent Variable: $\Delta \ln(\text{lights}_t)$				
	wind	precip.	drought	cold
weather <sub>t</sub>	-0.0019** (0.0009)	-0.0329*** (0.0070)	0.0091* (0.0048)	-0.0752*** (0.0152)
weather <sub>t-1</sub>	-0.0090*** (0.0009)	0.0222*** (0.0069)	0.0012 (0.0048)	-0.0318** (0.0149)
W · weather <sub>t</sub>	-0.0000 (0.0002)	0.0052*** (0.0013)	-0.0046*** (0.0009)	0.0219*** (0.0027)
W · weather <sub>t-1</sub>	0.0008*** (0.0002)	-0.0023* (0.0013)	0.0011 (0.0009)	-0.0200*** (0.0027)
ln(pop <sub>t</sub> )	0.0276*** (0.0013)	0.0286*** (0.0013)	0.0302*** (0.0014)	0.0273*** (0.0013)
W · ln(pop <sub>t</sub> )	0.0113*** (0.0006)	0.0117*** (0.0006)	0.0119*** (0.0006)	0.0110*** (0.0006)
ln(lights <sub>t-1</sub> )	-0.4381*** (0.0011)	-0.4360*** (0.0011)	-0.4321*** (0.0011)	-0.4373*** (0.0011)
$\rho$	0.0672*** (0.0000)	0.0672*** (0.0000)	0.0676*** (0.0000)	0.0672*** (0.0000)
Observations	507,780	501,942	468,111	505,953

Note: \*\*\*, \*\*, \* denote significance at the 1%, 5% and 10% level. All specifications are SDEM and are estimated by Maximum Likelihood. Standard errors in parentheses. Cell and year fixed effects included but not reported. Spatial radius is r=80 km. Yearly weather intensities reflect time-weighted rolling averages over 12 subsequent monthly observations. Dependent variable excludes top-coded pixels.



Table 3.B.7: Sensitivity to Bottom-Coding: Setting Pixels &lt;DN3 to Zero

Dependent Variable: $\Delta \ln(\text{lights}_t)$				
	wind	precip.	drought	cold
weather <sub>t</sub>	-0.0007 (0.0009)	-0.0265*** (0.0070)	0.0082* (0.0048)	-0.0852*** (0.0154)
weather <sub>t-1</sub>	-0.0106*** (0.0009)	0.0290*** -0.0069	0.0015 (0.0048)	-0.0291* (0.0150)
W · weather <sub>t</sub>	-0.0001 (0.0002)	0.0042*** (0.0013)	-0.0041*** (0.0009)	0.0242*** (0.0027)
W · weather <sub>t-1</sub>	0.0010*** (0.0002)	-0.0022* (0.0013)	0.0007 (0.0009)	-0.0217*** (0.0027)
ln(pop <sub>t</sub> )	0.0265*** (0.0013)	0.0275*** (0.0013)	0.0296*** (0.0014)	0.0262*** (0.0013)
W · ln(pop <sub>t</sub> )	0.0108*** (0.0006)	0.0112*** (0.0006)	0.0116*** (0.0006)	0.0105*** (0.0006)
ln(lights <sub>t-1</sub> )	-0.4395*** (0.0011)	-0.4376*** (0.0011)	-0.4338*** (0.0011)	-0.4388*** (0.0011)
$\rho$	0.0672*** (0.0000)	0.0672*** (0.0000)	0.0676*** (0.0000)	0.0672*** (0.0000)
Observations	507,024	501,228	467,460	505,197

Note: \*\*\*, \*\*, \* denote significance at the 1%, 5% and 10% level. All specifications are SDEM and are estimated by Maximum Likelihood. Standard errors in parentheses. Cell and year fixed effects included but not reported. Spatial radius is r=80 km. Yearly weather intensities reflect time-weighted rolling averages over 12 subsequent monthly observations.

Table 3.B.8: Time Varying Country Characteristics

Dependent Variable: $\Delta \ln(\text{lights}_t)$				
	wind	precip.	drought	cold
weather <sub>t</sub>	0.0004 (0.0010)	-0.0312*** (0.0070)	0.0062 (0.0049)	-0.0360** (0.0179)
weather <sub>t-1</sub>	-0.0049*** (0.0010)	0.0117* (0.0069)	0.0009 (0.0049)	-0.0390** (0.0175)
W · weather <sub>t</sub>	0.0003** (0.0002)	0.0043*** (0.0013)	-0.0041*** (0.0009)	0.0165*** (0.0029)
W · weather <sub>t-1</sub>	0.0009*** (0.0002)	-0.0022* (0.0013)	0.0017* (0.0009)	-0.0144*** (0.0028)
ln(pop <sub>t</sub> )	0.0140*** (0.0013)	0.0145*** (0.0013)	0.0158*** (0.0014)	0.0140*** (0.0013)
W · ln(pop <sub>t</sub> )	0.0040*** (0.0006)	0.0041*** (0.0006)	0.0044*** (0.0006)	0.0039*** (0.0006)
ln(lights <sub>t-1</sub> )	-0.4768*** (0.0011)	-0.4759*** (0.0011)	-0.4728*** (0.0012)	-0.4764*** (0.0011)
$\rho$	0.0671*** (0.0000)	0.0671*** (0.0000)	0.0068*** (0.0000)	0.0671*** (0.0000)
Observations	507,864	502,026	468,174	506,037

Note: \*\*\*, \*\*, \* denote significance at the 1%, 5% and 10% level. All specifications are SDEM and are estimated by Maximum Likelihood. Standard errors in parentheses. Cell and country-year fixed effects (with nested year fixed effects) included but not reported. Spatial radius is r=80 km. Yearly weather intensities reflect time-weighted rolling averages over 12 subsequent monthly observations.

Table 3.B.9: Simple Annual Mean of Weather Shocks

Dependent Variable: $\Delta \ln(\text{lights}_t)$				
	wind	precip.	drought	cold
weather <sub>t</sub>	-0.0032*** (0.0007)	-0.0289*** (0.0055)	0.0243*** (0.0039)	-0.0613*** (0.0137)
weather <sub>t-1</sub>	-0.0064*** (0.007)	0.0011 (0.0055)	-0.0060 (0.0038)	-0.0540*** (0.0133)
W · weather <sub>t</sub>	-0.0002 (0.0001)	0.0018* (0.0010)	-0.0037*** (0.0007)	0.0337*** (0.0025)
W · weather <sub>t-1</sub>	0.0008*** (0.0001)	0.0030*** (0.0010)	-0.0000 (0.0007)	-0.0504*** (0.0019)
ln(pop <sub>t</sub> )	0.0247*** (0.0013)	0.0257*** (0.0013)	0.0276*** (0.0014)	0.0245*** (0.0013)
W · ln(pop <sub>t</sub> )	0.0109*** (0.0006)	0.0113*** (0.0006)	0.0115*** (0.0006)	0.0107*** (0.0006)
ln(lights <sub>t-1</sub> )	-0.4385*** (0.0011)	-0.4367*** (0.0011)	-0.4329*** (0.0011)	-0.4376*** (0.0011)
$\rho$	0.0672*** (0.0000)	0.0672*** (0.0000)	0.676*** (0.0000)	0.0672*** (0.0000)
Observations	507,864	502,026	468,174	506,037

Note: \*\*\*, \*\*, \* denote significance at the 1%, 5% and 10% level. All specifications are SDEM and are estimated by Maximum Likelihood. Standard errors in parentheses. Cell and year fixed effects included but not reported. Spatial radius is r=80 km. Yearly weather intensities reflect non-weighted mean over all monthly observations within a year.

Table 3.B.10: Maximum Weather Shock Intensities, Non-Weighted

Dependent Variable: $\Delta \ln(\text{lights}_t)$				
	wind	precip	drought	cold
weather <sub>t</sub>	-0.0004*** (0.0001)	-0.0023** (0.0009)	0.0072*** (0.0017)	-0.0105*** (0.0040)
weather <sub>t-1</sub>	-0.0004*** (0.0001)	-0.0016* (0.0009)	0.0005 (0.0017)	0.0043 (0.0040)
W · weather <sub>t</sub>	-0.0001** (0.0000)	-0.0003 (0.0002)	-0.0017*** (0.0003)	0.0089*** (0.0007)
W · weather <sub>t-1</sub>	0.0001** (0.0000)	0.0006*** (0.0002)	-0.0002 (0.0003)	-0.0115*** (0.0007)
ln(pop <sub>t</sub> )	0.0251*** (0.0013)	0.0257*** (0.0013)	0.0276*** (0.0014)	0.0248*** (0.0013)
W · ln(pop <sub>t</sub> )	0.0111*** (0.0006)	0.0113*** (0.0006)	0.0115*** (0.0006)	0.0108*** (0.0006)
ln(lights <sub>t-1</sub> )	-0.4379*** (0.0011)	-0.4367*** (0.0011)	-0.4329*** (0.0011)	-0.4376*** (0.0011)
$\rho$	0.0672*** (0.0000)	0.0672*** (0.0000)	0.0676*** (0.0000)	0.0672*** (0.0000)
Observations	507,864	502,026	468,174	506,037

Note: \*\*\*, \*\*, \* denote significance at the 1%, 5% and 10% level. All specifications are SDEM and are estimated by Maximum Likelihood. Standard errors in parentheses. Cell and year fixed effects included but not reported. Spatial radius is r=80 km. Yearly weather intensities reflect non-weighted maxima of weather shocks within a year.

Table 3.B.11: Spatial Radius r=160km

Dependent Variable: $\Delta \ln(\text{lights}_t)$				
	wind	precip.	drought	cold
weather <sub>t</sub>	-0.0016** (0.0007)	-0.0249*** (0.0057)	0.0125*** (0.0041)	-0.0849*** (0.0136)
weather <sub>t-1</sub>	-0.0052*** (0.0007)	0.0158*** (0.0057)	-0.0075* (0.0040)	-0.0129 (0.0133)
W · weather <sub>t</sub>	-0.0000 (0.0000)	0.0008** (0.0004)	-0.0015*** (0.0003)	0.0061*** (0.0009)
W · weather <sub>t-1</sub>	0.0001* (0.0000)	-0.0000 (0.0004)	0.0005* (0.0003)	-0.0060*** (0.0008)
ln(pop <sub>t</sub> )	0.0245*** (0.0013)	0.0252*** (0.0013)	0.0264*** (0.0014)	0.0240*** (0.0013)
W · ln(pop <sub>t</sub> )	0.0057*** (0.0003)	0.0059*** (0.0003)	0.0061*** (0.0003)	0.0055*** (0.0003)
ln(lights <sub>t-1</sub> )	-0.4375*** (0.0011)	-0.4360*** (0.0011)	-0.4328*** (0.0011)	-0.4371*** (0.0011)
$\rho$	0.0220*** (0.0000)	0.0221*** (0.0000)	0.0226*** (0.0000)	0.0220*** (0.0000)
Observations	515,130	509,166	475,083	513,282

*Note:* \*\*\*, \*\*, \* denote significance at the 1%, 5% and 10% level. All specifications are SDEM and are estimated by Maximum Likelihood. Standard errors in parentheses. Cell and year fixed effects included but not reported. Spatial radius is r=160 km. Yearly weather intensities reflect time-weighted rolling averages over 12 subsequent monthly observations.

Table 3.B.12: Global Spillovers

Dependent Variable: $\Delta \ln(\text{lights}_t)$				
	wind	precip.	drought	cold
weather <sub>t</sub>	-0.0046*** (0.0007) [-0.0044]	-0.0279*** (0.0060) [-0.0259]	-0.0016 (0.0041) [-0.0029]	-0.0974*** (0.0122) [-0.0794]
weather <sub>t-1</sub>	-0.0095*** (0.0007) [-0.0093]	0.0198*** (0.0059) [0.0189]	0.0017 (0.0041) [0.0017]	-0.0858*** (0.0119) [-0.0908]
W · weather <sub>t</sub>	0.0005*** (0.0001) [0.0000]	0.0037*** (0.0009) [0.0001]	-0.0010* (0.0006) [-0.0001]	0.0217*** (0.0017) [0.0010]
W · weather <sub>t-1</sub>	0.0008*** (0.0001) [0.0000]	-0.0021** (0.0009) [-0.0001]	-0.0001 (0.0006) [0.0000]	0.0015 (0.0017) [-0.0003]
ln(pop <sub>t</sub> )	0.0228*** (0.0014) [0.0383]	0.0242*** (0.0014) [0.0397]	0.0256*** (0.0015) [0.0412]	0.0225*** (0.0014) [0.0383]
W · ln(pop <sub>t</sub> )	0.0116*** (0.0004) [0.0009]	0.0122*** (0.0004) [0.0009]	0.0121*** (0.0005) [0.0009]	0.0118*** (0.0004) [0.0009]
ln(lights <sub>t-1</sub> )	-0.3300*** (0.0009)	-0.3270*** (0.0009)	-0.3232*** (0.0009)	-0.3289*** (0.0009)
λ	0.0671*** (0.0000)	0.0671*** (0.0000)	0.0675*** (0.0000)	0.0671*** (0.0000)
Observations	508,158	502,320	468,384	506,394

Note: \*\*\*, \*\*, \* denote significance at the 1%, 5% and 10% level. All specifications are SDM and are estimated by Maximum Likelihood. Standard errors in parentheses. Average effects translated with spatial multiplier in square brackets. Cell and year fixed effects included but not reported. Spatial radius is r=80 km. Yearly weather intensities reflect time-weighted rolling averages over 12 subsequent monthly observations.

Table 3.B.13: Non-Linear Damage Functions, Squared

Dependent Variable: $\Delta \ln(\text{lights}_t)$				
	wind	precip	drought	cold
weather <sub>t</sub> <sup>2</sup>	-0.00005** (0.0000)	-0.0382*** (0.0075)	0.0011 (0.0040)	-0.0789*** (0.0179)
weather <sub>t-1</sub> <sup>2</sup>	-0.00017*** (0.0000)	0.0250*** (0.0074)	0.0007 (0.0039)	-0.0272 (0.0173)
W · weather <sub>t</sub> <sup>2</sup>	0.00000 (0.0000)	0.0052*** (0.0014)	-0.0028*** (0.0008)	0.0236*** (0.0032)
W · weather <sub>t-1</sub> <sup>2</sup>	0.00002*** (0.0000)	-0.0020 (0.0014)	0.0009 (0.0008)	-0.0253*** (0.0031)
ln(pop <sub>t</sub> )	0.0247*** (0.0013)	0.0257*** (0.0013)	0.0276*** (0.0014)	0.0246*** (0.0013)
W · ln(pop <sub>t</sub> )	0.0109*** (0.0006)	0.0113*** (0.0006)	0.0115*** (0.0006)	0.0107*** (0.0006)
ln(lights <sub>t-1</sub> )	-0.4385*** (0.0011)	-0.4367*** (0.0011)	-0.4328*** (0.0011)	-0.4378*** (0.0011)
$\rho$	0.0672*** (0.0000)	0.0672*** (0.0000)	0.0676*** (0.0000)	0.0672*** (0.0000)
Observations	507,864	502,026	468,174	506,037

Note: \*\*\*, \*\*, \* denote significance at the 1%, 5% and 10% level. All specifications are SDEM and are estimated by Maximum Likelihood. Standard errors in parentheses. Cell and year fixed effects included but not reported. Spatial radius is r=80 km. Yearly weather intensities reflect time-weighted rolling averages over 12 subsequent monthly observations. Yearly weather intensities are expressed as non-linear damage functions in squared terms.

Table 3.B.14: Non-Linear Damage Functions, Cubic

Dependent Variable: $\Delta \ln(\text{lights}_t)$				
	wind	precip	drought	cold
weather <sub>t</sub> <sup>3</sup>	-0.000001** (0.0000)	-0.0389*** (0.0084)	-0.0025 (0.0030)	-0.0937*** (0.0225)
weather <sub>t-1</sub> <sup>3</sup>	-0.000004*** (0.0000)	0.0215*** (0.0082)	0.0008 (0.0030)	0.0144 (0.0213)
W · weather <sub>t</sub> <sup>3</sup>	0.000000 (0.0000)	0.0041** (0.0016)	-0.0015** (0.0007)	0.0276*** (0.0042)
W · weather <sub>t-1</sub> <sup>3</sup>	0.000000*** (0.0000)	-0.0008 (0.0016)	0.0007 (0.0007)	-0.0385*** (0.0040)
ln(pop <sub>t</sub> )	0.0248*** (0.0013)	0.0257*** (0.0013)	0.0276*** (0.0014)	0.0249*** (0.0013)
W · ln(pop <sub>t</sub> )	0.0109*** (0.0006)	0.0113*** (0.0006)	0.0115*** (0.0006)	0.0108*** (0.0006)
ln(lights <sub>t-1</sub> )	-0.4383*** (0.0011)	-0.4367*** (0.0011)	-0.4328*** (0.0011)	-0.4377*** (0.0011)
$\rho$	0.0672*** (0.0000)	0.0672*** (0.0000)	0.0676*** (0.0000)	0.0672*** (0.0000)
Observations	507,864	502,026	468,174	506,037

Note: \*\*\*, \*\*, \* denote significance at the 1%, 5% and 10% level. All specifications are SDEM and are estimated by Maximum Likelihood. Standard errors in parentheses. Cell and year fixed effects included but not reported. Spatial radius is r=80 km. Yearly weather intensities reflect time-weighted rolling averages over 12 subsequent monthly observations. Yearly weather intensities are expressed as non-linear damage functions in cubic terms.

Table 3.B.15: All Weather Categories Together

<b>Dependent Variable: <math>\Delta \ln(\text{lights}_t)</math></b>		
	(1)	(2)
wind <sub>t</sub>	-0.0007 (0.0010)	-0.0068*** (0.0007)
wind <sub>t-1</sub>	-0.0097*** (0.0010)	
W · wind <sub>t</sub>	-0.0001 (0.0002)	0.0004** (0.0001)
W · wind <sub>t-1</sub>	0.0008*** (0.0002)	
prec <sub>t</sub>	-0.0373*** (0.0083)	-0.0271*** (0.0080)
prec <sub>t-1</sub>	0.0303*** (0.0082)	
W · prec <sub>t</sub>	0.0013 (0.0016)	0.0006 (0.0015)
W · prec <sub>t-1</sub>	-0.0023 (0.0016)	
drought <sub>t</sub>	-0.0010 (0.0054)	-0.0001 (0.0051)
drought <sub>t-1</sub>	0.0089* (0.0054)	
W · drought <sub>t</sub>	-0.0040*** (0.0011)	-0.0044*** (0.0010)
W · drought <sub>t-1</sub>	0.0000 (0.0010)	
cold <sub>t</sub>	-0.0960*** (0.0163)	-0.1305*** (0.0146)
cold <sub>t-1</sub>	-0.0265* (0.0160)	
W · cold <sub>t</sub>	0.0239*** (0.0029)	0.0214*** (0.0027)
W · cold <sub>t-1</sub>	-0.0226*** (0.0028)	
ln(pop <sub>t</sub> )	0.0261*** (0.0014)	0.0267*** (0.0014)
W · ln(pop <sub>t</sub> )	0.0106*** (0.0014)	0.0112*** (0.0006)
ln(lights <sub>t-1</sub> )	-0.4342*** (0.0011)	-0.4338*** (0.0011)
$\rho$	0.0676*** (0.0000)	-0.0676*** (0.0000)
Observations	468,174	468,174

*Note:* \*\*\*, \*\*, \* denote significance at the 1%, 5% and 10% level. All specifications are SDEM and are estimated by Maximum Likelihood. Standard errors in parentheses. Cell and year fixed effects included but not reported. Spatial radius is r=80 km. Yearly weather intensities reflect time-weighted rolling averages over 12 subsequent monthly observations.

Table 3.B.16: Income Interaction

Dependent Variable: $\Delta \ln(\text{lights}_t)$								
	wind		precip.		drought		cold	
	estimate	combined	estimate	combined	estimate	combined	estimate	combined
weather <sub>t</sub>	-0.0015 (0.0016)		0.0171 (0.0118)		-0.0120 (0.0093)		0.2442*** (0.0389)	
weather <sub>t-1</sub>	-0.0042*** (0.0015)		0.0249** (0.0117)		0.0081 (0.0092)		-0.0680* (0.0384)	
W · weather <sub>t</sub>	-0.0001 (0.0003)		0.0015 (0.0021)		-0.0020 (0.0016)		0.0077 (0.0059)	
W · weather <sub>t-1</sub>	0.0006** (0.0003)		-0.0040* (0.0021)		0.0029* (0.0016)		-0.0224*** (0.0059)	
weather <sub>t</sub> × low income	-0.0006 (0.0019)	-0.0021* (0.0011)	-0.0705*** (0.0146)	-0.0534*** (0.0087)	0.0267** (0.0108)	0.0147*** (0.0056)	-0.3575*** (0.0423)	-0.1133*** (0.0169)
weather <sub>t-1</sub> × low income	-0.0076*** (0.0019)	-0.0119*** (0.0011)	-0.0057 (0.0144)	0.0192** (0.0085)	-0.0092 (0.0107)	-0.0010 (0.0055)	0.0484 (0.0416)	-0.0193 (0.0165)
W · weather <sub>t</sub> × low income	0.0003 (0.0003)	0.0001 (0.0002)	0.0049* (0.0026)	0.0064*** (0.0016)	-0.0032* (0.0019)	-0.0052*** (0.0011)	0.0114* (0.0067)	0.0191*** (0.0031)
W · weather <sub>t-1</sub> × low income	0.0003 (0.0003)	0.0009*** (0.0002)	0.0033 (0.0026)	-0.0007 (0.0016)	-0.0029 (0.0019)	0.0000 (0.0010)	0.0054 (0.0066)	-0.0170*** (0.0030)
ln(pop <sub>t</sub> )	0.0247*** (0.0013)		0.0258*** (0.0013)		0.0277*** (0.0014)		0.0241*** (0.0013)	
W · ln(pop <sub>t</sub> )	0.0109*** (0.0006)		0.0112*** (0.0006)		0.0115*** (0.0006)		0.0103*** (0.0006)	
ln(lights <sub>t-1</sub> )	-0.4386*** (0.0011)		-0.4366*** (0.0011)		-0.4328*** (0.0011)		-0.4382*** (0.0011)	
ρ	0.0672*** (0.0000)		0.0672*** (0.0000)		0.0676*** (0.0000)		0.0672*** (0.0000)	
Observations	506,142		500,787		467,691		504,525	

Note: \*\*\*, \*\*, \* denote significance at the 1%, 5% and 10% level. All specifications are SDEM and are estimated by Maximum Likelihood. Standard errors in parentheses. Cell and year fixed effects included but not reported. Spatial radius is r=80 km. Yearly weather intensities reflect time-weighted rolling averages over 12 subsequent monthly observations.





---

## Lights out? Earthquakes and local economic activity<sup>\*</sup>

---

### 4.1 Introduction

In this paper I study the local economic impacts of earthquakes by investigating their effect on local emission of night light. Earthquakes are among the most destructive and costly natural disasters. The EM-DAT database records earthquakes as deadliest of all natural disasters over the last decade with over 400,000 fatalities, and causing over 435 billion US dollars of direct damages between 2005-2015 (CRED, 2021). While much is known about seismic risk and immediate impacts, little systematic analysis exists of the aftermath of earthquakes on the local economy.

One of the reasons for our limited understanding of local economic effects of natural disasters in general is that most existing economic studies use aggregated national income data. They thus study the effects of natural disasters at the national level (see e.g. Felbermayr and Gröschl, 2014). Earthquakes, however, are distinctly local phenomena, causing the local effect to be absorbed in national aggregated averages. This seriously limits our ability to study earthquakes' effects since substitution effects may occur within a country (as shown by my findings in Chapter 3 and Xiao and Nilawar, 2013). For example, potential direct negative effects in one location can be offset by positive indirect effects in other areas, causing disaster effects to average out at the national level. This concern is especially relevant when countries are geographically large. For example, Strobl (2011) shows that hurricanes have a significant negative impact on the economic growth rate of US counties, but this effect dissipates within a year at the state level. At the national US level, no impact is identified at all. A second reason is that an earthquake of a given size will affect a small country's national GDP much more than that of a large country – compare e.g. the 2010 Haiti earthquake with the 2008 Sichuan earthquake

---

<sup>\*</sup>This chapter is based on a single-authored paper (Schippers, 2022) that is currently in working paper status.

in China.<sup>1</sup> To make the comparison adequate, one therefore should analyze effects in comparable geographical units that are adequately sized to capture earthquakes' potential effects. At least three challenges make this kind of analysis difficult.

First, administrative data on GDP or income typically does not allow studying affected areas globally at a scale below the national level. However, with systematic recording of anthropogenic light emission at night at high spatial detail, it is possible to explore local impacts of shocks at a lower aggregation level with globally comparable data. While night light is evidently only a proxy for economic activity, this new type of data comes with a number of advantages. Night lights as observed from space are available whenever we have clear skies, as opposed to subnational GDP data which is only available for some countries. Moreover, night lights are able to capture the spatial heterogeneity in economic activity within countries. This allows us to assess the degree to which natural disasters affect an economy, relative to the normal economic activity on site.<sup>2</sup> On top of that, it is available for any regional aggregation that we desire.<sup>3</sup>

A second challenge is the time frequency of data: globally comparable economic statistics typically come at an annual interval. This also holds for the now increasingly used annual stable DMSP-OLS light images produced by NOAA.<sup>4</sup> However, earthquakes are relatively short in duration, and emergency response and reconstruction can start quickly after the potential series of aftershocks has receded. As this all takes place within the year of occurrence, annual average light intensity captures a mix of direct impact and recovery (for similar discussions on estimating hurricane impacts, see Mohan and Strobl, 2017; Del Valle et al., 2018). With the launch of the Suomi NPP satellite, the new VIIRS-DNB sensor has been detecting night lights for which NOAA has produced monthly composite images since April 2012 (Elvidge et al., 2017). These images provide us with high-detail monthly night light composites, that allow the study of short-term impacts of shocks. This makes it possible to systematically quantify earthquakes' direct impact on their socioeconomic environment, but also to separately study recovery after the event. In doing so, this paper aims at increasing our understanding of the short and

---

<sup>1</sup>While the literature typically controls for country size in these estimations, i.e. taking damages or fatalities over area size (see e.g. Skidmore and Toya, 2002), this hardly addresses the issue of taking into account local geographical, climatic, and cultural conditions, which show high heterogeneity especially within large countries. Moreover, local economic conditions ultimately determine potential impact, and can only be controlled for adequately by included at-site economic exposure, rather than country averages.

<sup>2</sup>Note that national GDP statistics implicitly assume a homogenous distribution of economic activity across space, which is especially problematic when used for studying growth effects of natural disasters that are local in nature – it matters **where** an earthquake occurs in countries the size of Russia or Brazil, as economic activity is highly unevenly spread.

<sup>3</sup>A sidenote concerns the general discussion on national income statistics; they are by construction unable to capture activity in the informal sector, which can account for up to 40% of national economies for developing countries (see Schneider and Enste, 2000; Schneider, 2005, 2007). Instead, night lights reflect any economic activity that requires the use of electric light at night, such that it reflects a part of economic activity that is related to the informal sector (for a recent application, see Tanaka and Keola, 2017)

<sup>4</sup>See <https://ngdc.noaa.gov/eog/dmsp/downloadV4composites.html>

medium-run effects of earthquakes on local economic activity.

A third challenge is to adequately quantify a disaster's intensity across geographical space. Until recently, most of the economic literature used outcome variables such as fatalities and damages, usually normalized by population size, geographical area, or GDP, as a proxy for intensity (see e.g. Botzen et al., 2019). As Felbermayr and Gröschl (2014) show, using these outcome variables as intensity measures results in substantial endogeneity bias – damages correlate positively with income. Besides, these kind of outcome variables typically have no geographical component. Instead, studying the economic effects of natural disasters should be approached by using the exogenous physical intensity of the natural hazard. But doing so is not straightforward since most data is not readily available.<sup>5</sup> This is especially challenging for earthquakes. The physical extent, direction, and strength of destructive force depends on a large number of factors that makes quantification of physical intensity in a given location hard (Allen et al., 2008). The typical measure for earthquakes is their magnitude, which represents the total energy release associated with an earthquake event.<sup>6</sup> While this measure is the most comprehensive description of an earthquake event as a whole, it is agnostic about how heavily the surface area was affected, and – more importantly – where the shaking took place. Instead of relying on a point source with general earthquake magnitude, I make use of a dataset of ground shaking maps, as compiled in the Shakemap Atlas provided by the United States Geological Survey (USGS) (Allen et al., 2008; García et al., 2012). This Atlas quantifies the geographical location and intensity of ground shaking of a set of significant earthquakes, of which I use events between 2012-2016. Recent contributions in the literature on the economics disasters have made use of shakemaps to identify earthquake impacts (see Skoufias et al., 2020, 2021; Nguyen and Noy, 2020). I follow this approach and expand the analysis to the global level, using the intensity of ground shaking on site as a measure of physical intensity of the shocks. The central question is how earthquakes affect local economic activity in the first year after the quake, as proxied by night light emission.

The empirical strategy is relatively straightforward. I collect, clean, and combine the monthly VIIRS night light composites for the period 2012-2016 and merge this data with the shakemaps of 456 earthquakes from the USGS Shakemap Atlas in a globally uniform manner. This involves a major data collection in which a global dataset of both monthly night lights and ground shaking from earthquakes is constructed at a resolution of 450 meters, containing close to a billion observations. I then relate intensity of ground shaking to changes in night light intensity over subsequent months through a panel fixed effects analysis. I split the analysis in two ways of spatial aggregation. Following the examples of Felbermayr et al. (2022)

---

<sup>5</sup>See Felbermayr et al. (2022) (Chapter 3) for the first attempt to do this systematically and globally for weather and climatic disaster types.

<sup>6</sup>Studies that examine the relation between earthquakes and economic activity typically take either magnitude as a measure for physical intensity (e.g. Felbermayr and Gröschl, 2014; Fabian et al., 2019), or refrain from using physical intensities altogether and rather use fatalities or monetary losses to quantify the severity of an event (e.g. Noy, 2009; Cavallo et al., 2013; Klomp, 2016).

(Chapter 3) and Fabian et al. (2019), I start with a global set of over 20,000 grid cells with a resolution of 0.5 degrees.<sup>7</sup> In a second step, I refrain from any spatial aggregation and instead do the analysis at the resolution of the VIIRS data, i.e. at 15 arc seconds or roughly 450 by 450 meters at the equator, as is more customary in the strand of literature that focuses on local impacts of hurricanes (Bertinelli and Strobl, 2013; Mohan and Strobl, 2017; Skoufias et al., 2020, 2021; Del Valle et al., 2018; Ishizawa et al., 2019; Miranda et al., 2020). This comprises a dataset of 1.3 million pixels, all of which are affected by shaking from earthquakes at some point in the time frame. In doing so, this paper aims to contribute to the emerging literature on economic impacts of natural disasters by assessing the impacts of earthquakes on night light emission at different spatial scales.

As opposed to the clear effect identified in the literature on hurricanes and night light, my findings do not suggest a clear-cut effect of earthquakes on night light intensity is present. I test for various specifications and controls in terms of fixed effects, and test for heterogeneity in income groups. However, no significant effect is found across the models, either at 0.5° or at pixel-resolution. These findings resemble those by Skoufias et al. (2021), who report similar results for some case studies and country-level results for Southeast-Asian countries. I discuss potential issues from both a methodological and data point of view, and form an agenda for future research.

The remainder of this paper is structured as follows: Section 4.2 reviews the related literature. Section 4.3 discusses the data sources used for this paper, describing first the night light data and subsequently the construction of the shakemap data. In Section 4.4 I explain the empirical strategy, and discuss results in Section 4.5. Section 4.6 discusses implications of the findings and concludes.

## 4.2 Literature

In this paper I build on several distinct literatures from economics and remote sensing. First, the use of night lights as a proxy for economic activity has become increasingly popular for a range of applications. Studies showing the relation between the relationship between night lights and socioeconomic information go back two decades (Sutton and Costanza, 2002; Doll et al., 2006; Sutton et al., 2007; Ghosh et al., 2009, 2010). In economics, night lights are being increasingly used to study local economic development, and more recently to study the effect of shocks on local economies. Henderson et al. (2012) investigate the informational value of night lights in estimating economic growth at the country level, while an emerging literature investigates smaller sub-national units.<sup>8</sup> The broad consensus is that

---

<sup>7</sup>These cells are approximately 55 by 55 kilometers at the equator, becoming narrower in east-west in Euclidean distance as one moves towards the poles. Given the data range of the VIIRS night lights, I only use cells between 65°South and 75°North, and drop seas and oceans.

<sup>8</sup>Michalopoulos and Papaioannou (2013, 2014) focus on economic growth in ethnic homelands, Hodler and Raschky (2014b) on economic development of sub-national administrative units,

growth in remotely sensed nighttime light provides a useful proxy for GDP growth over the long run. But night lights can also be used to track short-run fluctuations in economic development. For example, Henderson et al. (2012) show that e.g. the 1991 Rwandan genocide in Kigali can clearly be seen from the sky, as can the 2007/8 financial crisis in e.g. Jakarta. The authors further test this in a global panel and confirm that night lights are capable of predicting both economic expansions and downturns.<sup>9</sup> Recent studies on the newer monthly VIIRS light data show their potential to capture economic activity at the very local scale (e.g. Li et al., 2013b; Ma et al., 2014). The informational value of night lights for studying local economic dynamics is therefore evident, and I will exploit this in this paper.

The literature on using night lights to study economic impacts of natural disasters is growing fast. Early papers stem from the remote sensing and hazards literature, where remotely sensed images of night lights are primarily used for the purpose of identifying potentially damaged areas after disaster events as soon as possible. Kohiyama et al. (2004) are among the first to use DMSP night lights to study the immediate impacts of earthquakes. The authors design an automated program that detects anomalies in light intensity in potential earthquake zones to identify damaged areas, and show that day-to-day DMSP night light images do a fairly good job at identifying damaged areas even distant from the epicenter.<sup>10</sup> Making use of the newer VIIRS night light data, Fan et al. (2019) compare day-to-day night light changes after earthquake impacts to pre-earthquake mean radiance to rapidly predict damaged areas after impact. The authors report reasonable success in predicting damage from earthquakes by cross-referencing pixels with light change to USGS's Shakemaps for a number of major earthquakes.<sup>11</sup> Overall, light reduction

---

Storeygard (2016) on trade and urban growth, Henderson et al. (2017a) on urbanization for uniform grid cells and Bleakley and Lin (2012) on locations along rivers as natural features, Bruederle and Hodler (2018) on local wealth and human development in Sub-Saharan Africa, and De Janvry et al. (2016) on post-disaster growth in Mexican municipalities.

<sup>9</sup>Miranda et al. (2020) have recently revisited this issue in the context of hurricanes and find similar evidence specifically for Central American countries.

<sup>10</sup>In earlier work, Hashitera et al. (1999) explore the possibility of using the DMSP night lights to identify damaged areas after the Marmara earthquake in Turkey, using daily images. The authors report a high degree of correspondence between ex-post identified real damaged areas and areas identified from night light reduction. Moreover, Takashima et al. (2000) investigate to what extent the identified light reduction captures 1) deaths, 2) damaged housing, and 3) power outage. While power outage is detected in the areas where the power supply had not recovered over night yet, the night light reduction is clearly captured in areas even where power has come back online. In particular, the spatial distribution of reduction in night lights fits reasonably well with the distribution of casualties, and more importantly with the distribution of wounded and collapsed and moderately damaged housing. The estimated reduction in night light thus captures more than power outage alone, giving further support for the use of night lights to estimate post-disaster impacts. For a discussion on disaster-related power outages, see appendix section 4.B.1

<sup>11</sup>In their study (Fan et al., 2019), light reduction correlates strongly with ground shaking above MMI 5 and especially above MMI 6. Accuracy is in the order of 85% for the two studied earthquakes in Chile ( $M_w$ 8.2 April 2014 and  $M_w$ 8.3 September 2015). For the April 2015 Gorkha earthquake in Nepal, however, accuracy is only in the order of 15%, potentially due to cloud cover at the time of the earthquake, as well as generally lower intensities of light in the affected areas in Nepal versus the affected areas in coastal Chile.

correlates well with high shaking intensities, as modelled in the Shakemaps by USGS. The approach of the authors, however, is very case-specific, and they consider only the first days after impact to identify damaged areas. Instead, I am interested in tracking light levels over the months following an event to evaluate the impact and recovery phase, and moreover expand the analysis to a global sample.

In economics, with administrative data typically lacking for small regions of interest, studying changes in light over time for a particular area has also been helpful for studying the economic impact of sudden-onset events.<sup>12</sup> Hurricanes are covered most extensively in the literature. The first application of attempting to study local economic effects of natural disasters using night lights in the economics literature is presented by Bertinelli and Strobl (2013). The authors model wind speed from hurricanes on a 1km grid and establish negative local impact of hurricanes on intensity of recorded night light emission in the Caribbean. In a similar fashion, Gillespie et al. (2014) study the impact of the 2004 tsunami and find depressed luminosity in damaged areas for Indonesia.<sup>13</sup> A growing body of literature has followed these examples, and is studying the local economic impact of natural disasters – primarily hurricanes – using local responses in night light intensity. Elliott et al. (2015) study the effect of typhoons (i.e. tropical cyclones or hurricanes) in coastal China and similarly identify a short-term substantial negative impact on local economic activity as captured by night lights, but find no effect beyond the year of occurrence. A second follow-up study assesses the effects of cyclone Pam on the South Pacific Islands in March 2015, for the first time using the VIIRS monthly night light imagery (Mohan and Strobl, 2017). The authors find a sharp drop in night light intensity in the month of the storm, but find positive effects on light intensity after roughly half a year after the storm. These findings further confirm the need for studying disaster impacts at relatively high temporal frequency. Ishizawa et al. (2019) and Miranda et al. (2020) continue this discussion and record longer-lasting effects in the Dominican Republic and Central America respectively. Turning to flood events, Kocornik-Mina et al. (2020) study the effect of large-scale floods in urban areas using the annual DMSP night light data. The authors analyze the negative shock and recovery of city lights and find substantial effects in the year of occurrence, but no effect thereafter, except for more recently populated urban areas. Felbermayr et al. (2022) (Chapter 3) make the first attempt to bring the approach together in a systematic manner, and propose to study the local impacts of extreme weather events at a uniform scale of 0.5° grid cells. The authors collect and bring together spatially detailed data on storms, precipitation, temperature events, and droughts, and study the impact of extreme events on cells' local light emissions at annual frequency. As with the previous studies, temporary reductions in night light are found, while recovery seems to occur within 2 years for most event

---

<sup>12</sup>While not related to natural disasters per se, the VIIRS night lights have also been demonstrated to be useful in studying e.g. cities going dark in the Syrian crisis, as well as refugee camps showing up (see Román et al., 2018). Similarly, see Li and Li (2014) and Li et al. (2015) for a discussion on observing the Syrian crisis in Iraq and Syria from space.

<sup>13</sup>For a more recent discussion on the effects of the 2004 tsunami, also incorporating night lights, see Heger and Neumayer (2019).

types. I follow their approach in this paper, but instead study specifically the effects of earthquakes on night light intensity for affected areas in the subsequent months after the initial shock.

## 4.3 Data

I now turn to the data collection for this paper. For the baseline analysis I need night light intensity and the spatial distribution of ground shaking of earthquakes per grid cell per month. I first describe the data collection and cleaning for the night lights.

### 4.3.1 VIIRS night lights

Economists working with night light data have typically relied on annual stable night light composites from the Defense Meteorological Satellite Program (DMSP). With the launch of the Suomi-NPP satellite in 2011 a new suite of nighttime recordings has become available from the Visible Infrared Imaging Radiometer Suite (VIIRS) Day/Night Band (DNB). The VIIRS-DNB night light data has two major advantages over the older and more widely used DMSP-OLS data: (1) a much higher spatial resolution of 15 arc seconds versus 30 arc seconds, and (2) no saturation of light intensity and a much lower light detection limit and thus improved capacity to detect low-intensity light sources.<sup>14</sup> The 15 arc second night light pixels, from now on referred to as grid cells, form the core of the dataset. They are sized roughly 450 by 450 meters at the equator, and all data that is collected in addition to the night light data is processed at the same resolution and extent of 15 arc second cells of the VIIRS night light images.

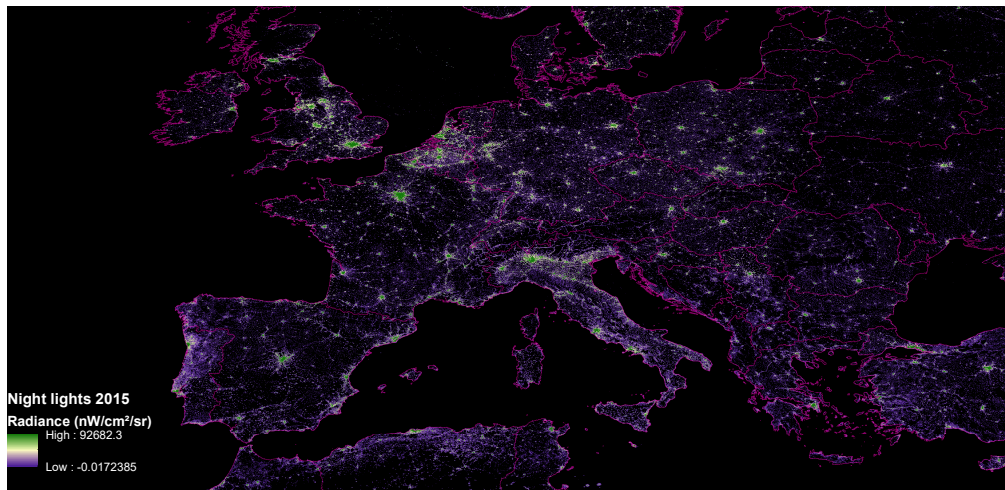
As with the annual composites of the DMSP-OLS data, NOAA processes the data to produce composite images of average visible light, but now at monthly intervals. The monthly DNB composites version 1.0, as delivered by NOAA at the time of writing, are raw cloud-free composites at a resolution of 15 arc seconds (for a detailed discussion, see Elvidge et al. (2017)). Before averaging to monthly composites, the data is filtered to exclude data impacted by stray light, lightning, lunar illumination, high-energy particles, and cloud-cover. The images cover the entire globe between 65°S and 75°N. The cleaning process by NOAA is less thorough than for the DMSP annual composites and leaves a number of issues unresolved in the data. Known contamination that remains in the images is reflection from snow cover and water body reflection, and ephemeral events such as forest fires and aurora (Levin and Zhang, 2017; Coesfeld et al., 2018). A further important caveat of the

---

<sup>14</sup>Note that the Suomi-NPP satellite has an overpass time at roughly 1.30 am. This is substantially later than that of the older DMSP satellites, which had an overpass time between 8.00-10.00 pm (Elvidge et al., 2013). The VIIRS night lights therefore arguably record a different type of night light than the DMSP satellites. As e.g. discussed by Gibson et al. (2020), rural lights are likely to be turned off at this time of night, while light from urban street lamps, car parks, and industrial facilities may still be lit.

raw data is that the monthly images are strongly affected by stray light in summer months, which occurs at mid-to-high latitudes – roughly matching the temperate zones on both the Northern and Southern hemisphere. As a result, large parts of the northern hemisphere have missing night light data for these months.<sup>15</sup> There is currently no solution for this issue, other than recording missing pixel-month observations for the affected areas.

Figure 4.3.1: Night light emission over Europe



*Note:* Average stable night light composite for 2015, as provided by NOAA.

Some further cleaning of the data is warranted before I construct the dataset for this analysis. I exclude all pixels that are not on land and exclude pixels for which no cloud-free observation is available. This results in a pixel-resolution dataset of roughly 855 million pixels between 65°S and 75°N. This dataset is too large to process, let alone to analyze econometrically. Ideally, one would simply drop all pixels with zero light intensity. However, the monthly images have no absolute zero radiance value floor, and instead have a range of small positive and negative values around zero (see Elvidge et al., 2017). As of yet, there is no consensus in the literature on how to deal with these (for a discussion, see Skoufias et al., 2021). As a first step, I make use of the more thoroughly cleaned annual stable VIIRS light product for 2015 to identify pixels that are considered dark after outlier removal, and drop these pixels accordingly (Elvidge et al., 2017).<sup>16</sup> While this is evidently

<sup>15</sup>On the northern hemisphere, the stray light border shifts across the globe from 65°North in winter time down to 35°North in June, roughly extending as far south as Tokyo. On the southern hemisphere, the border similarly moves towards the equator, up to 40°South in December, affecting the visibility of e.g. Melbourne in the southern hemisphere’s respective summer months. A separate version of the monthly images is distributed by NOAA, which include reconstruction of light intensity in stray-light affected zones, based on models of solar radiance. Since these values are imputed and do not account for potential shocks, I do not work with this version of the data. See Mills et al. (2013) for a discussion on the stray-light corrected images.

<sup>16</sup>I make use of the outlier-corrected stable light vcm-orm-ntl product for 2015. At the time of writing, no other annual stable VIIRS light products are available from NOAA.



inferior to dropping pixels that are dark throughout the entire period, there is no non-arbitrary way of deciding which cells are to be considered 'dark' and which are not based on the monthly images, because the monthly images have not undergone cleaning for outliers, and because there is no absolute zero in the monthly data. Moreover, there is no suggestion in the literature on how to distinguish between noise and signal in the lower spectrum of light intensity data. To refrain from having to make assumptions and to make the most transparent choice, I therefore rely on the annual stable 2015 product and set light intensity for pixels to zero for all pixels that have zero light in the annual stable image.<sup>17</sup>

Cells may be populated while emitting very little light, which is for example the case for many medium-sized cities in developing countries. Some of these areas are hard to distinguish from truly dark pixels in the raw light data (for a discussion, see Elvidge et al., 2017)). Simply removing remaining low-light grid cells may therefore omit areas of interest from the dataset. Instead I follow a different approach. Earthquakes cause damage to buildings and infrastructure, which are concentrated in urban areas. As night light intensity poorly reflects agricultural activity (Keola et al., 2015), impacts of earthquakes on rural areas will be hard to gauge through the use of night lights. I therefore focus the analysis on urban cells only. As a first step, I follow Kocornik-Mina et al. (2020) and use CIESIN's Global Rural-Urban Mapping Project (GRUMP) urban extent dataset (Center for International Earth Science Information Network (CIESIN) at Columbia University, 2017) to identify urban pixels. However, even urban extents from GRUMP have dark areas, and more importantly dark areas which are likely unpopulated as well. While disaggregated population datasets exist (see e.g. Center for International Earth Science Information Network (CIESIN) at Columbia University, 2016), they are typically based on population data from census areas and thus cannot be used to isolate populated from unpopulated pixels.

Instead, I use a different solution. To further reduce the data to urban pixels of interest only, I limit by presence of buildings, unambiguously signalling the presence of man-made structures. It is these areas that produce human-made light and that are exposed to seismic risk, and these are the areas of interest. I make use of the novel GHSL-BUILT dataset from JRC's Global Human Settlement Layer project, which records the proportion of building footprint area in pixel (Corbane et al., 2018).<sup>18</sup> Based on this, I drop all pixels that contain no built-up area.

Globally, 95% of roughly 855 million grid cells between 65°S and 75°N are entirely non-built-up. Of the remaining 42.6 million built-up cells, a further 18 million are persistently dark in the annual stable light product of 2015. After dropping the

---

<sup>17</sup>Note that one may argue this interferes with the very effect this paper is trying to find, namely reduced night light intensity after earthquakes. If this were a worry, it would affect the estimations only if night light intensity is reduced to zero for prolonged periods time starting before 2015, and would thus be considered dark in the annual 2015 product. However, as will be discussed in the results later, there is no sign of this happening in the data.

<sup>18</sup>GHSL-BUILT comes in World Mollweide projection and was downloaded at 250 meters resolution. The data was then reprojected to 15 arc seconds in WGS84 to match the resolution of the VIIRS night light data.

non-built-up, and built-up but persistently dark cells, the resulting dataset consists of 24.6 million grid cells. These represent 2.9% of all land cells. The result of this cleaning process is plotted in Figure 4.3.2. Cells in blue are built-up, but emit no persistent light. The pink cells are both built-up and persistently lit and make up the final dataset. Unsurprisingly, the majority of built-up and lit cells are located on the northern hemisphere, with the eastern half of North America, Europe, India, and east China being the most represented world regions. Note that large parts of South America, Africa, and Australia have unpopulated and thus non-built-up and non-lit areas, which are not included in the dataset.

Plotted in shades of green to red in Figure 4.3.2 are the levels of shaking from earthquakes as reported in the shakemaps that form the core data on the earthquakes for this analysis. I now turn to discussing this part of the data in detail.

### 4.3.2 Earthquakes

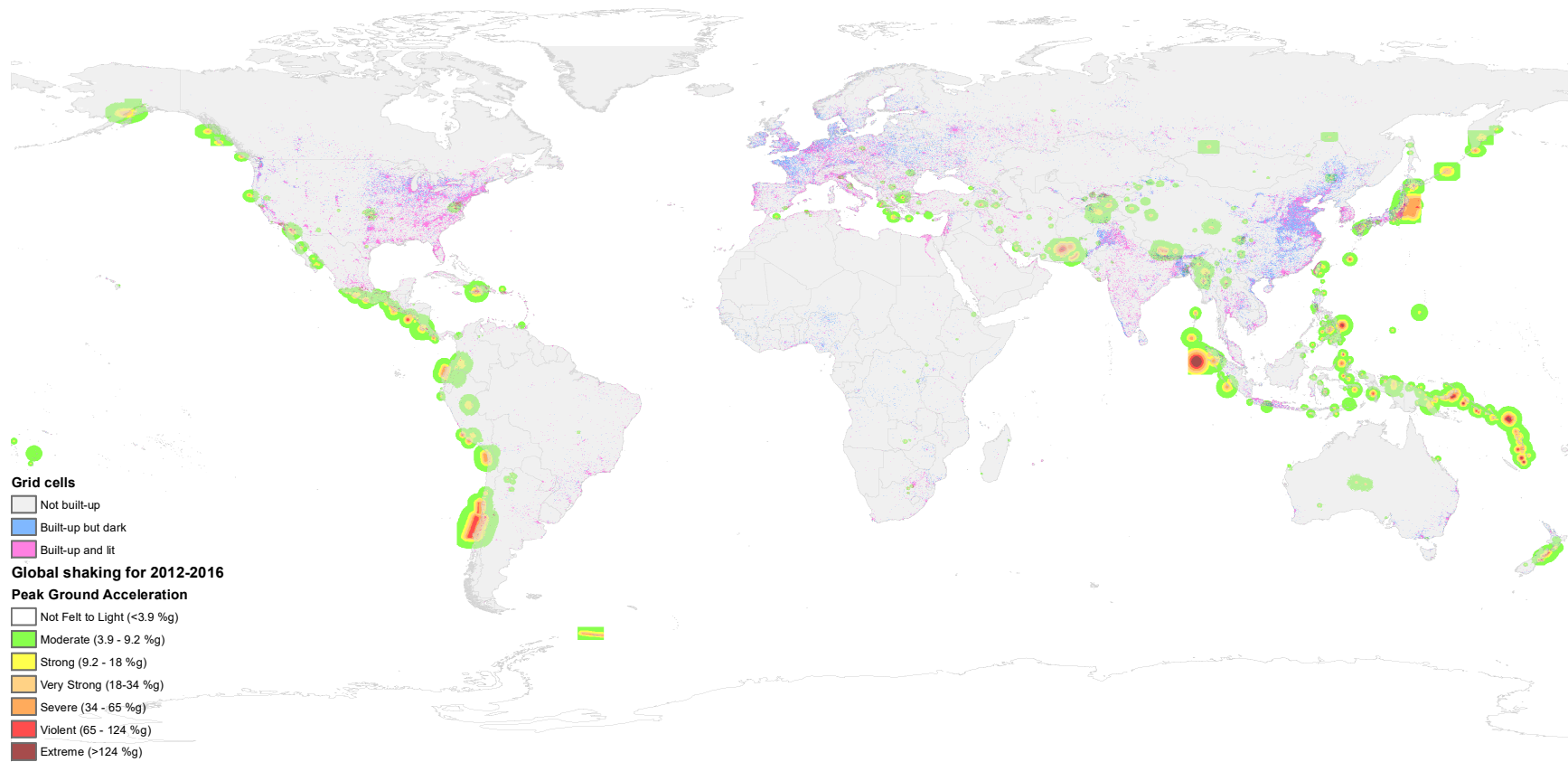
Earthquake information comes from the Shakemap Atlas 2.0, compiled and distributed by the United States Geological Survey (Allen et al., 2008). From the Shakemap Atlas, I take shakemaps for a set of significant earthquakes, giving intensity of ground shaking in the affected area (for a detailed description, see García et al., 2012).<sup>19</sup> The most important information that I use from these shakemaps are ground motion parameters, and specifically Peak Ground Acceleration (*pga*). This measure models the maximum ground shaking at a location, expressed as a proportion of  $g$  – the acceleration of the Earth’s gravity, equivalent to  $g$ -force. The geographical distribution of shaking is modeled by combining measurements with available information on topography and soil layers. It is this intensity of ground shaking rather than the more general overall magnitude of earthquakes that most directly relates to the spatial pattern and degree of damage (Allen et al., 2009). Peak ground acceleration is widely used in earthquake engineering and is the common measure employed in the construction of seismic hazard maps, such as the Global Seismic Hazard Map project (GSHAP, see Giardini et al. (1999)).<sup>20</sup> In doing so I follow Skoufias et al. (2020, 2021) in their work on Indonesia and Myanmar, as well as Nguyen and Noy (2020) for the Canterbury earthquake sequence in New Zealand.

---

<sup>19</sup>The Shakemap Atlas does not provide shakemaps for the full universe of seismic events. Instead, a selection is made to include only earthquakes that had potential human impact. The inclusion rule is as follows: (1) Only include earthquakes where population exposure to Modified Mercalli Intensity (MMI) VI level shaking is 3,000 people or greater, (2) include only earthquakes with a hypocentral depth less than 100 km, unless the earthquake resulted in casualties, and (3) include only earthquakes below magnitude 6.5 if their hypocentral depth is less than 45 km, unless the earthquake resulted in casualties. This selection of events ensures that I only include events with potential exposure of population and capital. See Allen et al. (2008) for a detailed discussion.

<sup>20</sup>The set of ground motion parameters also includes peak ground velocity and peak ground displacement. Since peak ground acceleration is the most commonly used of the three in both earthquake engineering as well as for earthquake hazard maps, and data availability for this measure is good, I use peak ground acceleration as the parameter of choice for this study. See Lackner (2018) for a detailed discussion.

Figure 4.3.2: Global maximum shaking of earthquakes included in the Shakemap Atlas 2.0 for 2012-2016



*Note:* Maximum ground shaking between 2012 and 2016 in *pga* (%g), as provided by the USGS Shakemap Atlas 2.0 (García et al., 2012). Based on own computations using the full set of shakemaps from the USGS Shakemap Atlas 2.0 for 2012-2016, accessed January 2019. In the case of multiple earthquakes occurring in the same location between 2012-2016, this figure plots the maximum peak ground acceleration recorded for that location throughout this period. The panel of grid cells after cleaning is indicated in two colors: the final set of built-up and lit grid cells is indicated in pink, whereas blue indicates cells that are built-up but have zero night light intensity. The blue cells are excluded from the analysis.

To provide a basis for discussion, some intuition for this measure is required. Wald et al. (1999) estimate relationships between peak ground acceleration and Modified Mercalli Intensity (MMI) for eight significant California earthquakes, adopted directly in Figure 4.3.3. Most important for this application is the level of potential damage from any given level of shaking. While estimated for California specifically, other studies have done so for Central United States (Atkinson and Kaka, 2006, 2007), Western United States, Japan, and Southern Europe (Murphy and O’Brien, 1977), and for Costa Rica (Linkimer, 2008), the latter of which finds relations that are remarkably close to those of Wald et al. (1999). While the estimated relations vary from region to region (Atkinson and Wald, 2007), to the best of my knowledge no global study exists that provides average estimates. I therefore follow the most commonly used classification by Wald et al. (1999). At any shaking below  $3.9\%g$  – or an MMI of 5 or lower, no damage is to be expected. Very light to light damage is expected between  $3.9$  and  $18\%g$ , which translates into MMI scales 5-6. At any level of shaking above that, potential damage is likely, thus starting at an MMI of 7.

Figure 4.3.3: Peak ground shaking and potential damage

PERCEIVED SHAKING	Not felt	Weak	Light	Moderate	Strong	Very strong	Severe	Violent	Extreme
POTENTIAL DAMAGE	none	none	none	Very light	Light	Moderate	Moderate/Heavy	Heavy	Very Heavy
PEAK ACC.(%g)	<.17	.17-1.4	1.4-3.9	3.9-9.2	9.2-18	18-34	34-65	65-124	>124
PEAK VEL.(cm/s)	<0.1	0.1-1.1	1.1-3.4	3.4-8.1	8.1-16	16-31	31-60	60-116	>116
INSTRUMENTAL INTENSITY	I	II-III	IV	V	VI	VII	VIII	IX	X+

Note: Instrumental Intensity scale adopted from Wald et al. (1999).

Since the scale on which shaking is recorded is non-linear in nature, using the continuous version of ground shaking in any statistical analysis is problematic. Skoufias et al. (2020, 2021) make use of vulnerability curves based on building types for Indonesia, in part to address the non-linear relation between ground shaking and building damage.<sup>21</sup> The use of vulnerability curves, however, is too ambitious for a global sample. To the best of my knowledge, no database exists that specifies vulnerability to ground shaking for all countries in the world.

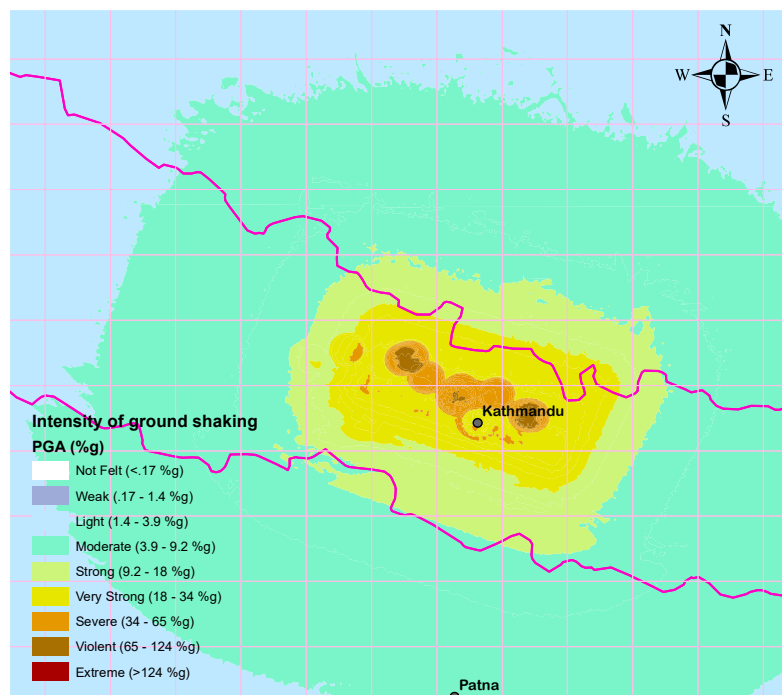
For the purpose of this paper, I will therefore make use of the classification by Wald et al. (1999), in which I consider shaking of MMI 4 or lower as no treatment, shaking in scales 5 and 6 as mild treatment, and any shaking of scale 7 or higher as heavy treatment. To be clear, all estimations are based on a pixel’s objective level of shaking in terms of peak ground acceleration, but classified into treatment dummies according to their potential for damage, and named according to the MMI classes in Wald et al. (1999). Later in the analysis, I relax the assumptions on thresholds for damage and estimate impacts using both linear and non-linear transformations of the *pga* variable, but find very similar results.<sup>22</sup>

<sup>21</sup>In the vulnerability curves presented by Skoufias et al. (2020), non-linearities become apparent starting at shaking levels of  $50\%$  *pga*. In the global dataset however, even for the pixel-months with shaking of MMI 7+, only roughly 5% of cases exceeds a *pga* of  $50\%$ .

<sup>22</sup>As an additional robustness test, I follow the literature on estimating relationships between

Figure 4.3.4 gives a graphical illustration of what a shakemap looks like, giving estimated *pga* over space for the April 2015 *M*7.8 Gorkha earthquake near Kathmandu, Nepal. Heavy shaking concentrates around the epicenter of the earthquake about 65 kilometers northeast of Kathmandu. Kathmandu was exposed to severe shaking reaching levels of up to 74%*g*, corresponding to an MMI of 9. This intensity of shaking is associated with heavy damage and a high death toll – both were, tragically, recorded. The most widely used database on fatalities and damages from natural disasters, EM-DAT (CRED, 2021), reports 8831 fatalities, and total damages of US\$ 5.2 billion. Note that while the decay of ground shaking is generally circular, hotspots of shaking are roughly parallel along the north-west to south-east fault line that generated the earthquake. Another important observation is that peak ground acceleration levels remain very strong over long distances, spanning well over 150 kilometers east to west. It is this type of non-random spatial heterogeneity in ground shaking that I deem essential to map to the grid cells that I study - a process that a general distance-decay rule cannot reproduce. Especially when focusing on relatively small spatial units as is done in this study, arbitrary distance-decay rules are likely to introduce more measurement error than they solve.

Figure 4.3.4: Intensity of ground shaking during the April 2015 Gorkha earthquake



*Note:* Ground shaking in *pga* (%*g*), as provided by the USGS Shakemap Atlas 2.0 (García et al., 2012). For reference, 0.5° grid cells that are used in the first part of the analysis are added in the background.

MMI and ground shaking (see Wald et al., 1999; Atkinson and Kaka, 2006, 2007; Linkimer, 2008), and test for a log-linear relationship between shaking and estimated impacts. Results are qualitatively similar.

I now turn to the global collection of shakemaps. Shakemaps for each individual earthquake are retrieved and I subsequently preserve maximum *pga* by pixel by month as the main variable of interest. Figure 4.3.2 shows the geographical distribution of the included earthquakes, as well as a the global set of cells that enter in the statistical analysis after the cleaning process described above. These cells are naturally concentrated around the ‘Ring of Fire’ (the Circum-Pacific belt) in the Pacific Ocean, stretching from the Andes in South America along the west coast of North America alongside Japan and south through Southeast Asia and the Pacific Islands. Other notable hotzones are central Asia with major earthquakes in Nepal and Pakistan, and the Mediterranean with many quakes in Italy, Greece, and Turkey among others. The heaviest shaking is experienced in Indonesia and the Pacific islands, as well as along the Andes range. Note that Central Europe, Russia, Canada, Australia, virtually entire Africa, and entire South America except for the Andes range do not experience any (serious) earthquakes in the studied period. As these areas are not by affected by earthquakes throughout the study period, I follow the strategy by Kocornik-Mina et al. (2020) and focus only on cells that are ever affected in the sample. I therefore drop all cells that never experience positive shaking through 2012-2016.

A total of 456 earthquakes for the period April 2012 - December 2016 are included for this analysis, leading to a total number of just over 1 million treatments across 700,000 unique cells. Magnitudes range from  $M4.5$  to  $M8.6$ , with a mean of  $M6.1$  and a standard deviation of  $M0.7$ .<sup>23,24</sup> Peak ground acceleration has a strongly right-skewed distribution, with a mean of 27% *pga* and 95% of MMI7+ shaking being below 50% *pga* (see Appendix Figure 4.A.2).

Throughout 2012-2016, 686,000 pixels are exposed to shaking of Modified Mercalli Intensity 5-6 (medium shaking of at most 18% *pga*) while a further 33,000 pixels experience heavy shaking of MMI 7+ (*pga* exceeding 18%). Average light intensity for this final sample is 10.8 nW/sr/cm<sup>2</sup>, with a standard deviation of 139.<sup>25</sup> To account for this heavily right-skewed distribution in the night lights, and as is customary in the literature, I take the natural logarithm of night light intensity as the dependent variable (see Appendix Figure 4.A.3 for a histogram of its distribution.) Finally,

---

<sup>23</sup>See Appendix 4.A Figure 4.A.1 for a histogram of magnitudes of the included earthquakes.

<sup>24</sup>Lackner (2018) investigates the representativeness of the Shakemap archive for total global earthquake ground shaking. The author concludes that coverage of significant events (in terms of shaking or human impacts) is nearly complete, with only 0.7% of earthquake with magnitude 5.5 or greater not having a shakemap. Recorded earthquakes without accompanying shakemaps are concentrated in the time period before 2006, while from 2006 onwards coverage in the Shakemap Atlas increases dramatically. In terms of geographical bias, the number of shakemaps is slightly biased towards North American events for earthquakes with a magnitude between 4.5 and 5.5. In total, 108 earthquake events, or roughly 15%, for this study have a magnitude in that range. Of these 108 events, only 18 are located in North America. According to Lackner (2018) the bias in the Shakemap dataset is more serious for earthquakes with a magnitude below 4.5, but none of these are included in this study.

<sup>25</sup>95% of observations has a radiance value larger than 0.5 nW/sr/cm<sup>2</sup>, corresponding to the highest threshold that e.g. Skoufias et al. (2021) use to limit the extent of the noise floor in the light data.

aggregated to  $0.5^\circ$  this makes for 4200 affected grid cells, for which I preserve mean light intensity and maximum *pga*.<sup>26</sup>

Table 4.3.1: Top 10 most damaging earthquakes between 2012-2016

	Country	Date	Magnitude	Peak ground acceleration (%g)	Total fatalities	Total affected	Total damage ('000 US\$)
1	Japan	16-Apr-2016	7.3	110%	49	298432	20,000,000
2	Italy	20-May-2012	6.0	18%	7	11050	15,800,000
3	China	20-Apr-2013	7.0	30%	198	2198785	6,800,000
4	Nepal	25-Apr-2015	7.8	74%	8831	5639722	5,174,000
5	Italy	24-Aug-2016	6.2	54%	296	4854	5,000,000
6	China	3-Aug-2014	6.5	34%	731	1120513	5,000,000
7	New Zealand	14-Nov-2016	7.8	198%	2	50	3,900,000
8	Ecuador	16-Apr-2016	7.8	54%	672	389364	2,000,000
9	China	7-Sep-2012	5.7	10%	81	744821	1,000,000
10	China	22-7-2013	5.9	22%	95	123887	1,000,000

*Note:* Top 10 highest damage earthquakes between 2012 and 2016, based on EM-DAT database. Magnitudes as reported by EM-DAT, maximum peak ground acceleration from the retrieved shakemaps from the Shakemap Atlas 2.0.

The most damaging earthquake is the very violent April 2016 Kumamoto earthquake in Japan, causing over 20 billion US\$ of damages (see Table 4.3.1). The majority of most damaging earthquakes is associated with very high levels of shaking, with the November 2016 earthquake in New Zealand leading with 198%g. However, a striking observation from Table 4.3.1 is that very large damages can occur even at levels of shaking at the lower end of shaking values in the high shaking category. The 2012 Northern Italy earthquake of 20 May was associated with shaking of 18%g, i.e. of MMI 7 shaking. Similar large damages are recorded in the September 2012 Sichuan earthquake in China ( $M_{5.7}$ ), even though peak ground acceleration was recorded at 10%g, therefore putting it not even in the category of heavy shaking, but at a category MMI6. Another noteworthy observation is that the number of fatalities evidently does not follow the same ranking as damages. Besides the 2015 Gorkha earthquake in Nepal, the second and third highest number of fatalities are found in the lower half of the top 10, and all are in middle or lower-middle income countries. While the 2012 Northern Italy earthquake was tremendously costly, EM-DAT reports only 7 fatalities. Similar relatively low numbers of fatalities are reported for the earthquakes in Japan and New Zealand. This is in line with earlier literature, that finds fatalities to be negatively, versus damages to be positively related to income per capita respectively (see Kahn, 2005; Strömberg, 2007) This brief top 10 clearly shows that we do not necessarily expect an unconditional linear relationship between shaking and disaster impact. This is of course widely

<sup>26</sup>For an earlier version of this paper, all data was organized at a resolution of  $0.5^\circ$ , following the strategy of Felbermayr et al. (2022) (Chapter 3). In this revision, all data has been recompiled at the 15 arc seconds resolution of the VIIRS data, after which the  $0.5^\circ$  grid cell resolution is compiled by aggregating up all pixels within the  $0.5^\circ$  grid cell boundaries after the cleaning process as described above.

acknowledged in the natural hazards literature, stressing that not only the hazard itself, but more importantly exposure and vulnerability determine ultimate disaster outcomes. For this reason, I will be conservative in my statistical analysis, and use the aforementioned three categories of no, mild, and heavy shaking as the starting point. I will come back to the issue of vulnerability in section 4.5.4, when I discuss heterogeneity within the panel.

### 4.3.3 Night lights and earthquakes: an example

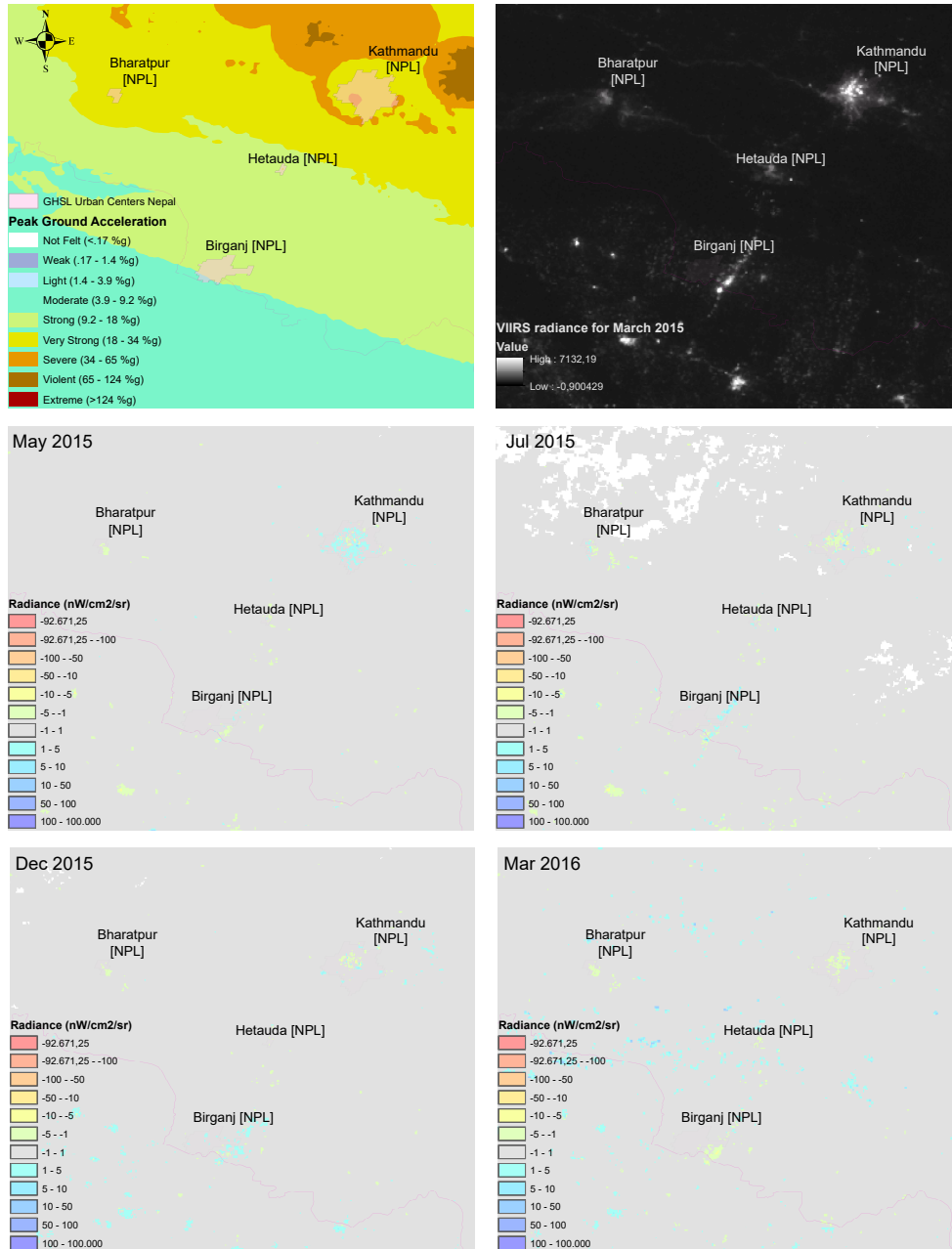
So what do the night lights show us when investigating earthquake events at this geographical and temporal scale? Before we turn to the statistical analysis, a graphical illustration is helpful. We return to the Gorkha earthquake of 25 April 2015 in Nepal, of which the shaking pattern was discussed in Figure 4.3.4. In Figure 4.3.5 below, I plot the night light intensity around Kathmandu before the earthquake, as well as the change in light intensity in the months after the earthquake. Strikingly, night light intensity in Kathmandu increases substantially in the month following the earthquake, signaling increased (outdoors) activity, while the settlements of Bharatpur, Hetauda, and Birganj show a decrease in light. These areas were exposed to shaking above  $9\%g$ , with Kathmandu and Bharatpur being most heavily shook at levels above  $18\%g$ .<sup>27</sup> There are no night light images available for June at this latitude due the earlier discussed stray light data issues in summer, so the first available subsequent observation is July. Already in July we see a decrease in night light with respect to March for Kathmandu, and also for Bharatpur and Hetauda. This pattern continues throughout the year 2015, as is shown in the bottom left panel of Figure 4.3.5, although Hetauda shows signs of recovery to pre-earthquake light levels. Indeed one year later in March 2016, night lights remain depressed in Kathmandu, as is the case for Bharatpur and Birganj. The persistent decrease in night light intensity for a large part of the city of Kathmandu shows how we can use night light imagery to study the impact of earthquakes on human settlements over time. However, a number of issues make visual evaluation of earthquake impacts difficult: first, there is large month-to-month variation in the recorded intensity of night light, such that changes in night light should be compared to 'average' changes in the area of interest. Indeed, entire regions or countries may experience an increase or decrease in recorded night light intensity from one month to the next (Levin, 2017). Comparison of images over time is therefore not trivial. Second, the visual inspection of the Gorkha earthquake reveals that while some parts of Kathmandu brighten, others become more dim. This spatial heterogeneity makes it hard to capture the overall effect on a city or a larger area. To flesh out the average effect, I use an econometric framework in which I account for such issues by making use of time fixed-effects that capture both year-to-year and month-to-month seasonal changes at the country level. The next section discusses the econometric model in detail.

---

<sup>27</sup>The highest level of shaking in Kathmandu was  $74\%g$ , corresponding to violent shaking of MMI 9.



Figure 4.3.5: Changes in night light around Kathmandu after April 2015 earthquake in Nepal



*Note:* The two top panels peak ground acceleration (left) and night light intensity in March 2015 (right) for the affected major settlements in Kathmandu. The four bottom panels show change in night light with respect to March 2015 (the earthquake occurred on the 25<sup>th</sup> of April). Green to yellow shades indicate a decrease in light intensity, blue shades indicate an increase. White represents missing radiance data. Based on own computations.

## 4.4 Empirical Strategy

I now turn to the identification strategy. The essential idea is simple: heavy ground shaking leads to physical destruction of capital and infrastructure and through these direct impacts affects local economic activity. When lights go out and stay out, this signals impediments to the local economy. It is this signal that I investigate. I approach this question with a panel fixed effects specification with a set of cell and time fixed effects, in which within-cell variation of month-to-month average night light intensity is related to the intensity of earthquake events in that cell over time:

$$\ln(\ell_{imy}) = \sum_{L=0}^k \beta_L \mathbf{D}_{imy-L} + \nu_i + \pi_{my} + \phi_{cy} + \eta_{cm} + \nu_i \cdot t + \mathbf{u}_{imy} \quad (4.4.1)$$

where  $\ln(\ell_{imy})$  is the natural logarithm of average night light intensity of cell  $i$  in month  $m$  in year  $y$  for each of the  $I$  grid cells. The earthquake treatment variable  $\mathbf{D}_{imy-L}$  captures earthquake intensity – peak ground acceleration – in two dummies: mild shaking ( $3.9 \leq \% pga < 18\%$ , corresponding to MMI 5-6), and heavy shaking ( $pga \geq 18\%$ , corresponding to MMI 7+). The omitted category is implicit and captures all cell-months with shaking below 3.9%  $pga$ . I allow for a contemporaneous effect in the month of occurrence ( $L = 0$ ) and a set of lagged intensity variables with a maximum lag length  $k$ , which I set to 12. Given the very limited availability of time-varying estimates of e.g. population numbers at the cell level, the only control variables are a set of fixed effects.  $\nu_i$  denote cell fixed effects controlling for time-invariant local unobservable variables, effectively controlling for geography, culture, and local economic and population conditions.<sup>28,29</sup> While data for ambient seismic risk is available, it is time-invariant and I therefore let cell fixed effects capture a cell's average long-run exposure to earthquakes. This is important, since there is large variation in the exposure of cells to earthquakes. The advantage of this approach is that shocks are therefore deviations from the mean for each individual cell (similar to Felbermayr et al., 2022, i.e. Chapter 3). Areas that experience mild shaking frequently are comparable to those that do not, through the cell fixed effects.  $\mathbf{D}_{imy-L}$  therefore represents random realizations of earthquake intensity for each cell, in turn allowing us to interpret  $\beta_L$  as the causal effect of earthquake intensity on monthly night light emission.

I then add a number of different time fixed effects. First, a flexible global time trend  $\pi_{my}$  captures global trends such as technological progress, energy costs, and the global business cycle, as well as potential month-to-month variation in measurement error of the satellite. Second, I follow Del Valle et al. (2018) and add country-by-year fixed effects  $\phi_{cy}$  to account for national economic growth or decline

---

<sup>28</sup>Note that light intensity strongly correlates with population size. However, for the short duration of the panel I only have a single population estimate (2015 from the Gridded Population of the World (v4, see Center for International Earth Science Information Network (CIESIN) at Columbia University (2016)). Since there is no credible globally systematic time-varying population estimate for this period, I let cell fixed effects account for initial population in 2012.

<sup>29</sup>Initial light level is implicitly controlled for with cell fixed effects.

throughout the panel. A completely flexible country-time trend (year-by-month fixed effects) would be ideal, but the analysis focuses only on cells that ever experience shaking in the study period. As such, country-time dummies would absorb at least part of the local treatment effect. Similar to the approach of Del Valle et al. (2018), I instead account for common recurring swings and seasonality in night light intensity at the country-level by including country-by-month fixed effects.<sup>30</sup> A final consideration is cell-specific growth in night lights throughout the time window of the panel. The fixed effects model is estimated in log-levels, and effectively demeans each cell's night light intensity over the study period. This ignores the fact that on average a cell's light intensity may grow or decline over the time period of the panel. To capture this, I include cell-specific linear time trends  $\nu_i \cdot t$ , that flexibly allow for growth or decline – or neither – at the cell level.

With the model I first study the contemporaneous effect of earthquake intensity  $\beta_0$  in the month of occurrence. The estimated lagged coefficients  $\beta_1$  through  $\beta_k$  then capture predicted deviations in the level of night light for a cell over time. Using these coefficients, I can plot predicted night light intensity over the months following an earthquake to give an estimate of the average duration of the shock effect and potential recovery.

As discussed in-depth in Felbermayr et al. (2022, Chapter 3), grid cells cannot be assumed to be independent from one another, as cells intersect and split true economic units such as cities and metropolitan areas. Night light emissions are highly spatially correlated, thus introducing spatial autocorrelation. In the ideal case, we would allow for spatial dependence between units through an explicit spatial model, like in Felbermayr et al. (2022, Chapter 3) and Nguyen and Noy (2020). However, due to serious limitations in the continuity of month-to-month observations for cells in the temperate zones, such a model is not feasible with these data. Moreover, due to the necessary cleaning steps described in the data section, pixels are not guaranteed to have a geographically meaningful set of neighboring pixels. Explicit modeling of spillovers is therefore not feasible. However, it remains necessary to address the presence of spatial autocorrelation. The most general, and most dominant approach in the literature on disaster impacts and night lights, is the use of Driscoll-Kraay standard errors (Driscoll and Kraay, 1998), which are robust to very general forms of spatial and temporal correlation in a panel.<sup>31</sup> I follow this example and correct for arbitrary spatial autocorrelation by using Driscoll-Kraay standard errors in the main estimations.<sup>32</sup> An alternative approach is to cluster standard errors by territories. Kocornik-Mina et al. (2020) take a conservative

---

<sup>30</sup>Rather than computing all these fixed effects, I absorb fixed effects by demeaning first. This is done with the 'ivreghdfe' package by Correia (Correia, 2016).

<sup>31</sup>For applications see Bertinelli and Strobl (2013); Skoufias et al. (2020); Ishizawa et al. (2019); Del Valle et al. (2018); Skoufias et al. (2021).

<sup>32</sup>Estimation of Driscoll-Kraay requires a maximum lag length. The choice for a lag length of 3 is based on the 'plug-in' estimator proposed by Hoechle (2007), which is based on the first step of Newey and West (1994) plug-in procedure. Because the optimal in the end depends on the underlying data, lag lengths have been tested for robustness from lag length 1 to 5. The lag length barely affects the standard errors, and does not change the results qualitatively. Therefore, I stick with the lag length as suggested by the heuristic in Hoechle (2007).

stance to this and estimate standard errors clustered at the country level in their country-year panel of flood effects on night light intensity for a sample of affected cities. Since by focusing the analysis on cells that are ever affected by earthquakes in the sample, my empirical strategy is close to that of Kocornik-Mina et al. (2020), and I test my results for robustness to this approach as well. Reassuringly, I find very similar results.

## 4.5 Results

### 4.5.1 Baseline results

I start the analysis with the  $0.5^\circ$  grid cell resolution, with the main results reported in Table 4.5.1. The most basic specification would be to either include a binary indicator for the occurrence of an earthquake, or to include a simple continuous measure of maximum groundshaking. As a reference, these are reported in models (1) and (2) of Table 4.5.1. Including the full set of fixed effects as discussed in Section 4.4 and computing Driscoll-Kraay standard errors, both the binary dummy and continuous maximum intensity of groundshaking indicate no contemporaneous effect of earthquakes.

However, there is a wide range of shaking intensities in the underlying data (see Section 4.3), and heavy shaking tends to be more impactful than mild shaking. A linear continuous term for maximum shaking can be problematic, since shaking is expressed in  $\%g$  and by no means needs to exhibit a linear increase in potential impacts. As discussed before, the ideal approach would be to have an explicit damage function, in which a relation between physical shaking and vulnerability of e.g. building stock is either estimated or assumed (see e.g. Skoufias et al., 2020, 2021). However, this is not feasible with the presented global sample.

Instead, I take a more conservative approach and allow for non-linearities by using categories of shaking following the classification by Wald et al. (1999), in which physical shaking is related to potential levels of damages that are associated with the Modified Mercalli Intensity (MMI) scale. I construct binary variables for shaking, making the distinction between no shaking ( $MMI \leq 4$ ), mild shaking ( $MMI 5-6$ ), and heavy shaking ( $MMI 7+$ ), reported in models (3)-(9). When I introduce only the contemporaneous shaking categories in model (3), I find a positive but insignificant effect for both mild and heavy shaking. The insignificant point estimate for mild shaking is expected, since hardly any potential damage is expected for this category (see Figure 4.3.3). The absence of a contemporaneous effect for heavy shaking may be unexpected but fits with the case-study of the April 2015 Kathmandu earthquake, in which night light intensity initially increases in Kathmandu (see Figure 4.3.5), and shows depressed levels only for the months following. Findings of Zhao et al. (2018) for the Central Italy earthquake in 2016 support this notion. The authors find that in the ten days after the earthquake, night light intensity increased rather than decreased possibly as a result of search and rescue activities directly following the event. If this is true more generally, I expect that this increase in light decreases

within a matter of days to weeks after the event, such that one would expect to see a depression in night lights in the lags of this model.<sup>33</sup>

Table 4.5.1: Baseline results: 0.5° grid cells

		Dependent Variable: $\ln(\text{lights}_{i,my})$								
		(1)	(2)	(3)	(4)	(5)	(6)	(7)	(8)	(9)
Earthquake occurrence (binary)	t	0.0190 (0.0134)								
Maximum PGA	t		0.1658 (0.1283)							
	t			0.0193 (0.0132)	0.0211 (0.0136)	0.0198 (0.0131)	0.0199 (0.0130)	0.0194 (0.0132)	0.0248* (0.0142)	0.0209 (0.0135)
	t-1				0.0033 (0.0154)	0.0013 (0.0162)	0.0022 (0.0158)	-0.0014 (0.0163)	-0.0038 (0.0160)	0.0024 (0.0132)
	t-2					-0.0203 (0.0129)	-0.0217* (0.0126)	-0.0211* (0.0126)	-0.0217 (0.0130)	-0.0239* (0.0134)
MMI 5-6	t-3						0.0055 (0.0113)	0.0028 (0.0115)	0.0005 (0.0113)	0.0000 (0.0117)
	t-4							0.0105 (0.0120)	0.0118 (0.0120)	0.0111 (0.0118)
	t-5								-0.0244** (0.0113)	-0.0258** (0.0115)
	t-6									-0.0091 (0.0098)
	t			0.0141 (0.0264)	0.0169 (0.0263)	0.0133 (0.0261)	0.0133 (0.0258)	0.0134 (0.0259)	0.0074 (0.0252)	0.0023 (0.0263)
	t-1				-0.0200 (0.0342)	-0.0157 (0.0340)	-0.0156 (0.0338)	-0.0154 (0.0342)	-0.0211 (0.0338)	-0.0293 (0.0359)
	t-2					-0.0193 (0.0286)	-0.0207 (0.0282)	-0.0206 (0.0288)	-0.0224 (0.0312)	-0.0300 (0.0313)
MMI 7+	t-3						-0.0115 (0.0236)	-0.0058 (0.0218)	-0.0118 (0.0224)	-0.0159 (0.0231)
	t-4							0.0014 (0.0167)	0.0042 (0.0174)	0.0013 (0.0175)
	t-5								-0.0733 (0.0467)	-0.0741 (0.0456)
	t-6									-0.0667* (0.0341)
Observations		218,388	218,388	218,388	214,331	211,179	208,621	205,480	201,429	197,324
No. of cells		4200	4200	4200	4200	4200	4200	4200	4200	4200
R-squared (within)		0.0000	0.0000	0.0000	0.0000	0.0001	0.0001	0.0001	0.0003	0.0003
Cell FE		Yes	Yes	Yes	Yes	Yes	Yes	Yes	Yes	Yes
Time FE		Yes	Yes	Yes	Yes	Yes	Yes	Yes	Yes	Yes
Country-year FE		Yes	Yes	Yes	Yes	Yes	Yes	Yes	Yes	Yes
Country-month FE		Yes	Yes	Yes	Yes	Yes	Yes	Yes	Yes	Yes
Linear cell-trend		Yes	Yes	Yes	Yes	Yes	Yes	Yes	Yes	Yes
Driscoll-Kraay SEs		Yes	Yes	Yes	Yes	Yes	Yes	Yes	Yes	Yes
AIC		124511	124512	124513	121382	118433	113241	107946	103767	99915
BIC		124521	124522	124534	121423	118495	113323	108048	103890	100058

Note: \*\*\*, \*\*, \* denote significance at the 1%, 5% and 10% level. Full set of fixed effects and cell-specific linear time trends included but not reported. Driscoll-Kraay standard errors with 3 lags for all models.

For this reason, I start with adding lags of the shaking dummies one-by-one up to 6 month lags initially in models (4)-(9), where the foremost coefficients of interest are those for MMI 7+ shaking. The results are clear: at 0.5° resolution, in the global average there is no statistically significant effect of heavy shaking on night light emission for the first 5 months. While point estimates are stable and

<sup>33</sup>The month of impact contains potential temporary power outages that may give limited insight in the negative effect of earthquakes on economic activity. As discussed in appendix section 4.B.1, temporary power outages typically last no longer than 2 days, while prolonged power outages evidently have detrimental effect on economic activity. For a discussion, see e.g. Rose et al. (1997) and Rose et al. (2007).

negative for most lags, standard errors are very large. Most point estimates for MMI 5-6 shaking are insignificant as well, with the exception of lag 5.

I continue to further extend the number of lags to a full year after the earthquake. Figure 4.5.1 graphically reports these estimates for a total number of 12 lags. The point estimates for MMI 7+ shaking are reported in Table 4.5.2 below. With a full year of lags included, none of the point estimates for mild shaking is significantly different from zero, with the exception of the 9<sup>th</sup> lag.

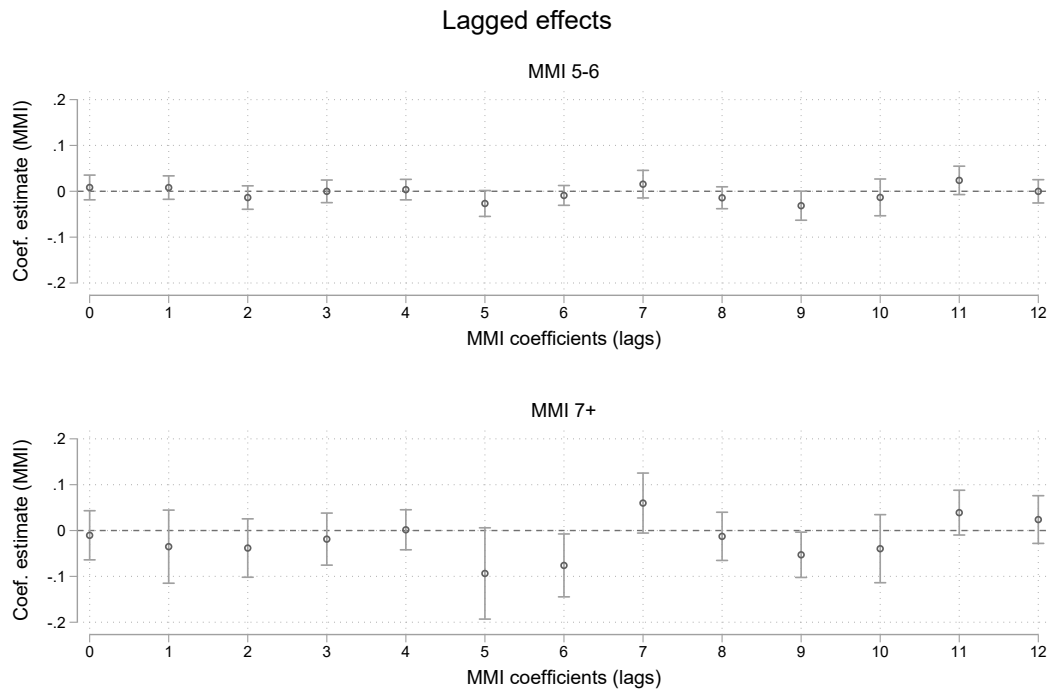
However, a similar conclusion must be drawn for heavy shaking. For the month of occurrence and the following four months, I find an - albeit consistently negative - insignificant effect of shaking on night light intensity. Surprisingly, months 5 and 6 show a substantial negative point estimate, of which the latter is significant at a 5% level. Without an immediate effect in at least the first few months after the quake, this estimated reduction in light intensity is hard to explain. The finding is stable across alternative fixed-effect specifications, in which I use linear country-trends instead of country-year dummies (following Kocornik-Mina et al. (2020), or when I exclude linear cell-trends and estimate country-by-year and country-by-month fixed effects only, thus staying closer to Del Valle et al. (2018) (see Table 4.B.1). I have tested for a linear, quadratic, and cubic transformation of the main independent variable, to account for potential non-linearities that may be poorly captured by the dummy approach, but find very similar results (see Appendix Figure 4.B.2). Since the relation between Modified Mercalli Intensity and peak ground acceleration is estimated to be approximately log-linear (see e.g. Wald et al., 1999), I also estimate equation 4.4.1 with logarithmic transformations of *pga*, and again find similar results. The same holds for using average shaking in a cell-month, rather than maximum shaking. In a final sanity test, I assess forwards rather than lags, and assess whether pre-earthquake coefficient estimates are approximately zero (see Appendix Figure 4.B.4). While insignificantly different from zero, the forwards are positive for the first three preceding months, with the month right before the earthquake spiking as the highest point estimate in the estimation. Reassuring as this may seem, the further forwards cast strong doubt as to whether the estimated point estimates in the lags contain an earthquake effect, or are simply the average result of the demeaning process of the fixed effects. In an attempt to take out seasonal swings and common changes over time in the VIIRS data, I have estimated country-by-year and country-by-month fixed effects. Regardless, the results are very stable across these alternative time fixed effects.

Table 4.5.2: Baseline results: 0.5° grid cells

		Dependent Variable: $\ln(\text{lights}_{i\text{my}})$												
		(1)	(2)	(3)	(5)	(6)	(7)	(8)	(9)	(10)	(11)	(12)	(13)	(14)
MMI 7+	t	0.0141 (0.0264)	0.0169 (0.0263)	0.0133 (0.0261)	0.0133 (0.0258)	0.0134 (0.0259)	0.0074 (0.0252)	0.0023 (0.0263)	-0.0012 (0.0270)	0.0065 (0.0259)	0.0050 (0.0275)	0.0069 (0.0307)	-0.0127 (0.0265)	-0.0104 (0.0266)
	t-1		-0.0200 (0.0342)	-0.0157 (0.0340)	-0.0156 (0.0338)	-0.0154 (0.0342)	-0.0211 (0.0338)	-0.0293 (0.0359)	-0.0268 (0.0370)	-0.0290 (0.0381)	-0.0284 (0.0388)	-0.0264 (0.0392)	-0.0228 (0.0401)	-0.0351 (0.0396)
	t-2			-0.0193 (0.0286)	-0.0207 (0.0282)	-0.0206 (0.0288)	-0.0224 (0.0312)	-0.0300 (0.0313)	-0.0329 (0.0321)	-0.0386 (0.0313)	-0.0408 (0.0310)	-0.0454 (0.0311)	-0.0432 (0.0319)	-0.0382 (0.0316)
	t-3				-0.0115 (0.0236)	-0.0058 (0.0218)	-0.0118 (0.0224)	-0.0159 (0.0231)	-0.0205 (0.0234)	-0.0193 (0.0245)	-0.0205 (0.0254)	-0.0207 (0.0245)	-0.0211 (0.0272)	-0.0187 (0.0282)
	t-4					0.0014 (0.0167)	0.0042 (0.0174)	0.0013 (0.0175)	0.0031 (0.0178)	0.0053 (0.0179)	0.0025 (0.0187)	0.0002 (0.0189)	-0.0007 (0.0203)	0.0016 (0.0217)
	t-5						-0.0733 (0.0467)	-0.0741 (0.0456)	-0.0721 (0.0448)	-0.0729 (0.0467)	-0.0766 (0.0467)	-0.0829* (0.0469)	-0.0966* (0.0487)	-0.0936* (0.0494)
	t-6							-0.0667* (0.0341)	-0.0713** (0.0354)	-0.0696* (0.0365)	-0.0706** (0.0350)	-0.0655* (0.0353)	-0.0655* (0.0349)	-0.0761** (0.0340)
	t-7								0.0568* (0.0326)	0.0560* (0.0311)	0.0507 (0.0315)	0.0512 (0.0333)	0.0524 (0.0325)	0.0599* (0.0325)
	t-8									-0.0204 (0.0245)	-0.0201 (0.0252)	-0.0200 (0.0250)	-0.0175 (0.0256)	-0.0127 (0.0261)
	t-9										-0.0614*** (0.0219)	-0.0580** (0.0225)	-0.0569** (0.0231)	-0.0529** (0.0245)
	t-10											-0.0450 (0.0341)	-0.0465 (0.0359)	-0.0396 (0.0368)
	t-11												0.0361 (0.0228)	0.0391 (0.0242)
	t-12													0.0240 (0.0258)
Observations		218,388	214,331	211,179	208,621	205,480	201,429	197,324	193,188	189,022	184,967	180,858	176,683	172,509
No. of cells		4200	4200	4200	4200	4200	4200	4200	4200	4200	4200	4200	4200	4200
R-squared (within)		0.0000	0.0000	0.0001	0.0001	0.0001	0.0003	0.0003	0.0004	0.0004	0.0005	0.0006	0.0007	0.0006
Cell FE		Yes	Yes	Yes	Yes	Yes	Yes	Yes	Yes	Yes	Yes	Yes	Yes	Yes
Time FE		Yes	Yes	Yes	Yes	Yes	Yes	Yes	Yes	Yes	Yes	Yes	Yes	Yes
Country-year FE		Yes	Yes	Yes	Yes	Yes	Yes	Yes	Yes	Yes	Yes	Yes	Yes	Yes
Country-month FE		Yes	Yes	Yes	Yes	Yes	Yes	Yes	Yes	Yes	Yes	Yes	Yes	Yes
Linear cell-trend		Yes	Yes	Yes	Yes	Yes	Yes	Yes	Yes	Yes	Yes	Yes	Yes	Yes
Driscoll-Kraay SEs		Yes	Yes	Yes	Yes	Yes	Yes	Yes	Yes	Yes	Yes	Yes	Yes	Yes

Note: \*\*\*, \*\*, \* denote significance at the 1%, 5% and 10% level. Full set of fixed effects and cell-specific linear time trends included but not reported. Driscoll-Kraay standard errors with 3 lags for all models.

Figure 4.5.1: Plotted estimates of lagged coefficients over time



*Note:* Plotted coefficient estimates up to 12 lags using the same model as reported for models (4)-(9) in Table 4.5.1. Dependent variable is  $\ln(\text{lights}_{imyt})$ , lag coefficients  $D_{imyt-L}$  reported on the x-axis, coefficient sizes  $\beta_j$  on the y-axis. Full estimation results for build-up of the model from zero to 12 lags are reported in Table 4.B.1. Whiskers indicate 95% confidence intervals.

A number of issues are now at play. First, the VIIRS data exhibits high month-to-month variability (Levin, 2017; Skoufias et al., 2021). The results shown here may be an example of how this may interfere with identifying local treatment effects of shocks. However, several studies have found at least immediate negative effects on light intensity in the case of hurricanes (Bertinelli and Strobl, 2013; Elliott et al., 2015; Mohan and Strobl, 2017; Del Valle et al., 2018), and some evidence exists for cases of earthquakes as well (Skoufias et al., 2020; Nguyen and Noy, 2020). In fact, while using a different approach for quantifying the strength of earthquakes - through total energy release related to magnitudes of the universe of earthquakes between 1992-2013 - Fabian et al. (2019) find negative effects on night light intensity for multiple years in larger  $1^\circ$  grids than I use, albeit using the annual DMSP night light data rather than the monthly VIIRS data. The results presented in this analysis are therefore troubling.

Apart from the temporal volatility in the light data, an alternative issue may be spatial aggregation. Aggregating up highly detailed data to larger units is always arbitrary to some degree, even though administrative units are typically the accepted norm. Following my approach in Chapter 3, I have so-far presented results for an aggregation level of  $0.5^\circ$  grid cells. However, earthquakes are localized events for which the scale may be much smaller than what  $0.5^\circ$  grid cells implicitly impose. As



a result, heterogeneity in both shaking intensity and potential impacts may be lost in the grid cell means. This may lead to attenuation bias, and may hence explain the statistically weak results. In order to investigate whether spatial aggregation may be the cause of not finding any consistent statistical pattern, I now turn to redoing the analysis at the resolution of the night light data, i.e. at 15 arc seconds cells - roughly 450 by 450 meters at the equator.<sup>34</sup> This places more focus on identification of directly damaged areas, following the early papers by Hashitera et al. (1999); Kohiyama et al. (2004) and is closely in line with the more recent literature on hurricane and flood impacts, in which pixel-level analysis is more common (Bertinelli and Strobl, 2013; Elliott et al., 2015; Kocornik-Mina et al., 2020).

### 4.5.2 Zooming in: pixel-resolution

The pixel-resolution results follow the exact same logic as those presented in the previous section. As discussed in Section 4.3, the dataset is constructed at the native resolution of the VIIRS data and is now analyzed at this native resolution.<sup>35</sup> I use the same MMI categorization of shaking, but rather than the maximum value of *pga* within a 0.5° cell, I record maximum *pga* by pixel by month. The model thus becomes much more precise in linking local seismic extremes with local light intensity. The model specification remains unchanged, with the notion that the linear cell-trend now refers to the 15 arc second pixel.

Results of the 12-lag model are presented in Figure 4.5.2. The results are strikingly similar to those for 0.5° grid cells. As before, point estimates for MMI 5-6 shaking are centered around zero and never statistically significant. Focusing on heavy shaking, point estimates for MMI 7+ shaking are very close to those reported for the 0.5° grid cells in Figure 4.5.1. Again, no immediate effect on night light intensity is found, and subsequent point estimates follow a very similar pattern. Again lags 5 and 6 have larger negative point estimates, but they are only half the size reported for 0.5° grid cells and are decisively insignificant. In line with the 0.5° results, lags 8 and 9 are negative, with the latter being significantly negative at 5%. However, more striking is the very large and positive point estimate for the 11-th month after the earthquake. While statistically insignificant, this positive spike is unexpected and can hardly be explained.<sup>36</sup>

As with the 0.5° grid cell results, estimation outcomes have been tested for robustness to the aforementioned alternative fixed effects, alternative clustering of standard errors at the country level, the lag length of the Driscoll-Kraay standard error estimation, and for the alternative use of the continuous *pga* variable (results not reported but available on request). Results are qualitatively similar, suggesting that aggregation is in fact not the problem.

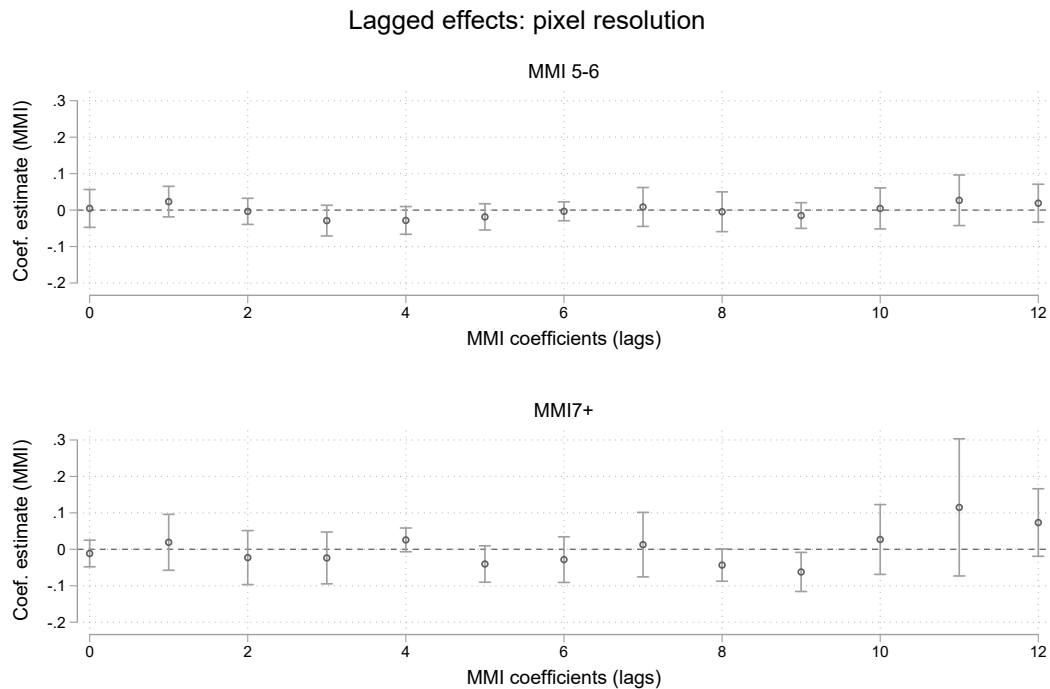
---

<sup>34</sup>I thank two anonymous reviewers and an editor from Environmental and Resource Economics for this suggestion.

<sup>35</sup>I gratefully acknowledge the high-performance computing facilities of SURFsara that allowed the data processing and analysis at the native resolution of the data presented in this chapter.

<sup>36</sup>Interestingly, Skoufias et al. (2021) report a similar positive spike in the 11-th lag for earthquakes in Myanmar, using the same monthly night light data.

Figure 4.5.2: Lagged coefficients over time: pixel resolution



*Note:* Plotted coefficient estimates up to 12 lags using the same model as reported for models (4)-(9) in Table 4.5.1, but now at pixel resolution. Dependent variable is  $\ln(\text{lights}_{imy})$ , lag coefficients  $D_{imy-L}$  reported on the x-axis, coefficient sizes  $\beta_j$  on the y-axis. Whiskers indicate 95% confidence intervals.

### 4.5.3 Reflecting on the findings

There are a number of studies to which I can directly relate my findings. The most closely related papers in terms of type of natural shock are the studies by Nguyen and Noy (2020), who study the impact of insurance on local economic recovery in New Zealand after the Canterbury earthquake sequence, and the work by Skoufias et al. (2020, 2021). Clearly, Skoufias et al. (2021) show that the VIIRS lights do not always show us what we expect to see.<sup>37</sup> The results presented so far may be another piece of evidence to this puzzle, and may point us to asking whether the noise in the VIIRS data is so large that earthquake effects may not be observable. Nguyen and Noy (2020) show that there is merit in using the data for recovery after the Canterbury earthquake sequence in New Zealand, but only after aggregating the monthly data to quarters, and aggregating from the pixel-resolution to the level of several city-blocks (area units, geographical statistical units used by Statistics New Zealand). Several other papers have used monthly night lights to study local impacts of climatic disasters. The first is the earlier mentioned study of the local

<sup>37</sup>Skoufias et al. (2021) was published a few months after finishing the present draft of this paper. I have incorporated their findings in the discussion for this paper, and engage with their findings more deeply in the next chapter of this dissertation.

economic impacts of Cyclone Pam in the Southern Pacific Islands by Mohan and Strobl (2017). In this paper, the authors follow a similar methodology and report immediate negative effects on night light intensity for the first six months after the cyclone, while evidence for net positive effects are reported for month 7 onwards. The second and related paper is by Del Valle et al. (2018) who study the short-run impacts of tropical cyclones in Guangdong Province in Southern China. Strikingly, the authors find no impact beyond the month of occurrence, stressing that any discernable impacts in the night lights may be short-lived. More persistent findings are reported by Ishizawa et al. (2019) for the Dominican Republic (up to 15 lags reduction from hurricanes), and on light growth by Miranda et al. (2020) for Central America. However, both make use of monthly DMSP data instead of VIIRS data, giving rise to the question whether the very short-term effect reported by Del Valle et al. (2018), lack of clear effects reported in Skoufias et al. (2021), and the complete lack of effects in this chapter are driven by data-related issues specific to the VIIRS lights. Note, however, that Mohan and Strobl (2017) do find statistically significant effects of hurricanes for the Pacific Islands using VIIRS monthly data, leading to an alternative possibility that effects might really be country or region-specific. The currently presented results may add evidence to this notion, and show that for earthquakes specifically even an immediate impact on night light intensity is not obvious.

In this discussion, the current analysis and the papers by Mohan and Strobl (2017) and Del Valle et al. (2018) stand in stark contrast to the existing empirical literature that is mostly concerned with annual effects, based on the annual DMSP night lights. Most directly related is the work by Fabian et al. (2019), who study the effect of earthquakes on both night light intensity and growth at the grid cell level at the annual level, making use of the annual DMSP-OLS data.<sup>38</sup> Instead of a very short-lived effect, the authors report depressed night light intensity for up to five years after occurrence in a global panel of 1° grid cells, as well as for 2° grid cells although smaller in size. The authors also use a within-estimator to model deviations-from-mean at the 1° or 2° cell level, but distribute earthquake energy over space by making use of magnitude and a general distance decay function. The relatively short time frame of the VIIRS data does not allow testing this longer-run impact in my analysis, but results based on my approach and the monthly night light data do not suggest evidence for such a prolonged negative effect.

Furthermore, several studies use night lights at the annual level for climatic disasters, such that I can make a direct comparison: Bertinelli and Strobl (2013) study the effect of hurricanes in the Caribbean using very small grid cells of 30 arc seconds, and Elliott et al. (2015) study the effect of tropical storms on cities in coastal China. Studying large-scale floods, Kocornik-Mina et al. (2020) similarly use night light intensity at the annual level to investigate local economic effects at the city level and report a negative and significant effect on night light intensity

---

<sup>38</sup>Fabian et al. (2019) model earthquake intensity by mapping total energy over space, including all aftershocks that were associated with an earthquake event. Spatial decay is modeled linearly according to distance-decay functions provided by Geoscience Australia.

of 2 to 8 percentage points and only for the year of occurrence. All three papers report a negative and significant effect of storms on annual night light growth and on annual night light intensity respectively, but only for the year of occurrence, with no significant lagged effects thereafter. All these results hint at rather short-lived impacts on local economic activity, at least when studied through the lens of night light intensity. My results are in line with this latter conclusion, but add that for earthquakes specifically there may be no measurable effect on local night light emission when using night light emissions.

The reported results up to this point are of course global averages, and may hide differences between cells that are ignored in the general model. While other papers have studied single countries or limited geographical regions, this paper takes a global perspective and therefore has a substantially more heterogeneous sample. The advantage of this heterogeneity is that we can study moderating factors, and test several important hypotheses in the literature regarding heterogeneity in resilience to direct impacts and recovery. However, the absence of a global homogenous and statistically significant effect first and foremost leads to the question whether subsets of the global sample may exhibit significant impacts. For this reason, I now turn to underlying heterogeneity.

#### 4.5.4 Beyond the global average: heterogeneity

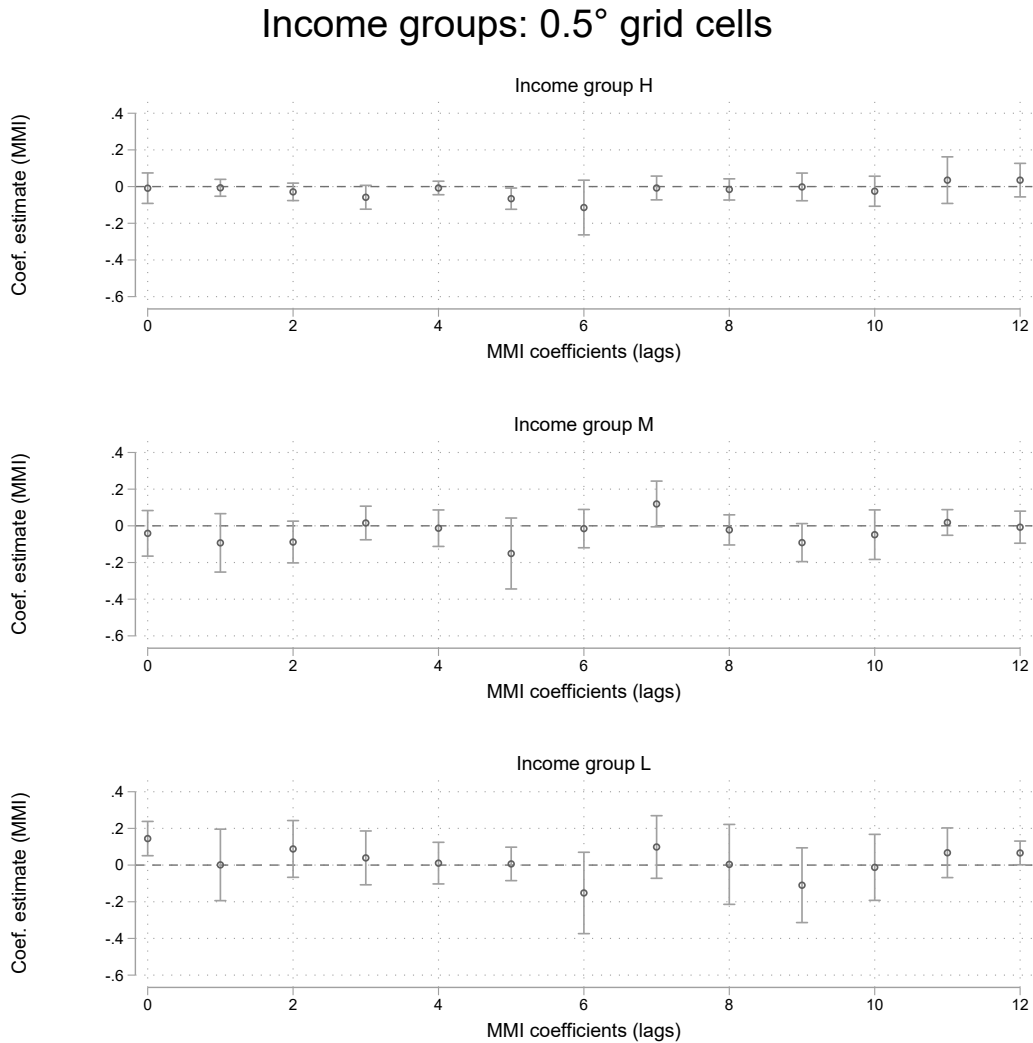
The baseline approach allows estimating a global average treatment effect, but hides much potential underlying heterogeneity. An important aspect that is omitted from the global model is the degree to which areas are prepared and/or resilient to the potential effects of earthquakes. Areas may be more or less resilient to disaster impacts depending on income per capita (Kahn, 2005), income inequality (Anbarci et al., 2005), institutional quality (Strömberg, 2007; Raschky, 2008), and a host of other potential determinants. Moreover, the most pressing question is whether the absence of a global homogenous impact can be partly answered by heterogeneity in subgroups.

I split the sample of cells into three income groups, based on the World Bank income group classification of 2012 and run the baseline model for the three income groups separately.<sup>39</sup> Results are reported in Figure 4.5.3. The short answer is that the coefficient estimates for the three groups hardly differ from the global average effect estimated in Figure 4.5.1 All three income groups show insignificant coefficient estimates, and - partly due to the relatively low number of earthquake cases per group - have no significant point estimates (at 5%). Note that there is one exception: the immediate effect is estimated to be positive and significant for the low-income group. However, given the spread of the other point estimates, I do not put much weight on this result.

---

<sup>39</sup>I combine 'low' and 'lower middle' into one category 'low' due to the very small number of cells that belong to the lowest income group (20 with *pga* levels of MMI 7+) and to have a sufficient number of earthquake treatments in each group. Cut-offs are  $\leq \$4086$ ,  $\leq \$12615$ , and  $> \$12615$  for low, middle, and high income groups respectively.

Figure 4.5.3: Effects by income group: 0.5° grid cells



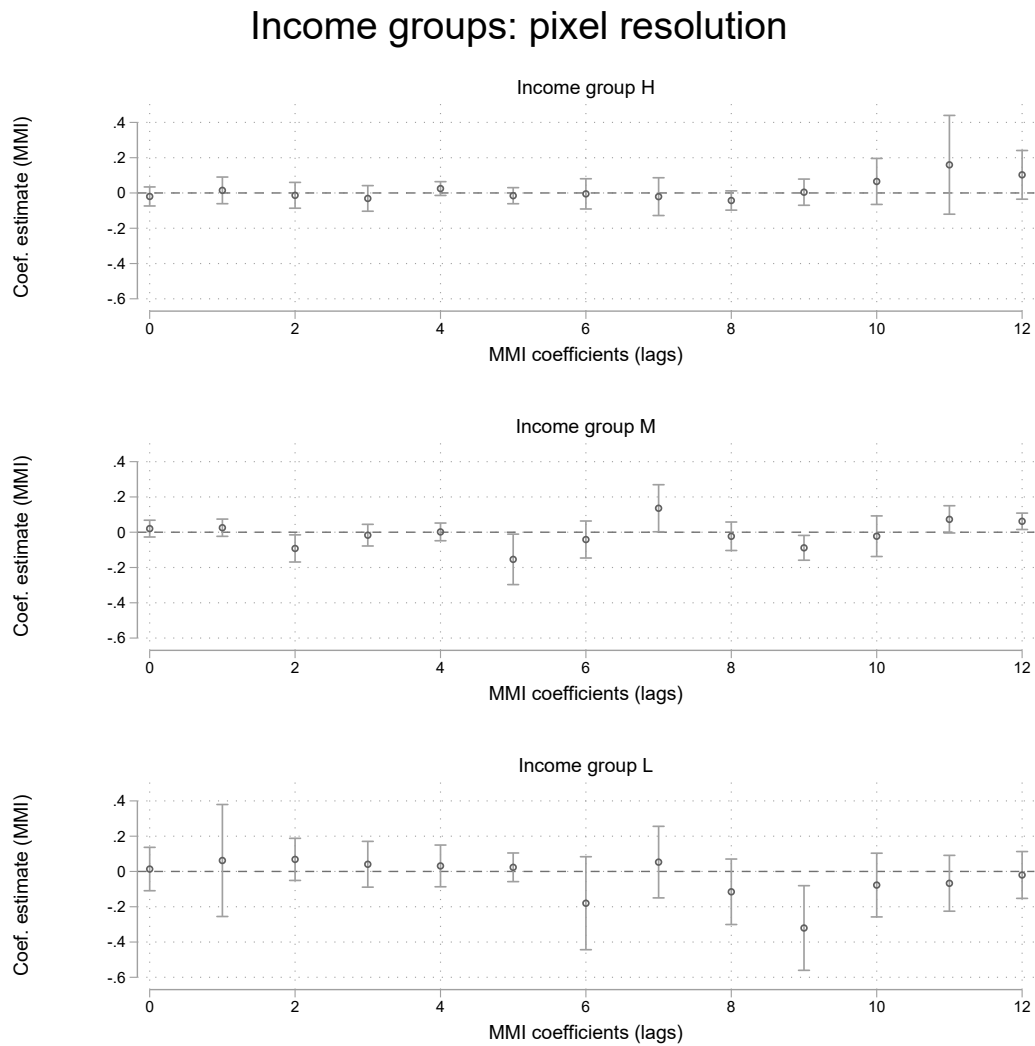
*Note:* Plotted coefficient estimates for MMI 7+ up to 12 lags as estimated in model (13) in Table 4.B.1 split by country group for the period 2012-2016. High-income by *H*, upper-middle income by *M*, and low and lower-middle income indicated by *L* respectively. Whiskers indicate 95% confidence intervals.

I then repeat the analysis at the pixel resolution. Results are reported in Figure 4.5.4. As for the baseline results, the income-group split results show strong similarity to those presented for the 0.5° grid cells.<sup>40</sup> Again most point estimates are insignificant. Note that the positive immediate effect estimated at 0.5° aggregation for the low-income group disappears at the pixel-resolution level. For the low-income group I find a significant effect in the 9<sup>th</sup> month after the earthquake, but with no meaningful impact before I cannot explain this point estimate. A similar argument

<sup>40</sup>Note that the mentioned positive spike for the pixel-resolution baseline results 11 months after the quake is driven by pixels in high-income countries.

holds for the 5<sup>th</sup> lag, which is just significant at 5%, but is surrounded by insignificant zero estimates. All-in-all, there is no sign that income group splits give more insight in the baseline results.

Figure 4.5.4: Effects by income group: pixel resolution



*Note:* Plotted coefficient estimates for MMI 7+ shaking up to 12 lags split by country groups for the period 2012-2016. High-income by *H*, upper-middle income by *M*, and low and lower-middle income indicated by *L* respectively. Whiskers indicate 95% confidence intervals.

## 4.6 Conclusion

In this paper I have explored the local economic impacts of earthquakes in a global sample. While impact assessments of earthquakes are abundant, a way to systematically track economic recovery from natural disasters in the short to medium run has been difficult due to lack of administrative socioeconomic data at both an adequate temporal and geographical resolution. This seriously hinders our ability to assess how natural disasters affect economies, both locally and at a wider national scale. In this paper I attempt to overcome these issues through two innovations.

First, I make use of high-resolution monthly night light intensity as a proxy for local economic activity, that allow studying month-to-month changes in economic activity in the affected area. I have done so by employing a recently developed dataset of global monthly VIIRS night lights images from the Suomi-NPP satellite (Elvidge et al., 2013).

Second, to assess local intensity of earthquakes I make use of detailed shakemaps from the Shakemap Atlas 2.0 that record ground shaking at a very high geographical resolution (García et al., 2012), allowing precise and objective quantification of a location's exposure to destructive energy of the earthquake. A global panel of over 24 million grid cells of roughly 450 by 450 meters at the equator was constructed, to which I map both monthly light intensity and earthquakes for the years 2012-2016. I then use a panel fixed effects approach to study the relation between ground shaking and local economic activity, as proxied by night light intensity, at both the resolution of the data, as well as for  $0.5^\circ$  grid cells.

The answer to this analysis is short: I do not find a measurable effect of heavy shaking from earthquakes on night light intensity. This is true for the immediate impact, as well as the months after. This finding is robust to a range of variations of the model specification, and holds at both the  $0.5^\circ$  and pixel resolution. I follow a strategy very similar to that of the existing literature in this field, although this has mostly been applied to the effect of hurricanes on night light intensity. This gives rise to a number of questions, many of which are mostly empirical and closely related to the cited literature.

First, the model may be incapable of capturing true effects, through its limited ability to address temporal volatility in the VIIRS data. This is apparent, even after limiting the dataset to cells that are urbanized, contain built-up surface, and are not persistently dark. As discussed in Skoufias et al. (2021), effects may not be observed for events of which we know there were substantial damages. One solution is suggested by Nguyen and Noy (2020), who similarly state that their model was unable to capture local recovery at monthly resolution. Instead, effects were observed when the dataset was aggregated to quarters. While this may be a way forward, doing so in a global panel for which the estimation relies on country-time fixed effects is not straightforward. Alternatively, the model may be too coarse to capture cell-deviations from local means, implying that an explicit difference-in-difference method may be better suited. However, this requires identifying plausible counterfactuals, which - given the noise in the data - is far from trivial. Generally

speaking, addressing the issue of seasonality in the data remains a challenge (Coesfeld et al., 2018; Gao et al., 2020; Zhao et al., 2020). The currently presented results follow the standard in the literature (e.g. Elliott et al., 2015; Del Valle et al., 2018; Ishizawa et al., 2019; Miranda et al., 2020) and add evidence to earthquake effects on night lights being at the very least ambiguous.

Second, or rather related to the model, there may be an issue of intention-to-treat in the model, whereas in reality physical shaking may have done little harm. Note that the sample of earthquakes in the current paper is restricted to potentially damaging events, and that only shaking of levels sufficiently high to generate substantial damages were considered (following the classification by Wald et al., 1999). Lack of actual treatment is therefore unlikely. An alternative approach may be to construct country-specific vulnerability curves, following Skoufias et al. (2020) and Skoufias et al. (2021). These essentially translate objective physical shaking into damage proxies, which - although necessarily based on assumptions about the building stock in pixels - may bring shaking values closer to true potential impact. Nonetheless, the robustness tests presented in this paper do not point towards qualitatively different results when assessing non-linear transformations of the peak ground acceleration variable. Instead, a more promising approach would be to test the relation between materialized damages and economic effects of one or multiple earthquakes in a (comparative) case study, in which changes in light intensity can be related directly to materialized impacts. This takes out the uncertainty that the physical shaking measures bring, and allow analyzing the reflection of VIIRS night light changes in response to materialized impacts from a large earthquake.<sup>41</sup>

Finally, there is the question of whether earthquake impacts are on average visible in the VIIRS night lights. Skoufias et al. (2021) cast doubt to the validity of the night lights in relation to the 2016 Aceh earthquake, for which essentially no effect can be observed in the monthly light data. While I do see direct impacts in the discussed example of the 2015 Gorkha earthquake in Nepal, observed changes in night light may be both positive and negative in geographically close areas. The currently presented results point in a similar direction: globally the average effect of heavy shaking on night light intensity cannot be distinguished from zero, and the same is true in the subsamples of income groups.

This result has to be evaluated in the light of the existing literature, which focuses mostly on the effects of hurricanes. New papers have recently been published in which the much-used DMSP night light data is aggregated to months, rather than years (Ishizawa et al., 2019; Miranda et al., 2020). These do find longer-lasting impacts than those reported in Mohan and Strobl (2017) and Del Valle et al. (2018), specifically for hurricanes, giving rise to the question whether DMSP monthly data may be of different and possibly better quality than the VIIRS monthly data for studying month-to-month changes in local economic activity in response to natural shocks. However, monthly composites for the DMSP monthly data were not publicly

---

<sup>41</sup>I do so in the next chapter of this dissertation, in which I study the impact of the April 2016 Kumamoto earthquake in Japan on VIIRS night light intensity of affected municipalities. There, we use a difference-in-differences approach to isolate treatment effects; see Chapter 5.



available at the time of writing, but were made available in the summer of 2021. Finding the answer as to whether this is purely a data-quality or modelling problem, or whether the effect really isn't there is therefore an avenue for future research.

Given the huge computational demands for studying impacts over time at very fine geographical resolution, a lot of heterogeneity remains unexplored in this paper. While future work should not become a search for a needle in a haystack, questions on vulnerability, inequality, and institutional moderating factors abound (see e.g. Anbarci et al., 2005; Strömberg, 2007; Raschky, 2008). On basis of the current results, one cannot conclude that there is no relation anywhere between earthquakes and night light intensity. However, I can conclude - on basis of the presented data and applied methods - that on average there is no convincing evidence for a structural relation.

## 4.A Descriptives, tables and figures

Table 4.A.1: Summary statistics

Variable	Obs.	Mean	Std	Min	Max
light (radiance)	1005093	1.099033	3.265065	-.3958848	459.6929
$\ln(\text{light})$	968456	-0.8706961	1.347388	-13.23698	6.130558
$\Delta \ln(\text{light})$	872196	0.0028375	0.6352082	-10.07179	9.496824
$\ln(\text{light neighbors})$	1124426	-1.08248	1.147347	-13.00985	4.822206
Max(peak ground acceleration)	2913	0.0877789	0.1147311	0.04	1.96
Instrumental Intensity V-VI	2913	0.9007896	0.2989957	0	1
Instrumental Intensity VII+	2913	0.0992104	0.2989957	0	1
Unique earthquakes events	Obs.	Mean	Std	Min	Max
Magnitude	456	6.069035	0.690693	4.5	8.6

Figure 4.A.1: Magnitude distribution of included earthquakes

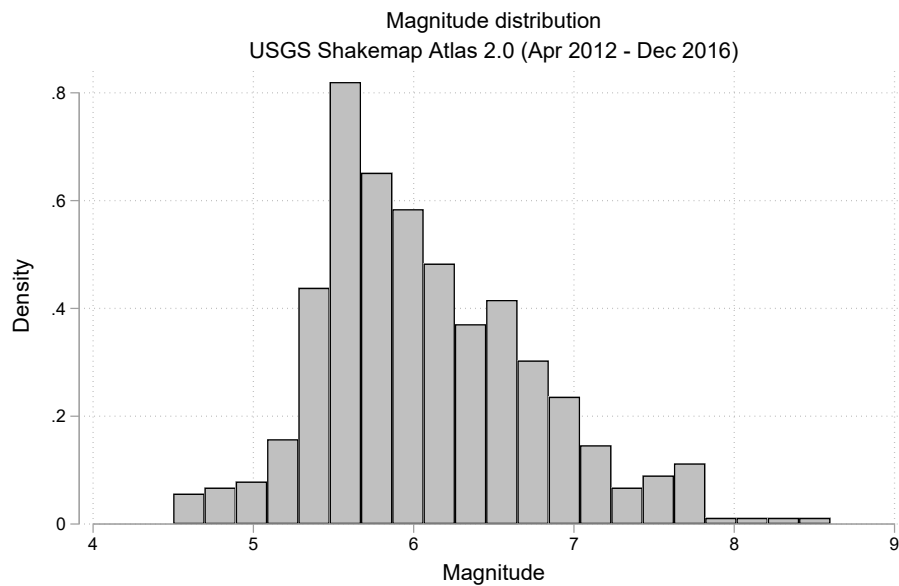


Figure 4.A.2: Distribution of peak ground acceleration of earthquakes included in the Shakemap Atlas 2.0 for 2012-2016

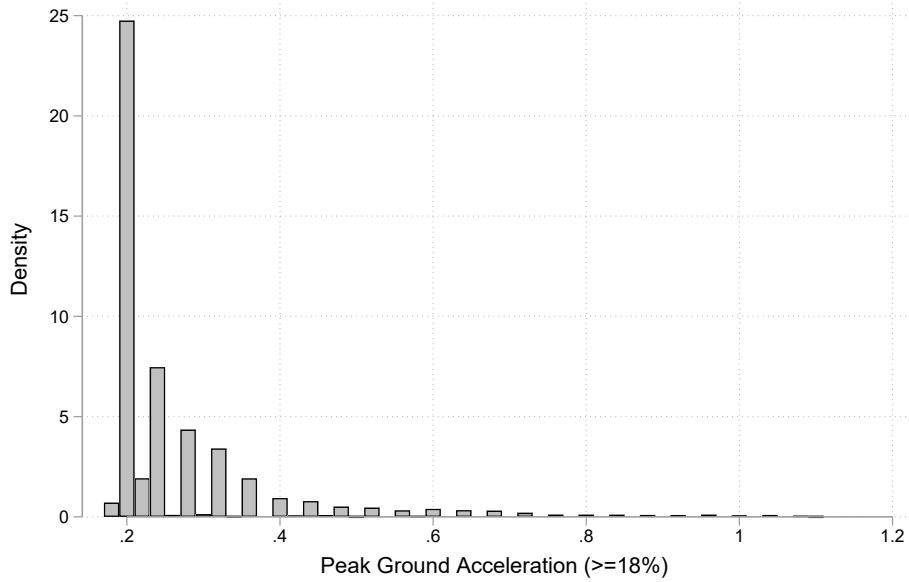
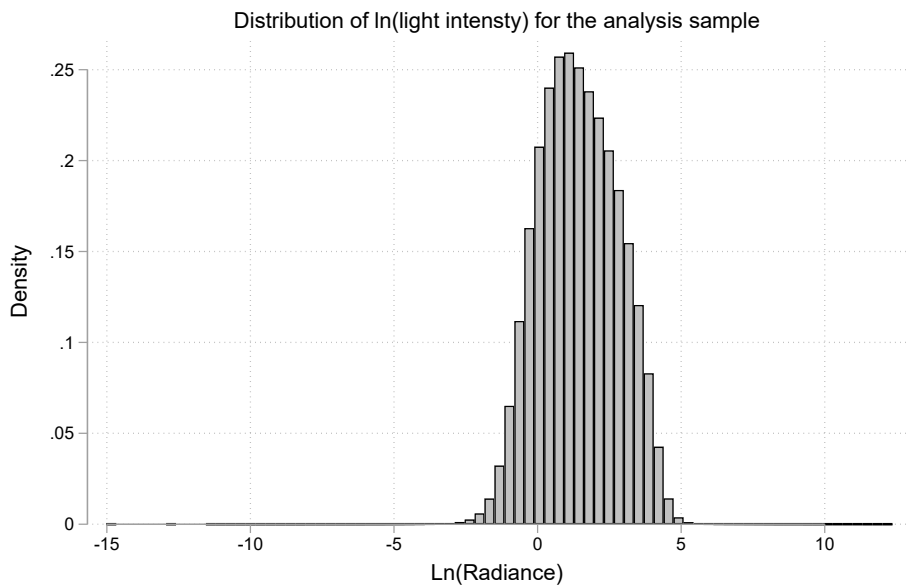


Figure 4.A.3: Distribution of log radiance for the analysis sample: built-up and persistently-lit pixels in GRUMP urban extents that ever experience non-zero shaking ( $pga > 0$ ) through 2012-2016.



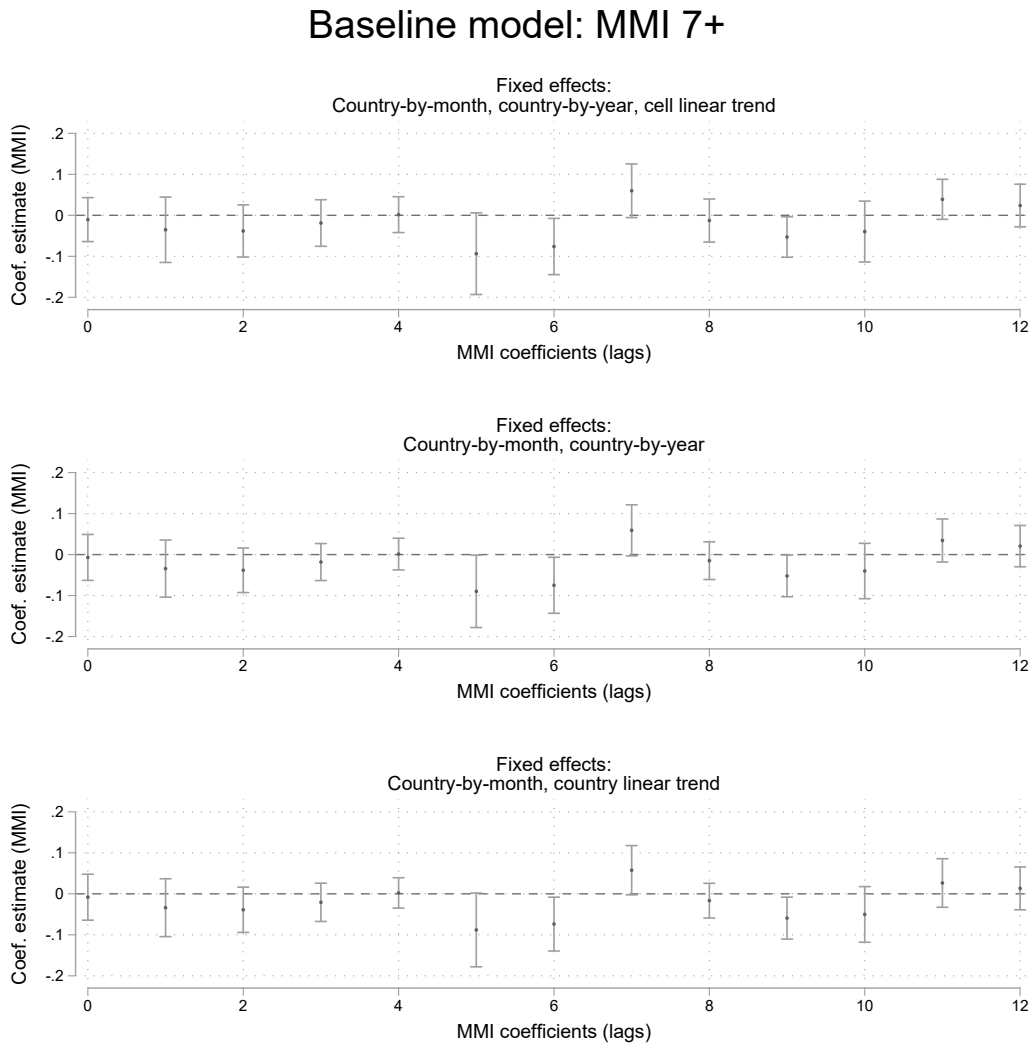
## 4.B Regression Tables and Figures

Table 4.B.1: Baseline results: 0.5° grid cells (extended)

		Dependent Variable: $\ln(\text{lights}_{i,t})$												
		(1)	(2)	(3)	(4)	(5)	(6)	(7)	(8)	(9)	(10)	(11)	(12)	(13)
MMI 5-6	t	0.0193 (0.0132)	0.0211 (0.0136)	0.0198 (0.0131)	0.0199 (0.0130)	0.0194 (0.0132)	0.0248** (0.0142)	0.0209 (0.0135)	0.0169 (0.0135)	0.0171 (0.0134)	0.0175 (0.0138)	0.0195 (0.0159)	0.0084 (0.0131)	0.0084 (0.0134)
	t-1		0.0033 (0.0154)	0.0013 (0.0162)	0.0022 (0.0158)	-0.0014 (0.0163)	-0.0038 (0.0160)	0.0024 (0.0132)	0.0123 (0.0107)	0.0115 (0.0119)	0.0090 (0.0127)	0.0091 (0.0135)	0.0162 (0.0149)	0.0081 (0.0127)
	t-2			-0.0203 (0.0129)	-0.0217* (0.0126)	-0.0211* (0.0126)	-0.0217 (0.0130)	-0.0239* (0.0134)	-0.0206 (0.0127)	-0.0165 (0.0127)	-0.0188 (0.0133)	-0.0181 (0.0133)	-0.0136 (0.0128)	-0.0136 (0.0127)
	t-3				0.0055 (0.0113)	0.0028 (0.0115)	0.0005 (0.0113)	0.0000 (0.0117)	-0.0053 (0.0127)	-0.0019 (0.0117)	0.0004 (0.0122)	-0.0018 (0.0124)	-0.0028 (0.0123)	-0.0001 (0.0122)
	t-4				0.0105 (0.0120)	0.0118 (0.0118)	0.0111 (0.0118)	0.0102 (0.0111)	0.0094 (0.0106)	0.0033 (0.0108)	0.0030 (0.0111)	0.0071 (0.0113)	0.0037 (0.0111)	0.0037 (0.0111)
	t-5						-0.0244** (0.0113)	-0.0258** (0.0115)	-0.0266** (0.0123)	-0.0254** (0.0126)	-0.0275** (0.0125)	-0.0294** (0.0132)	-0.0269* (0.0136)	-0.0265* (0.0140)
	t-6							-0.0091 (0.0098)	-0.0107 (0.0096)	-0.0092 (0.0097)	-0.0091 (0.0097)	-0.0087 (0.0097)	-0.0089 (0.0101)	-0.0090 (0.0107)
	t-7								0.0202 (0.0130)	0.0216 (0.0136)	0.0179 (0.0137)	0.0160 (0.0144)	0.0199 (0.0145)	0.0155 (0.0149)
	t-8									-0.0199* (0.0117)	-0.0204* (0.0122)	-0.0214* (0.0124)	-0.0163 (0.0119)	-0.0141 (0.0118)
	t-9										-0.0308* (0.0157)	-0.0326* (0.0162)	-0.0295* (0.0159)	-0.0314* (0.0157)
	t-10											-0.0165 (0.0182)	-0.0136 (0.0187)	-0.0133 (0.0199)
	t-11												0.0244 (0.0147)	0.0238 (0.0154)
t-12													-0.0001 (0.0126)	
MMI 7+	t	0.0141 (0.0264)	0.0169 (0.0263)	0.0133 (0.0261)	0.0133 (0.0258)	0.0134 (0.0259)	0.0074 (0.0252)	0.0023 (0.0263)	-0.0012 (0.0270)	0.0065 (0.0259)	0.0050 (0.0275)	0.0069 (0.0307)	-0.0127 (0.0265)	-0.0104 (0.0266)
	t-1		-0.0200 (0.0342)	-0.0157 (0.0338)	-0.0156 (0.0342)	-0.0154 (0.0338)	-0.0211 (0.0359)	-0.0293 (0.0370)	-0.0268 (0.0370)	-0.0290 (0.0381)	-0.0284 (0.0388)	-0.0264 (0.0392)	-0.0228 (0.0401)	-0.0351 (0.0396)
	t-2			-0.0193 (0.0286)	-0.0207 (0.0282)	-0.0206 (0.0288)	-0.0224 (0.0312)	-0.0300 (0.0313)	-0.0329 (0.0321)	-0.0386 (0.0313)	-0.0408 (0.0310)	-0.0454 (0.0311)	-0.0432 (0.0319)	-0.0382 (0.0316)
	t-3				-0.0115 (0.0236)	-0.0058 (0.0218)	-0.0118 (0.0224)	-0.0159 (0.0231)	-0.0205 (0.0234)	-0.0193 (0.0245)	-0.0205 (0.0254)	-0.0207 (0.0245)	-0.0211 (0.0272)	-0.0187 (0.0282)
	t-4					0.0014 (0.0167)	0.0042 (0.0174)	0.0013 (0.0175)	0.0031 (0.0178)	0.0053 (0.0179)	0.0025 (0.0187)	0.0002 (0.0189)	-0.0007 (0.0203)	0.0016 (0.0217)
	t-5						-0.0733 (0.0467)	-0.0741 (0.0456)	-0.0721 (0.0448)	-0.0729 (0.0467)	-0.0766 (0.0467)	-0.0829* (0.0469)	-0.0966* (0.0487)	-0.0936* (0.0494)
	t-6							-0.0667* (0.0341)	-0.0713** (0.0354)	-0.0696* (0.0365)	-0.0706** (0.0350)	-0.0655* (0.0353)	-0.0655* (0.0349)	-0.0761** (0.0340)
	t-7								0.0568* (0.0326)	0.0560* (0.0311)	0.0507 (0.0315)	0.0512 (0.0333)	0.0524 (0.0325)	0.0599* (0.0325)
	t-8									-0.0204 (0.0245)	-0.0201 (0.0252)	-0.0200 (0.0250)	-0.0175 (0.0256)	-0.0127 (0.0261)
	t-9										-0.0614*** (0.0219)	-0.0580** (0.0231)	-0.0569** (0.0245)	-0.0529** (0.0245)
	t-10											-0.0450 (0.0341)	-0.0465 (0.0359)	-0.0396 (0.0368)
	t-11												0.0361 (0.0228)	0.0391 (0.0242)
t-12													0.0240 (0.0258)	
Observations		218,388	214,331	211,179	208,621	205,480	201,429	197,324	193,188	189,022	184,967	180,858	176,683	172,509
No. of cells		4200	4200	4200	4200	4200	4200	4200	4200	4200	4200	4200	4200	4200
R-squared (within)		0.0000	0.0000	0.0001	0.0001	0.0001	0.0003	0.0003	0.0004	0.0004	0.0005	0.0006	0.0007	0.0006
Cell FE		Yes	Yes	Yes	Yes	Yes	Yes	Yes	Yes	Yes	Yes	Yes	Yes	Yes
Time FE		Yes	Yes	Yes	Yes	Yes	Yes	Yes	Yes	Yes	Yes	Yes	Yes	Yes
Country-year FE		Yes	Yes	Yes	Yes	Yes	Yes	Yes	Yes	Yes	Yes	Yes	Yes	Yes
Country-month FE		Yes	Yes	Yes	Yes	Yes	Yes	Yes	Yes	Yes	Yes	Yes	Yes	Yes
Linear cell-trend		Yes	Yes	Yes	Yes	Yes	Yes	Yes	Yes	Yes	Yes	Yes	Yes	Yes
Driscoll-Kraay SEs		Yes	Yes	Yes	Yes	Yes	Yes	Yes	Yes	Yes	Yes	Yes	Yes	Yes

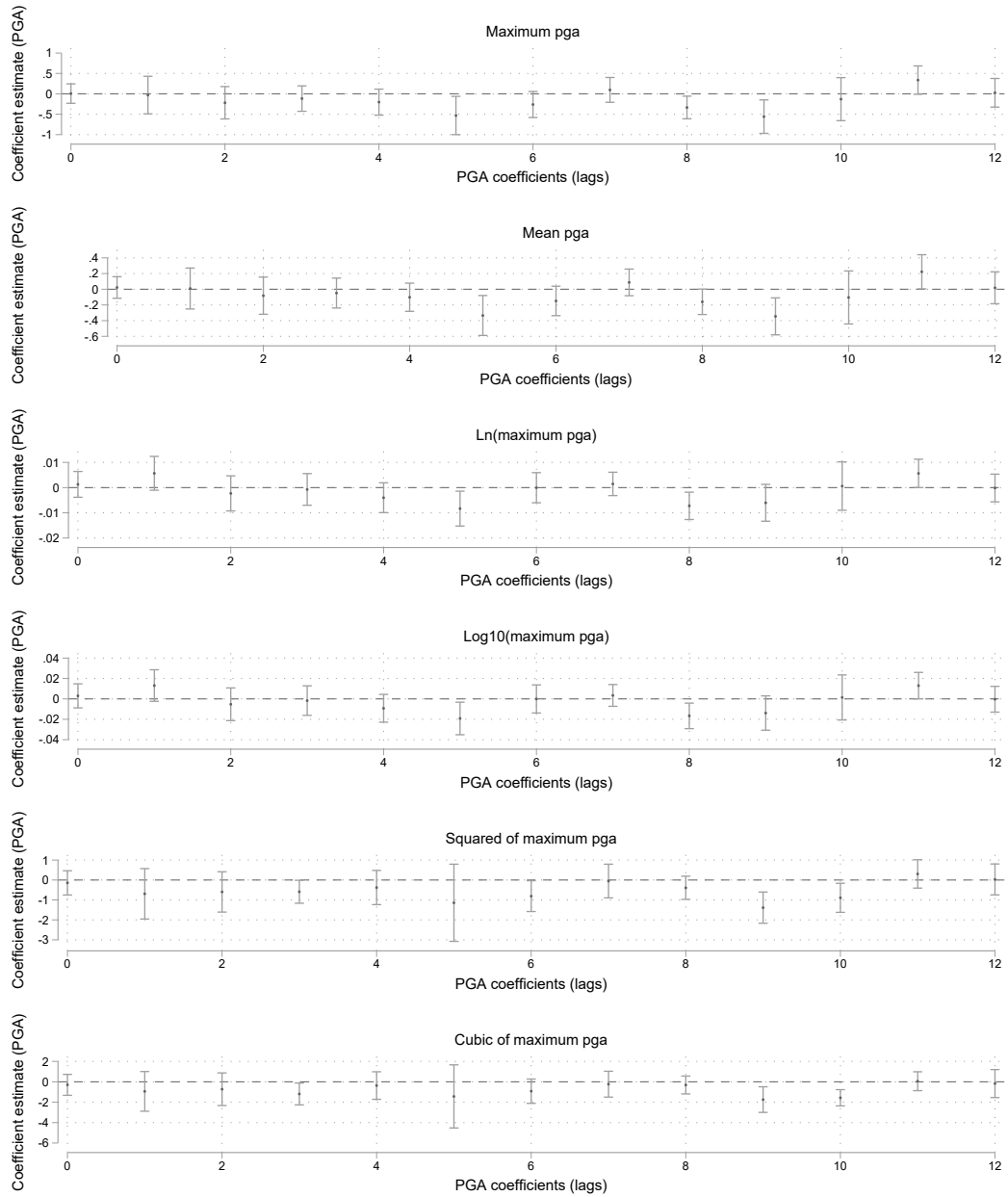
Note: \*\*\*, \*\*, \* denote significance at the 1%, 5% and 10% level. Full set of fixed effects and cell-specific linear time trends included but not reported. Driscoll-Kraay standard errors for all models, with 3 lags and clustered on time. Models (1)-(7) are exact replications of models (4)-(9) in table 4.5.1.

Figure 4.B.1: Robustness of the model to alternative fixed effects



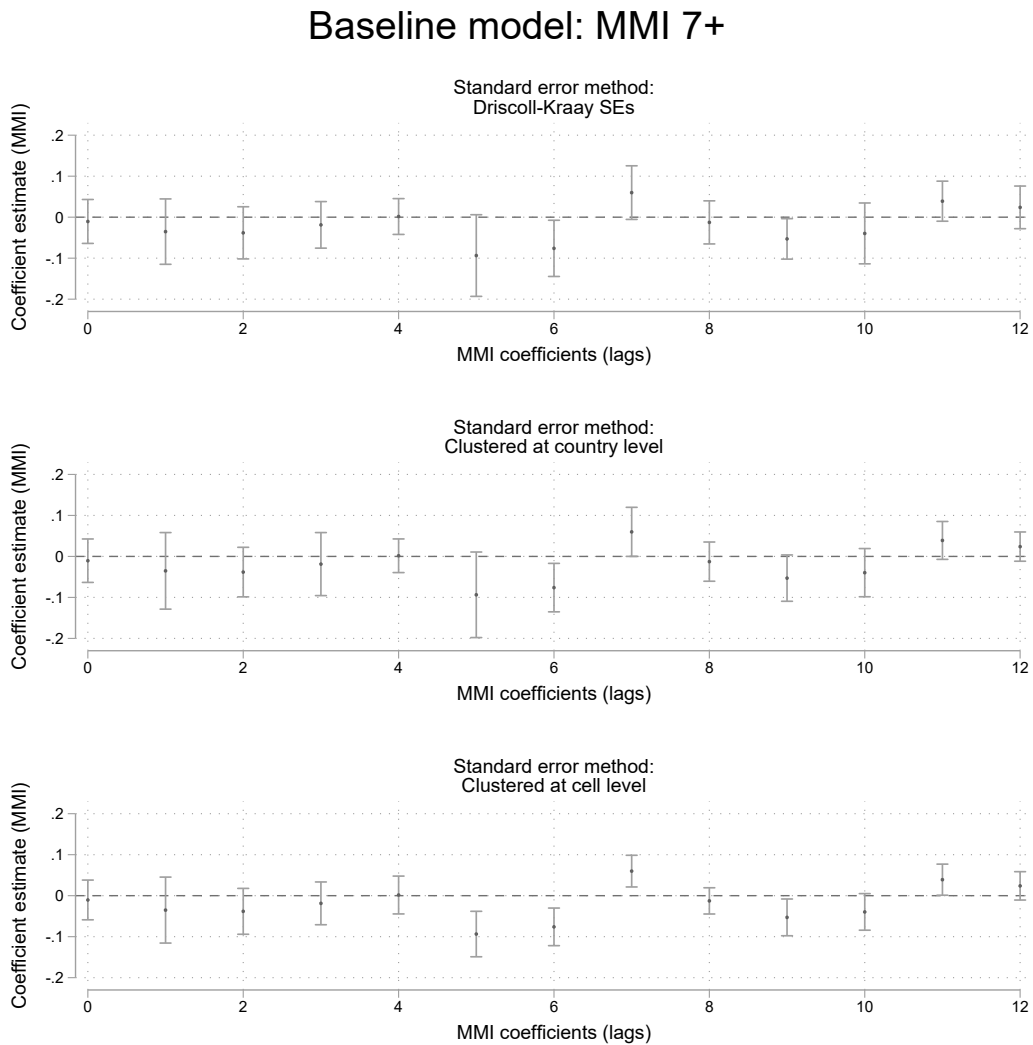
*Note:* Panels (1) through (3) reported the 12-lag model as estimated in Table 4.B.1, but for alternative fixed effect combinations. Panel (1) replicates the baseline results, with country-by-year FE, country-by-month FE, and linear cell-trends. Panel (2) omits the linear cell-trends. Panel (3) omits linear cell-trends and instead of country-by-year FE estimates linear country time trends, in line with Kocornik-Mina et al. (2020). Whiskers indicate 95% confidence intervals.

Figure 4.B.2: Robustness of the model to alternative shaking variable specifications



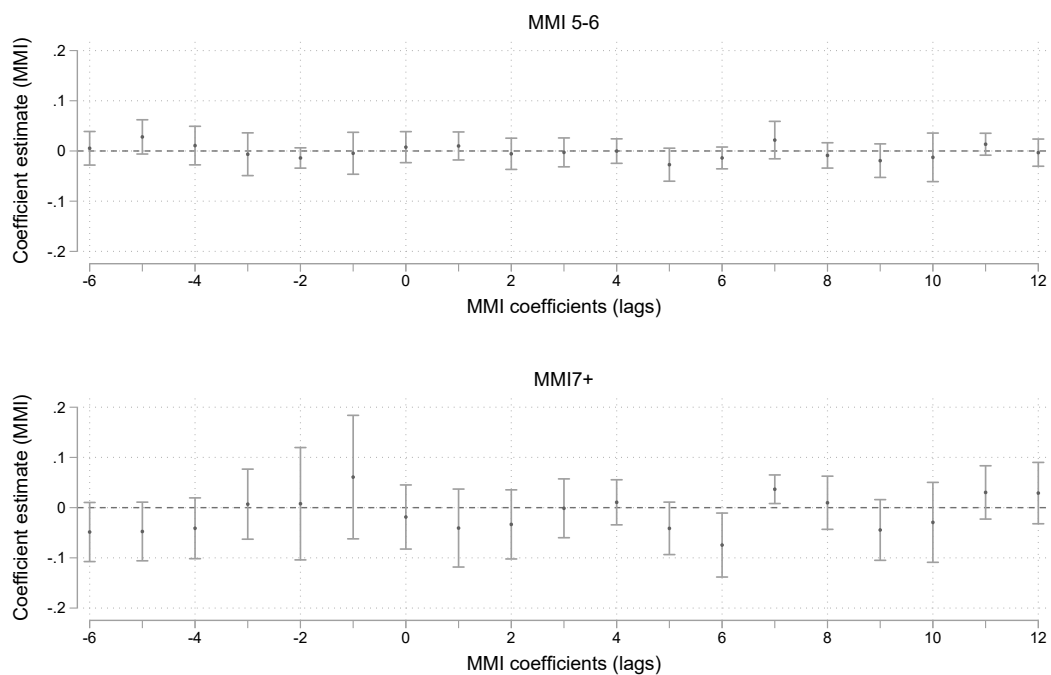
*Note:* Panels (1) through (6) reported the 12-lag model as estimated in Table 4.B.1, but for alternative specifications of the shaking variable. Whiskers indicate 95% confidence intervals.

Figure 4.B.3: Robustness of the 12-lag model to alternative clustering of standard errors



*Note:* 12-lag models estimated as in model (13) of Table 4.B.1. Whiskers indicate 95% confidence intervals. The top panel replicates Figure 4.5.1, with standard errors clustered on time and corrected for arbitrary spatial and temporal autocorrelation with the Driscoll-Kraay method. Panel (2) clusters standard errors at the country level, following Kocornik-Mina et al. (2020) - note that that the confidence intervals hardly differ with the top panel. Panel (3) instead has robust standard errors only, clustered at the cell level. This - as is to be expected - dramatically reduces standard errors, but does not change the results qualitatively.

Figure 4.B.4: The 12-lag model including pre-shock coefficients



*Note:* 12-lag models estimated as in model (13) of Table 4.B.1, but augmented with 3 pre-earthquake coefficients respectively. Whiskers indicate 95% confidence intervals. Note that the positive pre-occurrence coefficient estimates may be a sign that the cell fixed effects are being negatively affected by the prolonged negative effect from the earthquake itself. That is, being almost a quarter of the total available time period, average light intensity for the cell may already partly capture the negative effect from earthquakes. However, the differences are minor and highly insignificant.



### 4.B.1 Disaster-related power outages

Some discussion is warranted on what the changes in night lights may reflect in the face of disasters. In principle, there are three main components: (1) Direct damages to physical capital, (2) power outages due to disruption of the electricity grid, in part due to (1), and (3) reduction in day-to-day economic activity that stretches beyond the direct damages of (1) and (2). While direct damages evidently cause disruption to economic activity through the loss of productive assets, power outages may be of short duration while simultaneously having huge impact on total night light intensity that an area emits. Because of this particular relation between power outages and night lights, I now shortly discuss power outage durations and impacts.

It is evident that hurricanes, floods, earthquakes, wildfires, landslides, etc. can directly affect the electricity grid by causing physical destruction of buildings and infrastructure, and thus may lead to blackouts. Firms facing these blackouts have very little substitution possibilities and as a consequence direct losses from these outages can be very high (see e.g. Rose et al., 1997). This means that when areas directly powered by this grid black out, this translates into depressed night light intensity. Since the data products that researchers are using are either annual averages (DMSP-OLS) or monthly averages (VIIRS-DNB), these power outages go into the averages and may suppress light intensity, even though the power may come back online after a few days.<sup>42</sup> The critical question is then what changes in local economic activity this suppression of night light represents. This issue is left rather undiscussed in the present literature, and while it is beyond the scope of this paper to answer this question fully, a brief review of studies on power outages and their economic effects is therefore discussed here.

Global information on power outages is not readily available, but some information is available for the United States. In the U.S., about 1850 major power outages – defined as affecting more than 50,000 people – were recorded between 2000-2016 by the Department of Energy (DOE) (for a discussion, see Mukherjee et al., 2018). About 50% of these were caused by severe weather events, including hurricanes and wind and rain storms, snow, ice, and winterstorms, as well as thunderstorms, heatwaves, and wildfires (Mukherjee et al., 2018; Rentschler et al., 2019). In the study by Mukherjee et al. (2018), the vast majority of these outages lasted between 15-50 hours before supply was restored, and typically affected between 1 and 3 million people. Rentschler et al. (2019) do a similar study for U.S. power outages and find that power outages resulting from natural shocks, including storms, last on average 59 hours. For Europe, this is 9 hours on average. The majority of power outages – nearly 60% – is attributable to general storms, rather than hurricanes or ice storms alone (Kenward and Raja, 2014). Mukherjee et al. (2018) find that power outages on average last longer in more rural areas, with lower population densities. Exposed above-ground electrical infrastructure is more vulnerable in these areas, and lower on the priority ranking in the direct aftermath of a disaster. Furthermore,

---

<sup>42</sup>Note that in the new annual stable night light composites of the VIIRS-DNB data are processed with an outlier-removal algorithm that filters out power outages from the annual pixel average, see Elvidge et al. (2017).

Rentschler et al. (2019) also study the effect of annually recurring storms such as the ‘Nor’westers’ in Bangladesh. Even though Bangladesh is frequently exposed to these storms, they cause significant power outages.

Cao et al. (2013) explore the use of the VIIRS DNB images to study power outages on the east coast of the United States caused by the 2012 derecho storm near Washington D.C. and Hurricane Sandy in late October 2012. In both cases, estimated light reduction for selected affected urban areas is of the order of 30 to 50% with respect to pre-event light intensity. For the derecho storm, roughly 90% of customers had their power supply restored after 5 days, and for Hurricane Sandy light levels recovered to pre-storm levels within roughly two weeks.<sup>43</sup>

---

<sup>43</sup>Variability of night light intensity in normal times may also be a concern; Cao et al. (2013) assess day-to-day variability of light intensity in urban areas around Washington D.C. before the June 2012 derecho storm, and find variability in the range of 4-11%. While the power outages detected by the authors is an order of magnitude larger, filtering out the variability and likely seasonality of light use over time is essential to identifying shock impacts. I therefore apply country-by-month fixed-effects in the statistical analysis to capture month-to-month variation.

## CHAPTER 5

---

### Shaken, but not stirred?<sup>\*</sup> The local economic impacts of the 2016 Kumamoto earthquake in Japan

---

#### 5.1 Introduction

In this paper, we study the local economic impacts of the 2016 Kumamoto earthquake in southern Japan using night light intensity. We test the value of the high frequency monthly VIIRS night light data as a proxy for local economic activity in the aftermath of a large natural disaster. Population growth and urbanization, in combination with climate change, increase exposed populations around the world to natural hazards and thus disaster risk (IPCC, 2014; Hoeppe, 2016). Over the last decade, we have seen damages from natural disasters steadily increasing (Hoeppe, 2016; CRED, 2021). Studying the impacts that disasters have on communities, their resilience, how they recover from it, and moreover what explains differences in resilience and recovery patterns is therefore an important area of research. However, adequate data to study economic impacts in affected areas are often not available. While direct impacts in terms of damages and fatalities are typically well-documented and studied, indirect impacts on livelihoods are more difficult to capture. First, national statistics are inadequate to study the local effects of disasters (as discussed in Chapter 3 and Botzen et al., 2019). Natural disasters are typically localized events, that affect only part of a country. For example, Strobl (2012) shows that even the effects of large hurricanes on GDP growth dissipate within a year at the state level in the U.S., while national GDP growth rates show no effects of hurricanes

---

<sup>\*</sup>This chapter is based on a paper that was written with help of Lia Alscher, who I supervised as a BA student for her thesis on this topic. I thank her for her dedicated help with data collection and analysis. She is co-author on the paper, which is in working paper status at the time of writing (Schippers and Alscher, 2022).

at all. Instead effects at the county level are pronounced, as is the case for e.g. New Orleans after Hurricane Katrina (Xiao and Nilawar, 2013, and Chapter 2). However, data at the appropriate spatial resolution is often not available. Especially for developing countries reliable subnational statistics on income are notoriously hard to come by, while they typically are more severely affected (Noy, 2009) and have higher fatalities (Kahn, 2005). Second, most economic data comes in annual frequency, whereas the time frame in which impact and recovery takes place is in the order of weeks to months for the majority of events. As discussed by Mohan and Strobl (2017), higher frequency data is therefore desirable.

In an attempt to bridge the gap between local impacts and economic data at higher aggregation levels, a growing literature that uses insights from both economics and remote sensing is using night light data as a proxy for economic activity to study the effects of natural disasters on the economies of affected areas.<sup>1</sup> This follows a large and growing literature that uses nighttime lights as a proxy for subnational GDP and local economic activity (e.g. Sutton and Costanza, 2002; Doll et al., 2006; Sutton et al., 2007; Ghosh et al., 2009, 2010). After the seminal contributions by Henderson et al. (2012) and Chen and Nordhaus (2011) on the structural relation between night light intensity and national GDP, an emerging literature investigates this relation for smaller sub-national units.<sup>2</sup> Most research on natural disaster impacts uses annual DMSP night light data as a proxy for economic activity in the desired area. Promising results have been presented, with the key finding that night light intensity is capable of capturing economic downturns and recovery from natural disasters.<sup>3</sup>

However, annual night light composites provide only the combination of the impact and recovery phase. The release of the newer Visible Infrared Imaging

---

<sup>1</sup>Field work and reconnaissance is the traditional way of monitoring disaster-struck areas after impact, but this is costly, time-consuming, and can sometimes be difficult when infrastructural connections are damaged. In the field of disaster studies and remote sensing, remote sensing data have therefore long been recognized as an important tool to aid humanitarian response and for coordinating emergency and recovery efforts (Eguchi et al., 2008; Dell'Acqua and Gamba, 2012; Wegscheider et al., 2013).

<sup>2</sup>Michalopoulos and Papaioannou (2013, 2014) focus on economic growth in ethnic homelands, Hodler and Raschky (2014b) on economic development of sub-national administrative units, Storeygard (2016) on trade and urban growth, Henderson et al. (2017a) on urbanization for uniform grid cells and Bleakley and Lin (2012) on locations along rivers as natural features, Bruederle and Hodler (2018) on local wealth and human development in Sub-Saharan Africa, and De Janvry et al. (2016) on post-disaster growth in Mexican municipalities.

<sup>3</sup>Bertinelli and Strobl (2013), Elliott et al. (2015), and Kocornik-Mina et al. (2020) show temporary declines in night light intensity in disaster-struck areas, mostly only in the year of the event. Gillespie et al. (2014) show for Sumatra, Indonesia, that night lights capture the economic damages and economic recovery from the 2004 Indian Ocean Tsunami. In related work on the 2004 tsunami effects in Aceh, Indonesia, Heger and Neumayer (2019) show that declines and subsequent recovery (in terms of economic growth) can be captured in night lights. In Chapter 2 I study the economic effects of Hurricane Katrina on the coastal counties of Louisiana and Mississippi and show that night lights are a reasonable proxy for economic downturn and recovery in the affected area. In an attempt to apply this approach globally, I show in Chapter 3 that weather anomalies typically depress local night light intensity, while positively affecting neighboring areas through spatial spillover effects.

Radiometer Suite (VIIRS) night light data suite, which provides monthly composites, allows studying natural disaster impacts at higher frequency and at more spatial detail.<sup>4</sup> Mohan and Strobl (2017) pioneered in this and used the monthly VIIRS night lights to study the effects of Cyclone Pam in 2015 on the South Pacific Islands. The authors report an enormous initial reduction in light intensity, but also find cumulative positive effects by the end of the year, stressing that the impact and recovery phase should be separated when studying disaster impacts. Yet other papers using the monthly night light composites present very different results. Findings range from a negative impact of typhoons in China only in the month of occurrence (Del Valle et al., 2018) to altogether insignificant effects of various disaster types on local light intensity in five Southeast-Asian countries in Skoufias et al. (2021). Similar to Skoufias et al. (2021), in Chapter 4 I find insignificant results for earthquakes and monthly night lights in a global panel. As the popularity of using night light data as a proxy for (local) economic activity in the context of natural disasters is growing, these recent findings call for caution.

We contribute to this discussion by critically assessing how well the monthly VIIRS night lights serve as a proxy for economic activity in the aftermath of natural disasters in the context of a large and damaging earthquake. We make three main contributions. The first is on the identification of changes in the light data. One of the potential underlying problems is that the monthly data is extremely volatile (see Levin, 2017; Coesfeld et al., 2018; Levin et al., 2020). This makes it challenging to separate true impacts from general temporal variability in the data. Indeed, some recent papers on disaster impacts in the remote sensing literature are dedicated specifically to addressing the issues of seasonality and volatility in the data (Zhao et al., 2020; Gao et al., 2020), reporting some degree of success in separating true disaster impacts from general volatility. However, even after incorporating these suggested solutions, Skoufias et al. (2021) find no statistically significant relation between large shocks and light intensity in a panel fixed effect approach at the pixel level. In this paper, we therefore take a different approach and use a difference-in-differences strategy to compare areas that are affected by a natural disaster to unaffected nearby areas. In doing so, we present an alternative solution to the volatility problem in the data and test whether we can identify local

---

<sup>4</sup>The annual DMSP data is not without its problems: first, (1) saturation in urban centers obscures true light intensity and therefore hinders identification of true impact and recovery especially in dense cities (for an example, see Chapter 2). Second, (2) other problems are lack of on-board calibration, which makes comparison of changes in light intensity over time challenging, and geolocation errors and spatial averaging which cause ‘glow’ – also known as blooming – around urban centers (for a detailed discussion see Gibson et al., 2021). The newer VIIRS data addresses all of these issues while also being freely distributed in monthly rather than only in annual frequency. The newer monthly VIIRS data is thus suggested to be the better alternative moving forward (Elvidge et al., 2013, 2017). However, the economics literature is still predominantly using the older annual DMSP data (Gibson et al., 2020; Gibson, 2021). This is true not just for disaster studies, but more generally for economic studies that make use of night lights to proxy economic activity. Some studies have come out recently that use the monthly DMSP data to study the impacts of hurricanes (Del Valle et al., 2018; Miranda et al., 2020). This solves problem (2) but does not address the inherent problems with the DMSP data mentioned under (1).

disaster impacts from a major natural disaster with the monthly VIIRS night light data.

Our second and most important contribution is combining changes in light data with recorded damage and socioeconomic data at the local level. A key problem in this literature is that studies typically lack true damage data. Instead, physical intensity of the natural hazard is either used directly, or through a damage function that translates e.g. ground shaking or wind speed to expected building damage to arrive at local proxies for disaster intensity (Bertinelli and Strobl, 2013; Elliott et al., 2015, and Chapter 3). This allows researchers to study large regions over long time periods, while having a geographically precise and timely estimate of local intensities of extreme natural events, often at the pixel level (Elliott et al., 2015; Kocornik-Mina et al., 2020; Skoufias et al., 2021). Moreover, this can be done without requiring insurance records or damage assessments. However, when no light changes are observed, the cause for this is then ambiguous. Either there is no effect of the natural disaster on light intensity per se, or the natural hazard – e.g. heavy ground shaking in the case of an earthquake – did not result in substantial physical damages and as such did not result in a natural disaster in the first place.<sup>5</sup> To resolve this ambiguity we propose to study the relation between night lights and materialized damages directly.

Moreover, studies typically only focus on (a proxy for) direct damages, but disregard the indirect economic effects that the disaster may have caused, for example in terms of business interruption and income losses (e.g. Bertinelli and Strobl, 2013; Miranda et al., 2020; Skoufias et al., 2021). These effects crucially determine how local economies are affected in the medium run, and thus how night light emissions may change in the months after a disaster. We therefore incorporate both direct and indirect effects in our study. In order to be able to compare night light changes with independently measured damage and economic impact data, we need some level of spatial aggregation. We therefore aggregate night lights to the lowest level of administrative areas for which we also have socioeconomic data available. In our case this means we aggregate to the municipal level. As we need detailed spatial information on both disaster fatalities and damages as well as on socioeconomic indicators, data collection is demanding. We therefore focus on an event in a high-income country with sufficient availability and quality of local economic data and fatality and damage records. Moreover, in order to have strong priors on the expected (negative) effect of the disaster on night light intensity, we study a large event with major damages and measurable economic downturn. Since we are limited by the time period for which we have VIIRS night light data available, i.e. starting in April 2012, we study a relatively recent event. To limit the scope of this paper and following up on findings in Chapter 4, we focus on earthquakes.

---

<sup>5</sup>Specifically related to earthquakes, Hashitera et al. (1999) and Kohiyama et al. (2004) are examples of early studies that attempt to use changes in night light intensity to identify areas that are possibly affected by earthquakes in the first days after the disaster. More recent examples using the monthly VIIRS night light data to identify damaged areas in the first days after an earthquake are Zhao et al. (2018) and Fan et al. (2019). The latter two, however, do not make use of damage records, but rather use modelled impact data instead.

Finally, our third contribution is that we build a comprehensive overview of how the various effects of the earthquake in terms of human losses, damage to buildings, infrastructure and assets, and business interruption are expected to affect night light intensity. Using this framework, we first collect the relevant information for the affected area. In doing so, our paper relates to more traditional analyses of disaster impacts. We connect to Chang (2010), who studies the regional impacts of the 1995 Kobe earthquake in Japan and shows that the reconstruction sector experiences a boom in the years following the quake. Cole et al. (2019) study the 1995 Kobe quake, specifically looking at manufacturing plant survival. Other important work is that by Rose et al. (1997) on lifeline disruptions and Eichenauer et al. (2020), who study aid patterns after the Gorkha earthquake in April 2015, Nepal. We add to this literature by studying a more recent large earthquake disaster in detail, and exploring its regional economic impacts. Based on the collected case information, we then form expectations on how night light intensity should be affected and compare these expectations to observed changes in night light emissions.

The case we study in this paper is one of the costliest earthquakes of the past decade: the April 2016 Kumamoto earthquake on southern Kyushu Island in Japan. The earthquake resulted in over 20 billion US dollars of damages, tens of thousands damaged houses of which 8,000 collapsed completely, and over 200 fatalities. Japan is an ideal case for our purposes as it provides high quality damage and socioeconomic statistics at very low levels of spatial aggregation: the municipal level. This provides an excellent opportunity to assess the link between local economic dynamics and night light intensity in the aftermath of a natural disaster.<sup>6</sup> We collect data on physical damages to buildings and infrastructure, fatalities, and income and business impacts at the municipal level to measure economic impacts as a result of the disaster. We then do a comparative case study in which we relate these impacts to changes in night light intensity for the affected municipalities to assess to what extent the materialized impacts are reflected in night lights.

Our findings are not supportive. We find that on average there is no effect of the earthquake on night light intensity of the affected municipalities in the month of the earthquake or in the months following, even though recorded direct and indirect impacts were sizeable. Instead, only one municipality that experienced the collapse of an important bridge and a major loss of business activity shows a sustained downturn in light intensity, while the municipality that was worst affected in terms of building damage instead experiences a substantial increase in light intensity in the year after the earthquake. In the latter case, this happens despite an income loss of over 30 percent in 2016. Overall, there appears to be no relation between changes in light intensity in the monthly VIIRS data and income losses as a result of the earthquake. Concluding, our findings do not support the use of monthly VIIRS night light data as a proxy for local economic activity in the aftermath of a large earthquake, at least for the case considered in this study.

---

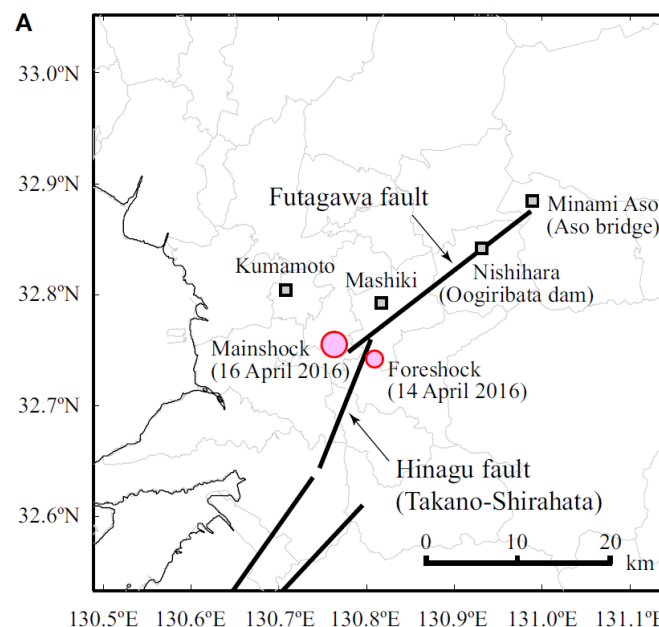
<sup>6</sup>Given the data demands and time window for a case, other candidate cases such as the April 2015 Gorkha earthquake in Nepal and the Central Italy earthquakes of 2016 were discarded. See Appendix 5.C for a discussion.

The remainder of this paper is organized as follows: in Section 2 we introduce and discuss the impacts of the Kumamoto earthquake in detail. Based on this we identify the areas that were hit most severely by the earthquake, for which we study changes in night light intensity in detail. Section 3 discusses the night light data and our methodology for identifying disaster impacts in the night lights. In section 4 we discuss results. Finally, Section 5 discusses the main results and limitations and concludes.

## 5.2 The April 2016 Kumamoto earthquake

On the 14th of April 2016 at 21:26 local time, Kumamoto prefecture was hit by a moderate earthquake along the Hinagu fault on the southern island of Kyushu, Japan (Cabinet Office Japan, 2017). The foreshock had an intensity of 6.5 Richter Scale and the epicenter was located to the east of Kumamoto City, at a shallow depth of approximately 10-12 km (see Figure 5.2.1). Two days later the main shock with an intensity of 7.3 occurred at 1.25 am local time close to the location of the first shock, followed by several smaller aftershocks. The damage was concentrated mainly around the Futagawa fault in the eastern part of Kumamoto prefecture, with Mashiki Town, Nishihara Village and Minamiaso Village being the most seriously damaged (Goda et al., 2016). We start with an account of direct impacts in terms of fatalities and damages, and then assess in detail indirect impacts in terms of disruptions to economic activity, infrastructure, and lifelines.

Figure 5.2.1: Earthquake location



*Note:* from “The 2016 Kumamoto Earthquakes: Cascading Geological Hazards and Compounding Risks”, by Goda et al. (2016). Reprinted under creative commons CC BY 4.0 license.



### 5.2.1 Direct impacts: fatalities and damages

The earthquakes caused in total 228 deaths and 2,753 people suffered from severe or minor injuries (Cabinet Office Japan, 2017). The disaster affected over 300,000 people (CRED, 2021), with over 100,000 evacuees in the first week after the earthquake (Cabinet Office Japan, 2017), and made 24,000 people homeless. Munich Re (2017) reports economic losses of 31.3 billion US Dollar, making it the third most expensive earthquake in Japan ever in nominal terms. Around 8,000 houses collapsed completely, and more than 140,000 were damaged out of which approximately 24,000 suffered major damage (Goda et al., 2016; Munich Re, 2017). In some areas such as in Nishihara Village, up to 56% of residents' houses were severely damaged (Tsuboi, 2019). More than 13,000 other non-residential buildings in Kumamoto prefecture were damaged (Kumamoto Prefectural Crisis and Disaster Prevention Division, 2020). We collect detailed data on building damage by municipality and summarize damages for the five worst-affected municipalities in Table 5.2.1 (for others see Appendix Tables 5.A.1 and 5.A.2). To allow comparison between affected municipalities, we divide building damage by population to construct a damage index that represents the total number of damaged buildings per capita. This damage index is reported in the final column of Table 5.2.1. To illustrate the degree of destruction, the five worst-affected municipalities record at least one damaged building for every four inhabitants. We plot the damage index for all municipalities of Kumamoto prefecture in Figure 5.2.2. Damage is highly concentrated along the Futagawa Fault, with Mashiki, Nishihara, Mifune, Kashima, and Minamiaso as the worst-affected municipalities. When focusing on total destruction of housing only, damages are limited to the hotspot of these same five municipalities (see Appendix Figure 5.A.1).

Table 5.2.1: Earthquake impact in selected municipalities

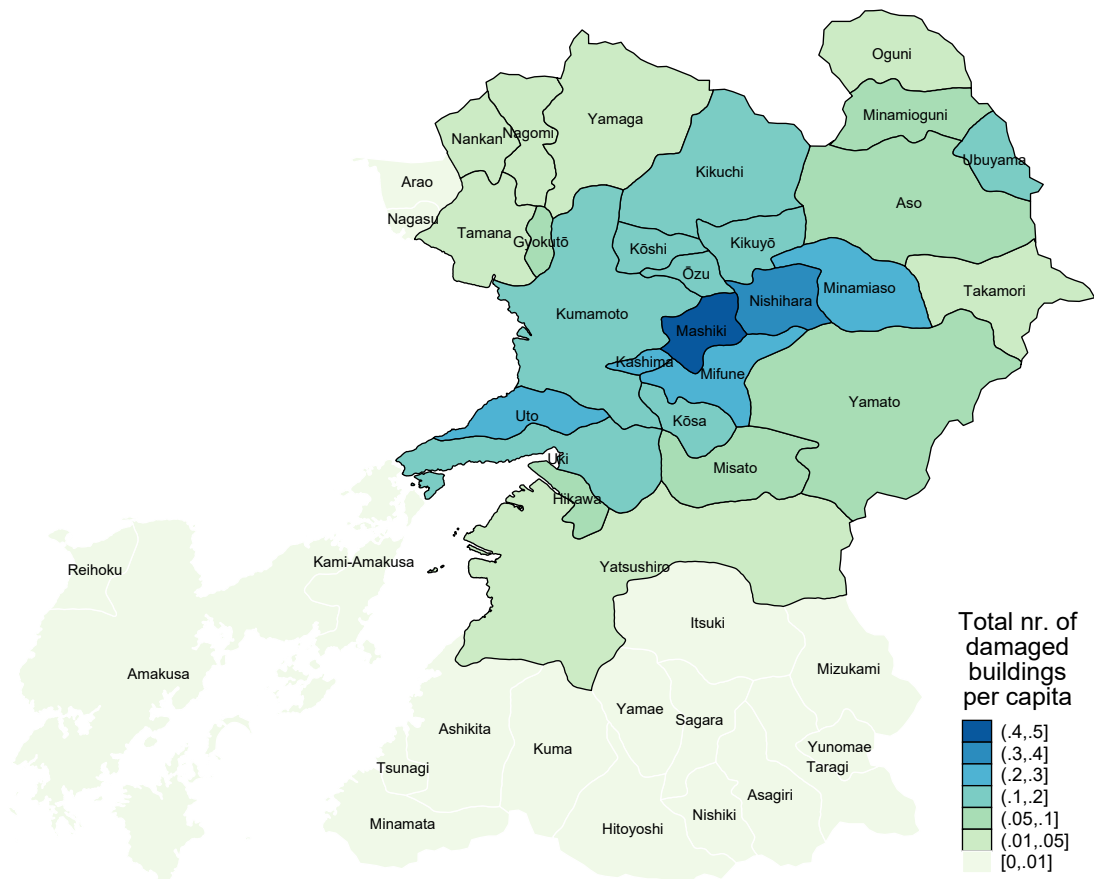
Municipality	Population	Total deaths	Total destruction of housing	Partial destruction of housing	Some damage of housing	Public building damage	Other non-residential building damage	Damage index
<b>Mashiki</b>	33611	45	3,026	3,233	4,325	104	5,902	0.494
<b>Nishihara</b>	6802	9	512	865	1,097	.	.	0.364
<b>Mifune</b>	17327	10	444	2,397	2,178	.	.	0.29
<b>Kashima</b>	9054	5	234	565	1,462	14	.	0.251
<b>Minamiaso</b>	11503	31	699	989	1,171	.	.	0.249

*Note:* Data on fatalities and injuries comes from the 2016 Kumamoto Earthquake Survey Report (Asian Disaster Reduction Center, 2016). Building damage information is taken from the 303rd Report on the Damage Situation of the 2016 Kumamoto Earthquake (Kumamoto Prefectural Crisis and Disaster Prevention Division, 2020).

## 5.2.2 Indirect impacts on economic activity, business, and lifelines

We use a combination of reports, statistics from the Statistical Bureau of Japan and from government departments, NGOs and insurance companies, and news articles to collect information on the impacts by municipality. The earthquake caused several landslides and especially had an impact on infrastructure such as airports, roads, and railways (Munich Re, 2017). However, most disruptions were short-lived. Only close to Minamiaso Village, a landslide caused severe damages including the collapse of an essential bridge, which led to sustained interruptions such as the suspension of service on two railway lines. Reconstruction took almost five years to complete.

Figure 5.2.2: Normalized damage distribution across municipalities in Kumamoto prefecture



*Note:* Total affected buildings calculated by the sum of totally destroyed housing, partially damaged housing, damaged public buildings, and damage of other non-residential buildings. Source: based on own calculations using data from the 303rd Report on the Damage Situation of the 2016 Kumamoto Earthquake (Kumamoto Prefectural Crisis and Disaster Prevention Division, 2020).

Next, we consider business interruption and potential closure due to loss of physical capital and changes in demand and supply in affected areas.<sup>7</sup> In the industrial area around Kumamoto City, several firms producing cars, electronic components and pharmaceuticals are located. Most buildings there only suffered minor damage, but nonetheless production was halted at least in the week following the disaster, thereby affecting global supply chains (Munich Re, 2017). Still, about half the businesses that suffered some kind of damage did not have to suspend operations at all, while 80% of businesses resumed operations within a week, and only less than 2% suffered from sustained business interruptions past June 2016 (Cabinet Office Japan, 2017, see Figure 5.A.3). Furthermore, all evacuation centers could be closed by November (Cabinet Office Japan, 2017, see Figure 5.A.4). On the other hand, sectors such as tourism experienced longer-term declines. The number of inbound tourists to Kumamoto Prefecture between October and December was 11.6% lower than in the previous year (Japan Times, 2017).

One of the main reasons for lights going out in the aftermath of natural disasters are power outages. However, electricity was fully restored in all municipalities within five days, and in most even earlier (detailed recovery times by municipality can be found in Figure 5.A.5). Therefore, in the case of the Kumamoto Earthquake power outages cannot be a substantial factor behind any observable decreases in night lights from May onwards. Even though the Cabinet Office Japan (2017) states that the infrastructure damages had a substantial impact on the daily lives of the population and business activities, in general recovery was rather swift. This is supported by a report of the Asian Disaster Reduction Center (2016) which concluded that, overall, the speed of recovery seemed high. It helped that damages were highly concentrated in Kumamoto City, and some other areas such as Mashiki Town and the Aso area. Moreover, most infrastructure damages were repaired within a month or an alternative connection was opened such that access to the damaged areas was restored.

Even though recovery was thus relatively quick, indirect damages to economies of the worst-affected municipalities in 2016 were quite serious. In the figures below, we report the effects of the Kumamoto earthquake on the municipalities of Kumamoto prefecture for 2016, focusing on municipal (taxable) income, net migration, and economic activity in terms of the number of business establishments.<sup>8</sup> Unsurprisingly, there is a striking similarity between these figures and the spatial distribution of direct damages reported in Figure 5.2.2. Income losses are especially large in Nishihara and Mashiki, which lose over 30 percent of taxable income in 2016 (see Figure 5.2.3a). Another striking observation is the overall positive growth of taxable income throughout Kumamoto prefecture, whereas the worst-affected area

---

<sup>7</sup>Such effects have been reported for e.g. Hurricane Katrina (see Xiao and Nilawar, 2013; Deryugina et al., 2018; Groen et al., 2020). For a discussion, see Chapter 2.

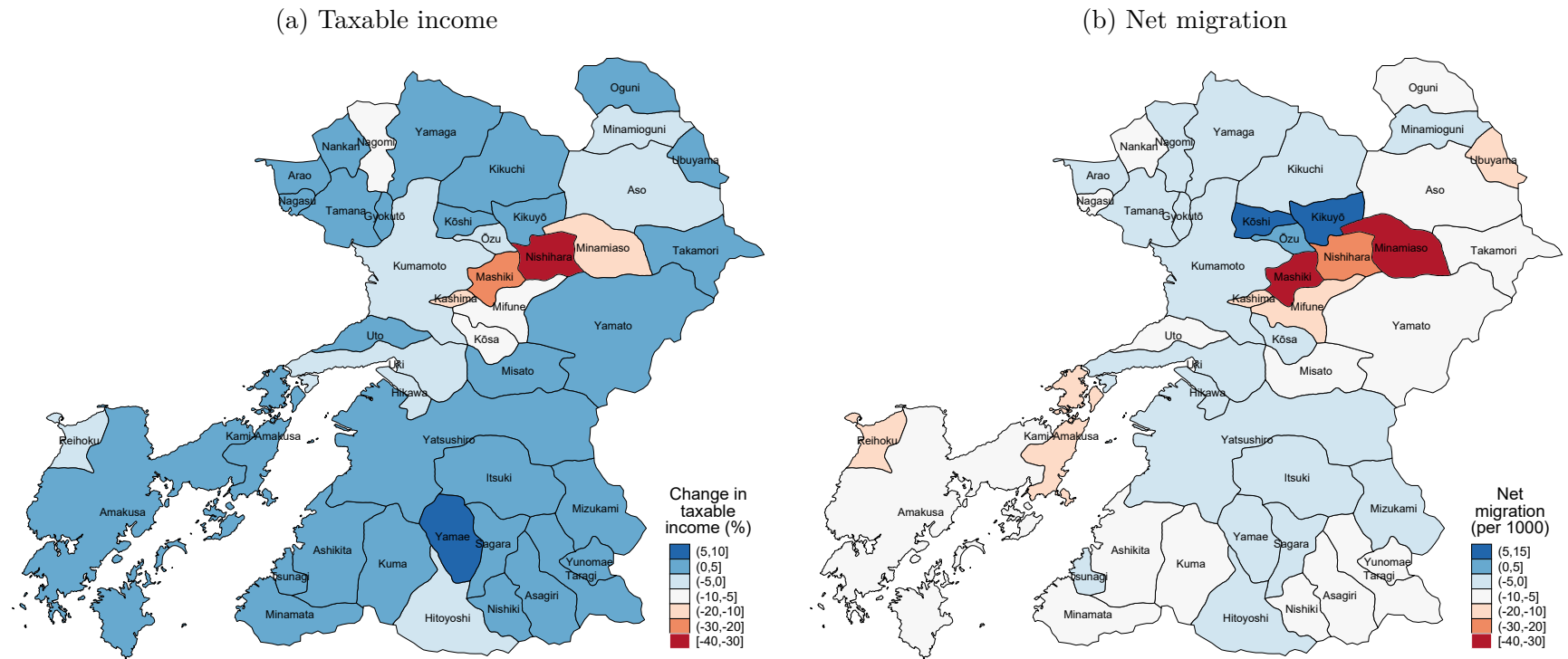
<sup>8</sup>An incidental but fortunate feature of the municipal data is that it is published per fiscal year, which runs from April to March. Figures for the year 2016 therefore coincide with the onset of the Kumamoto quake in April. Figures by municipality reported in detail in Appendix Figure 5.A.6a through 5.A.7b. Business establishments are defined as entities that occupy a certain place, have employees and equipment under a single management entity, and produce goods or services.

shows clear negative growth that is matched by moderate declines in neighboring municipalities. Similar to the income effect, the same worst-affected municipalities show substantial net migration rates of 15 to 40 outmigrants per 1,000, compared to an average of 5 (sd 6.9) before 2016 in Kumamoto prefecture (see Figure 5.2.3b).<sup>9</sup> In absolute terms, mean net migration from the municipalities is an outflow of 89 persons per year. By contrast, in 2016 this increases to 150 persons, indicating increased population movement due to the earthquake. Note that this hides substantial outliers such as Mashiki and Minamiaso, which experienced a net outmigration of 1319 and 485 people respectively, representing roughly 4% of their respective population numbers. Figures 5.2.4a and 5.2.4b then plot the change in the number of business establishments and number of engaged persons respectively. Changes are reported between 2014 and 2016, based on the 2017 business census (Cabinet Office Japan, 2017). As becomes obvious from the figures, decreases in the number of business establishments occur throughout Kumamoto prefecture. The average decrease is 5.1 percentage points (sd 6.9). The only municipalities that are more than one standard deviation above the mean are Mashiki and Nishihara, with 14% and 13% fewer business establishments respectively, and Minamiaso with a reduction of 44%. Reductions in Kashima, Mifune are close to the mean at roughly 5%. When instead focusing on persons engaged, it is really only Minamiaso that experiences an extraordinary reduction, again spiking with a reduction of over 42%.

---

<sup>9</sup>Figure 5.2.3b also shows clearly which municipalities were on the receiving part: in relative terms, immigration rates for 2016 were high in the neighboring municipalities of Koshi and Kikuyo.

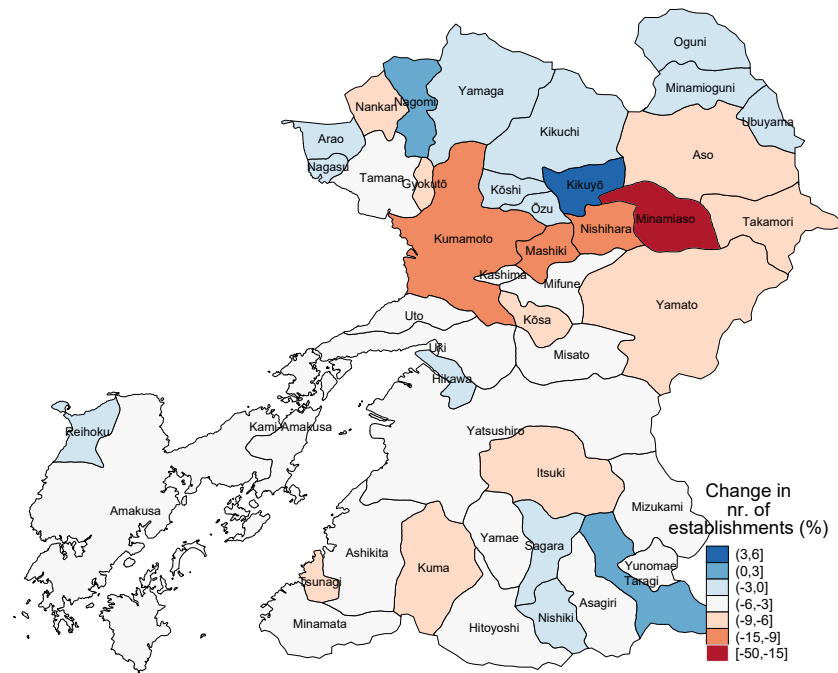
Figure 5.2.3: Changes in taxable income and net migration



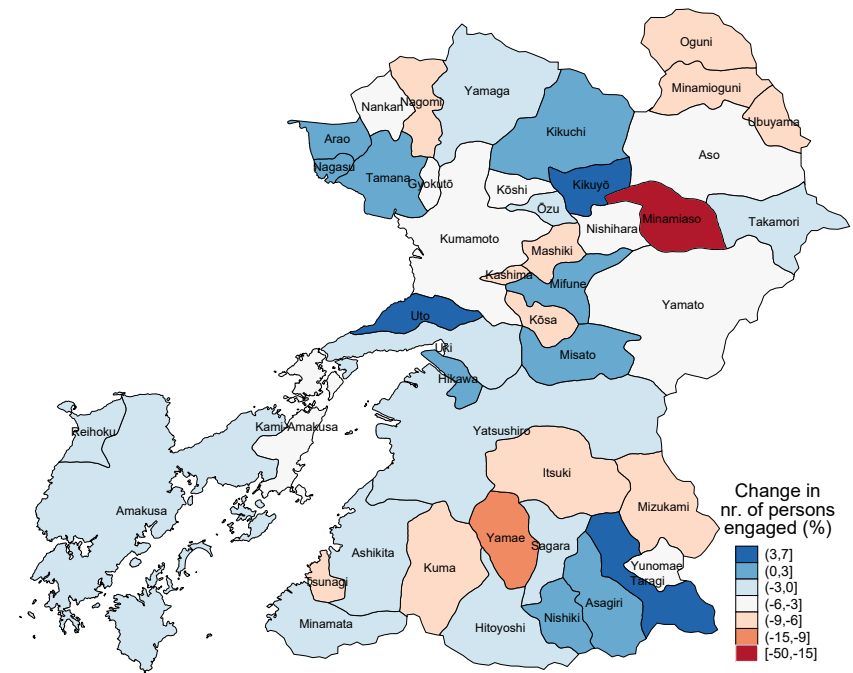
Note: (a) Source: own calculations. Difference between 2016 and 2015. (b) Source: own calculations. Migration data for 2016. Data from the System of Social and Demographic Statistics, Municipality Data (Official Statistics Japan, 2020).

Figure 5.2.4: Changes in business establishments and engaged persons

(a) Change in nr. of business establishments



(b) Change in nr. of persons engaged in business establishments



Note: Source: own calculations. Difference between 2016 and 2014. Data from the Economic Census for Business Activity for 2016 (Official Statistics Japan, 2020).

## 5.3 Methodology

With the stage being set, we now turn to testing to what extent night light intensity reflects the impacts identified in Section 5.2. We take a number of steps. We first formulate hypotheses on the relation between economic impacts and night light intensity for the short and medium run in Section 5.3.1. Second, we download, clean, and prepare the monthly VIIRS night light data, which is discussed in Section 5.3.2. In Section 5.3.3 we discuss our empirical strategy and analysis of the night lights.

### 5.3.1 Conceptual framework

We first set up a framework in which we relate the identified direct and indirect impacts to changes in light intensity for the short and medium run. To structure the analysis, we make use of standardized guidelines for damage assessments, for example from the OECD (2016). From this we identify five key factors: (1) social losses, including deaths and injuries; (2) property losses, of which both residential and non-residential building damage is the most important indicator; (3) damage to infrastructure and lifelines, such as roads and bridges, and electricity supply; (4) business interruption; and finally (5) emergency operations.<sup>10</sup> We first formulate hypotheses for the short run, which is limited to the month of the earthquake itself given the frequency of the data. We then turn to the medium run, in which the effects of social and property losses feed into the wider economy of the affected region in subsequent months. The factors and ways in which they affect economic activity and night light emissions are summarized below in tables 5.3.1 and 5.3.2, for the short and medium run respectively. We note that there is not much guidance in the literature, but we use established findings where available.

The expectations for night lights and economic activity generally coincide, as damages and impediments to normal daily life depress both economic activity and its associated night light emission. Considering the short run (Table 5.3.1), the effect of an earthquake is negative on both economic activity and night light emission for all but emergency operations. While there is no direct evidence in the literature to the best of our knowledge, Zhao et al. (2018) do find temporary increases in night light intensity in affected locations in the days after the 2016 earthquakes in Central Italy. The authors suggest that this may be due to emergency operations such as search and rescue activities. At the same time, emergency operations cause substantial costs and economic activity is hindered, because people in shelters cannot resume their daily lives. Furthermore, while fatalities and injuries may negatively affect economic activity in a municipality, we expect little effect on night light emissions if the death toll is as low as it was for the Kumamoto quake (228 fatalities, see Section 5.2.1). The opposite is true for damage to buildings, assets, and infrastructure, which should affect both economic activity and night light emissions negatively in the short run.

---

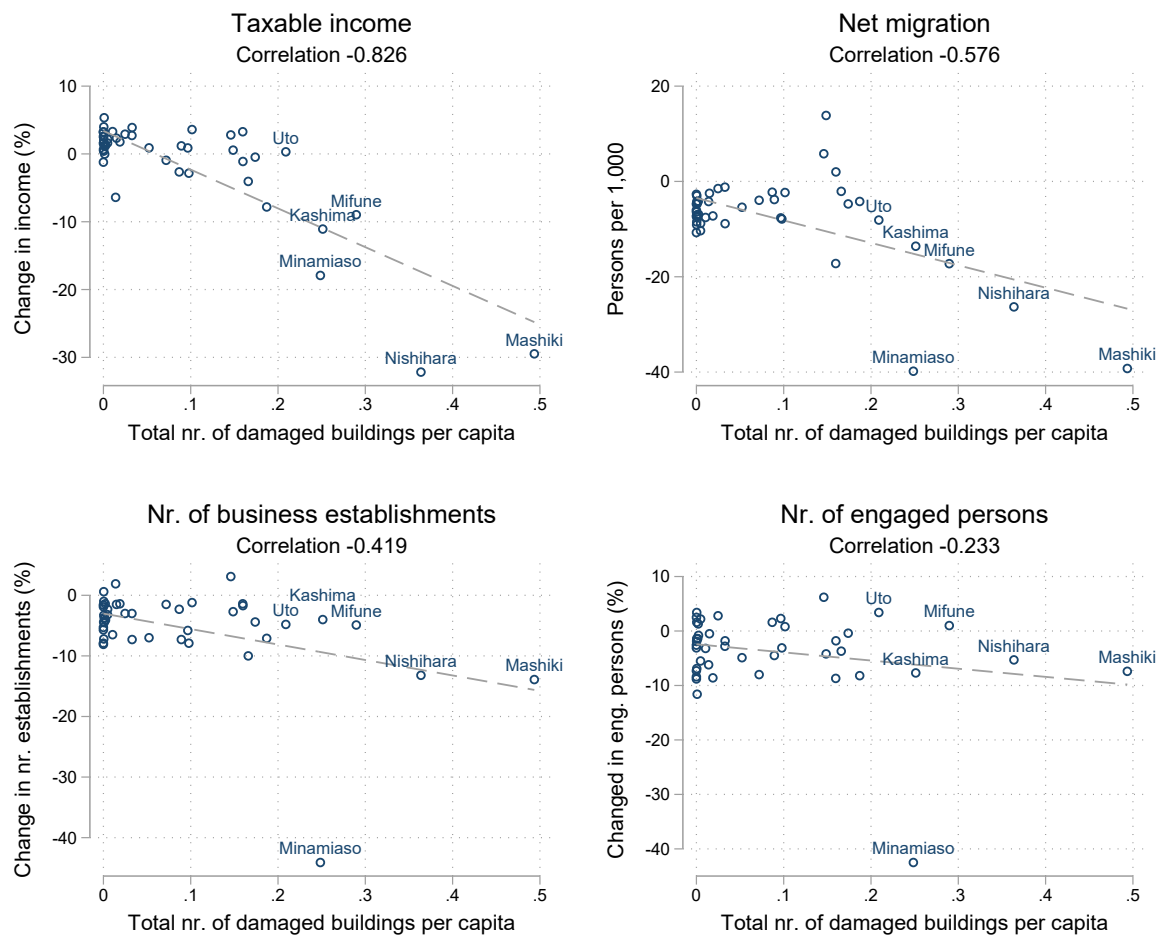
<sup>10</sup>Note that these same factors were also guiding in the data collection for damages and economic impacts discussed in Section 5.2.

Second, we consider the medium run (Table 5.3.2). An important factor is damage to buildings and infrastructure. While the loss of capital assets on the one hand depresses economic activity, damage to buildings and infrastructure also leads to reconstruction efforts, which give rise to a boom in the construction sector (see e.g. Chang, 2010; Xiao and Nilawar, 2013). These potential disparities between short and medium run and between night lights and economic activity demonstrate that some caution is needed when employing night lights as a proxy for economic activity in the context of a natural disaster. Moreover, it calls for studying the effects of disasters on economic activity at high temporal resolution in order not to mix negative direct damages with potential positive effects from reconstruction in the same post-disaster period.

We use the framework of Table 5.3.1 and 5.3.2 to form expectations on how and in which municipalities we should see changes in night light intensity (abbreviated to NTL in the tables) occurring based on the identified impacts in the previous section. We have identified clear negative earthquake impacts in terms of building and infrastructural damage, as well as economic impacts for 2016 in the worst-affected municipalities within Kumamoto Prefecture. Five municipalities along the Futugawa fault line stand out, ranked in order of normalized building damage: Mashiki, Nishihara, Mifune, Kashima, and Minamiaso. Figure 5.3.1 summarizes these findings. Pairwise correlations indicate that the relations with normalized building damage are especially strong for taxable income and net (out)migration. In line with the impacts discussed in the previous section, the relation with the number of business establishments and number of persons engaged is lower. The sharp outlier of Minamiaso forms the exception, which loses over 40% of both establishments and engaged persons between 2016 and 2014.



Figure 5.3.1: Summary of building damage and economic indicators by municipality



*Note:* Scatter plots and correlations between building damage and socioeconomic indicators for Kumamoto prefecture. Data on income and migration from the System of Social and Demographic Statistics, Municipality Data (Official Statistics Japan, 2020). The change in number of business establishments and engaged persons is based on data from Economic Census for Business Activity for 2016 (Official Statistics Japan, 2020), which reports changes with respect to 2014.

Table 5.3.1: Impact framework for the short run

Factor category	Factor	NTL +/0/-	Explanation	Econ. activity +/0/-	Explanation	References
<b>Social losses</b>	Fatalities	0/-	Large population decline may result in empty houses/buildings.	-	Loss of workforce and human capital.	Kohiyama et al. (2004)
	Injured	0	No change expected, as long as no additional (temporary) medical centers have to be set up.	-	Temporary reduction of workforce.	Kohiyama et al. (2004)
	Displaced population	0/-	Displaced population may move NTL with it. Either within same area (no change), or to another area (reduction of NTL).	-	Displaced workforce cannot resume daily activities, regardless whether displaced internally or to other areas.	Kohiyama et al. (2004); Xiao and Nilawar (2013); Li and Li (2014); Zhao et al. (2018); Chapter 1
<b>Property losses</b>	Housing	-	Destruction of an important light source.	-	Related to displaced workforce; daily activities cannot be resumed.	Kohiyama et al. (2004); Zhao et al. (2018); Fan et al. (2019)
	Public buildings	-	Destruction of an important light source.	-	Workplaces/public spaces cannot be visited; lower production, consumption, and related movement of people and capital.	
	Business assets	0/-	Indoor equipment will typically emit little to no light.	-	Loss of productive assets negatively affects production.	
<b>Damage to infrastructure/lifelines</b>	Damage to road infrastructure	-	Street lights and reduced traffic.	-	Reduced traffic/transportation hinders economic activity, both for production and consumption.	
	Damage to other transportation infrastructure (ports, railway, airports)	-	Street lights and reduced traffic.	-	Reduced capacity of central hubs in the transportation network puts additional stress on timely relief efforts, commute of employees, and on supply networks for local producers.	Chang (2010)
	Utilities disruption (power outages, disruption of water and gas supply, sewage damage)	-	Power outage directly results in loss of NTL.	-	Unavailability of essential lifelines (electricity, gas, water) strongly affects production. Short-run losses due to lack of refrigeration and other essential maintenance.	Rose et al. (1997); Kohiyama et al. (2004); Hallegatte et al. (2019)
<b>Emergency operation costs</b>	Search-and-rescue activities	+	Search-and-rescue at night requires emergency lighting, which may increase NTL intensity in the first days after a disaster (see e.g. the 2016 Central Italy earthquakes, as described by Zhao et al. 2018).	0	While valuable for human lives, search-and-rescue itself is not productive from a value-added perspective.	Zhao et al. (2018)
	Temporary structures such as evacuation centers	0/+	Typically in large stadiums and other existing structures built for large gatherings. Only positive if new centers are erected.	0/-	Temporarily replaces the intended function of the building, requires resources to run. Shifts resources away from value-adding processes to relief operations.	Félix et al. (2013)
<b>Business interruption</b>	Suspension of commercial activities and social life at night	-	Important source of light: factories, stores and advertisement lights.	-	Reduction of business activity and consumption of services (related to cultural institutions and traffic services).	Kohiyama et al. (2004)
	Disruption of other business activities	-	Any business activity at night requires light.	-	Reduction of business activity.	

Table 5.3.2: Impact framework for the medium run

Factor category	Factor	NTL +/0/-	Explanation	Econ. activity +/0/-	Explanation	References
<b>Social losses</b>	Fatalities	-	Substantial numbers of fatalities reduce both consumption and production in the medium run, and thus depress NTL.	-	Substantial fatalities translate into a smaller workforce and lower consumption. Psychological effects for individuals may affect productivity negatively.	
	Injured	0	Most injuries will be healed relatively quickly.	0/-	Most injuries will be healed relatively quickly. Longer-lasting injuries and possible disabling conditions may reduce the workforce and lower individual productivity.	
	Displaced population	-	Displaced population may move NTL with it. Within same area (approx. no change), or to another area (reduction of NTL).	-/+	Spatial shift of demand and supply. May benefit activity in the receiving region.	Xiao and Nilawar (2013); Li and Li (2014); Brata et al. (2018); Chapter 1
<b>Property losses</b>	Housing	+	Reconstruction and construction of (temporary) housing units is light-intensive. This should only result in a temporary increase of NTL.	+/0	(Re)construction efforts boost the construction sector and may attract workers from other regions (e.g. in the case for Aceh after the 2004 tsunami, or Hurricane Katrina in New Orleans).	Chang (2010); Xiao and Nilawar (2013); Heger and Neumayer (2019)
	Public buildings	+	Reconstruction is light-intensive. Public buildings that resume their intended function again may start emitting NTL again.	+/0	(Re)construction efforts boost the construction sector and may attract workers from other regions (e.g. in the case for Aceh after the 2004 tsunami, or Hurricane Katrina in New Orleans).	Chang (2010); Xiao and Nilawar (2013); Heger and Neumayer (2019)
	Business assets	0	As before, business assets themselves emit no light. Their indirect effect on production and productivity is more important.	+/0/-	Depending on investment effect: replacing capital may have no effect (0), lacking financial means to replace lost capital will negatively affect production (-), while creative destruction may positively affect productivity (+).	Skidmore and Toya (2002); Crespo Cuaresma et al. (2008); Leiter et al. (2009); Hallegatte and Dumas (2009); Zhou and Botzen (2021)
<b>Damage to infrastructure/lifelines</b>	Damage to road infrastructure	+/-	Reconstruction is light-intensive, but continued impediments to traffic may result in lower NTL.	-	Reconstruction efforts positively affect production, but a disrupted road network hurts regional business in the medium run.	Gillespie et al. (2014); Noy et al. (2021)
	Damage to other transportation infrastructure (ports, railway, airports)	-	Reconstruction of major transport hubs takes longer than road reconstruction. Depressed traffic through these hubs depresses NTL.	-	Reconstruction efforts may positively affect production, but disruption of major transport hubs hurts the regional economy (supply chains, spillover effects).	Chang (2010); Xiao and Nilawar (2013); Dekle et al. (2015); Brata et al. (2018)
	Utilities disruption (power outages, disruption of water and gas supply, sewage damage)	0/-	Prolonged power outage as a result of a damaged power grid results in longer duration of loss of NTL.	-	Unavailability of essential lifelines (electricity, gas, water) strongly affects production.	Rose et al. (1997); Kohiyama et al. (2004); Hallegatte et al. (2019)
<b>Business interruption</b>	Disruption of business activity	-	Business closure may lead to a reduction in economic activity in the affected area.	-	Loss of physical capital and changes in demand and supply in the affected area may negatively affect business activity.	Jarmin and Miranda (2009); Xiao and Nilawar (2013); Cole et al. (2019); Zhou and Botzen (2021)

Table 5.3.3 summarizes our expectations. Given the substantial damage to buildings and infrastructure in these municipalities we expect negative impacts on night light intensity at least in the month of the earthquake. For municipalities such as Mashiki, Nishihara, and Minamiaso, a visible impact beyond the short term is likely. As discussed in the previous section, Mashiki and Nishihara experience major reductions of taxable income in 2016 (around 30%), while also losing up to 14% of their business establishments. Minamiaso village stands out especially due to its substantial loss in terms of establishments within the municipality, and due to the collapse of the important Aso bridge that connects the municipality to the city of Kumamoto. We therefore expect negative effects on night light intensity in the months following April 2016. As a contrasting case, Uto is the sixth worst-affected municipality in terms of building damage (1 damaged building for every 5 inhabitants), but stands out in terms of an apparent absence of negative economic impacts. Instead of experiencing a loss in taxable income, income remains stable in 2016 (see Figure 5.3.1). Similarly, reduction of the number of business establishments was less than 5%, while the number of engaged persons instead rose by 3.4%.<sup>11</sup> We therefore expect a negative short-run impact on light intensity for Uto, but no effect in the medium run. In the main analysis of this study, we focus on these six municipalities.

Table 5.3.3: Expected night light impacts for the worst-affected municipalities

	Factor	Mashiki	Nishihara	Mifune	Kashima	Minamiaso	Uto	Others
<b>Short-run</b>	Social losses	0	0	0	0	0	0	0
	Property losses	-	-	-	-	-	-	-/0
	Infrastruct./lifelines	-	-	-	-	-	0	0
	Emergency operations	+	+	+	+	+	0	0
	Business interruption	-/0	-/0	-/0	-/0	-	0	0
<b>Medium-run</b>	Property losses	-	-	-	-	-	-	0
	Reconstruction	0/+	0/+	0/+	0/+	0/+	0/+	0
	Infrastruct./lifelines	0	0	0	0	-	0	0
	Business interruption	-	-	0	0	-	0	0

In practice, finding detailed information on emergency operations by municipality proved impossible. We therefore work with what anecdotal information we have from the disaster response agencies (Cabinet Office Japan, 2017). Since these activities take place in the first days to weeks after a disaster, this should only affect light emissions in the month of the disaster itself in the worst-affected municipalities. Finally, a similar notion on data availability holds for reconstruction efforts: we were unable to find detailed information on reconstruction efforts by municipality. However, anecdotal information clearly indicates that reconstruction was a multiyear effort. For example, reconstruction of the Aso bridge in Minamiaso took five years to complete. In other municipalities, reconstruction of damaged housing was similarly

<sup>11</sup>Interestingly, Uto is the sixth worst-affected municipality in terms of normalized total building damage, but damage records report only 116 completely destroyed houses (on a population of 37,000; compared to e.g. 512 in Nishihara, compared to a population of 6,800). If we instead look at normalized total destruction of housing only (Figure 5.A.1, Uto is ranks 12th and is hardly affected when compared to the top 5. Hence, Uto serves as an interesting comparative case.

projected to take years. Given the severe building damage in the worst-affected municipalities, we therefore expect the identified damages and income losses to outweigh the effect of reconstruction efforts in the first months after the quake.

For other places such as Kumamoto City we only expect short-term changes – if any – due to building damage and decreased activity in the industrial area in the immediate weeks following the disaster. While building damages were sizeable in many other municipalities, they were much less severe relative to population size. Moreover, economic impacts were much more limited. In addition, there were no major business interruptions past the first month post-quake and electricity supply was restored within a number of days. Damages were highly concentrated to Kumamoto prefecture and there even to a few municipalities. Consequently, for the other municipalities in Kumamoto prefecture, and moreover for the other prefectures on Kyushu Island, we do not expect noticeable changes in night light intensity as a result of the earthquake.<sup>12</sup>

### 5.3.2 Night lights

Next we collect and clean the monthly night light data for Kyushu Island. We make use of the VIIRS Day/Night Band (DNB) monthly night light composites, version 1.0, as provided by the Earth Observation Group at NOAA/NCEI (for a detailed discussion, see Elvidge et al., 2017). The data products record absolute radiance (in  $\text{nW}/\text{cm}^2/\text{sr}$ )<sup>13</sup> and the number of cloud-free nights that was used to construct the monthly average radiance value for each pixel, at a resolution of 15 arc seconds (roughly 450 meters at the equator). We aggregate all pixels within the administrative area of a municipality to compute its total sum of light (SOL) and the average number of cloud-free nights.<sup>14</sup> The mean sum of light by municipality is  $1160 \text{ nW}/\text{cm}^2/\text{sr}$  (sd 2773, median 521). The distribution is heavily right-skewed and contains substantial extreme values at the top end of the distribution even after the data filtering process by NOAA.<sup>15</sup> To facilitate comparison between municipalities

---

<sup>12</sup>Note that we exclude Oita prefecture from the analysis. While Oita prefecture does experience damages in the order of over 2200 damaged buildings (of which only 2 were completely destroyed), we have no detailed municipality-specific damage data. Overall, Kumamoto prefecture accounts for all but 2 totally destroyed houses, and accounts for 98% of overall building damage. See Appendix Table 5.A.2.

<sup>13</sup>In radiometry, radiance is measured as the amount of radiant energy emitted (measured in nanoWatts for the VIIRS data) per unit of time for a given surface area (square centimeters) at a particular angle (the steradian: sr). The data is then converted to give average radiance for a pixel sized roughly 450 by 450 meters at the equator. The average pixel on Kyushu Island emits  $1.89 \text{ nW}/\text{cm}^2/\text{sr}$ , while e.g. an average pixel in the municipality of Kumamoto, the largest city in Kumamoto prefecture, emits  $3.85 \text{ nW}/\text{cm}^2/\text{sr}$ .

<sup>14</sup>We use the Global Administrative Areas dataset (GADM, version 3.6) to delineate municipalities.

<sup>15</sup>Unlike the more widely used annual DMSP night light data, the monthly version 1.0 composites have not undergone the same thorough cleaning process. While the DNB data is filtered to exclude stray light, lightning, lunar illumination, high-energy particles, and cloud-cover, contamination from snow cover and water body reflection, as well as ephemeral events such as forest fires and aurora remain present in the data.

we take the natural logarithm of light intensity. This implies that we can interpret the change in intensity in percentage changes.

As cloud cover can be a major limitation in detecting light changes from natural hazards in the first days after an event, we inspect data coverage of cloud-free nights. Note that this is the case especially for meteorological events, but less so for earthquakes (Zhao et al., 2018; Levin et al., 2020). The average number of cloud-free nights is 8.4 (sd 3.4, median 8.3), meaning that on average less than a third of nights in a month is available. No municipality has a mean larger than 20 nights. This implies that the monthly radiance values in practice are computed based a subset of the month, with days potentially being clustered at the beginning or the end of the month. The monthly VIIRS images contain no information on which nights went into the monthly averages. However, given that we study a seismologic disaster, there is no systematic relation between cloud cover and our event of interest. If anything, limited availability of cloud-free nights therefore introduces measurement error, but no bias. To make sure our analysis is not impeded by missing data around the time of the quake, we inspect the distribution of cloud-free nights over time in detail. No months around the quake contain only missing data for any of the municipalities in Kumamoto prefecture.<sup>16</sup>

Related to measurement problems of the data, the monthly VIIRS images contain a noise floor that is affected by airglow contamination (for a detailed discussion, see Coesfeld et al., 2020). The way this airglow is corrected in the monthly images changed as of January 2017, causing an increase of average radiance by roughly 0.15 nW/cm<sup>2</sup>/sr. We regress absolute mean radiance for all municipalities in the dataset on a constant and a dummy for the years 2017-2018 and find a highly significant coefficient of 0.175 (sd 0.051, results not reported but available upon request). As this is insignificantly different from 0.15, we follow Coesfeld et al. (2020) and subtract 0.15 nW/cm<sup>2</sup>/sr from all pixel-level observations for January 2017 onwards, before moving on to the main analysis.<sup>17</sup>

While the VIIRS night light data improves over the older DMSP data in many respects (for a comprehensive overview, see Elvidge et al., 2017), an important difference is the overpass time of 1.30 am. This is substantially later than the overpass time between 8.00-10.00 pm of the older DMSP satellites (Elvidge et al.,

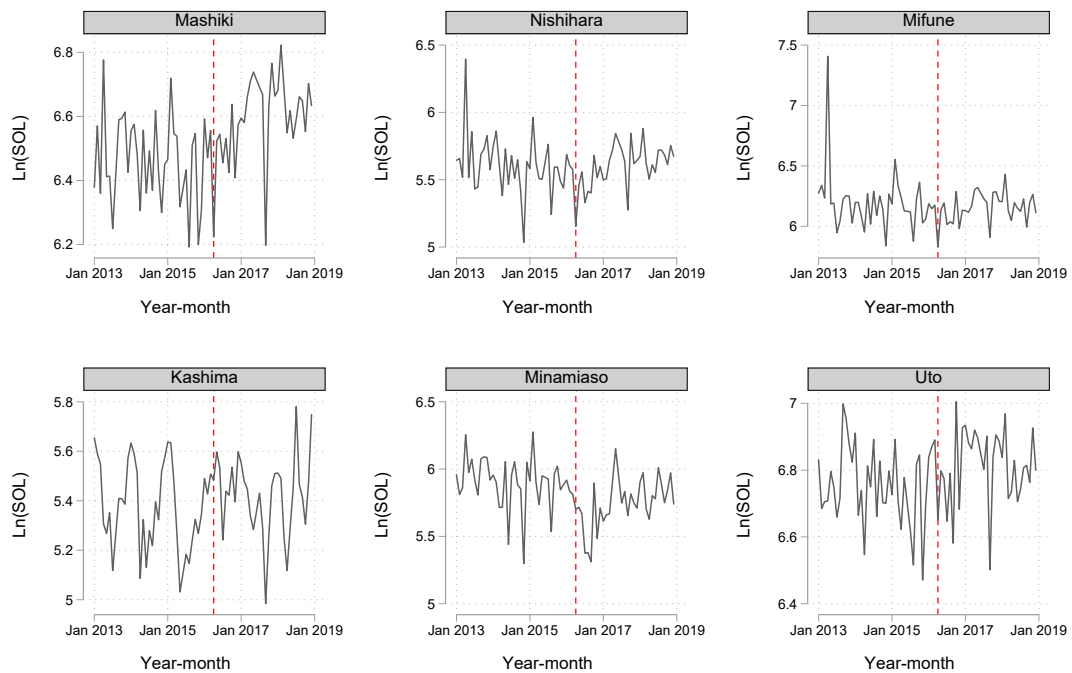
---

<sup>16</sup>While on average around 7.5 nights are available in the month April, April 2016 has a much lower mean number of nights across entire Kyushu Island (mean 3.6, sd 0.9). Specifically for the municipalities in Kumamoto prefecture, the mean is even lower at 2.6 (sd 0.7, see Appendix Figure 5.B.1). This affects our ability to observe changes in night light intensity for the impact month specifically, and the data contains no indication of which nights went into the average. However, the number of cloud-free nights in the subsequent months is considerably higher. Furthermore, the month June is associated with very low numbers of cloud-free nights (mean 2.4, sd 1.8, see Appendix Figure 5.B.2), with one outlier in 2015 in which radiance is missing for virtually all municipalities of Kumamoto prefecture (see Appendix Figure 5.B.3). We therefore set radiance in the month June 2015 to missing for all municipalities.

<sup>17</sup>While we can correct for such changes in measurement within a generic regression framework by using year dummies, not correcting for the level jump in the data contaminates descriptive graphs with a jump in the time series. Moreover, in a fully saturated difference-in-differences model that we apply later, we cannot use year dummies to take out this measurement difference.

2013). The VIIRS night light data may therefore record a different type of night light than the DMSP satellites did. As e.g. discussed by Gibson et al. (2020), rural lights are likely to be turned off at this time of night, while light from urban street lamps, car parks, and industrial facilities may still be lit. We stress that VIIRS night light data are therefore less likely than the DMSP data to capture social and cultural activities at night.

Figure 5.3.2: Total sum of light (in natural logarithm) by municipality for the worst-affected cases



*Note:* SOL = sum of light. The vertical red line indicates April 2016; i.e. the month of the earthquake.

We start with a simple descriptive of night lights for the worst-affected municipalities. The natural logarithm of the total sum of light by municipality is reported in Figure 5.3.2 below. Variability in light intensity over time within municipalities is clearly large, making it hard to visually assess whether the earthquake had any impact on night lights. While average change in night light intensity between 2013 and 2018 is roughly zero – i.e. the series are on average stationary – swings around this average can be rather large, indicated by a standard deviation of 22.3% on a mean of zero. This implies any potential impacts of the earthquake may be obscured by high variability of the month-to-month light intensity in the first place, such that simply eye-balling the time series does not provide much intuition. If anything, we observe a potential break in the series for Mashiki, which exhibits higher night light intensity values after the earthquake, whereas the series for Minamiaso show a noticeable immediate decrease in night light intensity, and a lower average for 2017-2018 than the years before the earthquake. For the other four, the raw data

provide little intuition, mostly due to the high variability of light levels over time. There is no established solution to this problem in the literature (Skoufias et al., 2021). We therefore now turn to discussing existing solutions and propose to use an alternative strategy in the form of a difference-in-differences framework to isolate the effect of the earthquake.

### 5.3.3 Empirical strategy

To identify the effect of the earthquake on night light emissions, we use a difference-in-differences framework in which we contrast night light intensity in affected municipalities to that in unaffected municipalities over time. This framework has been successfully applied by e.g. Heger and Neumayer (2019) to investigate the GDP growth effects of the 2004 Indian Ocean Tsunami on districts in Aceh, Indonesia. Following Heger and Neumayer (2019), we use a set of unaffected municipalities on the same island – in our case Kyushu island – as the control group, excluding the prefecture Oita.<sup>18</sup> Figure 5.3.3 shows the classification of treated and control municipalities for the entire island. Based on building damage per capita discussed in Section 5.2.1, we classify 27 municipalities as treated (orange), all within Kumamoto prefecture. 18 are classified as control municipalities within Kumamoto prefecture (yellow), with another 157 control municipalities in the other prefectures (green).<sup>19</sup>

The difference-in-differences framework comes with a number of advantages. First, since the exact location and timing of the Kumamoto earthquake cannot be known ex-ante, the shock is independent of economic activity and we can therefore interpret an identified difference between the treated and control groups as the causal effect of the earthquake on night light intensity. Second, inference of the potential impact of natural disasters on night lights typically relies on variation over time within spatial units, usually with a temporal resolution of years (e.g. Bertinelli and Strobl, 2013; Elliott et al., 2015; Kocornik-Mina et al., 2020, and Chapter 3). However, variability of monthly night light intensity makes the analysis more difficult with the monthly VIIRS data. Coesfeld et al. (2018) study this temporal variability in the USA and Canada and find the standard deviation of month-to-month radiance for individual pixels to be 15-20% of their mean even large light emitting urban and suburban areas. While we have other reasons to do our analysis at the municipal level, Coesfeld et al. (2018) suggest that aggregating light pixel values to larger geographical areas is suggested to reduce overall variation. We do so in our analysis, but still observe large standard deviations for changes in municipal total sum of light over time (as also illustrated by Figure 5.3.2). The mean (and median) growth rate of light intensity in our dataset is zero (i.e. the monthly series are stationary on average), but the standard deviation on this mean

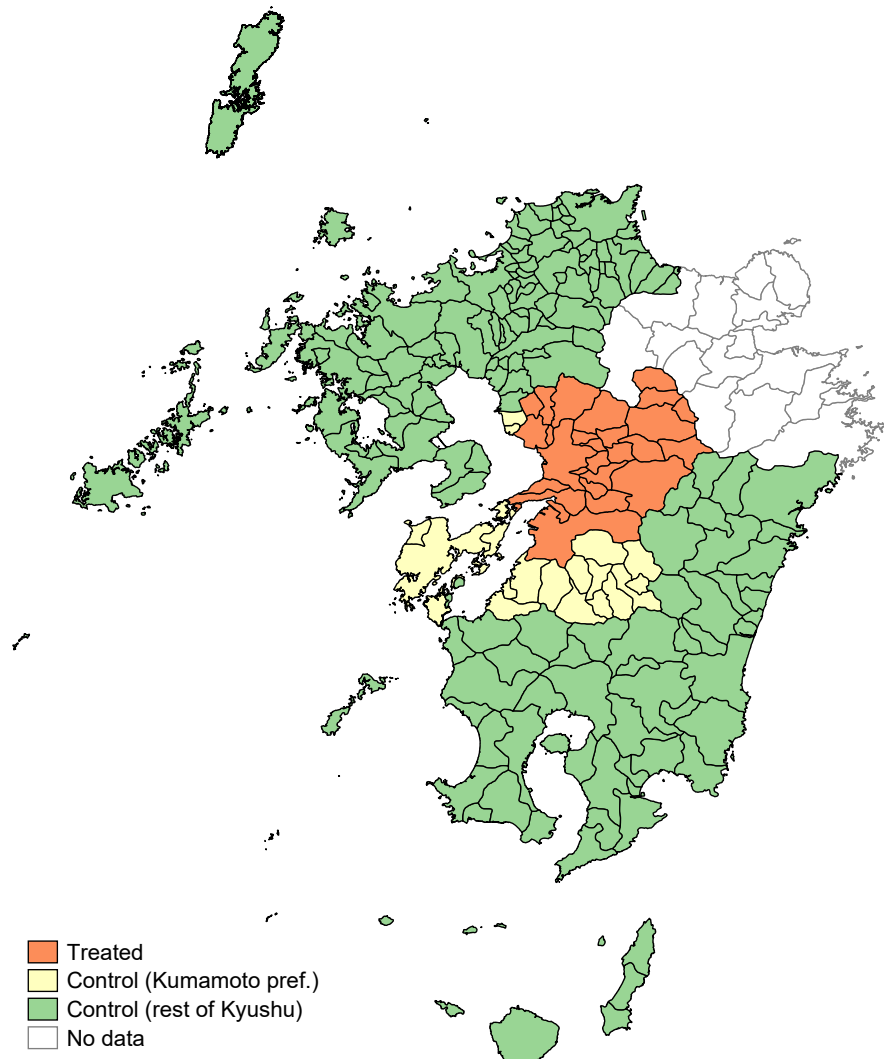
---

<sup>18</sup>As indicated before, the latter experienced smaller but noticeable building damage, affecting roughly 2200 houses (see Appendix Table 5.A.2 for detailed figures by prefecture). As we have no municipality-level damage information for this prefecture, we exclude this prefecture from the analysis.

<sup>19</sup>We exclude 13 southern island municipalities of Kagoshima prefecture due to their remote location.



Figure 5.3.3: Composition of treatment and control groups on the island of Kyushu



*Note:* 27 treated municipalities in Kumamoto prefecture in orange. 18 control municipalities within Kumamoto prefecture in yellow. The other 157 control municipalities from the other prefectures on Kyushu island. Note that Oita prefecture is excluded from the analysis (in shaded gray).

is roughly 50%. As our primary interest is in identifying changes in light intensity over time, the rather large temporal variation hinders graphical analysis and may obscure effects of the earthquake. In an attempt to account for potential seasonality in the temporal variation, as suggested by Levin (2017) and explored in Gao et al. (2020) and Zhao et al. (2020), we model seasonal patterns by municipality. However, taking out seasonality hardly affects the temporal variability of the series in our dataset (discussed in detail in Appendix 5.B.1).<sup>20</sup>

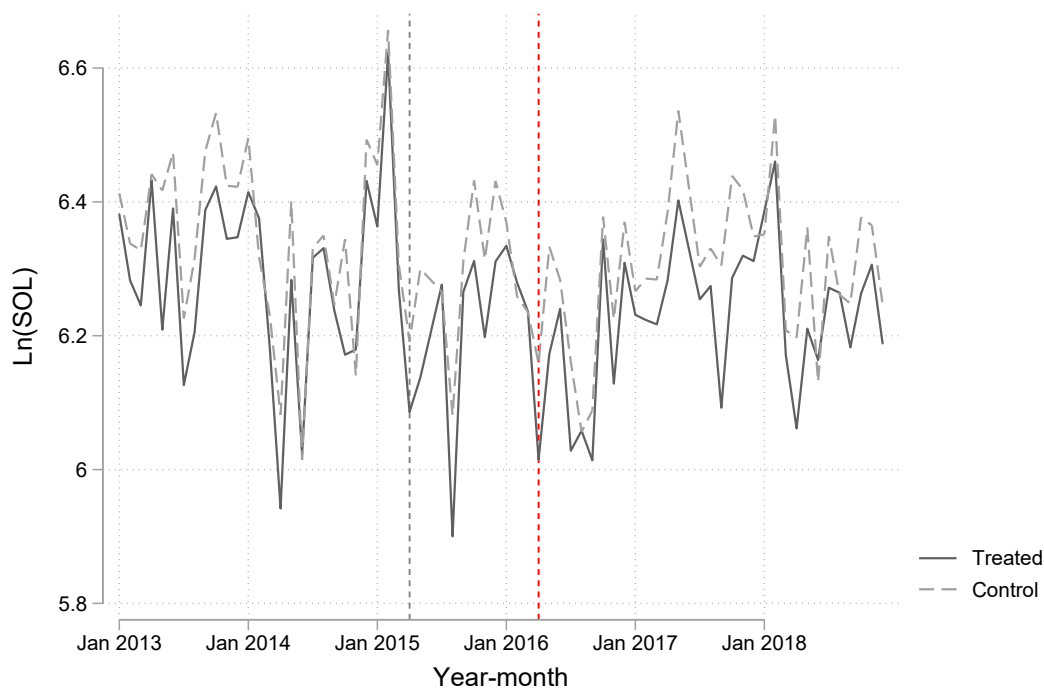
Instead, we observe a high degree of similarity in temporal variability of night

<sup>20</sup>For a detailed discussion on seasonality and volatility in the monthly VIIRS night light composites, see Levin (2017) and Coesfeld et al. (2018, 2020).

light intensity between affected and unaffected municipalities (see Figure 5.3.4). While the two groups do not overlay perfectly, average light intensity of the two groups evolves in tandem in the years prior to the earthquake. This parallel historic trend is the key to our identification strategy.<sup>21</sup> As a preface to the results, we note that the difference in average light values for the two groups is similar in April 2015 and April 2016, suggesting no average effect of the earthquake on the treated municipalities. We will test this formally later, using the difference-in-differences framework. To ensure comparability of the treatment and control group in terms of their population and economy, we report summary statistics by group on total population, taxable income, the size of the labor force, and sectoral employment in Table 5.3.4 below. The treatment and control groups are highly comparable on all covariates, with no significant differences except for the share of employment in the primary and tertiary sector, for which the difference is only small at 4 percentage points. The treatment and control group are thus highly comparable and share a parallel historic trend in the outcome variable to a large degree.

To illustrate the average effect of the earthquake on the treatment group, we plot

Figure 5.3.4: Average light intensity for the treated and control municipalities



*Note:* Treatment group consists of the 27 municipalities with building damage per capita of 0.01 and higher. The control group consists of all 175 other municipalities in the dataset. The vertical red line indicates the month of treatment (April 2016). The vertical gray line indicates April 2015, i.e. exactly one year before the earthquake.

<sup>21</sup>In Appendix Figure 5.B.6 we do the same comparison for log-differences rather than levels, thus comparing the growth rate of light intensity between the two groups. We find the same parallel pattern as reported in Figure 5.3.4.

Table 5.3.4: Summary statistics for the treated and control municipalities

	Treated	Control	Mean difference	t-stat	p-value
Mean light intensity (ln)	-0.581	-0.416	-0.166	-0.587	0.56
Total population (ln)	9.889	10.087	-0.198	-0.761	0.452
Taxable income (ln)	16.716	16.937	-0.221	-0.78	0.441
Size labor force (ln)	9.22	9.377	-0.157	-0.618	0.541
Employment in primary sector (%)	0.168	0.127	0.041	2.214	0.033
Employment in secondary sector (%)	0.227	0.227	0	-0.019	0.985
Employment in tertiary sector (%)	0.598	0.63	-0.032	-2.205	0.034
Number of observations	27	175			

*Note:* Means per group reported for the year 2015. Control group consists of all non-treated municipalities on Kyushu Island, excluding Oita prefecture. Mean light intensity is based on the annual VIIRS vrm-orm-ntl night light composite as provided by NOAA for January through December 2015. All other variables are reported for the fiscal year of 2015, which runs from April 2015 through March 2016.

the effects on taxable income and the net migration rate in Figure 5.3.5 below. The treatment group experienced a decline of taxable income of 2.8 percent, while the control group experiences roughly 2.2 percent growth. Similarly, the net migration rate remains roughly constant in the control group, while it nearly doubles in the treatment group. Figure 5.3.5 also shows that the deviation between the treatment and control group is only temporary, with both income and net migration numbers converging back to that of the control group by 2017. For this reason, we focus on the time window of the 12 months following the earthquake.

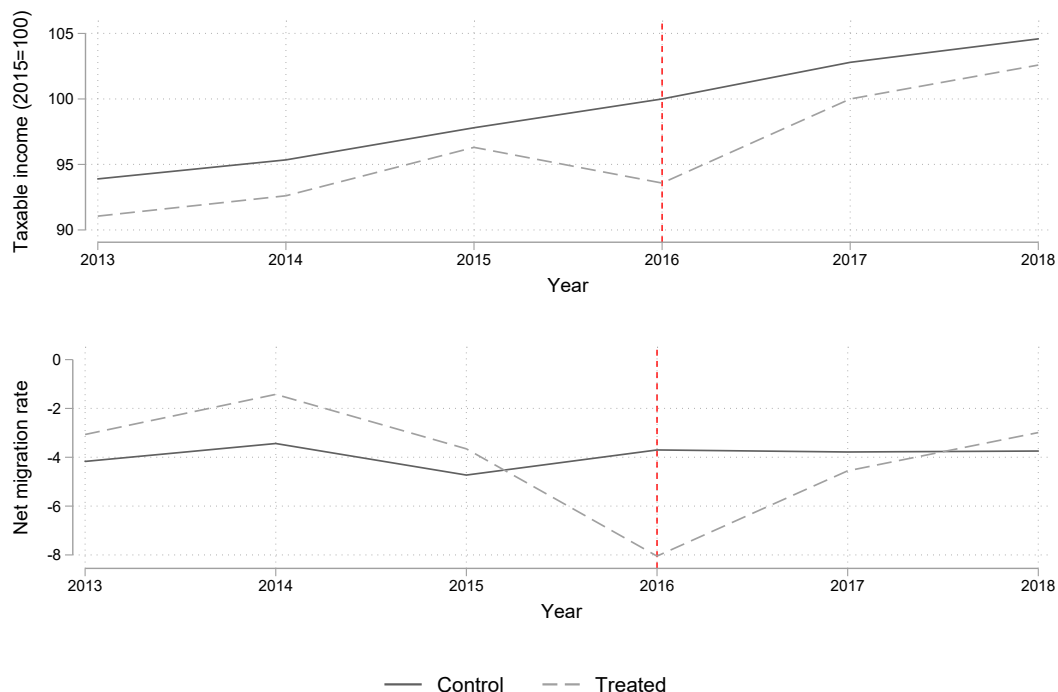
The identification strategy is then relatively straightforward. There are two groups of municipalities: those that were affected by the Kumamoto earthquake (treated municipalities;  $D = 1$ ) and those that were not (control municipalities;  $D = 0$ ). In a classical difference-in-differences framework, there are two time periods: before and after the treatment (pre-treatment  $T = 0$ ; and post-treatment  $T = 1$ ). However, in our case we are interested in immediate impacts and recovery post-earthquake. We therefore estimate the difference between the treated and control group in each time period (i.e. every month up to 12 months after the earthquake). Our effect of interest, the average treatment effect on the treated (ATE), is then estimated through a difference-in-differences estimation. Specifically, we compute the difference between treated and control before and after the treatment, for which the difference-in-differences between the two groups over time is then the treatment effect of interest. Formally, this can be written as:

$$\alpha_{ATE} = E[Y|D = 1, T = 1] - E[Y|D = 0, T = 1] - E[Y|D = 1, T = 0] + E[Y|D = 0, T = 0] \quad (5.3.1)$$

This identification strategy relies on a few crucial assumptions. First, to isolate a causal treatment effect, selection into treatment must be exogenous. Since the exact location and timing of the Kumamoto earthquake cannot be known ex-ante, violation of this assumption is unlikely. Second, the difference-in-differences framework requires a parallel trend prior to the moment of treatment, which we have

discussed above in relation to Figure 5.3.4.<sup>22</sup> While this cannot be formally tested, we test empirically for parallel trends by including coefficients for the differences between the treated and control units prior to treatment in the results section and report mostly insignificant coefficients. Finally, the stable unit treatment variable assumption (SUTVA) dictates that treated and control units cannot affect each other. We point out that while direct damages to buildings was highly localized to the worst-affected municipalities described in section 5.2.1, there are clear signs of negative effects to economic activity and income to neighboring municipalities as well (discussed in section 5.2.2). These can be either a sign of spatial spillovers or may be the direct result of damages in the respective municipalities. For this reason, we start with a rather large treatment group of 27 municipalities in Kumamoto, and gradually reduce the treatment group to higher thresholds of building damage per capita. Since the presence of spatial spillovers is possible after a large disaster (as discussed in Xiao and Nilawar, 2013, and shown in Chapter 3), we account for this issue in a robustness test by excluding control municipalities that are directly adjacent to treated municipalities, and later also exclude all unaffected

Figure 5.3.5: Indexed taxable income and net migration rate for the treated and control group



*Note:* Indexed taxable income (2015=100) in the top panel. Net migration rate (per 1,000) in the bottom panel. Treatment group consists of the 27 municipalities with building damage per capita of 0.01 and higher. The control group consists of all 175 other municipalities in the dataset.

<sup>22</sup>Note that the parallel trends prior to 2016 for taxable income (see Figure 5.3.5) also indicate that the parallel trend assumption is likely to hold.

municipalities in Kumamoto prefecture from the control group.

In practical terms, this implies that we estimate the following equation:

$$\ln(\text{light}_{it}) = \sum_{\tau=\text{May } 2015}^{\text{April } 2017} \beta_{\tau} \cdot 1[t = \tau] \cdot D_i + \alpha_i + \epsilon_{it} \quad (5.3.2)$$

in which the set of  $\beta_{\tau}$  coefficients leading up to April 2016 should be statistically insignificant (for the parallel historic trend assumption to hold), whereas  $\beta_{\tau}$  starting in April 2016 is the treatment effect of interest for the months following the earthquake. We include municipality fixed effects  $\alpha_i$  to control for unobserved heterogeneity between municipalities related to geography, size, and initial light levels. Standard errors are clustered at the municipality level.<sup>23</sup> We estimate this equation for the full set of affected municipalities, and later experiment with higher thresholds for the damage index.

Furthermore, as our case information leads us to conclude that only the worst-affected municipalities are likely to show substantial changes in night light intensity, we further analyze these cases in detail. As the group of treated municipalities then becomes very small, arbitrarily choosing entire Kumamoto prefecture or Kyushu Island as a control group may lead to comparing apples with oranges. We therefore follow previous applications in Coffman and Noy (2012), Cavallo et al. (2013), and Heger and Neumayer (2019) and use the synthetic control method to construct counterfactuals for the affected municipalities. This method is closely related to the difference-in-differences estimator but uses a weighted combination of a subset of control units from the pool of controls, rather than the (unweighted) control group as whole to construct an unobserved counterfactual (Abadie and Gardeazabal, 2003; Abadie et al., 2010). The goal of the synthetic control approach is to produce a synthetic counterfactual that best mimics the pre-treatment characteristics of the treated unit(s). In simple terms, we construct for each municipality a counterfactual that has a similar time series for night light intensity before the earthquake in 2016, to the best extent possible with the available pool of municipalities on Kyushu Island. We compute a single synthetic comparator for the individual municipalities based on pre-specified characteristics.<sup>24</sup> Following Heger and Neumayer (2019), the relevant characteristics are limited to the pre-treatment outcome variable. Still, as a robustness we include taxable income and total population for 2015 as covariates to ensure that the synthetic counterfactual is comparable to the treated municipality. Reassuringly, results are nearly identical.<sup>25</sup>

---

<sup>23</sup>While we would ideally estimate standard errors that are corrected for spatial autocorrelation, such as Driscoll-Kraay standard errors, this leads to symmetry and singularity issues in the variance matrix. We therefore rely on clustering of standard errors at the municipality level, which accounts for serial correlation and heteroskedasticity. For a similar discussion, see Heger and Neumayer (2019).

<sup>24</sup>We make use of the ‘synth’ package by Abadie et al. (2010).

<sup>25</sup>Note that we cannot use more traditional matching methods to ensure parallel historic trends, since none of the covariates are available in the same frequency as our dependent variable (monthly night light intensity).

## 5.4 Results

We now turn to the results. We first assess the average effect of the earthquake on night light intensity in the treatment group in Section 5.4.1. In Section 5.4.2, we zoom in on the worst-affected municipalities.

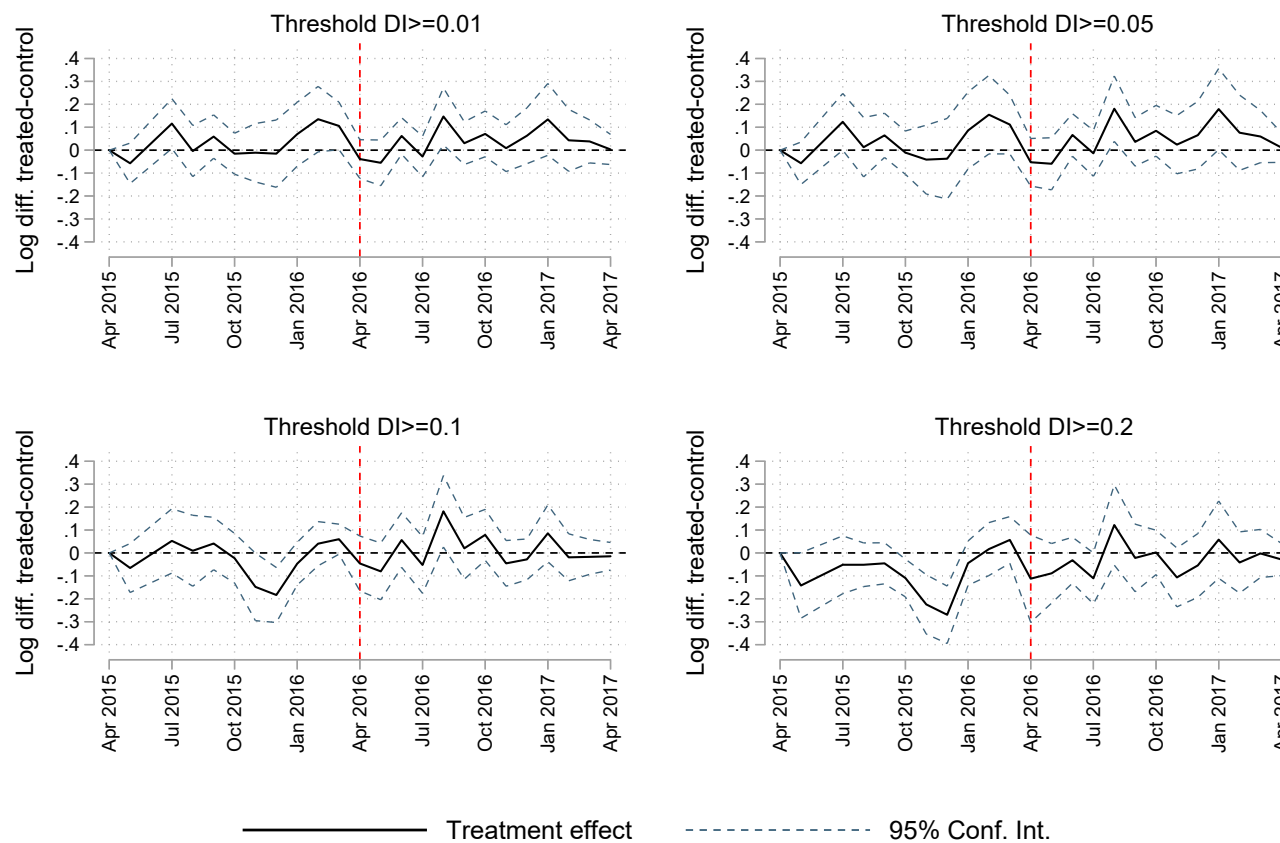
### 5.4.1 Average effects on night light intensity

We start with estimating a potential treatment effect of the earthquake on night light intensity for affected municipalities. We estimate equation 5.3.2 including all municipalities that experienced normalized building damage of at least 0.01 building per capita as the treatment group, effectively including 27 municipalities as treated. This gives us an estimate of the overall average effect of the earthquake on night light intensity in the region. We then gradually increase the threshold on the damage index to focus specifically on the more heavily affected areas. We set thresholds at 0.05 (20 treated), 0.1 (14 treated), and finally to 0.2 (6 treated), which involves only the six worst-affected municipalities in terms of normalized building damage – namely Mashiki, Nishihara, Mifune, Kashima, Minamiaso, and Uto.<sup>26</sup> The control group consists of all unaffected municipalities on Kyushu island, excluding the prefecture Oita. Results are reported below in Figure 5.4.1. On the y-axis, we report in black the estimated difference in log light intensity between the treated and the control group for each month in the data between April 2015 and April 2017, i.e. one year prior to the earthquake until one year after. The 95% confidence interval is plotted in blue. We focus first on the baseline estimate with a damage threshold of 0.01. Note that the estimated difference between the treatment and control group prior to treatment in April 2016 is not statistically significant except for the month prior to the quake and for July 2015, although an F-test on joint insignificance of the pre-event coefficients cannot be rejected. However, given the large temporal variability in the night light series, we are confident that this is our best possible estimate.

---

<sup>26</sup>When increasing the threshold, we drop all affected municipalities below the threshold from the estimation sample.

Figure 5.4.1: Baseline treatment effect estimates



*Note:* coefficient estimates of equation (1) reported in black, with a 95% confidence interval in blue. The vertical red line indicates the month of treatment (April 2016). The control group consists of all unaffected municipalities on Kyushu Island, excluding Oita prefecture (for a total of 175 municipalities). The treatment group varies by threshold of the damage index (DI): 27 for a threshold of 0.01, 20 for a threshold of 0.05, 14 for a threshold of 0.1, and 6 for the threshold of 0.2. In the latter case, only Mashiki, Nishihara, Mifune, Kashima, Minamiaso, and Uto are considered treated. Affected municipalities below the treatment threshold are excluded from the estimation sample.

We now turn to the immediate and medium-run impacts of the earthquake on night light intensity. As was suggested from the descriptive in Figure 5.3.4, we find no significant difference of night light intensity between the treatment and control groups for April 2016 (reported in the top left panel of Figure 5.4.1). On average the earthquake had no statistically significant effect on night light intensity. Focusing on the medium-run, i.e. the months in the year after the earthquake, we similarly find no evidence for an effect of the earthquake on night light intensity. However, as discussed in section 5.2.1, direct impacts were large in only a small number of municipalities within Kumamoto prefecture. To account for the possibility that light effects are visible only in those municipalities where impacts were more severe, we increase the normalized building damage threshold in three steps, reported in the remaining three panels of Figure 5.4.1. The conclusion on the immediate treatment effect does not change: even when limiting the estimation to only the six worst-affected municipalities, we estimate no statistically significant effect on night light intensity for the month of the earthquake, or in the year after. A concern may be that the control group includes municipalities that may be indirectly affected by the earthquake, specifically those in Kumamoto prefecture, as well as those that neighbor directly affected municipalities. Spillovers to nearby areas have indeed been identified by e.g. Xiao and Nilawar (2013) and in Chapter 3. To account for the possibility of spillover effects to nearby areas contaminating the estimated treatment effect, we test for robustness of the results to excluding all non-treated municipalities from Kumamoto prefecture from the control group, as well as all unaffected municipalities that are directly adjacent to a treated municipality (for reference, see Figure 5.3.3).<sup>27</sup> The results are hardly affected and are very similar to the baseline estimates of Figure 5.4.1 (see Appendix Figure 5.B.7). In their study on the recovery patterns of night lights after the Canterbury earthquakes in 2010-2011 in New Zealand, Nguyen and Noy (2020) suggest to aggregate the data to quarters before doing the analysis to smoothen temporal variability.<sup>28</sup> We aggregate the data to quarters starting in January, April, July, and October and re-run the estimation. Results remain qualitatively stable; again we find no sign for any treatment effect (see Appendix Figure 5.B.8a). In a final robustness check we aggregate to the annual level, in which we lose our ability to look at short-term dynamics, but are closer to the dominant approach in the literature. Again, we find no evidence for any treatment effect, either in the year of the earthquake or in the years following (see Appendix Figure 5.B.8b). We find no evidence for either a short or medium run impact of the earthquake on night light intensity in the affected area on average.

However, increasing the damage threshold also worsens the pre-treatment comparability of the treatment versus control group. While pre-trends are qualitatively similar, we estimate statistically significantly different light intensity values between the treated and control group for October through December 2015 for the highest damage threshold. This signals that the somewhat naïve approach of using the

---

<sup>27</sup>This removes 26 municipalities from the control group (149 control municipalities in total).

<sup>28</sup>Nguyen and Noy (2020) suggest that aggregating to quarters helps with smoothing the temporal variability, although no descriptives are provided. The authors indicate that none of their results are statistically significant at the monthly resolution.



unweighted average of all unaffected municipalities on Kyushu island performs worse as we reduce the size of the treatment group. This is not entirely unexpected, as the power of averaging out temporal variability over time is reduced when a smaller number of municipalities is considered, especially concerning the size of the treatment group. We therefore turn to an alternative approach in which we construct synthetic counterfactuals for the worst-affected municipalities in the next section.

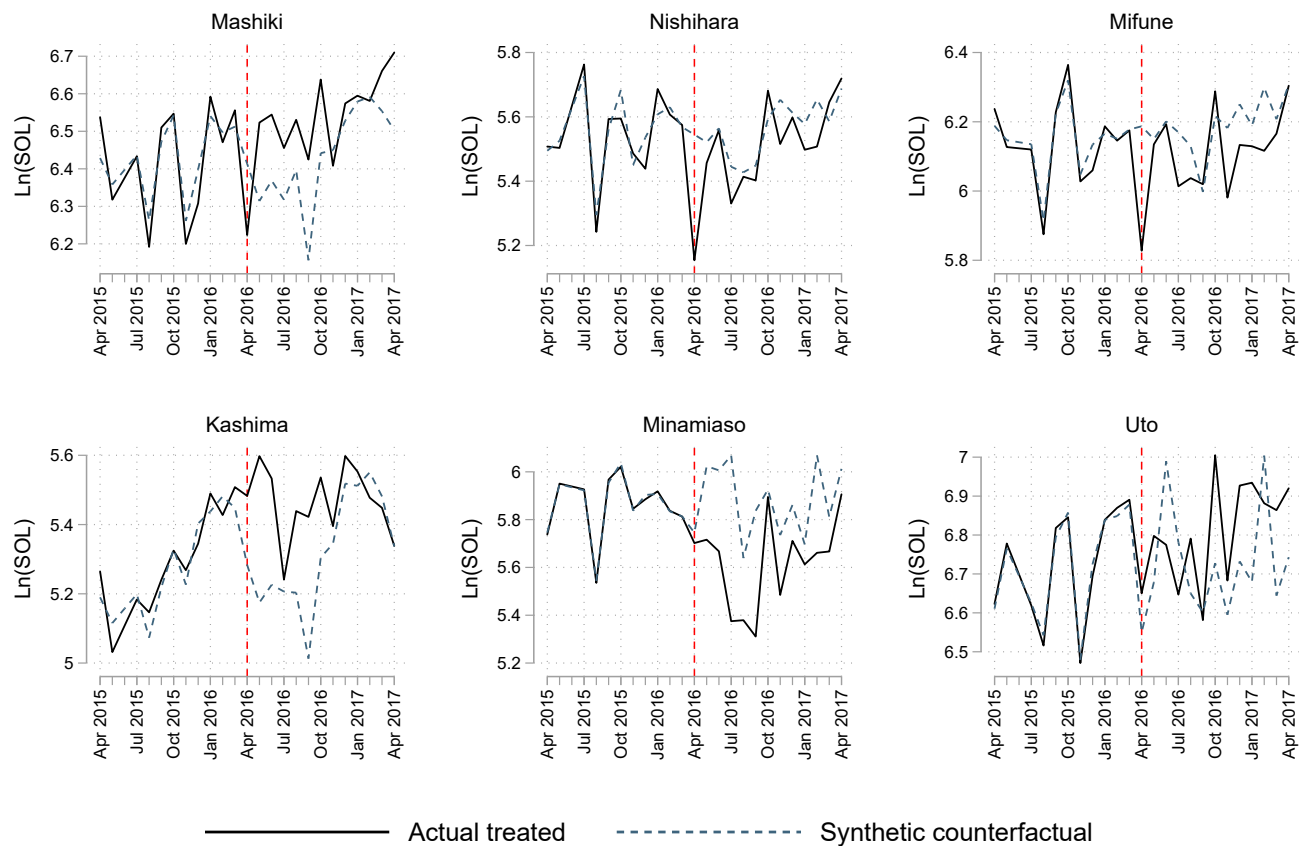
### 5.4.2 Zooming in: light intensity for the worst-affected municipalities

Our case information and the baseline results with no sign of an average treatment effect lead us to conclude that only the worst-affected municipalities – if any – remain to show substantial changes in night light intensity. We further analyze these cases in detail by constructing synthetic controls for each municipality individually. Results are reported below in Figure 5.4.2, with Figure 5.4.3 reporting the difference between the actual and synthetic municipalities. First, we observe that pre-earthquake night light intensity for the actual and synthetic counterfactual municipalities are closely aligned. This is to be expected as this is how the synthetic controls are computed by construction, but it also strongly signals that Kyushu Island is a suitable donor pool for counterfactuals for the worst-affected municipalities when we allow for a weighted combination of control units. However, the fits are not perfect; for Mashiki, Kashima, and Nishihara the deviation between the treatment and control group in the twelve months prior to the quake is somewhat larger than for the remaining other three.<sup>29</sup> As the synthetic control method provides no traditional confidence interval on the computed difference between the actual and synthetic counterfactual light levels, we report in Figure 5.4.3 an interval of plus and minus two standard deviations of the difference in the year prior to the earthquake. This gives a sense of how large the difference between the two groups in any month is relative to its average difference. We now turn to discussing expectations versus realized changes in night light intensity for the worst-affected municipalities.

---

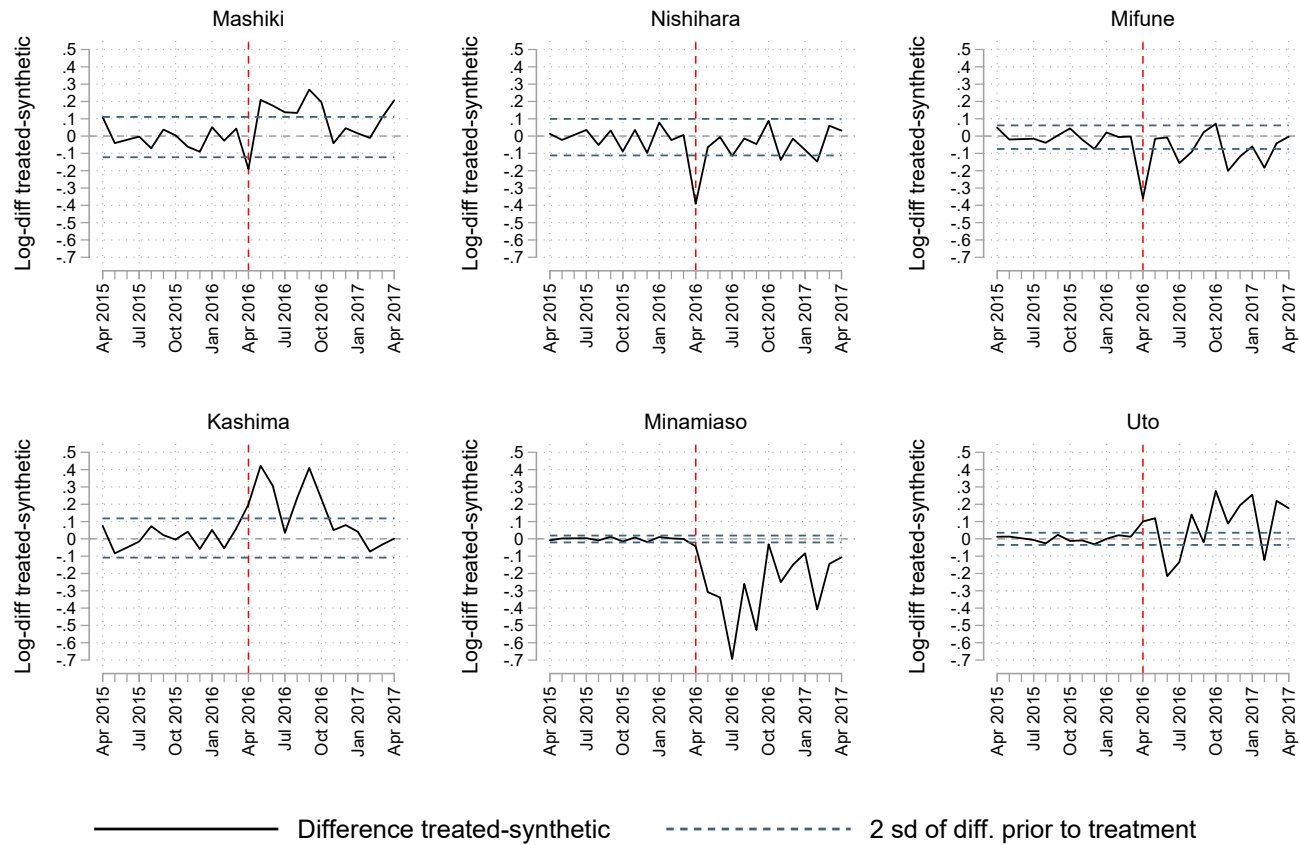
<sup>29</sup>Mean difference in  $\ln(\text{SOL})$  between the treated and control group is approximately zero, but the standard deviation on the difference is approximately twice as large for Mashiki, Nishihara, and Kashima versus the remaining three worst-affected municipalities (sd of 0.05 versus 0.02 respectively).

Figure 5.4.2: Night light intensity for the worst-affected municipalities versus synthetic counterfactuals



*Note:* actual and synthetic counterfactual time series for night light intensity for the worst-affected municipalities, ordered by building damage per capita. Since the synthetic counterfactual is constructed as a weighted average of control municipalities, there is no confidence interval for the time series of synthetic night light intensity. The donor pool consists of the municipalities on Kyushu Island, excluding those from the prefectures Kumamoto and Oita, as well as all municipalities that are directly adjacent to a treated municipality. The synthetic control method requires non-missing observations of the dependent variable. Due to the excessively low number of cloud-free nights in June 2015, radiance observations for June 2015 are replaced by an interpolated value between May and July 2015. Note that this is done after aggregating to the municipal level.

Figure 5.4.3: Difference in night light intensity between actual and synthetic counterfactuals for the worst-affected municipalities



*Note:* actual and synthetic counterfactual time series for night light intensity for the worst-affected municipalities, ordered by building damage per capita. Since the synthetic counterfactual is constructed as a weighted average of control municipalities, there is no confidence interval for the time series of synthetic night light intensity. The donor pool consists of the municipalities on Kyushu Island, excluding those from the prefectures Kumamoto and Oita, as well as all municipalities that are directly adjacent to a treated municipality. The synthetic control method requires non-missing observations of the dependent variable. Due to the excessively low number of cloud-free nights in June 2015, radiance observations for June 2015 are replaced by an interpolated value between May and July 2015. Note that this is done after aggregating to the municipal level.

Mashiki was the hardest-hit municipality in terms of building damage, with total destruction of over 3,000 houses, partial destruction of another 3,233, and another 4,325 houses with damage, on a total population of less than 34,000 in 2015. We observe a negative difference between the municipality's light level and its synthetic counterfactual of roughly 20 percentage points, which is unusually large for this municipality. Looking at the months after the earthquake, the synthetic counterfactual instead suggests that the earthquake resulted in a breaking point with higher light intensity directly following April 2016. Indeed average light intensity is roughly 4% higher in the 12 months after the quake, and is even 20% higher than before Kumamoto from April 2017 onwards. In contrast, taxable income declined by roughly 30 percentage points in the fiscal year 2016, while at the same time 4 percent of the municipality's population migrated out, and 14 percent of business establishments closed down. We therefore expected a negative or at least non-positive response of light intensity in the year following the earthquake. Within the bounds of our data collection, the only possible explanation for the increase in light intensity is that reconstruction efforts may be very light-intensive (as has been similarly suggested by Wang et al. (2018)), and are arguably most intense out of all affected municipalities especially in a relative sense. In addition, Mashiki directly borders Kumamoto City – the main economic hub of the region – which may affect recovery positively.<sup>30</sup> Reconstruction started in June 2016 and was planned to take years. However, as will become clear from the other cases, this seemingly plausible explanation is not consistent with other municipalities with a high degree of building damage.

For Nishihara, the observed immediate reduction in night light intensity for April 2016 in the raw data indeed appears to be stronger than what is to be expected on basis of the synthetic counterfactual. Given that over 50% of resident's houses in Nishihara Village were severely damaged, such a reduction in light intensity may be expected. The difference between actual and synthetic counterfactual light intensity is roughly 0.4 log points (49 percentage points) in April 2016. However, light intensity rebounds back to within the normal bounds of its synthetic counterfactual the next month already, even though the loss in taxable income for 2016 was over 40 percent. With additional substantial outmigration and a reduction of the number of business establishments of 13%, it is striking that no longer-run reduction in light intensity is visible. While building damage was less severe compared to that in Mashiki, Nishihara is still the second worst-affected municipality in terms of normalized building damage: over 2,400 buildings were affected of which roughly half were totally or partially destroyed. In light of a population of only 6,800 in 2015, it does not seem plausible that a lack of reconstruction efforts can explain the difference between Nishihara and Mashiki.

A similar observation can be made for Mifune, which experiences a notable deviation of night light intensity from its synthetic counterfactual in April 2016 of 0.36 log points (43 percentage points). Also similarly, light intensity in the month

---

<sup>30</sup>For example, Eichenauer et al. (2020) show that municipalities close to the capital were more likely to receive aid after the 2015 Kathmandu Earthquake in Nepal.

after the earthquake follows that of the synthetic counterfactual rather closely.<sup>31</sup> Yet, over 5,000 buildings were affected of which just under 3,000 were totally or partially destroyed. In light of a population of only 17,000 in 2015, it does not seem plausible that a lack of reconstruction efforts can explain the difference between Mifune and Mashiki either, similar to the observation for Nishihara. However, for Mifune it is important to note that the reduction in taxable income (roughly 10%) and business establishments (5%) was much smaller than that of Mashiki and Nishihara, and income was back at its 2015 level one year later. The similarity between Nishihara and Mifune is then rather striking, given that the former experiences a massive drop in annual income and a rather steep decrease in the number of business establishments, whereas the latter sees reductions of less than half on these variables. Yet their patterns of light intensity in these months appears similar.

Kashima shows a contrasting pattern, with higher light intensity in the year after the earthquake – a pattern that we observed earlier in the raw time series for the municipality as well. While there is a slight decrease in light intensity in the month of the earthquake, the synthetic counterfactual suggests that this decline should have been much larger in the absence of an earthquake. Between May and October 2016, we find even larger positive differences between the actual and counterfactual series. While July 2016 shows a temporary reduction, the pattern is rather similar to that of Mashiki. Similar to Mashiki, Kashima directly borders Kumamoto City and may thus be positively affected in terms of reconstruction efforts. Both findings are surprising however: while building damage was considerably smaller than in Mashiki, over 2,200 buildings were damaged with close to 800 being totally or partially destroyed on a population of approximately 9,000 in 2015. Combined with an income loss of 11%, it is again hard to explain the observed pattern in the night lights.

Minamiaso stands out as the outlier in this study. First, Minamiaso experiences – as the only municipality in our sample – a prolonged and clear depression of night light intensity throughout the year after the earthquake of roughly 25% on average. This pattern can be readily observed in the raw data and the synthetic counterfactual further confirms that the deviation is statistically highly exceptional. We find an immediate reduction of light intensity of roughly 10 percentage points in April 2016, with even larger declines in the months following. Strikingly, the strongest reduction in light intensity takes place in July until August 2016, when light intensity is up to 50 percentage points lower than the synthetic counterfactual. With no apparent other shocks being able to explain this rather large reduction, isolating why Minamiaso specifically experiences such a large decline is challenging. It is important to note that the reduction in taxable income was notably lower than that for e.g. Kashima and Nishihara (18% versus roughly 30% respectively). Yet, from the impact data that we have collected, Minamiaso is an outlier in terms of its enormous decline in business establishments and engaged persons (both around 40%), combined with major and long-lasting infrastructural damage that caused

---

<sup>31</sup>November 2016 appears to be an outlier. To the best of our knowledge, no other natural disaster can explain the deviation in Mifune in this month.

major disruptions to daily life and business activity in the municipality. However, as we have no comparable cases in which either the reduction in business establishments or the damage to road infrastructure can be held constant, identifying which is the crucial factor is not possible within our analysis. Nevertheless, Minamiaso can be said to be the real outlier in this analysis, essentially displaying the expected pattern in night light intensity as the only case in our comparative study.

Finally, for Uto the pre-trend is almost identical, but deviates immediately in the month of the earthquake in which the synthetic counterfactual suggests that light intensity should have been well over 20 percentage points lower than the observed intensity in April 2016. This is easily beyond the two standard deviations of its pre-treatment difference. This is therefore similar to the observation for Kashima; in both cases our results suggest an increase of light intensity over the synthetic counterfactual of roughly 20 percentage points. In both cases, this goes against our predictions, given the high degree of building damage. However, the observed post-earthquake pattern for Uto is more erratic and harder to interpret. We observe substantial under- and overshoots in the subsequent year, even though our case information suggests that Uto was not heavily affected beyond its sizeable building damage. Uto experienced significant damage but recorded only 116 collapsed houses on a population of 37,000. Building damage was thus sizeable but only limited in terms of completely destroyed buildings. In terms of economic impacts, Uto did not experience a reduction in taxable income, and experienced only moderate outmigration and reduction of the number of business establishments. The number of engaged persons in fact grew by 3.4%. Overall, we therefore expected no significant effect of the earthquake on Uto's night lights, but instead observe an erratic pattern of sizeable over- and undershooting of the synthetic counterfactual. Potentially reasons other than the April 2016 earthquake may be able to explain this observed pattern, but within the bounds of the current analysis the pattern remains rather puzzling.

We summarize our findings. For the worst-affected municipalities, we expected a downturn in light intensity at least in the first month(s) after the earthquake, but we observe a downturn in April 2016 in only 4 cases. Moreover, this downturn is followed by a return to pre-earthquake light intensity levels in two cases, and in the case of Mashiki even to a substantially higher light level than pre-earthquake from May until October. Instead, only for Minamiaso do we observe a sustained depression of light intensity. For the two remaining cases, we see an immediate increase in light intensity. In the case of Uto, this is followed by an erratic pattern of over- and undershooting of the synthetic counterfactual, which cannot be explained with the available data collected for this analysis. Finally, Kashima is the only municipality for which we observe an immediate and sustained higher light level than its counterfactual until October 2016. Overall, we can conclude quite clearly that there appears to be no relation with losses in income, which were by far largest in Mashiki and Nishihara (both around 30 percentage points). Instead, neither of these municipalities show a reduction in light intensity beyond the month of the earthquake itself. At the same time, there also appears to be no obvious relation with building damage: over 3,000 houses were completely destroyed in

Mashiki, representing a loss of 1 house for every 10 inhabitants. Yet, no sustained depression of night lights is visible. In fact, as we find no consistent pattern of sustained light reduction for municipalities with a high degree of building damage, our results suggest that the reductions in light intensity may reflect something other than building damage and may perhaps reflect the temporary power outage in the first days after the quake. The outage lasted for some days in the worst-affected municipalities; combined with the low number of cloud-free nights in April 2016, it is possible that average light intensity for the treatment month is reduced by one observation in a night with a power outage. With the current data at hand, we cannot tell for sure. We conclude that Minamiaso is the only municipality for which we observe the expected sustained depression in night light intensity. Based on our data collection, this can either be attributed to the extreme loss of business establishments (40% between 2014 and 2016), or to the collapse of the Aso bridge that cut the connection between Minamiaso and Kumamoto City for multiple years, or a combination of both.

## 5.5 Discussion and conclusion

In this paper, we have studied the local economic impacts of a large earthquake and have analyzed in detail the response of night light intensity to this shock at the municipal level for the April 2016 Kumamoto earthquake in Japan. We collect detailed damage data, as well as municipal economic statistics to describe in detail the impacts of the earthquake on the affected municipalities. We then analyze the average effect of the shock on night light intensity, and subsequently do a comparative case study with the worst-affected municipalities. Summarizing our main findings, we find no clear or unidirectional relation between building damage and a change in night light intensity: compared to unaffected counterfactual municipalities on the island, there appears to be no statistically significant difference in light intensity either in the month of the earthquake or in the months following. Instead, we find heterogeneous effects on night light intensity within the relatively small geographical area of Kumamoto prefecture. These patterns are not in line with our formulated expectations and cannot be explained by either differences in building damage or income losses. Especially the example of the municipality Mashiki shows that while income losses and outmigration may be substantial, we instead see a substantial increase in night light intensity. While the impacts on Minamiaso may be presented as an example where expectations and actual changes in night lights do match, this discrepancy casts serious doubt on the validity of the monthly VIIRS night lights as a proxy for changes in economic activity after a large earthquake, and possibly after natural disaster more generally. This echoes the findings presented in Skoufias et al. (2021), who similarly find essentially no observable effects on night light intensity for several large natural disasters in southeast Asia.

We do find substantial reductions in night light intensity in the month of occurrence for some of the worst-affected municipalities (similar to e.g. Del Valle

et al., 2018), but find no support for any sustained reductions in the subsequent months, other than for Minamiaso. Given the enormous amount of building damage, recovery within one month seems altogether implausible. More generally, the lack of any consistent negative impact of housing damage on night light intensity calls for caution in light of the existing literature. A growing number of studies relates a damage index for wind speeds from hurricanes to reductions in night light intensity and find statistically significant and sensible patterns (Bertinelli and Strobl, 2013; Elliott et al., 2015; Mohan and Strobl, 2017; Ishizawa et al., 2019; Miranda et al., 2020), while specifically for earthquakes we find similar evidence in Nguyen and Noy (2020) and in Fabian et al. (2019). Instead, our finding is more closely aligned with those of Zhao et al. (2018), who report mixed findings on night light intensity. Indeed, they find light intensity to grow in the days after the Central Italy Earthquakes in 2016. However, their study is focused on the first 10 days after the quake only; our study suggests that increase in night light intensity after an earthquake may last considerably longer. While Zhao et al. (2018) suggest that search-and-rescue activities may explain the increase in night light intensity post-earthquake, this cannot explain the prolonged increases in light intensity that we find for Mashiki and Kashima.

Especially for Mashiki and Nishihara, the lack of any negative medium-run impact on light intensity – and even a substantial increase in the case of Mashiki – stands in stark contrast to an income loss of over 30% in 2016, combined with unusually high outmigration and a loss of business establishments that is well over twice as large as the rest of the municipalities in the prefecture. Rather than seeing these substantial negative economic impacts being reflected in depressed light intensity, we find no such signal. We therefore conclude that the monthly night light images show little evidence in support of the use of monthly night light intensity as a proxy for changes in economic activity after the earthquake studied in this paper.

Our study cannot answer all remaining questions, so we discuss limitations here. Even though a thorough data collection was done, some pieces of information proved hard to come by. Ideally we would have had access to detailed search and rescue data, to get a grasp of the magnitude and extent of activities at night immediately after the quake, which arguably require artificial lighting. However, we find no reason to believe why search and rescue activities would be able to offset negative impacts of the degree of building damage and power outages in Kashima, whereas it would not in e.g. Mifune. Second, detailed (re)construction data by municipality would be helpful to answer whether the light intensity increases in Mashiki and Kashima can be explained by disproportionately larger (and faster) reconstruction efforts than in the other worst-affected municipalities. However, no such data were available. Future research may benefit from detailed reconstruction data. Given the data and anecdotal evidence that we collected for this study, however, it is implausible that differences in reconstruction efforts can explain the difference in the observed patterns between Mashiki and Kashima on the one hand (which show an increase in light intensity), and e.g. Nishihara and Mifune on the other (which show no such increase whatsoever).

Sufficient cloud-free data coverage remains an issue in the monthly composites.



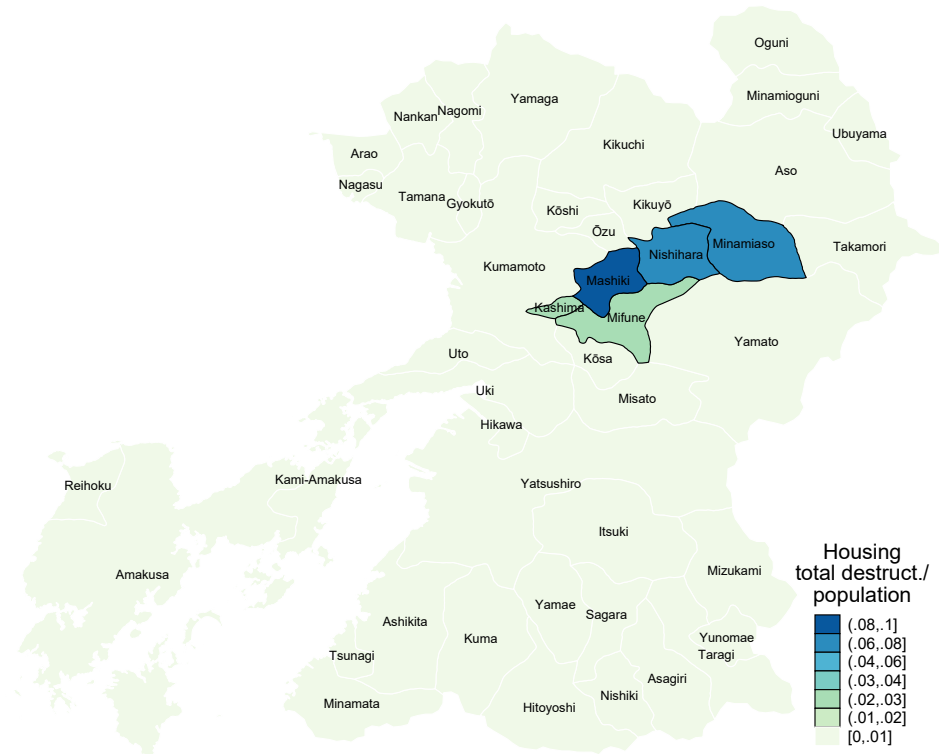
Like Zhao et al. (2018), we again find that a low number of cloud-free nights around the time of treatment may hinder identification of immediate impacts. While we ensured that we have no missing data for the affected municipalities, the unfortunate low number of cloud-free nights throughout entire Kyushu island in April 2016 makes the estimated immediate impacts somewhat less reliable than the point estimates in the subsequent months. Future research may benefit from identifying events with more available nights in the month of impact. Still, for municipalities such as Nishihara and Mashiki, we would not expect an immediate negative effect of housing damage in the month of occurrence to disappear one month later. Indeed, right after the disaster, reconstruction was suggested to take years.

A conceptual note is on the appropriate spatial and temporal resolution to study the effects of interest. In this paper, we have analyzed aggregate effects at the municipality level, so as to have data on economic activity to which to compare the night light data. However, there is also a more conceptual question of the appropriate level of spatial aggregation for which nighttime light emission functions as a suitable proxy for economic activity. Most studies that investigate the local economic effects of natural disasters choose to zoom in to the pixel resolution of the night light data and work with modeled physical intensity data in the form of wind speeds or seismic energy instead (e.g. Elliott et al., 2015; Kocornik-Mina et al., 2020; Skoufias et al., 2021), usually with little motivation for why that resolution is appropriate for studying the effect of interest. Only Nguyen and Noy (2020) speak of some necessary spatial aggregation in order for night light intensity to proxy local economic activity, but clearly there is no established practice yet in the literature. The fact that we find no convincing relation between changes in night light and either direct damages or indirect economic downturns on the level of municipalities then casts doubt on the value of zooming in further. We feel there is great need in this literature for sorting out the issue of appropriate spatial aggregation.

Finally, we note that the study focuses only on a region in Japan, a country that is famous for its earthquake preparedness. While building damage was substantial, this may explain the relatively low number of fatalities, compared to e.g. the Gorkha earthquake in Nepal, 2015. The analysis could be repeated for other cases to assess whether similar patterns hold in other countries, most notably in lower-income countries. Moreover, the findings in this study do not align with studies especially on hurricane impacts, for which reductions in night light are reported more frequently for various regions around the world. Future research can use the methodology applied in this paper to study in detail hurricane events or other disaster types with the monthly VIIRS data to find an answer to this discrepancy. As a closing note, and based on the presented evidence in this study, we conclude that caution is warranted when using the VIIRS monthly nighttime lights as a proxy for economic activity in the aftermath of natural disasters.

## 5.A Damages and economic data

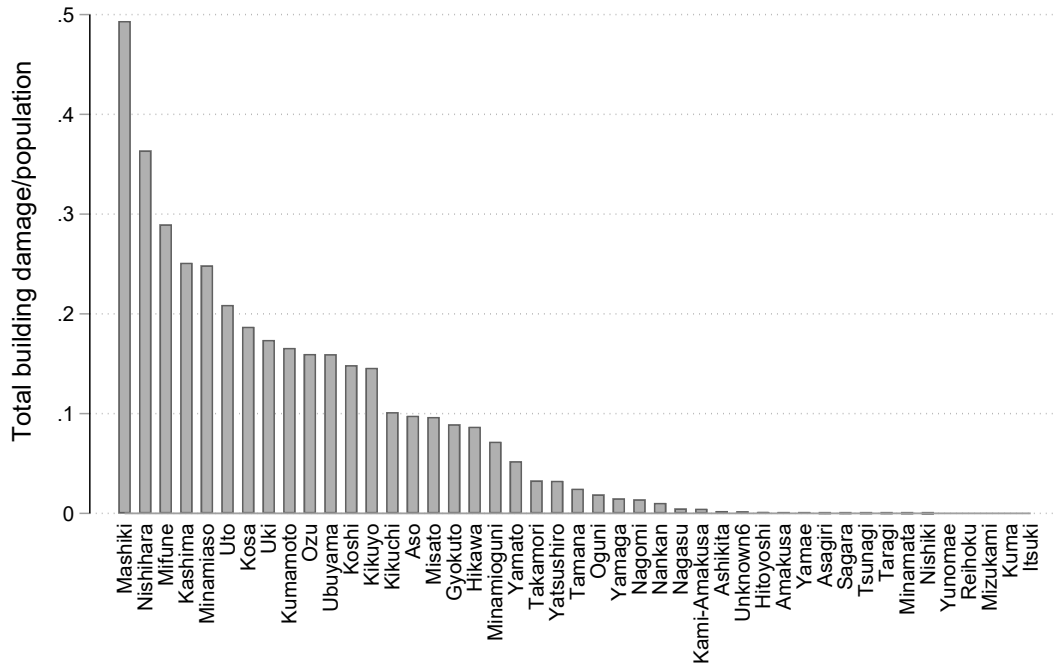
Figure 5.A.1: Normalized damages across municipalities in Kumamoto prefecture (total destruction of housing only)



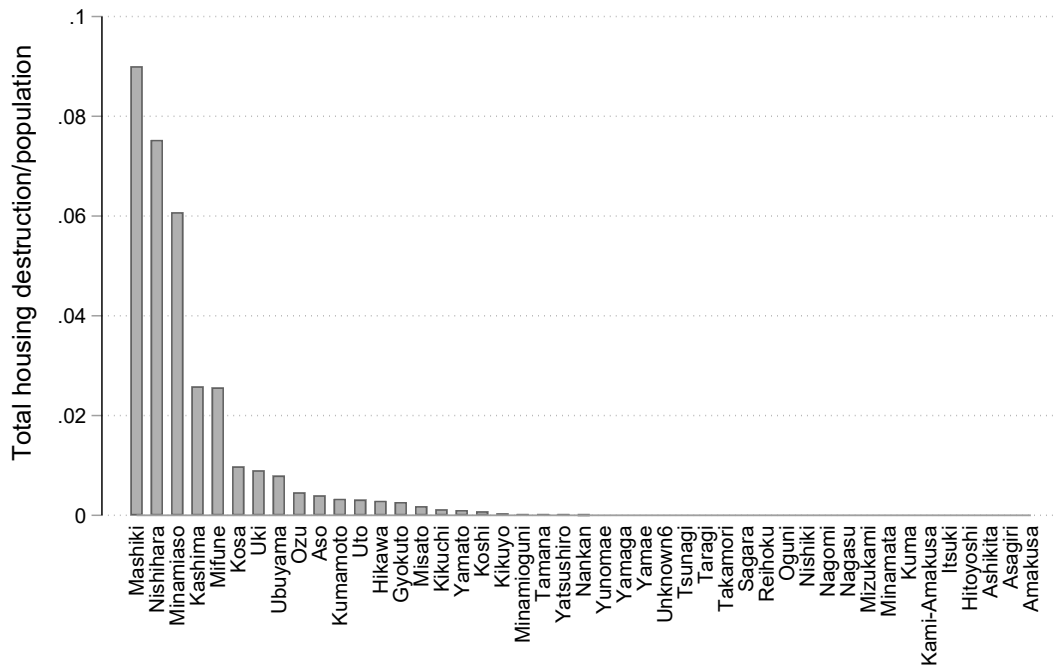
*Note:* Damage index limited to number of totally destroyed houses only. Source: based on own calculations using data from the 303rd Report on the Damage Situation of the 2016 Kumamoto Earthquake (Kumamoto Prefectural Crisis and Disaster Prevention Division, 2020).

Figure 5.A.2: Building damage in Kumamoto prefecture

(a) Total building damage normalized by population



(b) Total number of completely destroyed houses, normalized by population



Note: Based on own calculations using data from the 303rd Report on the Damage Situation of the 2016 Kumamoto Earthquake (Kumamoto Prefectural Crisis and Disaster Prevention Division, 2020). Total number of damaged buildings in (a) calculated by the sum of totally destructed housing, partially damaged housing, damaged public buildings, and damage of other non-residential buildings.

Table 5.A.1: Impact Numbers by Municipality

Municipality	Population in 2015 (2)	Total (1)	deaths	Seriously injured (1)	in-Minorly injured (1)	in-Minorly injured (1)	Total destruction of housing (1)	Partial destruction of housing (1)	Some damage of housing (1)	Public building damage (1)	Other non-resident building damage (1)
Mashiki	33,611	45		135		31	3,026	3,233	4,325	104	5,902
Nishihara	6,802	9		18		38	512	865	1,097		
Mifune	17,327	10		11		10	444	2,397	2,178		
Kashima	9,054	5		11			234	565	1,462	14	
Minamiaso	11,503	31		31		120	699	989	1,171		
Uto	37,026	12		24		18	116	1,747	4,386	7	1,482
Kosa	10,717	3		17		2	105	986	914		
Uki	59,756	13		48		95	539	2,396	5,673	28	1,755
Kumamoto	740,822	87		771		943	2,456	15,219	105,086	60	83
Ozu	33,452	4		26		10	154	1,372	3,820	1	
Ubuyama	1,510					2	12	46	180		3
Koshi	58,370	7		27		56	47	862	7,052	8	704
Kikuyo	40,984	6		14		15	15	672	5,133	1	160
Kikuchi	48,167	4		20		56	58	684	2,898		1,250
Aso	27,018	20		9		98	108	861	1,609	67	
Misato	10,333	2		5		1	19	284	694	2	
Gyokuto	5,265					1	14	146	291	12	7
Hikawa	11,994	3				3	35	194	813		
Minamioguni	4,048			1		2	1	38	175		77
Yamato	15,149	3					16	247	529		
Takamori	6,325	3		3				1	115		92
Yatsushiro	127,427	4		12		17	20	431	2,662	154	898
Tamana	66,782					18	11	95	1,550		
Oguni	7,187			2		4		1	135		
Yamaga	52,264					4		19	563		202
Nagomi	10,191					3		33	100	9	1
Nankan	9,786					1	1	2	82		18
Nagasu	15,889								69		8
Kami-Amakusa	27,006	1						1	127		
Ashikita	17,661							4	39		
Arao	53,407								88		23
Hitoyoshi	33,880					2			51		
Amakusa	82,739								79		1
Yamae	3,422								2		1
Asagiri	15,523								6		1
Sagara	4,468								2		
Tsunagi	4,673								2		
Taragi	9,791								2		
Minamata	25,411								5		2
Nishiki	10,766								3		
Yunomae	3,985								1		
Mizukami	2,232										
Itsuki	1,055										
Kuma	3,698										
Reihoku	7,739										
<b>Total</b>	<b>1,786,215</b>	<b>272</b>		<b>1,185</b>		<b>1,55</b>	<b>8,642</b>	<b>34,393</b>	<b>155,166</b>	<b>467</b>	<b>12,67</b>

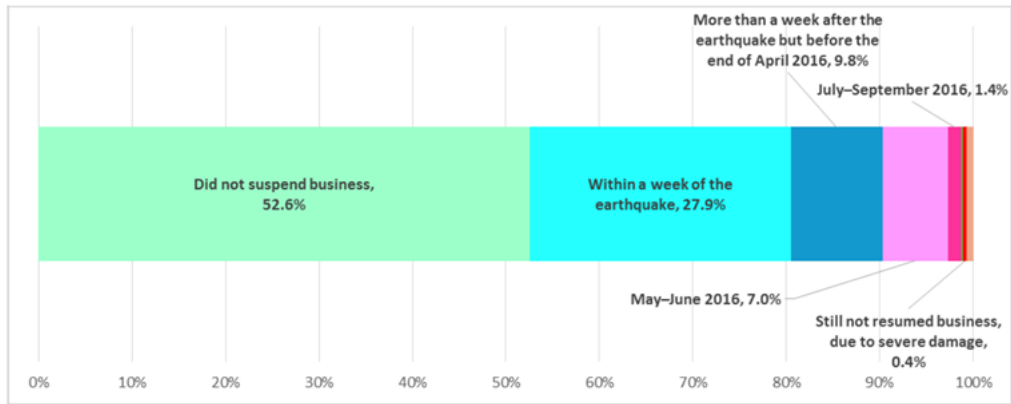
Note: Sources: (1) Kumamoto Prefectural Crisis and Disaster Prevention Division, 2020. (2) Statistical Data for Municipalities (Official Statistics Japan, 2020).

Table 5.A.2: Impact Numbers by Prefecture

Prefecture	Deaths (1)	Severely injured (1)	Slightly injured (1)	Fires (1)	Public build- ing dam- age (1)	Non- residential building damage (1)	Housing totally de- stroyed (1)	Housing half de- stroyed (1)	Housing some dam- age (1)	Number of in- quiries (2)	Number of set- tled cases (2)	Number of claim pay- ments (2)	Total amount of claims paid (in thousands of yen) (2)
Fukuoka		1	17			1		1	230	20,844	19,968	14,527	8,921,428
Saga		4	9			2			1	3,287	3,078	2,288	1,776,605
Nagasaki									1	866	828	559	328,728
Kumamoto	49	360	1,258	16	248	660	7,994	17,818	70,609	223,220	221,057	205,161	340,555,598
Oita		4	23			8	2	45	2,171	15,751	15,466	12,604	9,873,420
Miyazaki		3	5					2	20	501	478	329	275,550
Kagoshima										412	402	220	107,910
Yamaguchi									3				
Other Prefec- tures										680	645	379	279,384
<b>Total</b>	<b>49</b>	<b>372</b>	<b>1,312</b>	<b>16</b>	<b>248</b>	<b>671</b>	<b>7,996</b>	<b>17,866</b>	<b>93,035</b>	<b>265,561</b>	<b>261,922</b>	<b>236,067</b>	<b>362,118,623</b>

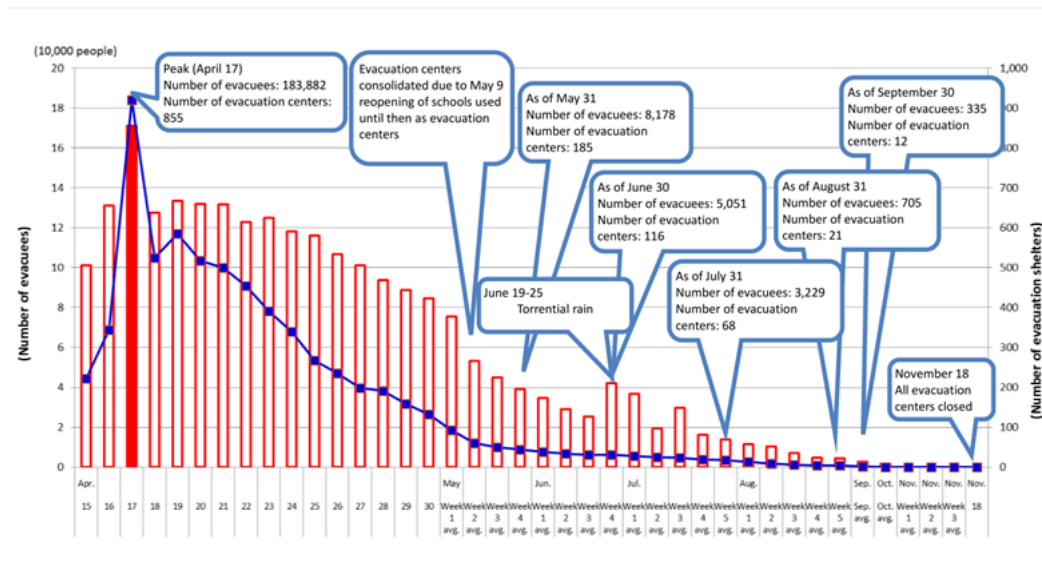
*Note:* These numbers are per 24.5.2016, so there is a difference with the final numbers for Kumamoto Prefecture. Reported deaths for Kumamoto prefecture are direct fatalities only. Sources: (1) 2016 Kumamoto Earthquake Survey Report (Preliminary) (Asian Disaster Reduction Center, 2016). (2) General Insurance Association Japan, 2016. Key figures related to insurance claims due to the 2016 Kumamoto Earthquake as of September 30, 2016. Available at: [https://www.sonpo.or.jp/en/news/2016/1610\\_01.html](https://www.sonpo.or.jp/en/news/2016/1610_01.html) (accessed 25.5.2020).

Figure 5.A.3: Timing of the resumption of business



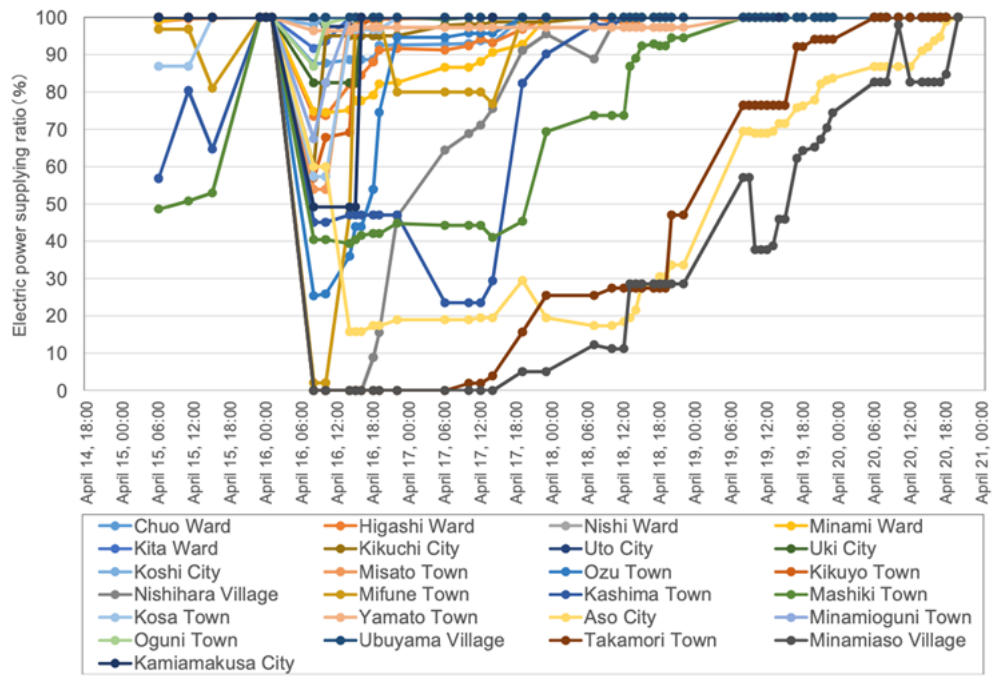
*Note:* The data describes “companies in the affected area” that suffered “some kind of damage” (n =1002) Produced by the Cabinet Office Japan from Survey of the Impact of the Kumamoto Earthquake on Business Continuity for Companies (Cabinet Office Japan, 2017).

Figure 5.A.4: Changes in the number of evacuees and evacuation centers



*Note:* Produced by Cabinet Office Japan (2017) from various materials, including the Report on the Review of Responses to the Kumamoto Earthquake Over a Period of Approximately Three Months (March 2017, Kumamoto Prefecture).

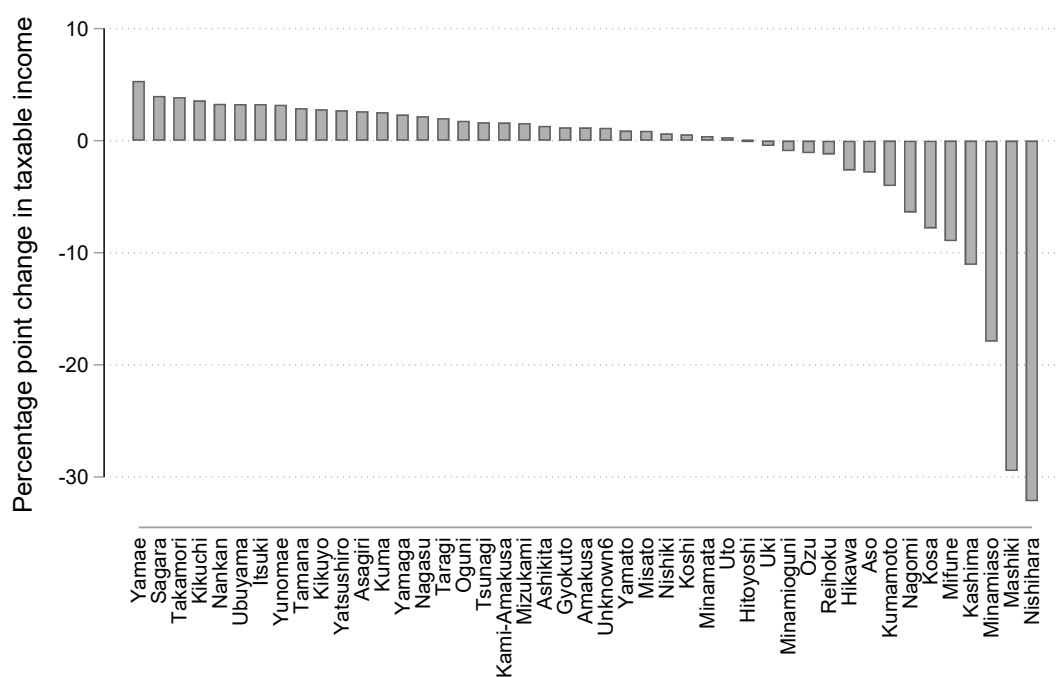
Figure 5.A.5: Electric power supplying ratios in Kumamoto prefecture



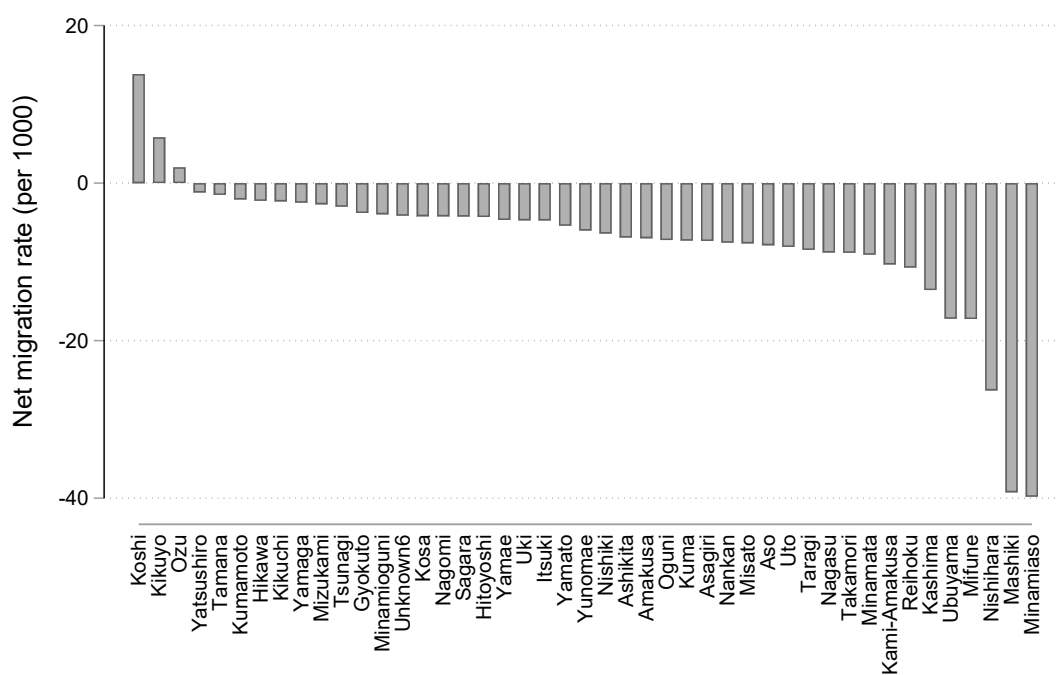
*Note:* reprinted from “Comparison of Functional Damage and Restoration Processes of Utility Lifelines in the 2016 Kumamoto Earthquake, Japan with two Great Earthquake Disasters in 1995 and 2011”, by Nojima and Maruyama (2016).

Figure 5.A.6: Change in income and migration

(a) Change taxable income (2016)



(b) Net migration (2016)

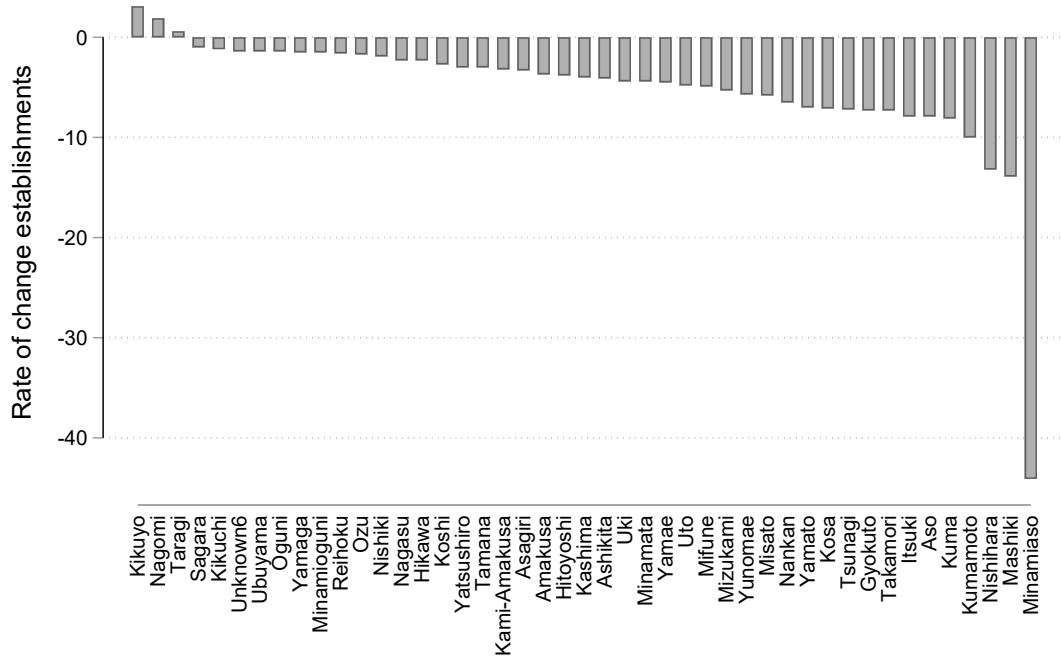


*Note:* own calculations. Data from the System of Social and Demographic Statistics, Municipality Data (Official Statistics Japan, 2020). (a) Difference between 2016 and 2015. Note that taxable income is accounted with one year delay (see technical description of Official Statistics Japan, 2020). (b) Migration data for 2016.

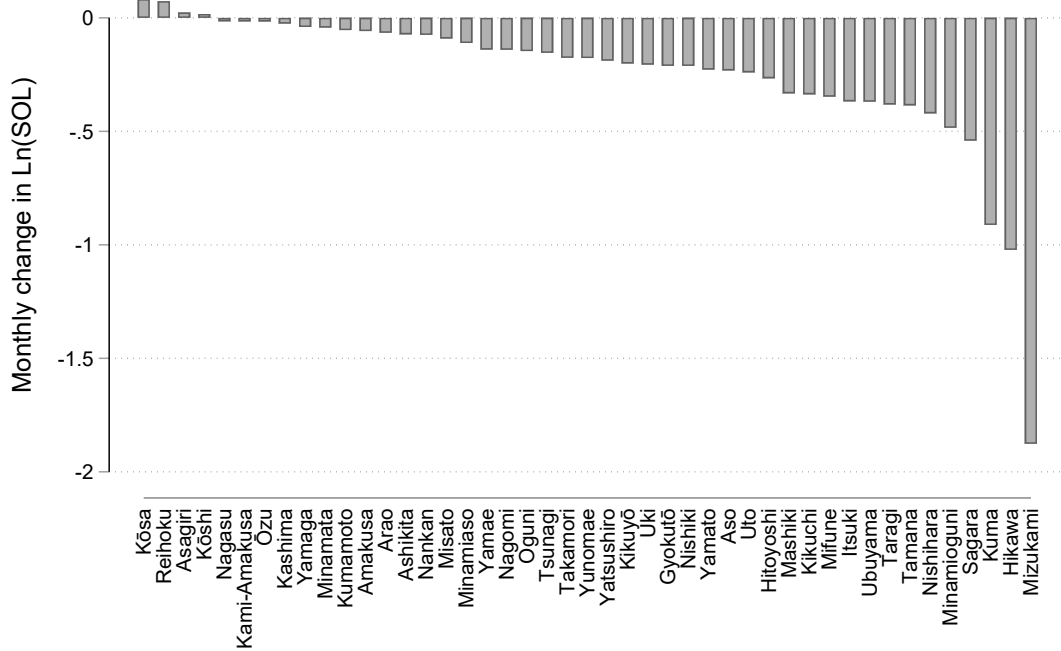


Figure 5.A.7: Change in business activity

(a) Change in number of business establishments (2016 w.r.t. 2014)



(b) Change in number of people engaged in business establishments (2016 w.r.t. 2014)



Note: own calculations. Difference between 2016 and 2014. Data from the Economic Census for Business Activity (Official Statistics Japan, 2020).

## 5.B Summary statistics and robustness tests

Figure 5.B.1: Number of cloud-free nights in April 2016, Kumamoto prefecture

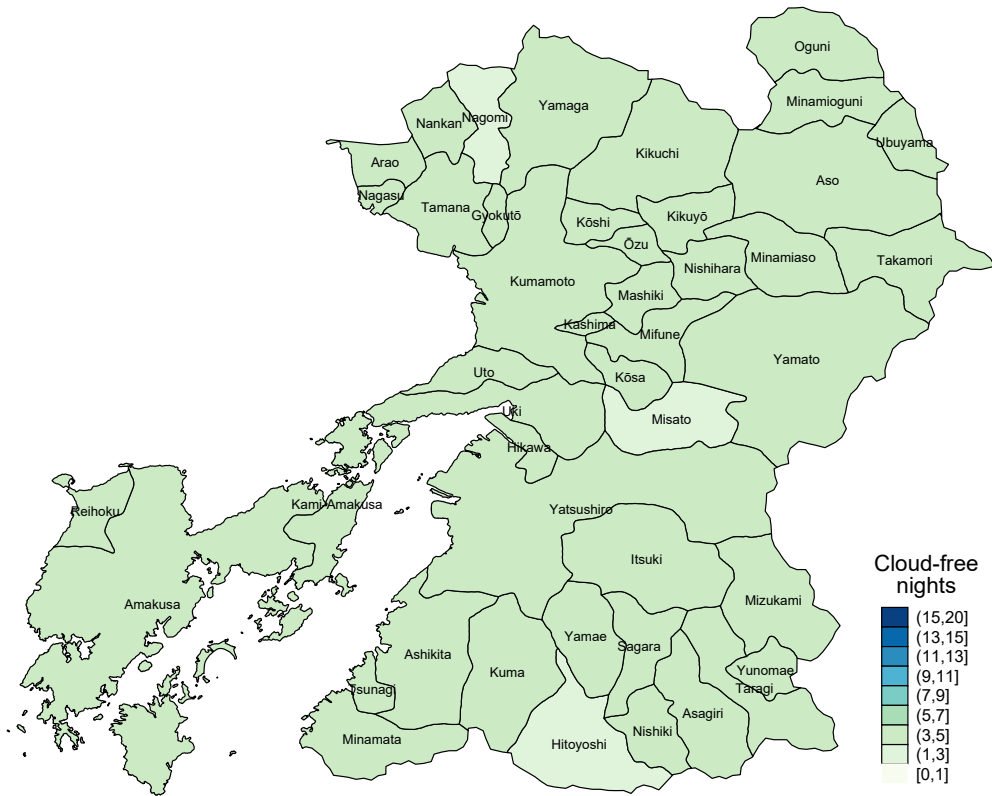


Figure 5.B.2: Number of cloud-free nights by month, 2013-2018 for the 6 prefectures on Kyushu Island

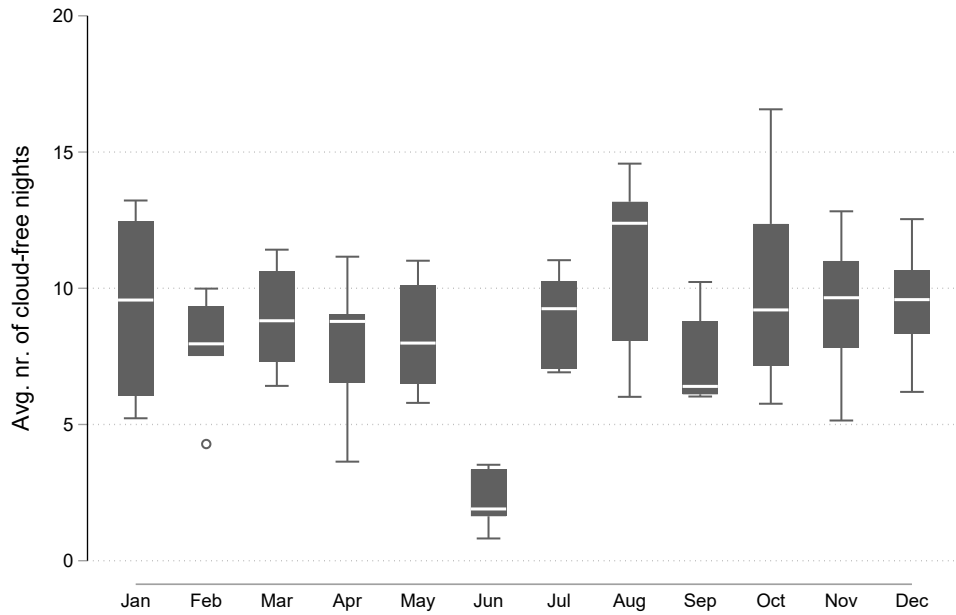


Figure 5.B.3: Number of cloud-free nights in June 2015, Kumamoto prefecture

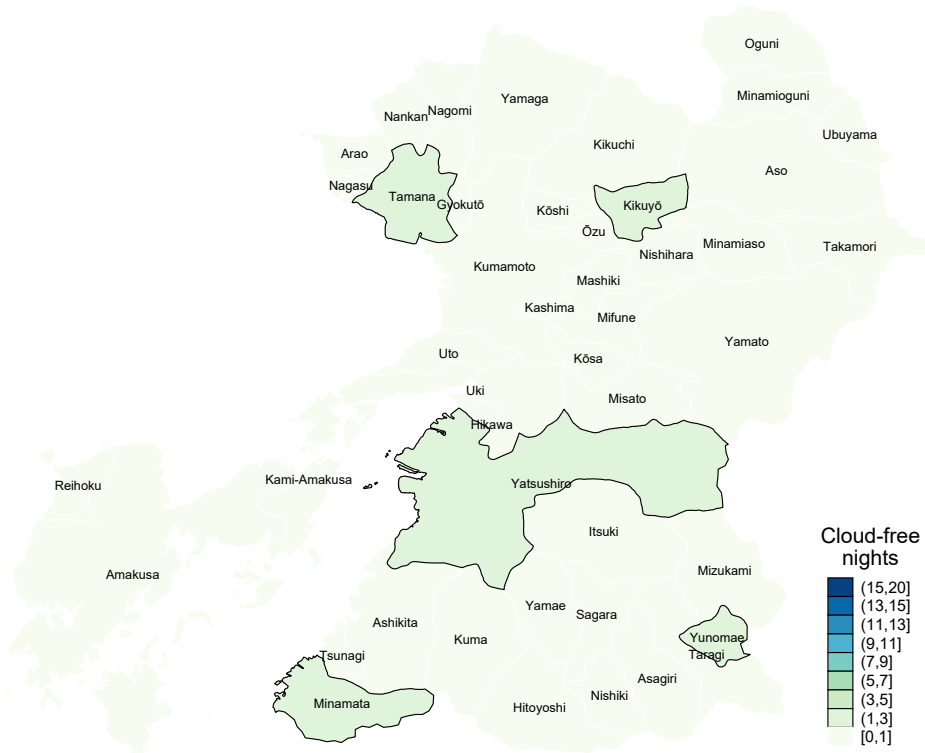


Table 5.B.1: Other natural extremes

Date	Event	Total deaths	Number of injured	Number of affected	Number of homeless	Total affected	Insured losses ('000\$)	Total damage ('000\$)	Affected prefectures
16 Apr 2016	Kumamoto earthquake	49	1684	272,763	23,985	298,432	5,000,000	20,000,000	Kumamoto, Fukuoka, Saga, Oita, Miyazaki
12-13 Jul 2012	Riverine floods	7	30	48135		48135		1,400,000	Kumamoto, Oita
7-10 Jul 2014	Typhoon Neoguri	7	66	600		666		156,000	Ehime, Kagawa, Kooti, Tokushima, Hukuoka, Kagosima, Kumamoto, Miyazaki, Nagasaki, Ooita, Saga, Hukusima, Nagano, Hokkaidoo
20-23 Jun 2016	Torrential rain	7		6,000		6,000			Kumamoto
6-7 Jul 2017	Tropical storm Nanmadol	37	34	2,610	300	2944	140,000	700,000	Fukuoka (Asakura), Oita prefectures (Kyushu Isl.), Shimane, Kumamoto, Hiroshima, Nagasaki, Miyazaki, Kagoshima
17-19 Sep 2017	Typhoon Talim	2	56	21,600		21,656	330,000	500,000	Oita, Kagawa, Okayama, Ehime, Kochi, Kyoto, Miyazaki, Hyogo

*Note:* List of other natural extremes affecting Kyushu Island in the study period 2012-2018. Based on EM-DAT records for Japan, last accessed June 2021 (CRED, 2021).

### 5.B.1 Seasonality in the VIIRS time series

A potential solution for the substantial temporal variability in the monthly VIIRS data is to account for seasonality, a feature in the data described by Levin (2017). Gao et al. (2020) and Zhao et al. (2020) propose to correct for this seasonality by first taking the seasonality component out of the raw data. To do so, we follow Gao et al. (2020) and Zhao et al. (2020) and assume that the time series for the night lights can be decomposed into three elements: a trend, a seasonal component, and a remainder component. We take out any systematic seasonal variation by regressing the logarithm of the total sum of light by municipality on municipality-specific month dummies, year dummies, and a constant. These capture in the most flexible way municipality-specific deterministic seasonal patterns. Specifically, we estimate for each municipality:

$$\ln(\text{light}_{imt}) = \alpha_i + \gamma_t + \delta_m + \epsilon_{imt} \quad (5.B.1)$$

in which  $\ln(\text{light}_{imt})$  is the natural logarithm of the sum of light intensity for municipality  $i$  in month  $m$  of year  $t$ ,  $\gamma_t$  is a set of year dummies that account for a flexible time trend by municipality, while  $\delta_m$  represents the month dummies, and  $\alpha_i$  is the municipality-specific constant – i.e. its mean sum of light in the data period. We estimate this regression using data for 2013–2018 for each of the six worst-affected municipalities.<sup>32</sup> We then use the estimated coefficients for the month dummies to take the seasonal component out of each municipality’s time series, in order to look at the trend plus remainder component of each time series respectively in Figure 5.B.4. Ideally, this would result in lower month-to-month variability. However, the standard deviation on monthly change in night light intensity is virtually unchanged, as is reflected by rather similar patterns between the raw and deseasonalized series in Figure 5.B.4.<sup>33</sup> Moreover, for most of the municipalities, the coefficients for the month dummies are highly insignificant, indicating that a deterministic seasonal pattern is rejected. Neither allowing for a stochastic rather than deterministic seasonal pattern, or pooling the regression to include only common month and year dummies changes this conclusion.<sup>34</sup> A similarly weak seasonal component is

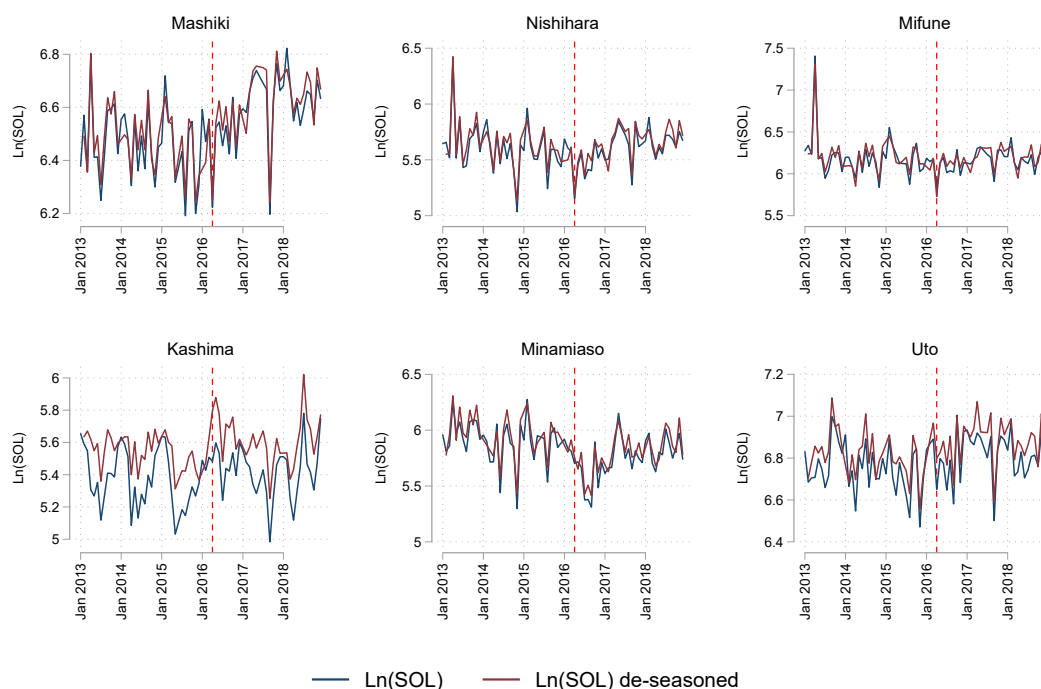
<sup>32</sup>To assess whether the night light series prior to the Kumamoto earthquake are unaffected by previous disasters, we check the EM-DAT records on natural disasters in Japan, and specifically for Kyushu Island in the years prior to the 2016 earthquake (see Table 5.B.1). Kumamoto and Oita prefectures were affected by riverine floods in July 2012. The floods affected almost 50,000 people and caused damages amounting to 1.4 billion US\$ (CRED, 2021). While we did not study this case in detail, a sharp drop in night light intensity is visible across all prefectures in Kyushu Island for July 2012. We therefore drop the year 2012 from the analysis.

<sup>33</sup>The exception is Kashima, for which a deterministic seasonal pattern yields highly significant estimates for all but two month dummies (December and February, with January as the base period). Here, we do see a dramatic reduction of temporal variability, and now see a potential positive impact of the earthquake on night light intensity. The difference is striking and not easily explained, as Kashima is geographically close to its neighboring worst-affected municipalities and therefore has no obvious differences in seasonality of its light emission. Note, however, that Kashima has a notably higher mean light intensity than the other five municipalities (3.28 compared to 1.13 nW/cm<sup>2</sup>/sr respectively).

<sup>34</sup>Employing common variation over time within the broader prefecture of Kumamoto, we

reported by Zhao et al. (2020) for their case study on the effects of hurricanes Irma and Rita on light emission in Puerto Rico. We conclude that trying to model the seasonality in the time series of night lights is challenging, which in turn makes inference on the impact of the Kumamoto quake on night light intensity difficult. We therefore turn to an alternative approach that relies on similarity in temporal variation between municipalities over time. This allows us to use cross-sectional differences over time in a difference-in-differences framework, without having to model the temporal variability explicitly. The approach is discussed in detail in section 5.3.3.

Figure 5.B.4: Total sum of light (in natural logarithm) by municipality for the worst-affected cases



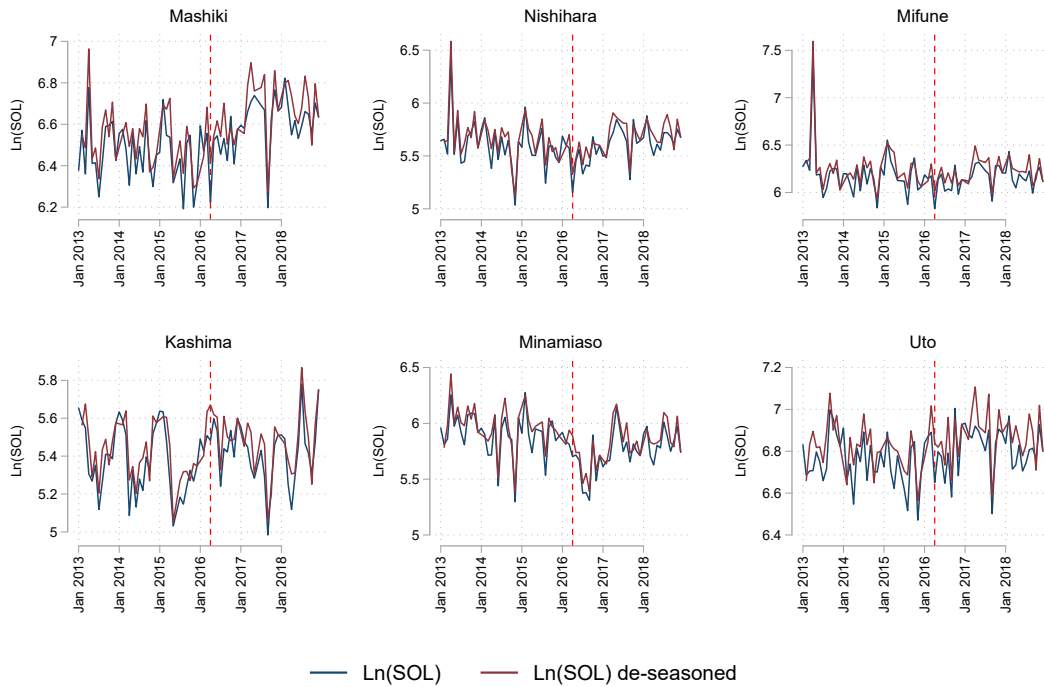
*Note:* SOL = sum of light. The vertical red line indicates April 2016; i.e. the month of the earthquake. The deseasonalized series are adjusted using unique coefficient estimates for month and year dummies by municipality.

---

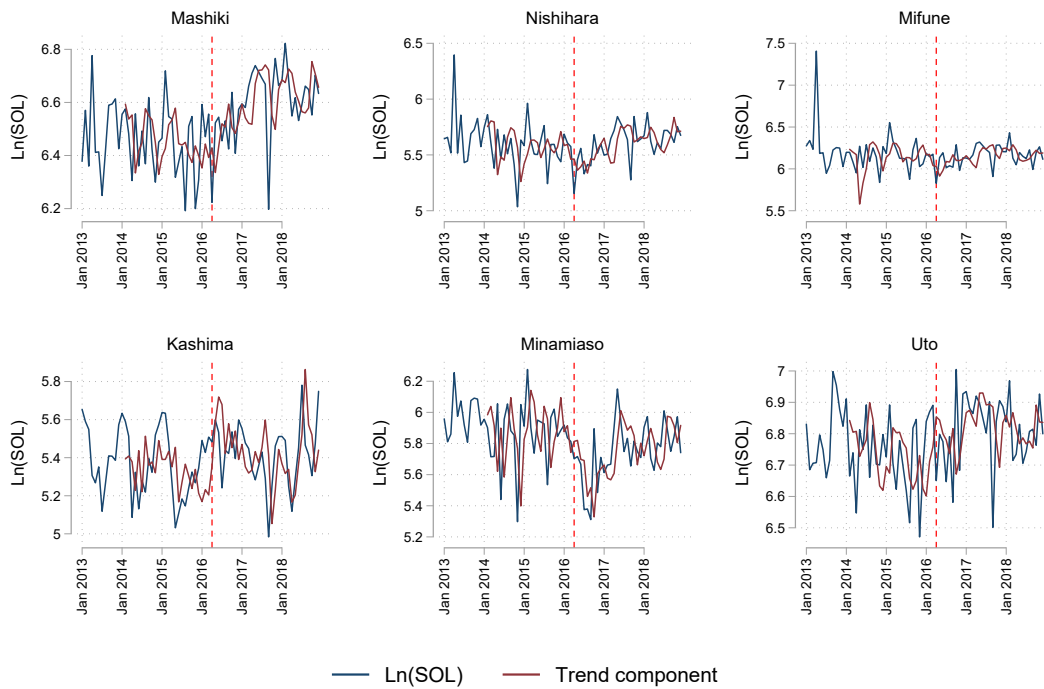
estimate equation 5.B.1 in a pooled regression for all municipalities in the prefecture. Results are highly comparable and reported in Appendix Figure 5.B.5a. An alternative approach is to include stochastic seasonality in the individual series. Including a random walk with drift and a seasonal period of 12 months (following Zhao et al., 2020) smooths the trends somewhat, but results remain qualitatively similar. Results are reported in Appendix Figure 5.B.5b.

Figure 5.B.5: Deseasonalized time series by municipality

(a) Deseasonalized time series by municipality for the worst-affected cases



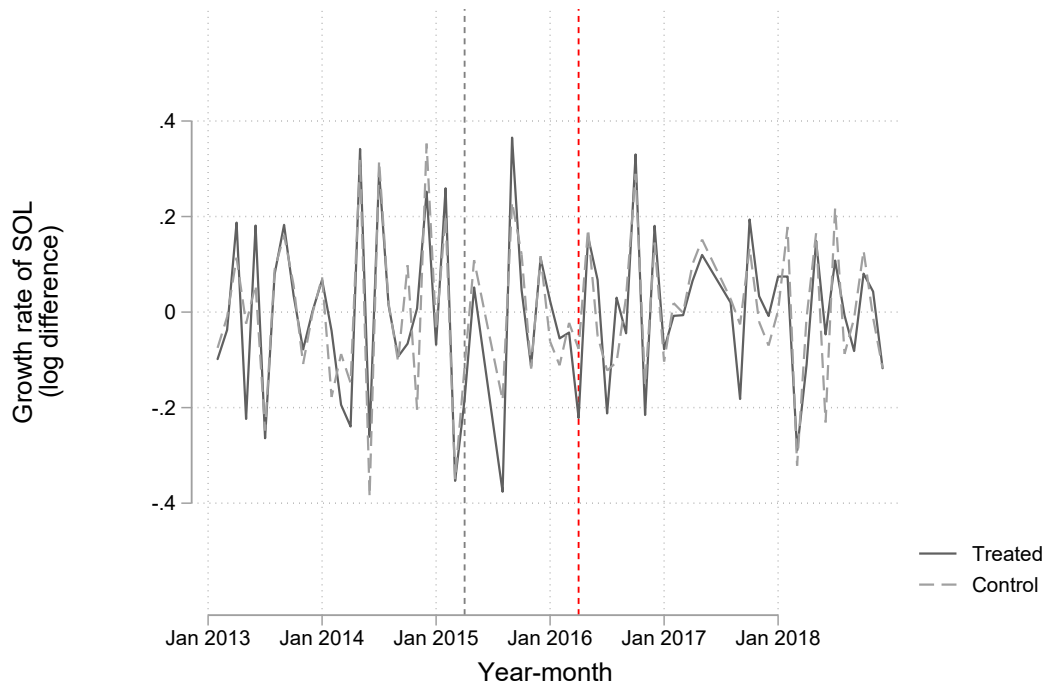
(b) Deseasonalized trends by municipality with stochastic seasonality



*Note:* (a) Residuals for the pooled regression of equation 5.B.1, using all municipalities in Kumamoto prefecture. The vertical red line indicates April 2016; i.e. the month of the earthquake. (b) Computed with unobserved components model with a random walk with drift and a seasonal period of 12 months. Note that the pattern hardly changes compared to a deterministic seasonal pattern reported in Figure 5.B.4, and is notably worse for Kashima.

### 5.B.2 Difference-in-differences robustness

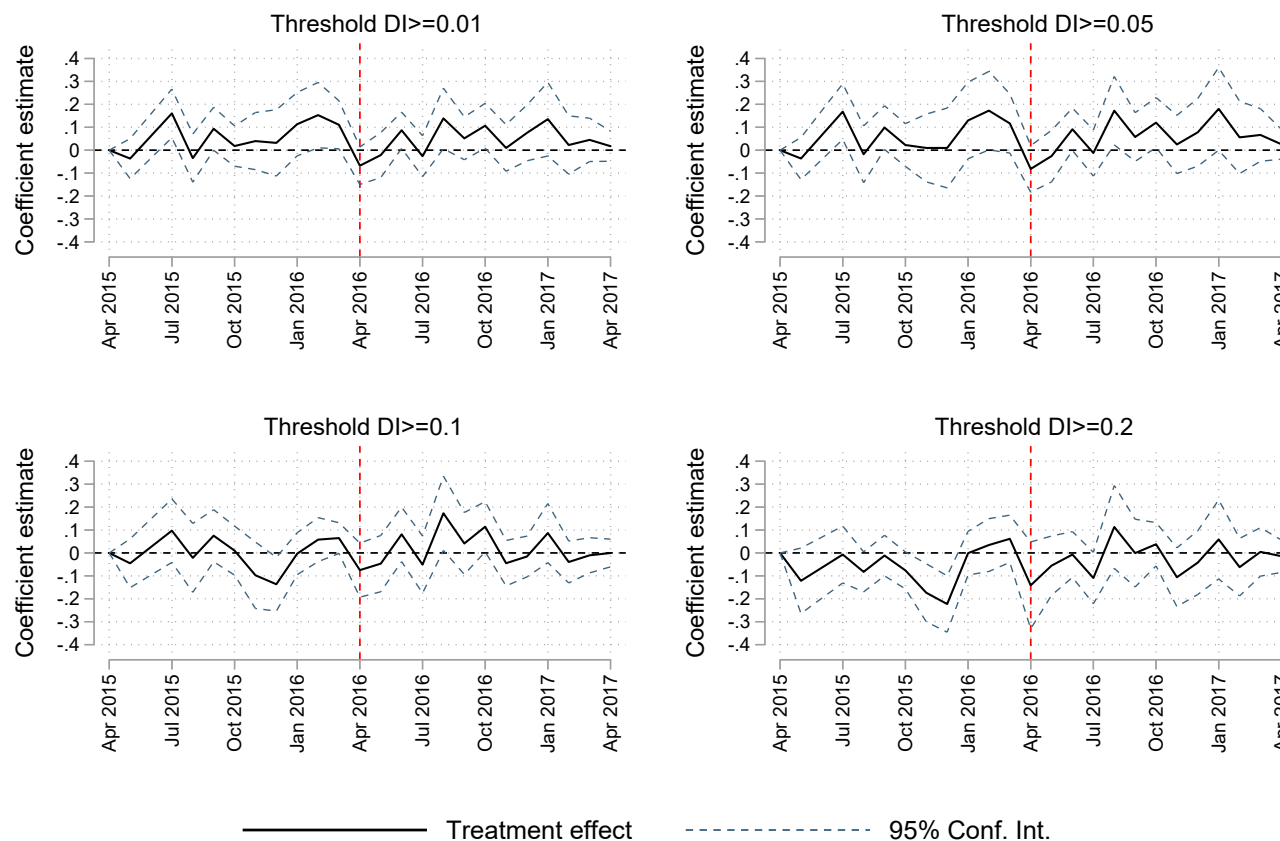
Figure 5.B.6: Log difference of light intensity for treated vs. control group



*Note:* Treatment group consists of the 27 municipalities with normalized building damage of 0.01 and higher. The control group consists of all 175 other municipalities in the dataset. The vertical red line indicates the month of treatment (April 2016). The vertical gray line indicates April 2015, i.e. exactly one year before the earthquake.



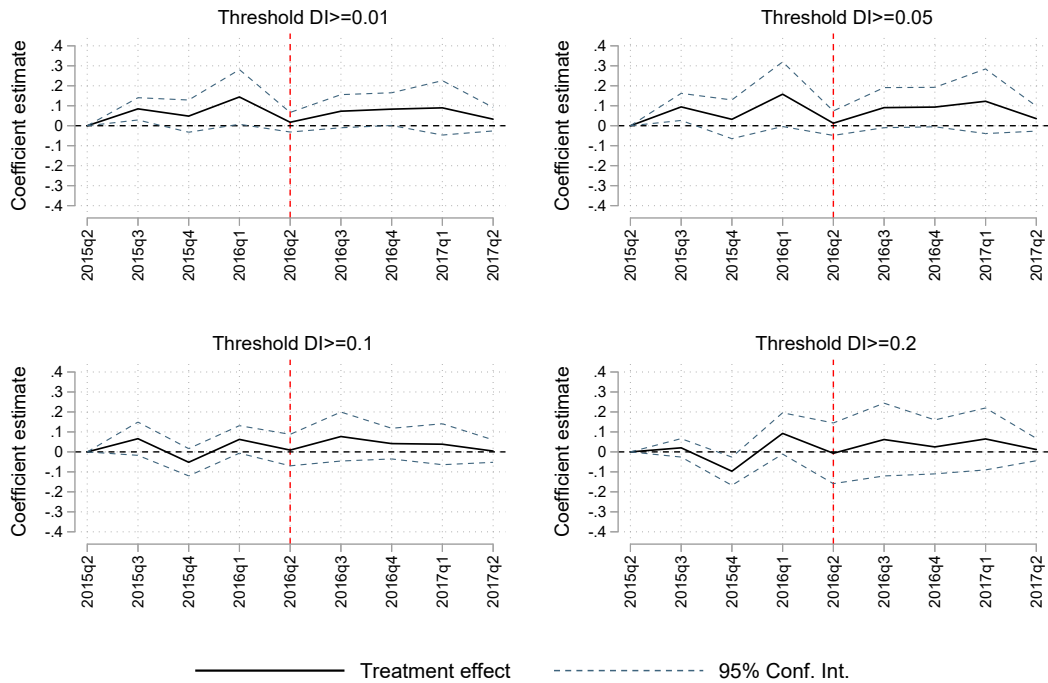
Figure 5.B.7: Baseline treatment effect, alternative control group



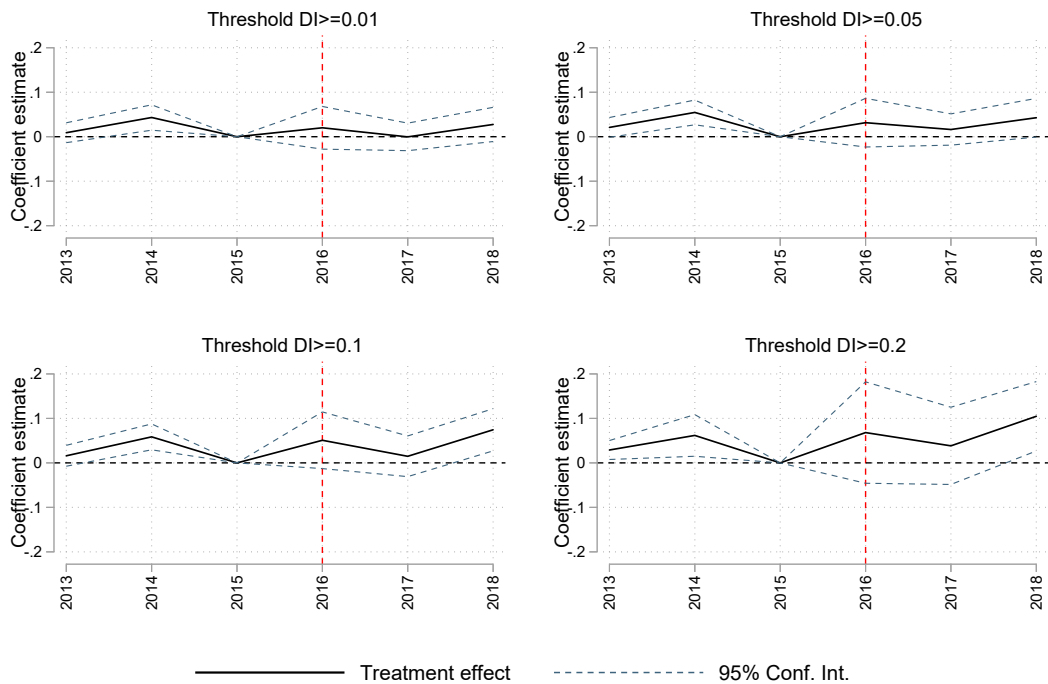
*Note:* Coefficient estimates of equation (1) reported in black, with a 95% confidence interval in blue. The vertical red line indicates the month of treatment (April 2016). The control group consists of all unaffected municipalities on Kyushu Island, excluding Oita prefecture, all unaffected control municipalities from Kumamoto prefecture, and any unaffected municipalities that directly neighbor a treated municipality (for a total of 149 control municipalities). The treatment group varies by threshold of the damage index (DI): 27 for a threshold of 0.01, 20 for a threshold of 0.05, 14 for a threshold of 0.1, and 6 for the threshold of 0.2. In the latter case, only Mashiki, Nishihara, Mifune, Kashima, Minamiaso, and Uto are considered treated. Affected municipalities below the treatment threshold are excluded from the estimation sample.

Figure 5.B.8: Treatment effect, aggregating to months and years

(a) Treatment effect estimates for quarters rather than months



(b) Treatment effect estimates for years rather than months



*Note:* Coefficient estimates of equation (1) reported in black, with a 95% confidence interval in blue. The vertical red line indicates the year of treatment (2016, starting in April). The control group consists of all unaffected municipalities on Kyushu Island, excluding Oita prefecture and all unaffected control municipalities from Kumamoto prefecture and any unaffected municipalities that directly neighbor a treated municipality (for a total of 149 control municipalities). Damage thresholds as in Figure 5.B.7.

## 5.C Case selection

Case selection was based on the subset of earthquakes between 2012 and 2016 with severe consequences, limited by the years for which VIIRS night light data is available. We rely on the EM-DAT database (CRED, 2021) for disaster impact figures in terms of fatalities and damages, for which the 5 worst cases in this period on both are listed below in Table 5.C.1.

Table 5.C.1: Worst earthquakes between 2012-2016

	<b>Top fatalities</b>	<b>Top damages</b>
1	Nepal, April 2015	Japan Kumamoto, Apr 2016
2	Yunnan, Aug 2014	Northern Italy, May 2012
3	Ecuador, Apr 2016	Sichuan, Apr 2013
4	Pakistan, Sep 2013	Nepal, Apr 2015
5	Iran, Aug 2012	Yunnan, Aug 2014

The following selection criteria apply for selection of the case study: (1) The affected area must be sufficiently populated and lit; (2) The earthquake must be associated with high damages; (3) Non-missing night light data in the months prior to, during, and after the earthquake; (4) Access to detailed damage reports (in a language that is accessible to the researcher); (5) Administrative statistics (municipal/district GDP, income, population statistics) to benchmark medium-run developments.

Especially the last requirement turned out to be the limiting factor (for Nepal, Ecuador, Pakistan, and Iran), while other earthquakes were (also) unfit candidates due to missing night light data – either because of stray light or because of clouds obscuring the area.

The earthquake with the highest social toll was the April 2015 Gorkha earthquake in Nepal. Its close to 9000 casualties are over ten-fold of the next disaster on this list – the August 2014 Yunnan earthquake in China. However, as has become clear from our impact framework, the effects that we expect to see reflected in night light intensity are concentrated on property losses rather than losses of human lives. In terms of property losses, the Nepal earthquake ranks 4th in this period. While this makes the disaster an excellent case, a number of issues make it less suitable for our presented framework: first, and most crucially, one of the months directly following the earthquake (June) contains only missing night light data, hence making the assessment of medium-run impacts difficult. Second, we do not have access to administrative statistics for Nepalese municipalities – most notably GDP statistics. In fact, Eichenauer et al. (2020) use VIIRS night lights to proxy for municipal GDP in the Nepalese case in their study on aid distortions after the Gorkha earthquake. Lacking this information and missing the month June, we discard the Gorkha earthquake as a potential case.

The Kumamoto quake is by far the most damaging in the period, with EM-DAT reporting over 20 billion US\$ of damages (and other estimates ranging up to 30

billion US\$). The epicenter was located near major urban centers and both the level and spatial extent of shaking was enormous – stretching almost the entire island of Kyushu. The quake affected close to 300,000 people, claimed over 200 lives, and resulted in the collapse of 8,000 houses and tens of thousands more damaged. The only earthquakes that come close to this level of destruction in this period are the May 2012 earthquake in Northern Italy (estimated 16 billion US\$ damages), and the two earthquakes in China (April 2013 in Sichuan, and August 2014 in Yunnan). While the Italian case of 2012 is interesting from numerous angles, and with administrative data being available, the VIIRS night light sensors are blinded by stray light in the summer months, resulting in zero valid observations of night light for the months May to July.<sup>35</sup> As a result, this case is also unfit. The Chinese cases are associated with lower damages (about a third to a fourth of Kumamoto), which makes us prefer the Japanese case over them. Concluding, the April 2016 Kumamoto earthquake is selected as the case for this study.

---

<sup>35</sup>The same is true for the August 2016 earthquake in Central Italy. Again, the months May-July prior to the earthquake are missing, making an impact assessment from night lights impossible.

# CHAPTER 6

---

## Conclusion

---

In this dissertation I have investigated the local economic impacts of natural disasters by making use of remotely sensed night light data. I have analyzed natural extremes ranging from hurricanes to earthquakes, and the interaction between these hazards and the local economies that they affect. This interaction increasingly materializes into natural disasters, that claim lives and cause destruction. Natural disasters are localized phenomena, and often occur in places where no adequate socioeconomic data is available to study their impacts. In order to bridge this gap, in this dissertation I study how nighttime light can help us understand how natural disasters affect local economic activity around the world. In chapters 2 and 5 I have studied this approach from a methodological perspective using case studies, while in chapters 3 and 4 I study the effects of extreme weather and earthquakes on local economic activity around the world. I start with summarizing my main contributions and findings by chapter. I then reflect on the overall answer to the central research question and discuss limitations and avenues for future research.

### 6.1 Main contributions

This work finds itself in the nexus between a growing interest among economists in the economic impacts of natural disasters, and rapid developments of the use of remote sensing techniques by disaster and remote sensing scholars to study natural hazards and their impacts. With an increasing attention for the effects of climate change on the world economy, economists turned their attention to studying GDP and GDP growth effects of natural disasters in the 2000s and 2010s, with the aim to understand how such risks may affect growth patterns and development. Whereas the answer to the effect of natural disasters on GDP growth would intuitively be ‘naturally negative’ (Felbermayr and Gröschl, 2014), this literature instead presented a range of findings ranging from negative (Raddatz, 2009; Hochrainer, 2009; Noy,

2009), to insignificant (Cavallo et al., 2013), and even positive (Skidmore and Toya, 2002; Loayza et al., 2012; Fomby et al., 2013). There are several explanations for this ambiguity, of which I have studied a number in this dissertation.

First, studying the impacts of natural disasters by statistically linking monetary damages to GDP leads to an endogeneity bias, as monetary damages tend to be positively correlated to income per capita, while coverage of events is similarly more complete in high income countries (Felbermayr and Gröschl, 2014). In order to estimate a causal effect of natural disasters on income growth, researchers should therefore instead make use of exogenous measures of disaster intensity. I do so by collecting and compiling a range of physical intensity measures of natural extremes for meteorological, climatological, and seismic hazards.

Second, there is a mismatch between the spatial scale of a natural hazard and the outcome measures of GDP or GDP growth at the national level. Natural hazards, and even more so the disasters they cause, are typically localized events. Local adverse impacts may therefore be small compared to national aggregate income. It is also of crucial importance whether an extreme natural event occurs in a densely populated area or in deserted hinterland. Moreover, local adverse impacts may affect neighboring areas through economic linkages and in turn may cause spatial spillovers to nearby locations. Depending on relations of complementarity or substitution, these linkages may aggravate or instead dampen the aggregate impacts of the disaster respectively. There is therefore a clear need to go beyond the national aggregate statistics. In this dissertation I have done so by shifting the focus to the local level.

As discussed at length in this dissertation, local socioeconomic data is difficult to obtain even in many highly developed countries, whereas even national level GDP statistics are of low quality in many developing countries. In search of alternative ways to gauge economic growth in and compare development across countries in the world, the seminal papers by Henderson et al. (2012) and Chen and Nordhaus (2011) showed convincingly that night lights can be used as a proxy for GDP or GDP growth, being especially valuable in countries with low-quality national income statistics. The two studies started a quickly growing strand of literature using (changes in) nighttime light as a proxy for (changes in) GDP or income. Numerous studies then started using the evidently valuable spatial component of the data, which allows researchers to be much more flexible in their spatial scope than previously allowed by administrative socioeconomic statistics (for excellent overviews, see Donaldson and Storeygard, 2016; Gibson et al., 2020, 2021). In the literature on natural disasters, studies by Bertinelli and Strobl (2013) and Elliott et al. (2015) similarly started using the night light data and showed how hurricanes result in darkened skies in the worst-affected areas in the Caribbean and China respectively. Independently from the economic literature, similar observations were made in the natural hazard and remote sensing literature (Kohiyama et al., 2004; Gillespie et al., 2014).

These developments combined then naturally led to the central question of this dissertation: *"How can nighttime light help us understand how natural disasters affect local economic activity around the world?"* The very premature state of the

literature was the starting point of this dissertation, in which I have explored this avenue of research. As has become clear from my chapters, this has deepened my insights in this matter and has produced valuable contributions to this literature. I have shown how night lights can be a powerful proxy for capturing the economic downturn caused by Hurricane Katrina in Louisiana, U.S., and how night lights illuminate spatial patterns of spatial spillovers in a global study on the impact of weather anomalies on local night light growth. However, it has also led to findings that call for some caution in using the night light data, especially the newer suite of monthly VIIRS data.

My main contributions are threefold: first, to the best of my knowledge, this dissertation is the first comprehensive work in which night lights are not only used to study local economic impacts of natural disasters, but in which the validity of this proxy is put to the test. I show that the effects of natural disasters are reflected in annual DMSP luminosity that can be observed from space. As has become clear from my final chapter, the use of the newer VIIRS data may be contested and questions have to be answered concerning the value of over-time comparison of light intensity as a proxy for changes in economic activity. I elaborate on these issues in the discussions of Chapters 4 and 5 below.

Second, the work in my dissertation is among the first that attempts to find a globally consistent way to study the local economic effects of natural disasters. Developing such an approach is an important step forward for research that aims to systematically compare resilience and recovery between areas with different levels of development and institutions. Together with my co-authors on Chapter 3, I provide a dataset to the literature that allows studying these questions. Moreover, we are the first to systematically study in a global dataset how such shocks may propagate to neighboring areas through spatial spillovers, and show convincing evidence for their existence.

Third, in this dissertation I bring together insights from the literature in economics, natural hazards and disasters, and remote sensing. For the most part, the economic literature on disaster impacts and growth communicates with these literatures only in a very limited way. I believe that combining insights from these literatures enriches literatures in two ways: remote sensing studies that focus on income or GDP distributions around the world can benefit from sound economic theory, while empirical economic studies on local development and growth benefit greatly from the in-depth knowledge on the pros and cons of night light and other remote sensing data from remote sensing specialists. In this dissertation I have attempted to bring insights and knowledge together. Chapter 2 is an example of bringing together insights on disaster impacts from disaster scholars on local impacts (Logan, 2006; Xiao and Nilawar, 2013) with insights from economists on labor market outcomes (Groen and Polivka, 2008; Deryugina et al., 2018; Groen et al., 2020) and insights from remote sensing scientists on the appropriate use and quality of night light data (Elvidge et al., 2013; Gillespie et al., 2014). While Chapter 3 is positioned more strictly within the economics literature, Chapters 4 and 5 explicitly engage with discussions in the natural hazard and remote sensing

literatures on the use of the newer VIIRS night light data, which is still hardly used in the economics literature even as this dissertation is coming to a close. Similar to the approach of Chapter 2, I bridge a gap between these literatures by studying in detail the economic impacts of the 2016 Kumamoto earthquake in Japan and by applying economic statistical tools to address measurement issues in the VIIRS data. In doing so, I have aimed at making these literatures communicate and to engage in discussions that will hopefully further this field of research. Fortunately economists are becoming increasingly aware of the value of other fields in this inherently multidisciplinary field (see e.g. Gibson et al., 2021; Gibson, 2021). I now summarize my contributions by chapter.

### 6.1.1 Chapter 2: Night lights and Hurricane Katrina

In Chapter 2 I investigate how and to what extent changes in night lights reflect the immediate impact and subsequent population and economic recovery of affected areas in the context of a large natural disaster. The central question of this chapter is: *"How do changes in night light intensity relate to economic activity in the aftermath of a large natural disaster?"* As the use of night lights to proxy local economic activity in the context of natural disasters has become increasingly popular in both the economic and remote sensing literature (e.g. Gillespie et al., 2014; Elliott et al., 2015; Zhao et al., 2018; Kocornik-Mina et al., 2020), I assess in this chapter how we should interpret changes in night lights as a result of the disaster. I study how the economies of the affected counties in Louisiana and Mississippi are affected by the hurricane, and subsequently analyze to what extent these patterns are reflected in their respective night lights. The case study of Hurricane Katrina is particularly suited for this purpose, as both detailed night light data and sub-national economic and population statistics are available for the areas impacted by Katrina. Furthermore, numerous studies have analyzed the social and economic consequences of Katrina (Logan, 2006; Groen and Polivka, 2008; Vigdor, 2008; Deryugina et al., 2018; Groen et al., 2020). This allows me to place our results in the broader body of evidence on the impacts of this event.

In light of the broader objectives of the dissertation, the analysis produces promising findings. First, I find that the pattern of housing and infrastructural damage along the coastline is reflected very well in the night lights. The hardest-hit counties show the largest declines in night light intensity, and light intensity recovers to pre-disaster levels in the subsequent years. However, recovery of night light intensity towards pre-Katrina levels is much faster than recovery of population, employment and income in the hardest-hit counties. Moreover, the results show that change in light intensity is mostly reflective of changes in resident population and the total number of employed people within the affected area, and is less so but positively related to aggregate income and real GDP. As I study a dense urban area in a high-income country, the saturation threshold of the satellite's sensor likely plays a significant role. Being unable to detect changes above the saturation threshold of the satellite's sensor, our estimated changes are therefore likely an underestimate of the true changes in light intensity in the affected areas (see e.g.



Elvidge et al., 2009b, 2014; Bluhm and Krause, 2018). This is accentuated by the fact that the correlation between night light intensity and the considered economic indicators is much stronger after Hurricane Katrina struck than before.

The positive and – in the case of population and employment – strong correlations with economic activity show that changes in night light intensity can be used successfully to capture local effects on economic activity of a large natural disaster, such as Hurricane Katrina. I therefore conclude that changes in night light intensity prove a valuable proxy for changes in local economic activity following a natural disaster, despite its various shortcomings discussed in the chapter. Analyses of disaster impacts using night light data are ideally complemented with detailed analysis of economic data which provide additional more in-depth insights into disaster impacts. Nevertheless, in areas where such economic data is unavailable, the results of this chapter suggest that night light data can be used to approximate the impacts of natural disasters on regional economies, at least in the case of sudden-onset events like floods and storms.

### 6.1.2 Chapter 3: A global perspective on local weather anomalies

The work in my first chapter is neither the first nor the only such effort in the literature. Multiple studies, some published shortly prior to or at the start of my PhD research (such as Bertinelli and Strobl, 2013; Elliott et al., 2015; Mohan and Strobl, 2017) and others in the years following (e.g. Nguyen and Noy, 2020; Kocornik-Mina et al., 2020), use the advantages of the light data discussed in the first chapter to analyze local impacts of natural disasters, predominantly for storms (hurricanes) and floods. Like my first chapter in this dissertation, these studies break ground for this approach and suggest that studying the effects of and resilience to natural extremes systematically around the world is possible with the night light data.

In Chapter 3, I therefore explore this approach by taking a global perspective, and make a number of contributions to this literature. First, I present novel findings with which I contribute to the economic development literature, that studies disaster impacts and their differential effects around the world (Noy, 2009; Loayza et al., 2012; Cavallo et al., 2013; Felbermayr and Gröschl, 2014; Heger and Neumayer, 2019; Kocornik-Mina et al., 2020). Second, I do so at a much more appropriate spatial scale; namely in geographically more confined areas that are directly affected by a natural hazard. The central subquestion here is: *"How do weather extremes affect local economic activity around the world?"* Together with my co-authors from CESifo in Munich, I take the first steps in doing so by studying a global grid of uniform grid cells, for which we map the universe of weather anomalies throughout the 1990s and 2000s. This allows us to study systematically how weather extremes affect economic activity around the world, which ultimately enables researchers to study how differing levels of development and institutional quality moderate the potential effects of natural disasters (related among many more to Anbarci

et al., 2005; Raschky, 2008; Barone and Mocetti, 2014; Berlemann and Wenzel, 2018). While there is literature that asks these questions at the national level, we argue that this is the wrong scope for investigation as the direct economic impact takes place locally rather than nationally, and impacts crucially depend on local exposure and vulnerability. Moreover, substitution effects between regions within a country may offset effects in the directly affected region. We therefore disentangle possibly opposing effects of local (adverse) shocks and economic spillover effects to neighboring areas through mechanisms of complementarity and substitution. In doing so we aim to answer the second subquestion of this chapter: *"Can we observe indirect effects of local weather extremes on local economic activity in neighboring areas?"*

Together with my co-authors, I present a new data set, the gridded GAME-LIGHTS database, which allows us to analyze the economic impacts of weather anomalies at the grid-cell level. Being limited by the best available resolution of global climate data, we divided the globe in grids with a resolution of  $0.5^\circ \times 0.5^\circ$  (approximately  $55 \times 55$  km at the equator). We compiled this data set by matching data on weather-related events to data on nighttime light emissions as a proxy for local economic activity. The resulting data set contains a balanced panel of over 24,000 grid-cells covering the land area of 197 countries from 1992 to 2013. Using spatial econometric panel techniques, we analyze this data and provide new evidence on the local impact of various types of weather events on the growth of nighttime light emissions, as well as spatial spillover effects from affected cells to neighboring cells.

Our results show that storms, cold spells, and precipitation anomalies all tend to reduce local light growth and have positive contemporaneous or lagged spatial spillover effects within an 80-km radius, corresponding to the 8 directly adjacent grid cells of an affected cell on the equator. These effects are economically significant. In contrast, the link between local light emission and droughts is weakly positive, with negative spillovers on neighboring cells. That result is mostly driven by urban cells, where droughts cause light emissions to rise, while spillovers from rural to urban cells are negative. Finally, our results show that low- and medium-income countries tend to respond more to weather anomalies than high-income countries.

Our results then point to a number of practical implications. Similar to findings in the literature on disaster impacts at the national level (e.g. Kahn, 2005; Strömberg, 2007; Felbermayr and Gröschl, 2014; Berlemann and Wenzel, 2018), we find that low- and middle-income countries suffer larger consequences than high-income countries. The global fight against climate change is thus in the interest of low income countries especially. Given that high-income countries have been a major driver of climate change, effort sharing only seems fair from an equity point of view. However, from a more regional perspective we estimate that the economic impacts of weather anomalies tend to be quite localized, and can be split up in predominantly negative local effects, and positive spillover effects in neighboring cells. We thus find evidence for economic substitution effects across space which can help cushion the negative impacts in an affected cell, suggesting that insurance schemes can be efficient in pooling risks even within regions of countries.

Finally, a major contribution of this paper is to break ground for future research by providing a global data set for analysing the impact of exogenous natural extremes to local economies and the spatial distribution of economic activity.<sup>1</sup> As I have indicated, model predictions on the (local) impacts of natural disasters on economic activity are still ambiguous and imprecise (Botzen et al., 2019). Our results and presented data can guide future theory development in this area while our data allow for more rigorous empirical testing. Next steps include investigating what mechanism dominates in causing spatial spillovers at the local level or how various economic factors, households, or firms react to the weather anomalies studied here. As indicated, the dimension of income and development levels warrants special attention in this respect.

### 6.1.3 Chapter 4: Zooming in on local impacts of earthquakes

The second half of this dissertation investigates questions similar to the ones in the first two chapters, but explores the use of a new suite of night light data - the Suomi-NPP Visible Infrared Imaging Radiometer Suite (VIIRS) - that provides monthly images of considerably higher quality than the widely used annual DMSP data. The remote sensing literature forcefully argues that this newer suite of data is the future of tracking remote sensed light from space (Elvidge et al., 2013, 2017; Levin et al., 2020), but the economic literature has hardly picked up on it even at the time of writing the concluding chapter of this dissertation (Gibson et al., 2020, 2021). The VIIRS data have no saturation issues and contain on-board calibration that allows direct comparison of images over time. Moreover, the higher temporal resolution allows distinguishing the impact phase from the recovery phase and thus disentangles two important distinct phases of the disaster cycle (see e.g. van Bavel et al., 2020). This makes this suite of data especially useful for studying sudden-onset events and their immediate aftermath, of which earthquakes are a prime example. While impact assessments of earthquakes are abundant, a way to systematically track economic recovery from natural disasters in the short to medium run has been difficult due to lack of administrative socioeconomic data at both an adequate temporal and geographical resolution. In Chapters 4 and 5, I have therefore explored the potential benefits of this data with special attention for its higher temporal resolution.

In Chapter 4, I explore the new VIIRS night light data that for the first time allows proxying changes in local economic activity at monthly intervals at high spatial resolution (see also Mohan and Strobl, 2017; Nguyen and Noy, 2020). I aim to answer the following research question: *"How do earthquakes affect local economic activity around the world?"* Similar to the work on the GAME-LIGHTS database, I collect, clean, and compile light intensity and global intensity maps of earthquake intensity for each month in the period 2012-2016. The result is a global

---

<sup>1</sup>The dataset is published with the publication of the paper in World Development (see Felbermayr et al., 2022), on which this chapter is based. The dataset is available publicly and freely under DOI-number: 10.7805/Game-Lights-2021. It can be downloaded at: <https://www.ifo.de/en/ebdc-data/ifo-game>.

panel of over 24 million built-up and lit grid cells of roughly 450 by 450 meters at the equator, to which I map both monthly light intensity and ground shaking intensity for the years 2012-2016. I then use a panel fixed effects approach to study the relation between ground shaking and local economic activity, as proxied by night light intensity, similar to the approach of Chapter 3 and the broader literature in this field. This analysis is done at two levels of spatial resolution: the pixel resolution of the monthly night light data (15 arc seconds, roughly 450 by 450 meters) and  $0.5^\circ$  grid cells, to relate findings to the approach of Chapter 3.

In contrast to the findings in Chapters 2 and 3, the results presented in this chapter are not promising. I do not find a measurable effect of heavy shaking from earthquakes on night light intensity. This is true for the immediate impact, as well as the months thereafter. The result is robust to a range of variations of the model specification, and moreover holds at both the  $0.5^\circ$  and pixel resolution. This implies that the results found for climatological and meteorological events at  $0.5^\circ$  are not resonated when looking specifically at earthquakes.

I identify two potential issues which are both of empirical nature. First, month-to-month variability in the VIIRS data is substantial even within small regions. Addressing the issue of temporal variability in the data has been acknowledged as a challenge in the literature (Coefield et al., 2018; Gao et al., 2020; Zhao et al., 2020; Skoufias et al., 2021). Rather than attempting to model this variability explicitly with time fixed effects, a difference-in-differences framework may be better-suited to control for this variation. I apply this alternative identification strategy to a comparative case study on a single earthquake event in Chapter 5. Second, there may be an issue of intention-to-treat in the model, whereas in reality physical shaking may have done little harm. That is, the natural hazard may not have triggered a natural disaster. However, the sample of earthquakes in the current paper is restricted to potentially damaging events, implying that only shaking of levels sufficiently high to generate substantial damages were considered (following the classification by Wald et al., 1999). Lack of actual treatment is therefore unlikely. Still, in order to exclude this possible explanation, a promising approach is to test the relation between materialized damages and economic effects of one or multiple earthquakes in a (comparative) case study, in which changes in light intensity can be related directly to materialized impacts. Again, I do so in a comparative case study on a single earthquake event in Chapter 5. Finally, contributions to the literature that were published after the main work of Chapter 4 was completed raise serious concerns about the extent to which the monthly VIIRS lights reflect impacts from natural disasters. Skoufias et al. (2021) cast doubt on the validity of using the VIIRS night lights in relation to several disasters, for which essentially no effect can be observed in the VIIRS light data even though a sizeable socioeconomic disaster was recorded. Combined with the results from this chapter, these findings call for a serious scrutiny of the application of the monthly VIIRS data for the purpose of studying local economic impacts of natural disasters, which I do in the final chapter of my dissertation.

### 6.1.4 Chapter 5: Shaken, but not stirred

In Chapter 5 I turn to the concerns raised by the results of Chapter 4: can we use the monthly night light data to study the local economic impacts of earthquakes? Studies in the literature so far combine physical intensity data on the natural hazard with changes in night light intensity, similar to my approach in Chapters 3 and 4, but usually for limited geographical areas (Mohan and Strobl, 2017; Miranda et al., 2020; Ishizawa et al., 2019) or single disaster events (Gao et al., 2020; Zhao et al., 2020). Therefore, they lack the information on realized impacts to explain what is happening when such changes are not observed despite the occurrence of a sizeable natural hazard. The lack of a robust statistical relation between earthquakes and light intensity presented in Chapter 4 is a clear example of this, and has recently been resonated by findings of Skoufias et al. (2021). In this chapter I take a step back and essentially do another falsification test on the lights data in the context of a large natural disaster, similar to chapter 2. The central question to this chapter is: *"To what extent can we use monthly VIIRS night lights as a proxy for local economic activity in the aftermath of natural disasters?"* This time I use the monthly VIIRS light data, rather than the yearly DMSP data that I used to study Hurricane Katrina. The question is simple: do we observe expected changes in light intensity in areas where we observe (1) large materialized damages and (2) adverse economic impacts? Answering this requires high-quality disaster impact and socioeconomic data at low levels of spatial aggregation. However, neither impact nor socioeconomic data at subnational levels are readily available, making data collection for this study challenging. This study is the first to bring such information together with night light intensity.

Given the effort to collect the different types of data even for a single area, I focus on a large and damaging event with substantial material damages. Being restricted by the limited time window of the VIIRS data set and the demands on high-quality local socioeconomic data, the choice for the case for this study fell on the April 2016 Kumamoto earthquake on the southern island of Kyushu, Japan. I collect detailed records on building damage and socioeconomic statistics at the municipal level. Using this unique combination of data, I do a comparative case study in which we relate damage records and changes in socioeconomic conditions to changes in monthly night light intensity at the municipal level. Making use of the spatial variation in disaster impacts in a difference-in-differences framework, I then assess to what extent the monthly night lights reflect the impacts from the earthquake.

Summarizing the main findings, I find no clear or unidirectional relation between building damage and a change in night light intensity: compared to unaffected counterfactual municipalities on the island, there appears to be no statistically significant difference in light intensity either in the month of the earthquake or in the months following. Instead, I find heterogeneous effects on night light intensity within the relatively small geographical area of Kumamoto prefecture. These patterns are not in line with our formulated expectations and cannot be explained by either differences in building damage or income losses. For example, I observe substantial

income losses and outmigration in the municipality of Mashiki, where I instead observe a substantial increase in night light intensity that cannot be explained by factors in our analysis. The impacts on the severely affected municipality of Minamiaso may be presented as an example where expectations and actual changes in night lights do match. However, combined with the findings on the other worst-affected municipalities, this discrepancy casts serious doubt on the validity of the monthly VIIRS night lights as a proxy for changes in economic activity for the case we study here. Naturally, this raises the question whether this notion holds more generally, especially for other types of disasters (for example for hurricanes, see Mohan and Strobl, 2017; Zhao et al., 2020) and in other countries (in particularly lower-income countries, as studied in e.g. Zhao et al., 2018, 2020; Skoufias et al., 2021). This debate is still ongoing, but I provide clear evidence in favor of being cautious of using this data for the present purpose.

Ideally we would have had access to detailed search and rescue data, to get a grasp of the magnitude and extent of activities at night immediately after the quake, which arguably require artificial lighting. However, we find no reason to believe that search and rescue activities would be able to offset negative impacts of the degree of building damage and power outages in one municipality, whereas it would not in another. Moreover, detailed (re)construction data by municipality would be helpful to answer whether the light intensity increases that we identified for some municipalities can be explained by disproportionately larger (and faster) reconstruction efforts than in the other worst-affected municipalities, but no such data were available. Within the bounds of our analysis, however, it is implausible that differences in reconstruction efforts can explain the qualitative differences in the observed light intensity patterns between municipalities, all of which had reconstruction going on in the months to years after the quake. We note that the study focuses only on a region in Japan, a country that is famous for its earthquake preparedness. This is likely part of the reason that fatality numbers were relatively low, even when building damage was severe. The analysis could be repeated for other cases to assess whether similar patterns hold in other countries, most notably in lower-income countries. Moreover, the findings in this study do not align with studies especially on hurricane impacts, for which reductions in night light are reported more frequently for various regions around the world. This discrepancy warrants further inquiry, which I put on the agenda for future research. Concluding, my final chapter presents new and important evidence to the growing literature that uses night lights to proxy local economic activity in times of natural disasters. Acknowledging the limitations of the study, I conclude that caution is warranted when using the VIIRS monthly nighttime lights as a proxy for economic activity in the aftermath of natural disasters, at least in the case of earthquakes.

## 6.2 Discussion on the main findings

Between the four main chapters of this dissertation, I present two contrasting answers to the use of night light data for studying local economic impacts of natural

disasters. In the first two chapters, the annual DMSP night light data correspond well with disaster impacts for the case of Katrina and show great promise in the global study on the effects of local weather anomalies. I show that local weather extremes affect local economic activity and present evidence for temporary spatial shifts of economic activity to neighboring regions. We show that these effects are limited in their geographical scope and that they are most pronounced in low- and middle-income countries. In doing so, we break new ground for an approach to study the effect of natural disasters on economic development and growth, as well as exploring new ways to study regional and network effects of shocks more generally. Follow-up work is ongoing in which we find that the presented spillover effects follow sensible economic channels (national borders and roads to start with). As such, night light data has proven to be valuable in opening up ways to study economic dynamics following natural extremes at a spatial scale in countries where no or no reliable socioeconomic statistics are available.

Findings in the following two chapters, however, tell a different story. Using the newer and supposedly better suite of monthly VIIRS night light data to study the local effects of earthquakes, I am unable to find essentially any robust link between impacts from earthquakes and changes in night light intensity. In hindsight, studying weather extremes in this context may have provided a better comparison with the findings in the first two chapters. However, recently published and related literature finds similar evidence for some cases of weather events (Skoufias et al., 2021).

A critical reflection is therefore necessary. Part of the problem with the VIIRS data appears to be data-related. Cleaning is not as thorough as it is for the annual DMSP data (Elvidge et al., 2017), while seasonality and generic temporal variability are topics that are still being discussed in the remote sensing literature (Coesfeld et al., 2018; Zhao et al., 2020; Gao et al., 2020). Use of this data by non-specialists may therefore still be premature, in contrast to the well-documented and well-understood issues with the DMSP data (and summarized especially for an economic audience by Gibson et al., 2021).

Apart from data issues, however, Chapter 5 shows convincing evidence that even extensive building damage from the Kumamoto earthquake is barely reflected in the VIIRS data at all. This stands in stark contrast to the results of Chapter 2 on Hurricane Katrina using the annual DMSP data, and other studies that use the DMSP data to identify e.g. damaged urban areas from earthquakes (e.g. Hashitera et al., 1999; Kohiyama et al., 2004). Instead I find no evidence that the VIIRS light data provide a reasonable proxy for either immediate damages or recovery in the case of the Kumamoto earthquake. My answer is therefore that economists and academics in general should be cautious in using the newer monthly data for studying the economic impacts of natural disasters at least in the case of earthquakes, even when a growing literature suggests that these data are the way forward. As a general remark, my results show that night lights may not always respond as theory would predict. They are a proxy for economic activity, but at the end of the day night light data measures light, not GDP.

### 6.3 Limitations and directions for future research

The methods and findings presented in this dissertation evidently come with limitations. First, one of the issues in the literature with which I engage closely in this dissertation, is the unprecisely defined concept of local economy. There is a lack of theoretical underpinning of what the appropriate spatial scale of 'local' economy is, and in the existing literature choices are made more on an ad-hoc basis than on the basis of a sound theoretical idea of what the unit of interest should be. First and foremost, this is a data-driven approach. The night light data allow analyzing changes at essentially any level of spatial aggregation, down to the resolution of the satellite records themselves. Many studies in this literature choose this seemingly non-arbitrary limit of the data and analyze disaster impacts at the pixel resolution. Changes in pixel-level night light intensity are then interpreted as changes in local economic activity. In my fourth chapter, I choose a similar strategy when analyzing the effects of earthquakes on night light emissions.

A number of reflections on this matter are appropriate. First, the final pixel resolution of the annual DMSP data is roughly 1km at the equator. As discussed in the introduction, however, spatial smoothing and geolocation errors imply that the true ground footprint of the DMSP-OLS sensor is roughly  $5 \times 5$ km (Elvidge et al., 2013). This causes substantial spatial autocorrelation between nearby pixels and blurring of light e.g. along urban edges and in zones between urban centers (referred to as glooming, for a discussion see Gibson, 2021). Changes in a single pixel in the final DMSP data are therefore the smoothed average of changes in a larger area, introducing measurement error into estimations of the effect of shocks on night light intensity as the dependent variable when the analysis is at the pixel-level. For this reason, I have not worked with pixel-level analyses with the DMSP data in this dissertation. Aggregation to larger (administrative) units, as I have done in Chapter 2 and 3, reduces the magnitude of this problem substantially. It is also important to note that the newer VIIRS night light data are not contaminated by this issue, and have a true ground footprint of  $742 \times 742$  meters. The strategy in Chapter 4 is therefore not affected by the issue of spatial smoothing, as opposed to studies that use pixel-level DMSP data (e.g. Bertinelli and Strobl, 2013; Elliott et al., 2015; Kocornik-Mina et al., 2020).

Second, a less data-oriented and more conceptual discussion is similarly thin in the literature. Nguyen and Noy (2020, pp. 861), in their analysis of the effect on insurance payments for local economic recovery after the 2011 Canterbury earthquake sequence in New Zealand, loosely discuss that "the correlation between night-time light and economic activity tends to be weaker at very small unit levels (e.g. one pixel), so some aggregation appears to be necessary." While this is arguably true, no guidance for this is currently available in the literature. In turn, the authors aggregate the night light pixels to the lowest level of statistical area units (AUs) in New Zealand, arguably again an ad-hoc and data-driven approach that cannot be generalized across the globe. Rather than applying an aggregation strategy, as I do in most analyses for this dissertation, many studies instead simply choose the pixel



level as the spatial unit of interest, without further discussing how this may or may not be appropriate when using night light intensity as a proxy for local economic activity. Clearly, there is a need for a better understanding of how night lights reflect economic activity and moreover at what spatial scale this is appropriate. This is true both conceptually and theoretically from a regional economics point of view (for a discussion, see Chapter 3 and Botzen et al., 2019).

Third, from a more geographical point of view the previous point clearly relates to the Modifiable Area Unit Problem (MAUP). This has to do with statistical bias that may arise from varying shapes and aggregations of point-based data into administrative units or grid cells (both of which are used in this dissertation). I implicitly engage with this problem in Chapter 4, when comparing estimation results of the impacts of earthquakes on night light emissions at both  $0.5^\circ$  grid cells and at the 15 arc seconds pixel-resolution of the VIIRS data (roughly 450 by 450 meters at the equator). However, there appears to be a need for further scrutiny as to how spatial aggregation may affect (1) the correlation between night light intensity and economic activity, and (2) how this interacts with potential treatment effects (both local, and in terms of spatial spillovers as in Chapter 3).

In light of Chapter 2 and 5, an interesting comparison is that of population changes. Hurricane Katrina caused a very large population displacement of roughly half a million people, resulting in entire neighborhoods essentially being deserted for weeks to months or multiple years in the case of the poorest and most severely flooded districts. This resulted in some parts of New Orleans city going dark altogether in the year of the hurricane. Instead, as discussed in Chapter 5 the displacement effects of the Kumamoto earthquake were more modest. While the disaster affected over 300,000 people and resulted in a peak of over 100,000 evacuees in the first week after the quake, the number of homeless is set at roughly 24,000 (CRED, 2021). Being spread across multiple municipalities throughout Kumamoto prefecture, and with electricity being restored within a number of days, we do not observe areas going dark in the same way as we do for New Orleans in Chapter 2. While barely discussed in the economic literature that uses nighttime lights as a proxy for economic activity, this may be indicative of changes along the extensive margin being more pronounced than changes along the intensive margin. That is, areas going from lit to unlit drive at least part of the recorded reduction in night light intensity after Hurricane Katrina. Instead, in the case of the Kumamoto earthquake areas remain lit and reductions in light intensity are more modest, in line with population displacement being much more limited and less prolonged than in the case of Hurricane Katrina.

As income reductions are hardly reflected in the case of the Kumamoto quake, this may be indicative of night light changes being more closely related to population changes rather than income changes. This echoes the findings of Chapter 2, where we similarly find a stronger correlation with population changes than with changes in income. In simple terms, lights go out when people leave, but perhaps less so when they stay but experience a drop in income (or savings). Of course, this is conceptually easy to grasp and the inverse of it happens when e.g. rural areas experience economic development and growth and start emitting light (e.g. Gibson

et al., 2017). In the case of natural disasters, however, this has not yet been studied in detail and I therefore put it on the agenda for future research.

One of the initial goals of the research in this dissertation was to investigate the mechanisms through which development and institutions affect resilience to natural hazards. Institutions (Raschky, 2008; Barone and Mocetti, 2014), inequality (Anbarci et al., 2005), and more generally development (Kahn, 2005; Strömberg, 2007) clearly matter for resilience in both *ex-ante* preparedness and *ex-post* recovery. As has been discussed at length in this dissertation, however, studying this requires a means to quantify both natural extremes and potential impacts thereof at the appropriate spatial scale. Especially the latter proved to be challenging. Night light emissions are one way of assessing this, but as I show in Chapter 5 we have at least some reason to believe that they do not form the holy grail for this research agenda.

I stress that research into the area of resilience and mitigation strategies is important. Especially in many developing countries, societies face challenges in light of a rapidly changing climate combined with population growth and urbanization in hazard-prone areas. The methods applied in this dissertation do pave the way for comparative case studies that make use of differences (discontinuities) in institutional arrangements along regional borders, as is the case in e.g. the divide between North and South Italy, which experiences major earthquakes along the divide (for an example, see e.g. Barone and Mocetti, 2014). However, data limitations on the VIIRS data did not allow the study of this particular and interesting case. Data coverage allowing, future events in Italy or similar regions of interest may be successfully studied using this approach. Alternatively, different and likely more conventional outcome variables can be used to facilitate comparative studies where night light data proves insufficient (e.g. Brata et al., 2018; Heger and Neumayer, 2019).

I have investigated one possible way to gain a better understanding of how natural shocks affect the economic systems that they affect, but there are many other ways. Data popularly referred to as big data, such as information from social media (Indaco, 2020) or mobile phone data (Blumenstock et al., 2015; Šćepanović et al., 2015) and possibly other types of data, may provide new ways of capturing economic dynamics on the surface rather than using the ‘eyes from the sky’ alone. It is worthwhile to notice that in disaster management and relief studies the value of these types of data have long been recognized (Gao et al., 2011; Houston et al., 2015). These alternatives may prove equally or perhaps even more valuable than remote sensing data *per se*. Moreover, these different types and sources of data are likely complementary in creating a fuller and richer picture as opposed to using them in isolation.

At the closing of this dissertation, I propose an agenda for future research. First, I have discussed how natural disasters may affect the economies that they hit directly in an adverse way. In Chapter 3, however, I have presented evidence for how disasters may indirectly affect neighboring areas through spatial spillovers. Evidently, the question is how these spillovers materialize and how we can understand the mechanism behind them. In follow-up work on the study presented in Chapter 3 of

this dissertation (not included in this dissertation), I study these spillovers in more detail with my co-authors Thomas Steinwachs and Jasmin Gröschl (see Gröschl et al., 2020). We investigate whether the spatial spillovers we identify in Chapter 3 are more pronounced between areas that are more strongly linked than others, as captured by shared national borders and by connectivity through major road networks. Indeed we find the spillover effects to be more pronounced between cells sharing the same national border, and between cells that have a larger number of road connections between them. Given these preliminary findings, this avenue of research is promising and I therefore stress that future research may look into these mechanisms further. Not only will this help us in understanding how the effects of local adverse shocks dissipate over space and through economic networks, but it also helps in understanding that these dynamics may be helpful when considering mitigation strategies in the face of climate change as well as when considering regional insurance schemes for natural disasters.

Second, given the issues identified in Chapters 4 and 5, one of the questions is whether night light data holds much promise for economic research at all. To this, my answer is twofold. First, I provide evidence to a debate in which opposing views and evidence are presented. Recent studies by Ishizawa et al. (2019), Zhao et al. (2020), and Miranda et al. (2020) show clear evidence that night lights do capture adverse impacts from various hurricanes around the world. To discard night lights as a means to study the economic impacts of natural disasters would therefore be strictly premature. New data possibilities open up further research possibilities. As the work of this dissertation was coming to a close in the summer of 2021, NOAA published a new suite of monthly DMSP night light data that allows the short-term analysis of disasters through 1992-2013. New papers have recently been published that use these monthly DMSP data, rather than the monthly VIIRS data (Ishizawa et al., 2019; Miranda et al., 2020). These studies find longer-lasting local impacts of hurricanes than those reported in earlier papers by Mohan and Strobl (2017) and Del Valle et al. (2018) who instead make use of the VIIRS data. This gives rise to the question whether DMSP monthly data may be of different and possibly better quality than the VIIRS monthly data for studying month-to-month changes in local economic activity in response to natural shocks. Having both the DMSP and VIIRS data available at monthly intervals allows a follow-up study of Chapters 4 and 5, in which an answer can be found to whether the lack of observable effects of ground shaking on night light emissions is specific to the VIIRS night light data, or whether we find similar patterns in the DMSP data. An especially promising avenue may be to analyze the same events with the two different suites of monthly night light data, being limited to the only and relatively short overlapping period of April 2012 through December 2013 – the short period of time during which both satellite suites were operational simultaneously.

Another important observation is that virtually all studies in this field are concerned with hurricanes. While these are also localized events, the geographical extent of destruction is typically (much) larger than that of earthquakes. I am among the first to present evidence against the use of night lights in the case of earthquakes, both from a global point of view (Chapter 4) and for a detailed case study of the

devastating Kumamoto quake (Chapter 5). The contrasting results that I present here thus call for more attention to studying different types of disasters, rather than windstorms alone, with special attention for slower disasters like heatwaves, coldwaves, and droughts.

Zooming out, I believe that night lights and remote sensing more broadly hold great promise for the social sciences. Specifically for night lights, the application presented in this dissertation presents numerous challenges on both the measurement of light intensity itself and on how changes in light intensity relate to changes in economic conditions on the ground. These challenges make this application intellectually challenging, but may obscure a more uncontested and obvious quality: when comparing across space rather than across time, the images from space give a truly objective reflection of the spatial distribution of economic activity across the globe. Studying the economic impacts of natural disasters essentially means studying (temporary) deviations from an economic equilibrium. Instead, patterns of gradual growth, especially in poor rural areas of the world, are much more stable processes which are reflected strongly by gradual growth of light intensity of population centers (the intensive margin) and by new places lighting up (the extensive margin). Studying rural development in developing countries, and the effect of otherwise poorly measurable effects like road construction (Asher and Novosad, 2020) and political gains for regions that are poorly captured by administrative boundaries (such as ethnic homelands in Sub-Saharan Africa, see Michalopoulos and Papaioannou (2013, 2014)), is enabled by this type of remotely sensed information. I believe that remote sensing data will prove to be of great value to social scientists around the world trying to understand these matters (for an excellent discussion on this, see Gibson, 2021; Gibson et al., 2021).

Finally, this dissertation has focused heavily on the use of night light data as a proxy for local economic activity in the context of natural disasters. With the continuously expanding number of satellites orbiting the earth, new and different types of remote sensing data are becoming available to social scientists free of charge. Humans emit more than light alone. For example, gaseous emissions can also be detected through remote sensing and can inform us in related but possibly different ways about consumption and production activity at high spatial detail. For example, data on nitrogen and CO<sub>2</sub> emissions provide promising avenues of research into remotely sensed economic activity, as is illustrated for example by the strong declines in nitrogen dioxide emissions and air pollution in the early phase of the global COVID-19 crisis as captured by the Copernicus Sentinel-5P satellite.<sup>2</sup> In this context, the methods and findings discussed in this dissertation are just one way forward of how remotely sensed footprints of human activity on earth can inform us about development, growth, and shocks.

---

<sup>2</sup>This discussion was widely covered by ESA's Copernicus program throughout the COVID-19 pandemic. For applications, see [https://www.esa.int/Applications/Observing\\_the\\_Earth/Copernicus/Sentinel-5P](https://www.esa.int/Applications/Observing_the_Earth/Copernicus/Sentinel-5P)

---

## Bibliography

---

- Abadie, A., Diamond, A., Hainmueller, J., 2010. Synthetic control methods for comparative case studies: estimating the effect of California's tobacco control program. *Journal of the American Statistical Association* 105, 493–505.
- Abadie, A., Gardeazabal, J., 2003. The economic costs of conflict: a case study of the Basque country. *American Economic Review* 93, 113–132.
- Acs, Z.J., Audretsch, D.B., Feldman, M.P., 1994. R&D spillovers and recipient firm size. *The Review of Economics and Statistics* 76, 336–340.
- Aerts, J.C., Botzen, W.W., Emanuel, K., Lin, N., De Moel, H., Michel-Kerjan, E.O., 2014. Evaluating flood resilience strategies for coastal megacities. *Science* 344, 473–475.
- Alesina, A., Michalopoulos, S., Papaioannou, E., 2016. Ethnic inequality. *Journal of Political Economy* 124, 428–488.
- Allen, T.I., Wald, D.J., Earle, P.S., Marano, K.D., Hotovec, A.J., Lin, K., Hearne, M.G., 2009. An atlas of shakemaps and population exposure catalog for earthquake loss modeling. *Bulletin of Earthquake Engineering* 7, 701–718.
- Allen, T.I., Wald, D.J., Hotovec, A.J., Lin, K.W., Earle, P.S., Marano, K.D., 2008. An Atlas of ShakeMaps for selected global earthquakes. Technical Report.
- Alonso, W., 1960. A theory of the urban land market. *Papers and Proceedings of the Regional Science Association* 6, 149–157.
- Anbarci, N., Escaleras, M., Register, C.A., 2005. Earthquake fatalities: the interaction of nature and political economy. *Journal of Public Economics* 89, 1907–1933.
- Anselin, L., 2013. *Spatial econometrics: Methods and models* (Vol. 4). Springer Science & Business Media.
- Asher, S., Novosad, P., 2020. Rural roads and local economic development. *American Economic Review* 110, 797–823.

- Asian Disaster Reduction Center, 2016. 2016 Kumamoto earthquake survey report (preliminary). URL: [https://www.adrc.asia/publications/201604\\_KumamotoEQ/ADRC\\_2016KumamotoEQ\\_Report\\_1.pdf](https://www.adrc.asia/publications/201604_KumamotoEQ/ADRC_2016KumamotoEQ_Report_1.pdf).
- Atkinson, G.M., Kaka, S.I., 2006. Relationships between felt intensity and instrumental ground motion for New Madrid ShakeMaps. Department of Earth Sciences, Carleton University.
- Atkinson, G.M., Kaka, S.I., 2007. Relationships between felt intensity and instrumental ground motion in the Central United States and California. *Bulletin of the Seismological Society of America* 97, 497–510.
- Atkinson, G.M., Wald, D.J., 2007. “Did You Feel It?” Intensity data: a surprisingly good measure of earthquake ground motion. *Seismological Research Letters* 78, 362–368.
- Audretsch, D.B., Feldman, M.P., 1996. R&D spillovers and the geography of innovation and production. *The American Economic Review* 86, 630–640.
- Auffhammer, M., Hsiang, S.M., Schlenker, W., Sobel, A., 2013. Using weather data and climate model output in economic analyses of climate change. *Review of Environmental Economics and Policy* 7, 181–198.
- Baltagi, B.H., Song, S.H., Jung, B.C., Koh, W., 2007. Testing for serial correlation, spatial autocorrelation and random effects using panel data. *Journal of Econometrics* 140, 5–51.
- Barone, G., Mocetti, S., 2014. Natural disasters, growth and institutions: a tale of two earthquakes. *Journal of Urban Economics* 84, 52–66.
- Basker, E., Miranda, J., 2018. Taken by storm: business financing and survival in the aftermath of Hurricane Katrina. *Journal of Economic Geography* 18, 1285–1313.
- Baugh, K., Elvidge, C.D., Ghosh, T., Ziskin, D., 2010. Development of a 2009 stable lights product using DMSP-OLS data. *Proceedings of the Asia-Pacific Advanced Network* 30, 114.
- van Bavel, B., Curtis, D., Dijkman, J., Hannaford, M., De Keyzer, M., Van Onacker, E., Soens, T., 2020. *Disasters and history: the vulnerability and resilience of past societies*. Cambridge University Press.
- Bennett, M.M., Smith, L.C., 2017. Advances in using multitemporal night-time lights satellite imagery to detect, estimate, and monitor socioeconomic dynamics. *Remote Sensing of Environment* 192, 176–197.
- Berlemann, M., Wenzel, D., 2018. Hurricanes, economic growth, and transmission channels: empirical evidence for countries on differing levels of development. *World Development* 105, 231–247.

- Bertinelli, L., Strobl, E., 2013. Quantifying the local economic growth impact of hurricane strikes: an analysis from outer space for the Caribbean. *Journal of Applied Meteorology and Climatology* 52, 1688–1697.
- Beyer, R.C., Chhabra, E., Galdo, V., Rama, M., 2018. Measuring districts' monthly economic activity from outer space. *World Bank Policy Research Working Paper* 8523 .
- Bickenbach, F., Bode, E., Nunnenkamp, P., Söder, M., 2016. Night lights and regional GDP. *Review of World Economics* 152, 425–447.
- Bleakley, H., Lin, J., 2012. Portage and path dependence. *Quarterly Journal of Economics* 127, 587–644.
- Bluhm, R., Krause, M., 2018. Top lights-bright cities and their contribution to economic development. *CESifo Working Paper No.* 7411 .
- Blumenstock, J., Cadamuro, G., On, R., 2015. Predicting poverty and wealth from mobile phone metadata. *Science* 350, 1073–1076.
- Botzen, W.W., Deschenes, O., Sanders, M., 2019. The economic impacts of natural disasters: a review of models and empirical studies. *Review of Environmental Economics and Policy* 13, 167–188.
- Boustan, L.P., Kahn, M.E., Rhode, P.W., Yanguas, M.L., 2020. The effect of natural disasters on economic activity in US counties: a century of data. *Journal of Urban Economics* 118, 103257.
- Brata, A.G., de Groot, H.L., Zant, W., 2018. The impact of the 2006 Yogyakarta earthquake on local economic growth. *Economics of Disasters and Climate Change* 2, 203–224.
- Bruederle, A., Hodler, R., 2018. Nighttime lights as a proxy for human development at the local level. *PLoS ONE* 13(9), e0202231.
- Cabinet Office Japan, 2017. White paper: Disaster management in Japan. URL: [http://www.bousai.go.jp/kyoiku/panf/pdf/WP2017\\_DM\\_Full\\_Version.pdf](http://www.bousai.go.jp/kyoiku/panf/pdf/WP2017_DM_Full_Version.pdf).
- Cao, C., Shao, X., Uprety, S., 2013. Detecting light outages after severe storms using the S-NPP/VIIIRS Day/Night Band radiances. *IEEE Geoscience and Remote Sensing Letters* 10, 1582–1586.
- Capello, R., 2015. *Regional economics*. Routledge, London.
- Carrera, L., Standardi, G., Bosello, F., Mysiak, J., 2015. Assessing direct and indirect economic impacts of a flood event through the integration of spatial and computable general equilibrium modelling. *Environmental Modelling & Software* 63, 109–122.

- Cavallo, E., Galiani, S., Noy, I., Pantano, J., 2013. Catastrophic natural disasters and economic growth. *Review of Economics and Statistics* 95, 1549–1561.
- Cavallo, E., Noy, I., et al., 2011. Natural disasters and the economy — A survey. *International Review of Environmental and Resource Economics* 5, 63–102.
- Center for International Earth Science Information Network (CIESIN) at Columbia University, 2016. Gridded Population of the World, Version 4 (GPWv4): Population Count. URL: <http://dx.doi.org/10.7927/H4X63JVC>.
- Center for International Earth Science Information Network (CIESIN) at Columbia University, 2017. Global Rural-Urban Mapping Project, Version 1 (GRUMPv1): Urban Extent Polygons, Revision 01. NY: NASA Socioeconomic Data and Applications Center (SEDAC). doi:<https://doi.org/10.7927/H4Z31WKF>. Accessed on 24 Sept 2020.
- Chang, S.E., 2010. Urban disaster recovery: a measurement framework and its application to the 1995 Kobe earthquake. *Disasters* 34, 303–327.
- Chen, X., Nordhaus, W.D., 2011. Using luminosity data as a proxy for economic statistics. *Proceedings of the National Academy of Sciences* 108, 8589–8594.
- Christaller, W., 1933. *Die zentralen Orte in Süddeutschland* (the central places in southern Germany). Gustav Fischer, Jena.
- Coesfeld, J., Anderson, S., Baugh, K., Elvidge, C., Schernthanner, H., Kyba, C., 2018. Variation of individual location radiance in VIIRS DNB monthly composite images. *Remote Sensing* 10, 1964.
- Coesfeld, J., Kuester, T., Kuechly, H.U., Kyba, C., 2020. Reducing variability and removing natural light from nighttime satellite imagery: A case study using the VIIRS DNB. *Sensors* 20, 3287.
- Coffman, M., Noy, I., 2012. Hurricane Iniki: measuring the long-term economic impact of a natural disaster using synthetic control. *Environment and Development Economics* 17, 187–205.
- Cole, M.A., Elliott, R.J., Okubo, T., Strobl, E., 2019. Natural disasters and spatial heterogeneity in damages: the birth, life and death of manufacturing plants. *Journal of Economic Geography* 19, 373–408.
- Conley, T.G., 1999. GMM estimation with cross sectional dependence. *Journal of Econometrics* 92, 1–45.
- Conley, T.G., 2008. Spatial econometrics, in: Durlauf, S.N., Blume, L.E. (Eds.), *The New Palgrave Dictionary of Economics*. Palgrave Macmillan, Basingstoke.
- Content, J., Frenken, K., 2016. Related variety and economic development: a literature review. *European Planning Studies* 24, 2097–2112.



- Corbane, C., Florczyk, A., Pesaresi, M., Politis, P., Syrri, V., 2018. GHS-BUILT R2018A-GHS built-up grid, derived from Landsat, multitemporal (1975–1990–2000–2014). European Commission, Joint Research Centre, JRC Data Catalogue .
- Correia, S., 2016. Linear models with high-dimensional fixed effects: An efficient and feasible estimator [unpublished manuscript]. Working Paper URL: <http://scorreia.com/research/hdfe.pdf>.
- CRED, D.G.S., 2021. EM-DAT: The Emergency Events Database. Université catholique de Louvain (UCL) – CRED, D. Guha-Sapir URL: [www.emdat.be](http://www.emdat.be).
- Crespo Cuaresma, J., Hlouskova, J., Obersteiner, M., 2008. Natural disasters as creative destruction? Evidence from developing countries. *Economic Inquiry* 46, 214–226.
- Croft, T.A., 1978. Nighttime images of the earth from space. *Scientific American* 239, 86–101.
- Damania, R., Desbureaux, S., Hyland, M., Islam, A., Moore, S., Rodella, A.S., Russ, J., Zaveri, E., 2017. *Uncharted waters: The new economics of water scarcity and variability*. Washington, DC: World Bank.
- Dartmouth Flood Observatory, 2005. DFO Event 2005-114 - Hurricane Katrina: New Orleans area - Rapid Response Inundation Map 1. URL: <https://floodobservatory.colorado.edu/2005114.html>.
- De Janvry, A., Del Valle, A., Sadoulet, E., 2016. Insuring growth: the impact of disaster funds on economic reconstruction in Mexico. The World Bank.
- De Luca, G., Hodler, R., Raschky, P.A., Valsecchi, M., 2018. Ethnic favoritism: An axiom of politics? *Journal of Development Economics* 132, 115–129.
- Deaton, A., Heston, A., 2010. Understanding PPPs and PPP-based national accounts. *American Economic Journal: Macroeconomics* 2, 1–35.
- Dekle, R., Hong, E., Xie, W., 2015. The regional spillover effects of the Tohoku earthquake. USC-INET Research Paper 15-13 .
- Del Valle, A., Elliott, R.J., Strobl, E., Tong, M., 2018. The short-term economic impact of tropical cyclones: Satellite evidence from Guangdong province. *Economics of Disasters and Climate Change* 2, 225–235.
- Dell, M., Jones, B.F., Olken, B.A., 2012. Temperature shocks and economic growth: evidence from the last half century. *American Economic Journal: Macroeconomics* 4, 66–95.
- Dell’Acqua, F., Gamba, P., 2012. Remote sensing and earthquake damage assessment: experiences, limits, and perspectives. *Proceedings of the IEEE* 100, 2876–2890.

- Deryugina, T., Kawano, L., Levitt, S., 2018. The economic impact of Hurricane Katrina on its victims: Evidence from individual tax returns. *American Economic Journal: Applied Economics* 10, 202–33.
- Doll, C., 2008. CIESIN thematic guide to night-time light remote sensing and its applications.
- Doll, C.H., Muller, J.P., Elvidge, C.D., 2000. Night-Time Imagery as a Tool for Global Mapping of Socioeconomic Parameters and Greenhouse Gas Emissions. *AMBIO: A Journal of the Human Environment* 29, 157–162.
- Doll, C.N., Muller, J.P., Morley, J.G., 2006. Mapping regional economic activity from night-time light satellite imagery. *Ecological Economics* 57, 75–92.
- Donaldson, D., Storeygard, A., 2016. The view from above: Applications of satellite data in economics. *Journal of Economic Perspectives* 30, 171–98.
- Driscoll, J.C., Kraay, A.C., 1998. Consistent covariance matrix estimation with spatially dependent panel data. *Review of Economics and Statistics* 80, 549–560.
- Earth Observation Group, 2016. Version 4 DMSP-OLS Night-Time Lights Time Series. URL: <https://eogdata.mines.edu/products/dmsp/>.
- Ebener, S., Murray, C., Tandon, A., Elvidge, C.C., 2005. From wealth to health: Modelling the distribution of income per capita at the sub-national level using night-time light imagery. *International Journal of Health Geographics* 4, 1–17.
- Eguchi, R.T., Huyck, C.K., Ghosh, S., Adams, B.J., 2008. The application of remote sensing technologies for disaster management, in: *The 14th World Conference on Earthquake Engineering*, Vol 17.
- Eichenauer, V.Z., Fuchs, A., Kunze, S., Strobl, E., 2020. Distortions in aid allocation of United Nations flash appeals: Evidence from the 2015 Nepal earthquake. *World Development* 136, 105023.
- Elliott, R., Strobl, E., Sun, P., 2015. The local impact of typhoons on economic activity in China: A view from outer space. *Journal of Urban Economics* 88, 50–66.
- Elvidge, C.D., Baugh, K., Zhizhin, M., Hsu, F.C., Ghosh, T., 2017. VIIRS night-time lights. *International Journal of Remote Sensing* 38, 5860–5879.
- Elvidge, C.D., Baugh, K.E., Kihn, E.A., Kroehl, H.W., Davis, E.R., Davis, C.W., 1997. Relation between satellite observed visible-near infrared emissions, population, economic activity and electric power consumption. *International Journal of Remote Sensing* 18, 1373–1379.
- Elvidge, C.D., Baugh, K.E., Zhizhin, M., Hsu, F.C., 2013. Why VIIRS data are superior to DMSP for mapping nighttime lights. *Proceedings of the Asia-Pacific Advanced Network* 35, 62. doi:10.7125/APAN.35.7.

- Elvidge, C.D., Hsu, F.C., Baugh, K.E., Ghosh, T., 2014. National trends in satellite observed lighting. *Global Urban Monitoring and Assessment through Earth Observation* 23, 97–118.
- Elvidge, C.D., Sutton, P.C., Ghosh, T., Tuttle, B.T., Baugh, K.E., Bhaduri, B., Bright, E., 2009a. A global poverty map derived from satellite data. *Computers & Geosciences* 35, 1652–1660.
- Elvidge, C.D., Ziskin, D., Baugh, K.E., Tuttle, B.T., Ghosh, T., Pack, D.W., Erwin, E.H., Zhizhin, M., 2009b. A fifteen year record of global natural gas flaring derived from satellite data. *Energies* 2, 595–622.
- Fabian, M., Lessmann, C., Sofke, T., 2019. Natural disasters and regional development – the case of earthquakes. *Environment and Development Economics* 24, 479–505.
- Fan, X., Nie, G., Deng, Y., An, J., Zhou, J., Li, H., 2019. Rapid detection of earthquake damage areas using VIIRS nearly constant contrast night-time light data. *International Journal of Remote Sensing* 40, 2386–2409.
- Felbermayr, G., Gröschl, J., 2014. Naturally negative: The growth effects of natural disasters. *Journal of Development Economics* 111, 92–106.
- Felbermayr, G., Gröschl, J., Sanders, M.W., Schippers, V.G., Steinwachs, T., 2022. The economic impact of weather anomalies. *World Development* 151, 105745.
- Félix, D., Branco, J.M., Feio, A., 2013. Temporary housing after disasters: a state of the art survey. *Habitat International* 40, 136–141.
- Fomby, T., Ikeda, Y., Loayza, N.V., 2013. The growth aftermath of natural disasters. *Journal of Applied Econometrics* 28, 412–434.
- Frame, D.J., Rosier, S.M., Noy, I., Harrington, L.J., Carey-Smith, T., Sparrow, S.N., Stone, D.A., Dean, S.M., 2020. Climate change attribution and the economic costs of extreme weather events: a study on damages from extreme rainfall and drought. *Climatic Change* 162, 781–797.
- Frenken, K., Van Oort, F., Verburg, T., 2007. Related variety, unrelated variety and regional economic growth. *Regional Studies* 41, 685–697.
- Gao, H., Barbier, G., Goolsby, R., 2011. Harnessing the crowdsourcing power of social media for disaster relief. *IEEE Intelligent Systems* 26, 10–14.
- Gao, S., Chen, Y., Liang, L., Gong, A., 2020. Post-earthquake night-time light piecewise (pnlp) pattern based on NPP/VIIRS night-time light data: a case study of the 2015 Nepal earthquake. *Remote Sensing* 12, 2009.

- García, D., Mah, R., Johnson, K., Hearne, M., Marano, K., Lin, K., Wald, D., Worden, C., So, E., 2012. ShakeMap Atlas 2.0: An improved suite of recent historical earthquake ShakeMaps for global hazard analyses and loss model calibration, in: World Conference on Earthquake Engineering.
- Geiger, T., Frieler, K., Bresch, D.N., 2018. A global historical data set of tropical cyclone exposure (tce-dat). *Earth System Science Data* 10, 185–194.
- Ghosh, T., Anderson, S., Powell, R.L.P.L., Sutton, P.C., Elvidge, C.D., 2009. Estimation of Mexico's informal economy and remittances using night-time imagery. *Remote Sensing* 1, 418–444.
- Ghosh, T., Anderson, S.J., Elvidge, C.D., Sutton, P.C., 2013. Using nighttime satellite imagery as a proxy measure of human well-being. *Sustainability* 5, 4988–5019.
- Ghosh, T., L Powell, R., D Elvidge, C., E Baugh, K., C Sutton, P., Anderson, S., 2010. Shedding light on the global distribution of economic activity. *The Open Geography Journal* 3, 147–160.
- Giardini, D., Grünthal, G., Shedlock, K.M., Zhang, P., 1999. The GSHAP global seismic hazard map. *Annals of Geophysics* 42.
- Gibson, J., 2021. Better night lights data, for longer. *Oxford Bulletin of Economics and Statistics* 83, 770–791.
- Gibson, J., Datt, G., Murgai, R., Ravallion, M., 2017. For India's rural poor, growing towns matter more than growing cities. *World Development* 98, 413–429.
- Gibson, J., Olivia, S., Boe-Gibson, G., 2020. Night lights in economics: sources and uses. *Journal of Economic Surveys* 34, 955–980.
- Gibson, J., Olivia, S., Boe-Gibson, G., Li, C., 2021. Which night lights data should we use in economics, and where? *Journal of Development Economics* 149, 102602.
- Gillespie, T.W., Frankenberg, E., Fung Chum, K., Thomas, D., 2014. Night-time lights time series of tsunami damage, recovery, and economic metrics in Sumatra, Indonesia. *Remote Sensing Letters* 5, 286–294.
- Goda, K., Campbell, G., Hulme, L., Ismael, B., Ke, L., Marsh, R., Sammonds, P., So, E., Okumura, Y., Kishi, N., et al., 2016. The 2016 Kumamoto earthquakes: cascading geological hazards and compounding risks. *Frontiers in Built Environment* 2, 19.
- Griliches, Z., 1957. Hybrid corn: An exploration in the economics of technological change. *Econometrica* 25, 501–522.
- Groen, J.A., Kutzbach, M.J., Polivka, A.E., 2020. Storms and jobs: the effect of hurricanes on individuals' employment and earnings over the long term. *Journal of Labor Economics* 38, 653–685.

- Groen, J.A., Polivka, A.E., 2008. The effect of Hurricane Katrina on the labor market outcomes of evacuees. *American Economic Review* 98, 43–48.
- Gröschl, J., Schippers, V., Steinwachs, T., 2020. Borders, roads and the relocation of economic activity due to extreme weather. CESifo Working Paper No. 8193 .
- Grossman, G.M., Helpman, E., 1991. Quality ladders and product cycles. *Quarterly Journal of Economics* 106, 557–586.
- Guha-Sapir, D., Below, R., Hoyois, P., 2021. EM-DAT: The CRED/OFDA International Disaster Database. [www.emdat.be](http://www.emdat.be).
- Hägerstrand, T., 1952. The propagation of innovation waves. *Lund studies in geography: Series B: Human geography* , 3–19.
- Halleck Vega, S., Elhorst, J.P., 2015. The SLX Model. *Journal of Regional Science* 55, 339–363.
- Hallegatte, S., 2008. An adaptive regional input-output model and its application to the assessment of the economic cost of Katrina. *Risk analysis* 28, 779–799.
- Hallegatte, S., Dumas, P., 2009. Can natural disasters have positive consequences? Investigating the role of embodied technical change. *Ecological Economics* 68, 777–786.
- Hallegatte, S., Green, C., Nicholls, R.J., Corfee-Morlot, J., 2013. Future flood losses in major coastal cities. *Nature Climate Change* 3, 802–806.
- Hallegatte, S., Rentschler, J., Rozenberg, J., 2019. *Lifelines: the resilient infrastructure opportunity*. Washington, DC: World Bank.
- Harris, I., Jones, P., Osborn, T., Lister, D., 2014. Updated high-resolution grids of monthly climatic observations – the CRU TS3. 10 Dataset. *International Journal of Climatology* 34, 623–642.
- Hashitera, S., Haruo, Kohiyama, M., Maki, N., Hayashi, H., Matsuoka, M., Fujita, H., 1999. Use of DMSP-OLS images for early identification of impacted areas due to the 1999 Marmara earthquake disaster, in: *Proceedings of the 20th Asian Conference on Remote Sensing*, pp. 1291–1296.
- Haslett, J., Raftery, A.E., 1989. Space-time modeling with long-memory dependence: Assessing Ireland’s wind power resource. *Applied Statistics* , 1–50.
- Heger, M.P., Neumayer, E., 2019. The impact of the Indian Ocean tsunami on Aceh’s long-term economic growth. *Journal of Development Economics* 141, 102365.
- Henderson, J.V., Squires, T., Storeygard, A., Weil, D., 2017a. The global distribution of economic activity: Nature, history, and the role of trade. *Quarterly Journal of Economics* 133, 357–406.

- Henderson, J.V., Storeygard, A., Deichmann, U., 2017b. Has climate change driven urbanization in Africa? *Journal of Development Economics* 124, 60–82.
- Henderson, J.V., Storeygard, A., Weil, D.N., 2012. Measuring economic growth from outer space. *American Economic Review* 102, 994–1028.
- Henderson, M., Yeh, E.T., Gong, P., Elvidge, C., Baugh, K., 2003. Validation of urban boundaries derived from global night-time satellite imagery. *International Journal of Remote Sensing* 24, 595–609.
- Hiemstra, P., Pebesma, E., Twenhofel, C., Heuvelink, G., 2008. Real-time automatic interpolation of ambient gamma dose rates from the Dutch radioactivity monitoring network. *Computers & Geosciences* 35, 1711–1721.
- Hochrainer, S., 2009. Assessing the macroeconomic impacts of natural disasters: Are there any? *World Bank Policy Research Working Paper* 4968 .
- Hodler, R., Raschky, P.A., 2014a. Economic shocks and civil conflict at the regional level. *Economics Letters* 124, 530–533.
- Hodler, R., Raschky, P.A., 2014b. Regional favoritism. *Quarterly Journal of Economics* 129, 995–1033.
- Hoechle, D., 2007. Robust standard errors for panel regressions with cross-sectional dependence. *The Stata Journal* 7, 281–312.
- Hoeppe, P., 2016. Trends in weather related disasters—consequences for insurers and society. *Weather and Climate Extremes* 11, 70–79.
- Hofstra, N., Haylock, M., New, M., Jones, P., Frei, C., 2008. Comparison of six methods for the interpolation of daily European climate data. *Journal of Geophysical Research: Atmospheres* 113.
- Hoover, E.M., 1948. *Location of economic activity*. McGraw-Hill Book Company, Inc., New York.
- Hornbeck, R., Naidu, S., 2014. When the levee breaks: black migration and economic development in the American South. *American Economic Review* 104, 963–90.
- Hotelling, H., 1929. Stability in competition. *Economic Journal* 39, 41–57.
- Houston, J.B., Hawthorne, J., Perreault, M.F., Park, E.H., Goldstein Hode, M., Halliwell, M.R., Turner McGowen, S.E., Davis, R., Vaid, S., McElderry, J.A., et al., 2015. Social media and disasters: a functional framework for social media use in disaster planning, response, and research. *Disasters* 39, 1–22.
- Hsiang, S.M., 2010. Temperatures and cyclones strongly associated with economic production in the Caribbean and Central America. *Proceedings of the National Academy of Sciences* 107, 15367–15372.

- Hsiang, S.M., Jina, A.S., 2014. The causal effect of environmental catastrophe on long-run economic growth: evidence from 6,700 cyclones. Working Paper 20352. National Bureau of Economic Research. URL: <https://www.nber.org/papers/w20352>.
- Indaco, A., 2020. From twitter to GDP: Estimating economic activity from social media. *Regional Science and Urban Economics* 85, 103591.
- IPCC, 2014. Climate Change 2014: Synthesis Report. Contribution of Working Groups I, II and III to the Fifth Assessment Report of the Intergovernmental Panel on Climate Change. [Core Writing Team, Pachauri, R.K., Meyer, L.A. (Eds.)]. IPCC, Geneva, Switzerland , 151.
- Ishizawa, O.A., Miranda, J.J., Strobl, E., 2019. The impact of hurricane strikes on short-term local economic activity: evidence from nightlight images in the Dominican Republic. *International Journal of Disaster Risk Science* 10, 362–370.
- Japan Times, 2017. Caught off guard by deadly quakes, Kumamoto still learning lessons one year on. URL: [https://www.japantimes.co.jp/news/2017/04/13/national/caught-off-guard-deadly-quakes-kumamoto-still-learning-lessons-one-year/#.Xr-rGC\\_37fY](https://www.japantimes.co.jp/news/2017/04/13/national/caught-off-guard-deadly-quakes-kumamoto-still-learning-lessons-one-year/#.Xr-rGC_37fY). Accessed 16.5.2020.
- Jarmin, R.S., Miranda, J., 2009. The impact of Hurricanes Katrina, Rita and Wilma on business establishments. *Journal of Business Valuation and Economic Loss Analysis* 4.
- Jean, N., Burke, M., Xie, M., Davis, W.M., Lobell, D.B., Ermon, S., 2016. Combining satellite imagery and machine learning to predict poverty. *Science* 353, 790–794.
- Jerven, M., 2010. The relativity of poverty and income: How reliable are African economic statistics? *African Affairs* 109, 77–96.
- Johnson, S., Larson, W., Papageorgiou, C., Subramanian, A., 2013. Is newer better? Penn World Table revisions and their impact on growth estimates. *Journal of Monetary Economics* 60, 255–274.
- Kahn, M.E., 2005. The death toll from natural disasters: The role of income, geography, and institutions. *Review of Economics and Statistics* 87, 271–284.
- Kenward, A., Raja, U., 2014. Blackout: Extreme weather, climate change and power outages. *Climate central* 10.
- Keola, S., Andersson, M., Hall, O., 2015. Monitoring economic development from space: Using night-time light and land cover data to measure economic growth. *World Development* 66, 322–334.
- Klomp, J., 2016. Economic development and natural disasters: a satellite data analysis. *Global Environmental Change* 36, 67–88.

- Klomp, J., Valckx, K., 2014. Natural disasters and economic growth: a meta-analysis. *Global Environmental Change* 26, 183–195.
- Knabb, R.D., Rhome, J.R., Brown, D.P., 2005. Tropical Cyclone Report Hurricane Katrina. Technical Report. National Hurricane Center. URL: [https://www.nhc.noaa.gov/data/tcr/AL122005\\_Katrina.pdf](https://www.nhc.noaa.gov/data/tcr/AL122005_Katrina.pdf).
- Knapp, K.R., Applequist, S., Diamond, H.J., Kossin, J.P., Kruk, M., Schreck, C., 2010a. NCDC International Best Track Archive for Climate Stewardship (IBTrACS) Project, Version 3 [v03r09]. NOAA National Centers for Environmental Information. DOI:10.7289/V5NK3BZP.
- Knapp, K.R., Kruk, M.C., Levinson, D.H., Diamond, H.J., Neumann, C.J., 2010b. The International Best Track Archive for Climate Stewardship (IBTrACS) unifying tropical cyclone data. *Bulletin of the American Meteorological Society* 91, 363–376.
- Kocornik-Mina, A., McDermott, T.K., Michaels, G., Rauch, F., 2020. Flooded cities. *American Economic Journal: Applied Economics* 12, 35–66.
- Kohiyama, M., Hayashi, H., Maki, N., Higashida, M., Kroehl, H., Elvidge, C., Hobson, V., 2004. Early damaged area estimation system using DMSP-OLS night-time imagery. *International Journal of Remote Sensing* 25, 2015–2036.
- Kraus, E., 1977. Subtropical droughts and cross-equatorial energy transports. *Monthly Weather Review* 105, 1009–1018.
- Krige, D.G., 1951. A statistical approach to some basic mine valuation problems on the Witwatersrand. *Journal of the Southern African Institute of Mining and Metallurgy* 52, 119–139.
- Krugman, P., 1979. A model of innovation, technology transfer, and the world distribution of income. *Journal of Political Economy* 87, 253–266.
- Kumamoto Prefectural Crisis and Disaster Prevention Division, 2020. About the damage situation of the 2016 Kumamoto Earthquake (303rd report). URL: [https://www.pref.kumamoto.jp/kinkyu/pub/detail.aspx?c\\_id=9&id=475&pg=1](https://www.pref.kumamoto.jp/kinkyu/pub/detail.aspx?c_id=9&id=475&pg=1). Accessed on 25.5.2020.
- Kunkel, K.E., Pielke Jr, R.A., Changnon, S.A., 1999. Temporal fluctuations in weather and climate extremes that cause economic and human health impacts: A review. *Bulletin of the American Meteorological Society* 80, 1077–1098.
- Lackner, S., 2018. Earthquakes on the surface: earthquake location and area based on more than 14 500 shakemaps. *Natural Hazards and Earth System Sciences* 18, 1665–1679.



- Leiter, A.M., Oberhofer, H., Raschky, P.A., 2009. Creative disasters? Flooding effects on capital, labour and productivity within European firms. *Environmental and Resource Economics* 43, 333–350.
- Lenzen, M., Malik, A., Kenway, S., Daniels, P., Lam, K.L., Geschke, A., 2019. Economic damage and spillovers from a tropical cyclone. *Natural Hazards and Earth System Sciences* 19, 137–151.
- LeSage, J.P., Pace, R.K., 2009. *Introduction to Spatial Econometrics*. Boca Raton, FL: Taylor and Francis.
- Levin, N., 2017. The impact of seasonal changes on observed nighttime brightness from 2014 to 2015 monthly VIIRS DNB composites. *Remote Sensing of Environment* 193, 150–164.
- Levin, N., Kyba, C.C., Zhang, Q., de Miguel, A.S., Román, M.O., Li, X., Portnov, B.A., Molthan, A.L., Jechow, A., Miller, S.D., et al., 2020. Remote sensing of night lights: A review and an outlook for the future. *Remote Sensing of Environment* 237, 111443.
- Levin, N., Zhang, Q., 2017. A global analysis of factors controlling VIIRS nighttime light levels from densely populated areas. *Remote Sensing of Environment* 190, 366–382.
- Li, X., Chen, X., Zhao, Y., Xu, J., Chen, F., Li, H., 2013a. Automatic intercalibration of night-time light imagery using robust regression. *Remote sensing letters* 4, 45–54.
- Li, X., Li, D., 2014. Can night-time light images play a role in evaluating the Syrian crisis? *International Journal of Remote Sensing* 35, 6648–6661.
- Li, X., Xu, H., Chen, X., Li, C., 2013b. Potential of NPP-VIIRS nighttime light imagery for modeling the regional economy of China. *Remote Sensing* 5, 3057–3081.
- Li, X., Zhang, R., Huang, C., Li, D., 2015. Detecting 2014 Northern Iraq insurgency using night-time light imagery. *International Journal of Remote Sensing* 36, 3446–3458.
- Lima, R.C.d.A., Barbosa, A.V.B., 2019. Natural disasters, economic growth and spatial spillovers: Evidence from a flash flood in Brazil. *Papers in Regional Science* 98, 905–924.
- Linkimer, L., 2008. Relationship between peak ground acceleration and Modified Mercalli Intensity in Costa Rica. *Revista Geológica de América Central* , 81–94.
- Loayza, N.V., Olaberria, E., Rigolini, J., Christiaensen, L., 2012. Natural disasters and growth: Going beyond the averages. *World Development* 40, 1317–1336.

- Logan, J.R., 2006. The impact of Katrina: Race and class in storm-damaged neighborhoods. Unpublished manuscript. Spatial Structures in the Social Sciences, Brown University.
- Lösch, A., 1944. Die räumliche ordnung der wirtschaft. G. Fischer.
- Ma, T., Zhou, C., Pei, T., Haynie, S., Fan, J., 2012. Quantitative estimation of urbanization dynamics using time series of DMSP/OLS nighttime light data: A comparative case study from China's cities. *Remote Sensing of Environment* 124, 99–107.
- Ma, T., Zhou, C., Pei, T., Haynie, S., Fan, J., 2014. Responses of Suomi-NPP VIIRS-derived nighttime lights to socioeconomic activity in China's cities. *Remote Sensing Letters* 5, 165–174.
- Malmberg, A., Maskell, P., 1997. Towards an explanation of regional specialization and industry agglomeration. *European Planning Studies* 5, 25–41.
- Mansfield, E., 1961. Technical change and the rate of imitation. *Econometrica* 29, 741–766.
- Mård, J., Di Baldassarre, G., Mazzoleni, M., 2018. Nighttime light data reveal how flood protection shapes human proximity to rivers. *Science Advances* 4, eaar5779.
- Michalopoulos, S., Papaioannou, E., 2013. Pre-colonial ethnic institutions and contemporary African development. *Econometrica* 81, 113–152.
- Michalopoulos, S., Papaioannou, E., 2014. National institutions and subnational development in Africa. *Quarterly Journal of Economics* 129, 151–213.
- Millo, G., 2014. Maximum Likelihood estimation of spatially and serially correlated panels with random effects. *Computational Statistics & Data Analysis* 71, 914–933.
- Millo, G., Piras, G., 2012. SPLM: Spatial Panel Data Models in R. *Journal of Statistical Software* 47, 1–38.
- Mills, S., Weiss, S., Liang, C., 2013. VIIRS day/night band (DNB) stray light characterization and correction, in: *Earth Observing Systems XVIII*, International Society for Optics and Photonics. p. 88661P.
- Miranda, J.J., Ishizawa, O.A., Zhang, H., 2020. Understanding the impact dynamics of windstorms on short-term economic activity from night lights in Central America. *Economics of Disasters and Climate Change* 4, 657–698.
- Mohan, P., Strobl, E., 2017. The short-term economic impact of tropical Cyclone Pam: an analysis using VIIRS nightlight satellite imagery. *International Journal of Remote Sensing* 38, 5992–6006.

- Moran, P.A., 1950. Notes on continuous stochastic phenomena. *Biometrika* 37, 17–23.
- Mukherjee, S., Nateghi, R., Hastak, M., 2018. A multi-hazard approach to assess severe weather-induced major power outage risks in the U.S. *Reliability Engineering & System Safety* 175, 283–305. URL: <http://www.sciencedirect.com/science/article/pii/S0951832017307767>.
- Munich Re, 2017. Natural catastrophes 2016 analyses, assessments, positions. URL: [https://www.munichre.com/content/dam/munichre/global/content-pieces/documents/TOPICS\\_GEO\\_2016-en4.pdf](https://www.munichre.com/content/dam/munichre/global/content-pieces/documents/TOPICS_GEO_2016-en4.pdf).
- Murphy, J.u., O'brien, L., 1977. The correlation of peak ground acceleration amplitude with seismic intensity and other physical parameters. *Bulletin of the Seismological Society of America* 67, 877–915.
- Muth, R.F., 1961. Economic change and rural-urban land conversions. *Econometrica*, 1–23.
- National Hurricane Center, 2018. Costliest U.S. tropical cyclones tables updated. Technical Report. National Hurricane Center. URL: <https://www.nhc.noaa.gov/news/UpdatedCostliest.pdf>.
- Newey, W.K., West, K.D., 1994. Automatic lag selection in covariance matrix estimation. *The Review of Economic Studies* 61, 631–653.
- Nguyen, C.N., Noy, I., 2020. Measuring the impact of insurance on urban earthquake recovery using nightlights. *Journal of Economic Geography* 20, 857–877.
- Nicholson, S.E., 1986. The spatial coherence of African rainfall anomalies: Inter-hemispheric teleconnections. *Journal of Climate and Applied Meteorology* 25, 1365–1381.
- Nojima, N., Maruyama, Y., 2016. Comparison of functional damage and restoration processes of utility lifelines in the 2016 Kumamoto earthquake, Japan with two great earthquake disasters in 1995 and 2011. *JSCE Journal of Disaster FactSheets* URL: [https://committees.jsce.or.jp/disaster/system/files/FS2016-L-0004\\_2.pdf](https://committees.jsce.or.jp/disaster/system/files/FS2016-L-0004_2.pdf).
- Nordhaus, W., Azam, Q., Corderi, D., Hood, K., Victor, N.M., Mohammed, M., Miltner, A., Weiss, J., 2006. The G-Econ database on gridded output: methods and data. Yale University, New Haven .
- Nordhaus, W., Chen, X., 2015. A sharper image? Estimates of the precision of nighttime lights as a proxy for economic statistics. *Journal of Economic Geography* 15, 217–246.
- Noy, I., 2009. The macroeconomic consequences of disasters. *Journal of Development Economics* 88, 221–231.

- Noy, I., Nguyen, C., Patel, P., 2021. Floods and spillovers: households after the 2011 great flood in Thailand. *Economic Development and Cultural Change* 69, 829–868.
- Noy, I., Nualsri, A., 2011. Fiscal storms: public spending and revenues in the aftermath of natural disasters. *Environment and Development Economics* 16, 113–128.
- OECD, 2016. Improving the evidence base on the costs of disasters to inform better policy making for disaster risk management: Toward a framework for accounting national risk management expenditures and losses of disasters. URL: <https://www-oecd-org.proxy.library.uu.nl/gov/risk/issues-paper.pdf>. Accessed 1.6.2020.
- Official Statistics Japan, 2020. Statistical observations by municipalities. Data retrieved from the System of Social and Demographic Statistics (SSDS), <https://www.e-stat.go.jp/en/regional-statistics/ssdsview/municipality>.
- Pandey, B., Zhang, Q., Seto, K.C., 2017. Comparative evaluation of relative calibration methods for DMSP/OLS nighttime lights. *Remote Sensing of Environment* 195, 67–78.
- Paxson, C., Rouse, C.E., 2008. Returning to New Orleans after Hurricane Katrina. *American Economic Review* 98, 38–42.
- Perroux, F., 1955. Note sur la notion de pôle de croissance. *Economie appliquée* 7, 307–320.
- Pinkovskiy, M., Sala-i Martin, X., 2016. Lights, camera . . . income! Illuminating the national accounts-household surveys debate. *Quarterly Journal of Economics* 131, 579–631.
- Pistrika, A.K., Jonkman, S.N., 2010. Damage to residential buildings due to flooding of New Orleans after Hurricane Katrina. *Natural Hazards* 54, 413–434.
- Raddatz, C., 2007. Are external shocks responsible for the instability of output in low-income countries? *Journal of Development Economics* 84, 155–187.
- Raddatz, C., 2009. The wrath of god: Macroeconomic costs of natural disasters. World Bank Policy Research Working Paper 5039 .
- Raschky, P.A., 2008. Institutions and the losses from natural disasters. *Natural hazards and earth system sciences* 8, 627–634.
- Rentschler, J., Obolensky, M., Kornejew, M., 2019. Candle in the wind? Energy system resilience to natural shocks. Background paper to the World Bank report *Lifelines: the resilient infrastructure opportunity* (Hallegatte, S., J. Rentschler, and J. Rozenberg, 2019).

- Rodriguez-Oreggia, E., De La Fuente, A., De La Torre, R., Moreno, H.A., 2013. Natural disasters, human development and poverty at the municipal level in Mexico. *The Journal of Development Studies* 49, 442–455.
- Román, M.O., Wang, Z., Sun, Q., Kalb, V., Miller, S.D., Molthan, A., Schultz, L., Bell, J., Stokes, E.C., Pandey, B., et al., 2018. NASA's Black Marble nighttime lights product suite. *Remote Sensing of Environment* 210, 113–143.
- Rose, A., Benavides, J., Chang, S.E., Szczesniak, P., Lim, D., 1997. The regional economic impact of an earthquake: direct and indirect effects of electricity lifeline disruptions. *Journal of Regional Science* 37, 437–458.
- Rose, A., Oladosu, G., Liao, S.Y., 2007. Business interruption impacts of a terrorist attack on the electric power system of Los Angeles: customer resilience to a total blackout. *Risk Analysis: An International Journal* 27, 513–531.
- de Ruig, L.T., Barnard, P.L., Botzen, W.W., Grifman, P., Hart, J.F., de Moel, H., Sadrpour, N., Aerts, J.C., 2019. An economic evaluation of adaptation pathways in coastal mega cities: an illustration for Los Angeles. *Science of the Total Environment* 678, 647–659.
- Salop, S.C., 1979. Monopolistic competition with outside goods. *The Bell Journal of Economics* , 141–156.
- Šćepanović, S., Mishkovski, I., Hui, P., Nurminen, J.K., Ylä-Jääski, A., 2015. Mobile phone call data as a regional socio-economic proxy indicator. *PloS ONE* 10, e0124160.
- Schippers, V.G., 2022. Lights out? Earthquakes and local economic acitivity. Working Manuscript .
- Schippers, V.G., Alscher, L., 2022. Shaken but not stirred? The local economic impacts of the 2016 Kumamoto earthquake in Japan. Working Manuscript .
- Schippers, V.G., Botzen, W.J.W., 2022. Uncovering the veil of night light changes in times of catastrophe. *Natural Hazards and Earth System Sciences Discussions* 2022, 1–37. URL: <https://nhess.copernicus.org/preprints/nhess-2022-23/>.
- Schneider, A., Friedl, M.A., Potere, D., 2009. A new map of global urban extent from MODIS satellite data. *Environmental Research Letters* 4, 044003.
- Schneider, F., 2005. Shadow economies around the world: What do we really know? *European Journal of Political Economy* 21, 598–642.
- Schneider, F., 2007. Shadow economies and corruption all over the world: New estimates for 145 countries. *Economics E-Journal* URL: [https://papers.ssrn.com/sol3/papers.cfm?abstract\\_id=636661](https://papers.ssrn.com/sol3/papers.cfm?abstract_id=636661).

- Schneider, F., Enste, D.H., 2000. Shadow economies: Size, causes, and consequences. *Journal of Economic Literature* 38, 77–114.
- Scrucca, L., Fop, M., Murphy, T.B., Raftery, A.E., 2016. `mclust` 5: clustering, classification and density estimation using Gaussian finite mixture models. *The R Journal* 8, 205–233.
- Skidmore, M., Toya, H., 2002. Do natural disasters promote long-run growth? *Economic Inquiry* 40, 664–687.
- Skoufias, E., Strobl, E., Breivik Tveit, T., 2020. Flood and tsunami damage indices based on remotely sensed data: an application to Indonesia. *Natural Hazards Review* 21, 04020042.
- Skoufias, E., Strobl, E., Tveit, T., 2021. Can we rely on VIIRS nightlights to estimate the short-term impacts of natural hazards? Evidence from five South East Asian countries. *Geomatics, Natural Hazards and Risk* 12, 381–404.
- Small, C., Pozzi, F., Elvidge, C.D., 2005. Spatial analysis of global urban extent from DMSP-OLS night lights. *Remote Sensing of Environment* 96, 277–291.
- Stein, M., 1999. *Interpolation of spatial data: some theory for kriging*. New York: Springer-Verlag.
- Storeygard, A., 2016. Farther on down the road: Transport costs, trade and urban growth in Sub-Saharan Africa. *Review of Economic Studies* 83, 1263–1295.
- Strobl, E., 2011. The economic growth impact of hurricanes: evidence from US coastal counties. *Review of Economics and Statistics* 93, 575–589.
- Strobl, E., 2012. The economic growth impact of natural disasters in developing countries: Evidence from hurricane strikes in the Central American and Caribbean regions. *Journal of Development economics* 97, 130–141.
- Strömberg, D., 2007. Natural disasters, economic development, and humanitarian aid. *Journal of Economic Perspectives* 21, 199–222.
- Sutton, P.C., Costanza, R., 2002. Global estimates of market and non-market values derived from night-time satellite imagery, land cover, and ecosystem service valuation. *Ecological Economics* 41, 509–527.
- Sutton, P.C., Elvidge, C.D., Ghosh, T., 2007. Estimation of gross domestic product at sub-national scales using night-time satellite imagery. *International Journal of Ecological Economics and Statistics™* 8, 5–21.
- Takashima, M., Hayashi, H., Kimura, H., Kohiyama, M., 2000. Earthquake damaged area estimation using DMSP/OLS night-time imagery-application for Hanshin-Awaji earthquake, in: *Geoscience and Remote Sensing Symposium, 2000. Proceedings. IGARSS 2000. IEEE 2000 International, IEEE*. pp. 336–338.

- Tanaka, K., Keola, S., 2017. Shedding light on the shadow economy: A night-time light approach. *Journal of Development Studies* 53, 32–48.
- Toya, H., Skidmore, M., 2007. Economic development and the impacts of natural disasters. *Economics Letters* 94, 20–25.
- Tsuboi, S., 2019. A study of Nishihara village's disaster response in the Kumamoto earthquake and the disaster victims' perception of life recovery and assessment of health, in: Asahi, C. (Ed.), *Building Resilient Regions. New Frontiers in Regional Science: Asian Perspectives*, Vol 35. Springer, Singapore, pp. 245–260.
- Tuttle, B.T., Anderson, S.J., Sutton, P.C., Elvidge, C.D., Baugh, K., 2013. It used to be dark here. *Photogrammetric Engineering & Remote Sensing* 79, 287–297.
- U.S. Bureau of Economic Analysis, 2020. *Regional Economic Accounts*. URL: <https://www.bea.gov/data/economic-accounts/regional>.
- U.S. Department of Housing and Urban Development, 2006. *Current Housing Unit Damage Estimates: Hurricanes Katrina, Rita, and Wilma*. URL: [https://www.huduser.gov/publications/pdf/gulfcoast\\_hsnngdmgest.pdf](https://www.huduser.gov/publications/pdf/gulfcoast_hsnngdmgest.pdf).
- Venables, A.J., 1996. Equilibrium locations of vertically linked industries. *International Economic Review* 37, 341–359.
- Vernon, R., 1966. International trade and international investment in the product cycle. *Quarterly Journal of Economics* 80, 190–207.
- Vicente-Serrano, S.M., Beguería, S., López-Moreno, J.I., 2010. A multiscalar drought index sensitive to global warming: the Standardized Precipitation Evapotranspiration Index. *Journal of Climate* 23, 1696–1718.
- Vigdor, J., 2008. The economic aftermath of Hurricane Katrina. *Journal of Economic Perspectives* 22, 135–54.
- Von Thünen, J.H., 1826. *Der isolierte Staat in Beziehung auf Landwirtschaft und Nationaloekonomie*. Puthes, Hamburg.
- Wald, D.J., Quitoriano, V., Heaton, T.H., Kanamori, H., 1999. Relationships between peak ground acceleration, peak ground velocity, and modified mercalli intensity in California. *Earthquake Spectra* 15, 557–564.
- Wang, J., Zhang, J., Gong, L., Li, Q., Zhou, D., 2018. Indirect seismic economic loss assessment and recovery evaluation using nighttime light images—application for Wenchuan earthquake. *Natural Hazards and Earth System Sciences* 18, 3253–3266.
- Weber, A., 1909. *Ueber den Standort der Industrien. Erster Teil. Reine Theorie der Standorte*. Mohr, Tübingen .

- Wegscheider, S., Schneiderhan, T., Mager, A., Zwenzner, H., Post, J., Strunz, G., 2013. Rapid mapping in support of emergency response after earthquake events. *Natural Hazards* 68, 181–195.
- Worden, C., Wald, D., 2016. Shakemap manual online: technical manual, user's guide, and software guide. online URL: <http://usgs.github.io/shakemap>.
- Wu, J., Wang, Z., Li, W., Peng, J., 2013. Exploring factors affecting the relationship between light consumption and GDP based on DMSP/OLS night-time satellite imagery. *Remote Sensing of Environment* 134, 111–119.
- Xiao, Y., 2011. Local economic impacts of natural disasters. *Journal of Regional Science* 51, 804–820.
- Xiao, Y., Nilawar, U., 2013. Winners and losers: analysing post-disaster spatial economic demand shift. *Disasters* 37, 646–668.
- Zhang, Q., Pandey, B., Seto, K.C., 2016. A robust method to generate a consistent time series from DMSP/OLS nighttime light data. *IEEE Transactions on Geoscience and Remote Sensing* 54, 5821–5831.
- Zhang, Q., Seto, K.C., 2011. Mapping urbanization dynamics at regional and global scales using multi-temporal DMSP/OLS nighttime light data. *Remote Sensing of Environment* 115, 2320–2329.
- Zhao, N., Liu, Y., Hsu, F.C., Samson, E.L., Letu, H., Liang, D., Cao, G., 2020. Time series analysis of VIIRS-DNB nighttime lights imagery for change detection in urban areas: a case study of devastation in Puerto Rico from hurricanes Irma and Maria. *Applied Geography* 120, 102222.
- Zhao, X., Yu, B., Liu, Y., Yao, S., Lian, T., Chen, L., Yang, C., Chen, Z., Wu, J., 2018. NPP-VIIRS DNB daily data in natural disaster assessment: evidence from selected case studies. *Remote Sensing* 10, 1526.
- Zhou, F., Botzen, W., 2021. Firm level evidence of disaster impacts on growth in Vietnam. *Environmental and Resource Economics* 79, 277–322.



---

## Nederlandse samenvatting

---

In dit proefschrift bestudeer ik de lokale economische impacts van natuurrampen. Natuurrampen kunnen enorme consequenties hebben en komen steeds vaker voor door klimaatverandering en bevolkingsgroei. Wereldwijd sterven jaarlijks zo'n 60.000 mensen door natuurgeweld. Alleen al de directe schade wordt geschat op rond de 100 miljard dollar per jaar. In combinatie met toenemende verstedelijking in gebieden die blootgesteld zijn aan extreem natuurgeweld, is de verwachting dat de consequenties van natuurrampen alleen maar zullen toenemen in de nabije toekomst.

Schade aan gebouwen, infrastructuur en bezittingen en verlies van mensenlevens beïnvloeden economische beslissingen. Productie en consumptiegedrag veranderen onder invloed van verlies van fysiek kapitaal, inkomen en reserves zoals spaargeld. De mate waarin natuurgeweld tot dergelijke gevolgen leidt heeft te maken met hoe samenlevingen zich wapenen tegen dit natuurgeweld. In Nederland hebben we hoge dijken gebouwd om het water buiten te houden, terwijl in Japan aardbevingsbestendig gebouwd wordt. Maar niet overal ter wereld heeft men de middelen of de organisatiekracht om dergelijke maatregelen te nemen. Sommige samenlevingen hebben leren leven met natuursextremen als jaarlijks terugkerend fenomeen, denk aan de jaarlijkse overstromingen in Bangladesh. Andere raken overvallen door buitengewoon extreem natuurgeweld, zoals bij de desastreuze aardbeving in Haïti in 2010.

Een opkomend veld binnen de economische wetenschap houdt zich bezig met de vraag hoe natuurrampen onze economieën beïnvloeden en hoe de verschillen in weerbaarheid tussen landen verklaard kunnen worden, met als breder maatschappelijk doel om meer kennis te vergaren over hoe mitigatie- en adaptatiestrategieën vormgegeven zouden moeten worden. De wijze waarop studies in deze literatuur naar deze vraag kijken is veelal door te analyseren wat het effect van natuurrampen is op het nationaal Bruto Binnenlands Product (BBP). Deze aanpak leidt tot een grote verscheidenheid aan resultaten, van negatief tot geen effect, of juist een positief effect op het BBP. Maar landen verschillen enorm in grootte van niet alleen hun oppervlak, maar ook van hun economieën. Belangrijk is daarbij ook dat het uitmaakt of een ramp plaatsvindt in een dunbevolkt deel van het achterland, of juist midden in de bevolkingscentra van een land. Dezelfde ramp is in verhouding tot een kleine economie, zoals die van Haïti, veel groter dan voor een grote economie zoals die

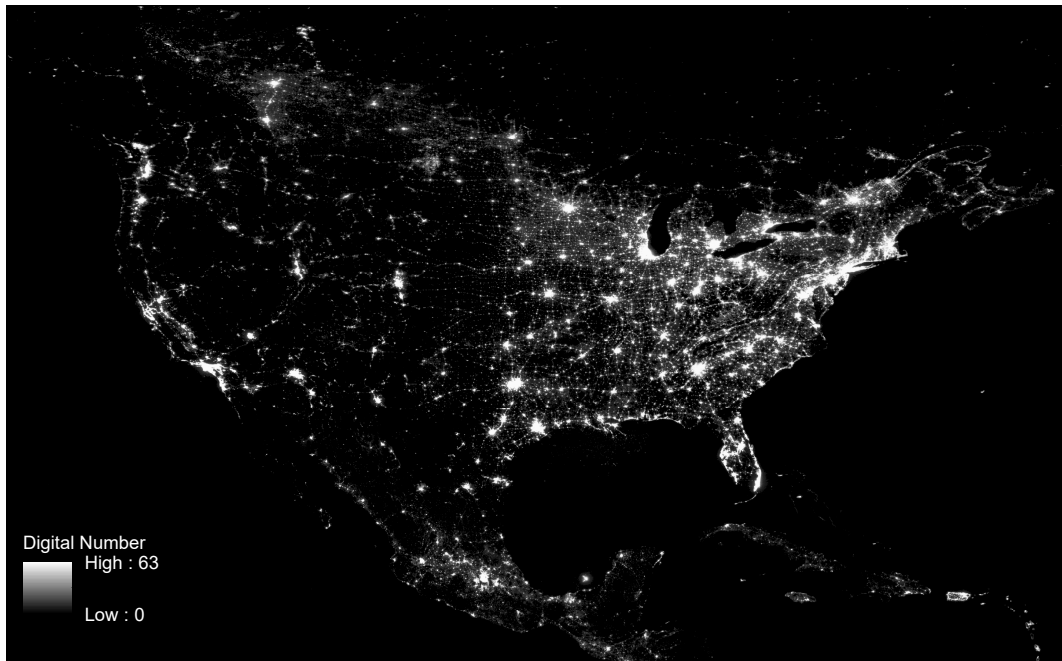
van de Verenigde Staten. Een vergelijking van de effecten van een dergelijke ramp tussen deze landen is dus misleidend.

Daarnaast kent een natuurramp verliezers en winnaars. De detailhandel kan stil komen te liggen omdat de vraag naar alledaagse producten (tijdelijk) wegvalt, terwijl de toegenomen vraag naar bouwmaterialen en -personeel voor wederopbouw die sector juist doet groeien. Maar ook tussen gebieden kan er sprake zijn van verschuivingen van mensen en economische activiteit. De vraag naar personeel voor wederopbouw kan mensen naar een rampgebied trekken, terwijl mensen die hun woning zijn kwijtgeraakt een nieuwe woonplaats en baan elders gaan zoeken. Hoe groter een land is, hoe groter de kans is dat deze dynamiek plaatsvindt binnen de nationale grenzen. Het totale BBP is dan een verzameling van al deze mogelijke effecten en geeft dus slechts een zeer beperkt beeld van wat er daadwerkelijk heeft plaatsgevonden.

In dit proefschrift beargumenteer ik dat het nationale perspectief het verkeerde startpunt is voor een analyse van de economische effecten van natuurrampen. In plaats daarvan zoom ik in op de lokale effecten, in gemeenten, provincies, en wereldwijd op cellen van halve graden. Dit inzoomen is echter verre van triviaal, omdat voor de meeste landen geen economische data beschikbaar zijn op dit schaalniveau. Terwijl het BBP zelfs op alledaagse nieuwspagina's een bekend begrip is, is het correct 'meten' van economische activiteit (voor BBP technisch gezien de totale hoeveelheid aan toegevoegde waarde van alle in een land geproduceerde goederen en diensten) verre van eenvoudig. Economen maken standaard gebruik van internationale databases waarin het BBP van landen door de tijd is becijferd. Maar de kwaliteit van deze gegevens verschilt sterk tussen hoge- en lage-inkomenslanden. In veel ontwikkelingslanden is de kwaliteit ervan dermate laag, dat gezocht wordt naar alternatieve manieren om BBP te benaderen – met zogenaamde proxies. Een van deze proxies die recent is voorgesteld, is de hoeveelheid licht dat een land 's nachts uitzendt. Een voorbeeld hiervan is weergegeven in onderstaand figuur, waarin Noord-Amerika is afgebeeld zoals het 's nachts door een satelliet met een lichtgevoelig instrument wordt waargenomen.

Opvallend is dat het patroon dat we waarnemen sterk overeenkomt met het patroon van de grote steden, ofwel bevolkingsdichtheid. We zien duidelijk de grote agglomeraties aan de oostkust, maar bijvoorbeeld ook Mexico Stad ten zuiden van de Verenigde Staten. Ook opvallend is het verschil tussen het sterk oplichtende oosten en het relatief donkere westen van de Verenigde Staten; een duidelijke weerspiegeling van de spreiding van bevolkingsdichtheid in de V.S., die sterk samenhangt met de hoeveelheid economische activiteit die weer optelt tot het BBP.

De relatie tussen nachtlucht en economische activiteit is dan ook in vele studies gelegd, die op hun beurt de basis hebben gevormd voor een grote literatuur waarin nachtlucht wordt gebruikt als proxy voor BBP of op meer lokaal niveau als proxy voor economische activiteit. Belangrijk is om op te merken dat dit niet alleen zo is voor de spreiding van economische activiteit over de ruimte, maar ook voor de verandering in economische activiteit in een land of een regio door de tijd. Als licht toeneemt, is dat een teken dat de economie is gegroeid. Deze relatie staat centraal in dit proefschrift, maar dan in beginsel in omgekeerde richting: natuurrampen



Figuur 1: Noord-Amerika in de nacht. Dit figuur laat de hoeveelheid nachtlucht zien die wordt waargenomen door een DMSP (Defense Meteorological Satellite Program) satelliet voor Noord-Amerika in het jaar 2010. De data is afkomstig van de Earth Observation Group van de National Oceanic and Atmospheric Association (NOAA) in samenwerking met de NASA, die dagelijkse beelden opschonen en aggregeren tot jaarlijkse datasets met stabiel aanwezig licht. De intensiteit van nachtlucht wordt weergegeven op een resolutie van 30 arc seconden (ongeveer  $1\text{km}^2$ ), op een schaal (Digital Number) van 0 tot 63.

leiden tot schade en een (tijdelijke) afname van economische activiteit en dus nachtlucht. In dit proefschrift gebruik ik deze relatie om meer inzicht te krijgen in hoe natuurrampen lokale economieën raken over de wereld.

De bijdragen van mijn onderzoek kunnen worden opgedeeld in vier hoofdstukken, die de kern vormen van mijn proefschrift. In de eerste helft van het proefschrift, hoofdstukken 2 en 3, werk ik met jaarlijkse nachtluchtdata – de dominante databron in de economische literatuur – die gebruikt wordt als proxy voor (jaarlijkse) economische activiteit, dan wel BBP. Een snel groeiende literatuur gebruikt nachtlucht als proxy voor economische activiteit in de context van natuurrampen, maar stelt de validiteit van deze proxy geenszins ter discussie.

In hoofdstuk 2 onderzoek ik de mate waarin deze relatie opgaat in de context van een catastrofale ramp. Ik bestudeer de casus van orkaan Katrina die in augustus 2005 de kust van de Amerikaanse staten Louisiana en Mississippi trof. Samen met Wouter Botzen verzamel ik gedetailleerde socio-economische data op county-niveau en breng door middel van schadedata en statistieken over bevolking, werkgelegenheid en inkomen de economische impacts van orkaan Katrina op de counties van deze twee staten in beeld. We contextualiseren de impact aan de hand van de economische literatuur over deze ramp om een zo volledig mogelijk beeld te schetsen van de gevolgen van Katrina voor de economieën van de getroffen staten. Daarna kijken we

naar veranderingen in nachtlucht en onderzoeken in welke mate deze de economische impacts reflecteren. Een voorbeeld hiervan is weergegeven in onderstaande figuur voor de stad New Orleans, die zwaar getroffen werd door de orkaan. De tijdelijke leegloop van de stad is duidelijk te zien vanuit de ruimte, terwijl vooral voor de zwaar getroffen oostelijke wijken van de stad ook in het jaar erop nog een duidelijke reductie van nachtlucht te zien is.

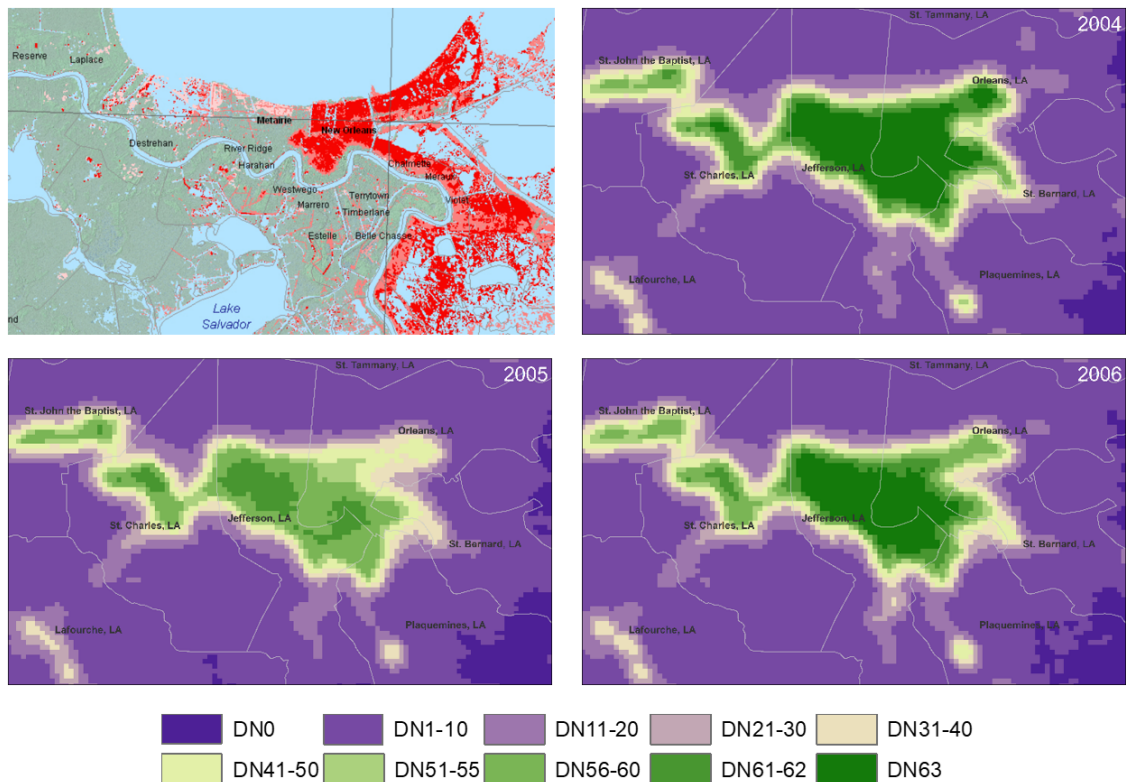
De resultaten in hoofdstuk 2 laten een zeer duidelijke relatie zien met de waargenomen schade aan woningen en met de sterke afname van bevolkingsaantallen in de getroffen counties. Daarnaast laten we zien dat er een sterke relatie bestaat met werkgelegenheid en vinden we een positieve relatie met het totale inkomen in de counties. We concluderen dat de veranderingen in nachtlucht zich niet één-op-één laten vertalen in de economische impacts die we hebben geïdentificeerd, maar dat ze wel een goede benadering vormen. In gebieden waar we geen lokale socio-economische data hebben, kan verandering in nachtlucht dus gebruikt worden als proxy voor de verandering van economische activiteit als gevolg van een grote natuurramp.

In hoofdstuk 3 bestudeer ik de lokale economische impacts van weersextremen in een mondiale setting. Samen met Gabriel Felbermayr, Jasmin Gröschl, Thomas Steinwachs en Mark Sanders presenteer ik een mondiale dataset waarin we op halve graden voor de hele wereld de intensiteit van weersomstandigheden en de hoeveelheid nachtlucht kwantificeren.<sup>1</sup> In dit hoofdstuk kijken we niet alleen naar hoe weersextremen lokale economische activiteit beïnvloeden, maar ook hoe omliggende gebieden hierdoor al dan niet geraakt worden. De stelling is dat nabijgelegen gebieden die niet direct geraakt zijn door natuurgeweld via indirecte links met het getroffen gebied wel degelijk gevolgen ervan kunnen ondervinden. Bij een relatie die berust op afhankelijkheid (complementariteit) zal een negatieve impact op het getroffen gebied ook zijn weerslag vinden in een negatieve impact op het omliggende gebied. Andersom kan in het geval van het overnemen van activiteit van de getroffen buurregio (substitutie) juist een positief effect ontstaan voor omliggende gebieden. In dit hoofdstuk zetten we een ruimtelijk econometrisch model op dat deze relaties toestaat, om zo een schatting te maken van lokale impacts en de aanwezigheid van spillover effecten van getroffen regio's naar buurregio's. Onze studie is de eerste die dergelijke spillover effecten laat zien op lokaal niveau in een systematische mondiale analyse.

Onze resultaten zijn duidelijk: weersextremen hebben in het geval van stormen, regenval, en kou een lokaal negatief effect op nachtlichtemissie, terwijl de omliggende regio's een positief effect op nachtlichtemissie ervaren. Wanneer we een uitsplitsing maken naar inkomensniveaus van landen, zien we dat het grootste deel van onze effecten gedreven wordt door regio's in lage-inkomenslanden. Opnieuw vestigt dit de aandacht op dat lage-inkomenslanden het zwaarst getroffen worden door natuurrampen, terwijl ook daar de komende decennia de zwaarste gevolgen van klimaatverandering op weersextremen wordt verwacht.

---

<sup>1</sup>Dit hoofdstuk is gepubliceerd in het wetenschappelijk tijdschrift *World Development* (Felbermayr et al., 2022).



Figuur 2: Nachtlucht voor New Orleans, van 2004 tot 2006. Linksboven een uitsnede van een overstromingskaart van de Darmouth Flood Observatory. Lichtintensiteit (in Digital Number, DN) is opgedeeld in kleurklassen: donkergroen geeft een hoge hoeveelheid licht weer, terwijl paars zeer weinig tot geen licht vertegenwoordigt. Een groot deel van de stad was zeer sterk verlicht in 2004, het jaar voordat orkaan Katrina de stad trof, maar neemt sterk af in lichtsterkte in 2005. Opvallend is dat vooral het armere oostelijke gedeelte van de stad zwaar getroffen wordt (zie overstromingskaart linksboven); dit vindt zijn weerslag in de sterkste afname in lichtintensiteit in dit deel van de stad. De lichtintensiteit herstelt zich in een groot deel van de stad in 2006, maar vooral het oostelijke gedeelte blijft lang donkerder. Het duurde meer dan 10 jaar tot het lichtniveau in deze buurten van de stad weer op zijn oude niveau was.

In de tweede helft van dit proefschrift, hoofdstukken 4 en 5, verleg ik de focus van jaar-op-jaar veranderingen naar het onderscheid tussen de fase van impact en de fase van herstel na een ramp. De jaarlijkse nachtluchtdata kunnen slechts de uitkomst van de combinatie van schade en herstel weergeven, terwijl de dynamiek als gevolg van een natuurramp zich logischerwijs binnen dit jaar voltrekt. Sinds enkele jaren is een nieuwe set van nachtluchtdata beschikbaar, de Visible Infrared Imaging Radiometer Suite (VIIRS) van de Suomi-NPP satellieten, die de oudere en in 2013 gestopte DMSP satellieten heeft vervangen. Deze data is nog vrij nieuw en is daarmee onontgonnen terrein binnen de economie. Ook toepassingen voor onderzoek naar natuurrampen zijn nog schaars. De VIIRS data zijn van hogere kwaliteit dan de oudere DMSP data en het is noodzakelijk om over te stappen op deze nieuwe databron om recentere rampen te kunnen bestuderen met nachtlucht. In hoofdstukken 4 en 5 gebruik ik deze data om de lokale effecten van aardbevingen

te bestuderen.

In hoofdstuk 4 gebruik ik de mondiale aanpak van hoofdstuk 3 om de lokale effecten van aardbevingen in kaart te brengen aan de hand van de nieuwe VIIRS data. Dit betekent dat de analyse plaatsvindt op maandelijkse in plaats van jaarlijkse resolutie, hetgeen gepaard gaat met de nodige uitdagingen rondom seizoensafhankelijke patronen van licht en de enorme hoeveelheid aan data en benodigde rekenkracht die gepaard gaat met een dergelijke analyse. Ik verzamel data over de intensiteit van aardbevingen (groundshaking, ofwel *peak ground acceleration*) en koppel dit aan lokale emissies van nachtlucht. In tegenstelling tot de resultaten van hoofdstuk 3, laten de analyses in hoofdstuk 4 een heel ander beeld zien. Ik vind geen relatie tussen nachtlichtemissies en aardbevingen voor cellen van halve graden. Omdat de hogere kwaliteit van de VIIRS data het mogelijk maakt om verder in te zoomen, doe ik de analyse opnieuw, maar dan op de resolutie van de nachtlichtdata zelf; zo'n 500 bij 500 meter. Ook hier vind ik geen relatie tussen de intensiteit van aardbevingen en nachtlichtemissies. In overeenstemming met mijn bevindingen in hoofdstuk 4, riepen nieuwe bijdragen van andere onderzoekers twijfel op over de waarde van de VIIRS data als proxy voor economische activiteit bij natuurrampen. Zo worden voor verschillende rampen in Zuid-Oost Azië geen effecten in het VIIRS nachtlucht waargenomen, zowel voor aardbevingen als voor orkanen. Om deze mogelijke verklaring voor de onverwachte resultaten in hoofdstuk 4 te onderzoeken, focus ik me in het laatste hoofdstuk opnieuw op de relatie tussen daadwerkelijk economische impact en veranderingen in nachtlucht in de VIIRS data.

De benodigde informatie voor een dergelijke vergelijking vereist dat we opnieuw gedetailleerde informatie hebben over zowel gerapporteerde schade als socio-economische statistieken op lokaal niveau. Daarom doe ik in hoofdstuk 5 opnieuw een case study met een vergelijkbare aanpak als in hoofdstuk 2. Ik onderzoek op gemeentelijk niveau de effecten van de Kumamoto aardbeving, die in april 2016 het zuidelijke Kyushu eiland van Japan trof. De aardbeving beschadigde en vernietigde deels tienduizenden huizen. De schade wordt tussen de 20 en 30 miljard dollar geschat. In het jaar van de aardbeving verloren de zwaarst getroffen gemeenten tot wel 30 procent van hun jaarlijkse inkomen. Ik verzamel gedetailleerde data over schade, bevolkings- en migratiecijfers en bedrijvigheids- en inkomensdata voor alle gemeenten in het getroffen gebied. Door nachtlucht in de getroffen gemeenten te vergelijken met niet-getroffen gemeenten, isoleer ik vervolgens het effect van de aardbeving op nachtlucht.

Terwijl de economische verschillen tussen de getroffen en niet-getroffen gemeenten evident zijn, vind ik geen duidelijk effect van de aardbeving op het nachtlucht van de getroffen gemeenten. De patronen kunnen niet verklaard worden door schade aan gebouwen, inkomensverliezen, of verliezen van bedrijvigheid in de gemeenten. Alleen in een gemeente waar een brug instortte die de primaire verbinding vormde met het economische centrum van de regio (Kumamoto stad), is een duidelijke afname in nachtlucht waar te nemen die ook langere tijd aanhoudt. Hoewel generaliseren van deze bevindingen lastig is door de focus op een enkele casus, biedt deze studie wel het eerste duidelijke bewijs van een geval waar de verwachte effecten in nachtlucht niet waargenomen worden. Daarmee is dit hoofdstuk ook een waarschuwing voor

de literatuur die de nieuwere VIIRS data gebruikt als proxy voor economische activiteit, zeker in de context van natuurrampen.

Ik concludeer dat het gebruik van nachlichtdata in de context van natuurrampen kansen biedt, maar dat dit niet zonder kanttekeningen komt. In hoofdstukken 2 en 3 presenteer ik veelbelovende resultaten die ons begrip over de lokale effecten van rampen en spillovers naar omliggende gebieden een stapje verder brengen. Ik laat zien dat het gebruik van nachlicht een oplossing biedt om veranderingen in lokale economische activiteit als gevolg van natuurrampen te bestuderen op plekken waar we geen socio-economische data voorhanden hebben. Daarnaast laat ik zien dat dit perspectief ook nieuwe inzichten brengt: effecten van natuurrampen zijn inderdaad lokaal, maar hebben ook weer hun weerslag op economische activiteit in buurregio's. Negatieve lokale effecten vertalen zich bij weersextremen bijvoorbeeld in positieve effecten in nabij gelegen gebieden, die op hun beurt dus de totale impact van een natuurramp kunnen verzachten. Vooral naar aanleiding van het tweede hoofdstuk is vervolgonderzoek voor de hand liggend om in kaart te brengen hoe deze spillovers tot stand komen, waar dit wel en waar dit niet het geval is, en hoe deze relaties al dan niet leiden tot het opvangen van lokale schokken op landelijk niveau. Aan een deel van dit vervolgonderzoek ben ik zelf al bezig, maar ik hoop met deze dissertatie ook anderen in dit onderzoeksveld aan te spreken.

Anderzijds laten hoofdstukken 4 en 5 zien dat onderzoek met de nieuwere VIIRS nachlichtdata problematisch is. Meer onderzoek is nodig naar andere casussen en wellicht met systematischere analyses, waarin gevolgen van verschillende rampen vergeleken worden om meer duidelijkheid te krijgen over waarom ik en anderen in de literatuur non-resultaten vinden. Speciale aandacht is nodig voor de oververtegenwoordiging van onderzoek naar orkanen en overstromingen, terwijl andere rampen als aardbevingen, maar ook langzamere rampen als droogtes, maar weinig aan bod komen. Economen maar ook andere academici moeten dus met voorzichtigheid te werk gaan wanneer zij de nieuwe nachlichtdata gebruiken voor hun onderzoek.

Dit betekent echter niet dat deze lijn van onderzoek geen toekomst heeft. Natuurrampen kunnen op velerlei manieren bestudeerd worden; de weg van nachlicht is daar slechts één van. Anderzijds vormen natuurrampen slechts één onderdeel van een breed pallet aan ontwikkelingsvraagstukken die met nachlicht bestudeerd kunnen worden. Processen die minder schoksgewijs gaan, maar te maken hebben met geleidelijke groei, zoals economische groei in rurale gebieden van ontwikkelingslanden, lenen zich juist bij uitstek om op deze manier bestudeerd te worden. Tot slot ontstaan met de groeiende hoeveelheid satellieten die de aarde bekijken, waarvan data steeds meer publiek toegankelijk wordt, ook nieuwe en andere mogelijkheden voor wetenschappelijk onderzoek. Zo is de uitstoot van gasen als CO<sub>2</sub> en stikstof uit de ruimte waar te nemen; tijdens de COVID-19 pandemie was een afname hiervan duidelijk te zien op de kaarten van de Europese Copernicus satellieten. Bezien in deze context zijn de methoden en bevindingen in dit proefschrift dus slechts één manier waarop waarnemingen van menselijke activiteit vanuit de ruimte ons kunnen informeren over ontwikkeling, groei, en schokken.





---

## Curriculum Vitae

---

Vincent Schippers was born in Leiderdorp, the Netherlands, in 1991. He grew up in Alphen aan den Rijn, where he attended the Groene Hart Lyceum and obtained his gymnasium diploma (cum laude) in 2009. He obtained a Bachelor's degree in Human Geography and Planning from Utrecht University (cum laude) in 2013, with an extensive minor in Economics, partly through an exchange semester at Hong Kong University. After finishing a Research Master in Multidisciplinary Economics (cum laude) at Utrecht University School of Economics in 2016, he carried out his PhD research at the same institute from 2016 to 2021. During his PhD, Vincent conducted an extensive research collaboration with co-authors from CESifo Munich, joined a research group on water, climate and future deltas at the Geosciences faculty of Utrecht University, and presented his work at numerous conferences. As of October 2021, Vincent works as a researcher at the Netherlands Bureau for Economic Policy Analysis (Centraal Planbureau).



---

## U.S.E. Dissertation Series

---

USE 001 **Bastian Westbrook** (2010): *Inter-firm networks: economic and sociological perspectives.*

USE 002 **Yi Zhang** (2011): *Institutions and International Investments: Evidence from China and Other Emerging Markets.*

USE 003 **Ryan van Lamoen** (2011): *The Relationship between Competition and Innovation Measuring Innovation and Causality.*

USE 004 **Martijn Dröes** (2011): *House Price Uncertainty in the Dutch Owner-Occupied Housing Market.*

USE 005 **Thomas van Huizen** (2012): *Behavioural Assumptions in Labour Economics: Analysing Social Security Reforms and Labour Market Transitions.*

USE 006 **Martijn Boermans** (2012): *International Entrepreneurship and Enterprise Development.*

USE 007 **Joras Ferwerda** (2012): *The Multidisciplinary Economics of Money Laundering.*

USE 008 **Federico D'Onofrio** (2013): *Observing the country: a history of Italian agricultural economics, 1900-1930.*

USE 009 **Saraï Sapulete** (2013): *Works Council Effectiveness: Determinants and Outcomes.*

USE 010 **Britta Hoyer** (2013): *Network Formation under the Threat of Disruption.*

USE 011 **Coen Rigtering** (2013): *Entrepreneurial Orientation: Multilevel Analysis and Consequences.*

USE 012 **Beate Cesinger** (2013): *Context and Complexity of International Entrepreneurship as a Field of Research.*

USE 013 **Jan de Dreu** (2013): *Empirical essays on the governance of financial institutions.*

USE 014 **Lu Zhang** (2013): *Industrial Specialization: Determinants, Processes and Consequences.*

USE 015 **Matthias Filser** (2013): *Strategic Issues in Entrepreneurship and Family Business Research.*

USE 016 **Mikko Pohjola** (2013): *A Compilation of Studies on Innovation in Firms: Capabilities, Strategies, and Performance.*

USE 017 **Han-Hsin Chang** (2013): *Heterogeneity in Development.*

USE 018 **Suzanne Heijnen** (2014): *Analyses of sickness absence.*

USE 019 **Mark Kattenberg** (2014): *The Economics of Social Housing: Implications for Welfare, Consumption, and Labor Market Composition.*

USE 020 **Daniel Possenriede** (2014): *The Economics of Temporal and Locational Flexibility of Work.*

USE 021 **Dirk Gerritsen** (2014): *The Relevance of Security Analyst Opinions for Investment Decisions.*

USE 022 **Shiwei Hu** (2014): *Development in China and Africa.*

USE 023 **Saara Tamminen** (2014): *Heterogeneous Firms, Mark-Ups, and Income Inequality.*

USE 024 **Marcel van den Berg** (2014): *Does Internationalization Foster Firm Performance?*

USE 025 **Emre Akgündüz** (2014): *Analyzing maternal employment and child care quality.*

USE 026 **Jasper Lukkezen** (2014): *From Debt Crisis to Sovereign Risk.*

USE 027 **Vesile Kutlu** (2015): *Essays on Subjective Survival Probabilities, Consumption, and Retirement Decisions.*

USE 028 **Brigitte Crooijmans** (2015): *Leiden fusies tot efficiëntere woningcorporaties? Een exploratieve studie naar schaalvoordelen in de sociale huisvesting.*

USE 029 **Andrej Svorenčik** (2015): *The Experimental Turn in Economics: a History of Experimental Economics.*

USE 030 **Secil Danakol** (2015): *Foreign Direct Investment, Foreign Aid and Domestic Entrepreneurship.*

USE 031 **Ioana Deleanu** (2015): *Anti-Money Laundering Efforts: Failures, Fixes and the Future.*

USE 032 **Jaap Oude Mulders** (2016): *Organizations, managers, and the employment of older workers after retirement.*

USE 033 **Malka de Castro Campos** (2016): *Private Consumption-Savings Behavior and Macroeconomic Imbalances.*

USE 034 **Tahereh Rezai Khavas** (2016): *Fairness concerns and cooperation in context.*

USE 035 **Joyce Delnoy** (2016): *Auctions with Competing Sellers and Behavioral Bidders.*

USE 036 **Krista Bruns** (2017): *Emergence and Diffusion of Institutions and their Effect on Economic Growth.*

USE 037 **Daan van der Linde** (2017): *Democracies under Rising Inequality: New Tests of the Redistributive Thesis.*

USE 038 **Swantje Falcke** (2017): *On the move: Analyzing immigration determinants and immigrant outcomes.*

USE 039 **Joep Steegmans** (2017): *House Prices and Household Mobility in The Netherlands: Empirical Analyses of Financial Characteristics of the Household.*

USE 040 **Najmeh Rezaei Khavas** (2017): *Essays in Information Economics.*

USE 041 **Maryam Imanpour** (2017): *The Role of Social Networks for Combating Money Laundering.*

USE 042 **Ye Li** (2018): *Hydrogen Infrastructure Decisions through a Real Option Lens.*

USE 043 **Li Lin** (2018): *Leadership across cultural contexts.*

USE 044 **Werner Liebregts** (2018): *Hidden entrepreneurship: Multilevel analyses of the determinants and consequences of entrepreneurial employee activity.*

USE 045 **Ian Koetsier** (2018): *Government debt: The economic consequences of natural disasters and pension funds' herding.*

USE 046 **Jordy Meekes** (2019): *Local Labour Markets, Job Displacement And Agglomeration Economies.*

USE 047 **Timur Pasch** (2019): *Essays On The Design Of The Management Accounting System: Determinants, Components And Effects.*

USE 048 **Jeroen Content** (2019): *The role of relatedness and entrepreneurship in regional economic development.*

USE 049 **Franziska Heinicke** (2019): *Essays on self-image and preferences for honesty.*

USE 050 **Rebean Al-silefanee** (2019): *Entrepreneurship and Private Sector Development: The Case of Kurdistan Region of Iraq.*

USE 051 **Markus Meinzer** (2019): *Countering cross-border tax evasion and avoidance: An assessment of OECD policy design from 2008 to 2018.*

USE 052 **Zornitza Kambourova** (2019): *Women's Adverse Health Events and Labor Market Participation.*

USE 053 **Tim van der Valk** (2019): *Household finance in France and the Netherlands 1960-2000: An evolutionary approach.*

USE 054 **Milena Dinkova** (2019): *Brace yourselves, Pension is coming: Consumption, financial literacy and tailored pension communication.*

USE 055 **Lisa Dumhs** (2019): *Finding the right job: School-to-work transitions of vocational students in the Netherlands.*

USE 056 **Dea Tusha** (2020): *FDI spillovers in developing countries: channels, conditions, challenges.*

USE 057 **Jingyang Liu** (2020): *Money and credit dynamics in the euro area.*

USE 058 **An Duong** (2020): *Financial integration, trade, and productivity.*

USE 059 **Katharina Weddige-Haaf** (2021): *Real and Financial Asymmetries in the Euro Area.*

USE 060 **Peter Gerbrands** (2021): *Tax Dynamics and Money Laundering. Simulating Policy Reforms in a Complex System.*

USE 061 **Timo Verlaat** (2022): *Carrot and Stick: Experiments with social welfare policies.*

USE 062 **Lucia Rossel Flores** (2022): *A multidisciplinary analysis of tax reform: from politics to human behavior.*

USE 063 **Wanxiang Cai** (2022): *Social capital and crowdfunding. A multilevel perspective.*